U.S. DEPARTMENT OF COMMERCE
National Technical Information Service

PB-282 780

Use of Dredgings for Landfill Technical Report No. 1. Engineering Characteristics of Polluted Dredgings

Northwestern Univ, Evanston, Ill Dept of Civil Engineering

Prepared for

Municipal Environmental Research Lab -Cincinnati, Ohio

May 78

TECHNICAL REPORT DATA
(Please read Instructions on the reverse before completing)

1. REPORT NO. EPA-600/2-78-088b

2.

3. PB 282 780

4. TITLE AND SUBTITLE
USE OF DREDGINGS FOR LANDFILL
Technical Report No. 1
Engineering Characteristics of Polluted Dredgings

5. REPORT DATE May 1978 (Issuing Date)

6. PERFORMING ORGANIZATION CODE

7. AUTHOR(S)
Raymond J. Krizek, Gabor M. Karadi, and Paul L. Hummel

8. PERFORMING ORGANIZATION REPORT NO.

9. PERFORMING ORGANIZATION NAME AND ADDRESS
Department of Civil Engineering
The Technological Institute
Northwestern University
Evanston, Illinois 60201

10. PROGRAM ELEMENT NO. 1BC611

11. CONTRACT/GRANT NO. R-800948

12. SPONSORING AGENCY NAME AND ADDRESS
Municipal Environmental Research Laboratory--Cin.,OH
Office of Research and Development
U.S. Environmental Protection Agency
Cincinnati, Ohio 45268

13. TYPE OF REPORT AND PERIOD COVERED Final

14. SPONSORING AGENCY CODE EPA/600/14

15. SUPPLEMENTARY NOTES Project Officers: Clifford Risley, Phone (312) 353-2200, and Richard P. Traver, Phone (201) 321-6677 8-340-6677. See also Technical Reports No. 2, 3, 4, & 5, EPA-600/2-78-088c, d, e, &f, available from the National Technical Information Service, Springfield, VA.

16. ABSTRACT

The engineering properties of most dredgings were found to be quite similar to those of fine-grained, organic soils, and the general notion that maintenance dredgings are soft and weak is only partially due to their inherent nature; the primary reason for this condition seems to be attributable to the environmental circumstances under which they are frequently placed, namely, in low lying swampy areas with poor drainage. Although the chemical composition of polluted maintenance dredgings is often quite unique compared to that of most soils, the influence of other major factors, such as water content and density, tends to control their engineering behavior, and the unique chemical nature of the dredgings is usually subjugated to a somewhat minor role.

Subject to appro~~pro~~priate handling, it appears that dewatered dredgings can be compacted to form a medium-density landfill which may be used for parking lots or residential construction. Although landfills of hydraulically-placed materials may ultimately serve this same purpose after suitable treatment, the time required would normally be much longer; however, proper planning during the fill process can enhance the quality of the fill and accelerate the time at which it can be used, thus increasing its economic value.

17. KEY WORDS AND DOCUMENT ANALYSIS

a. DESCRIPTORS	b. IDENTIFIERS/OPEN ENDED TERMS	c. COSATI Field/Group
Dredging, Dredges, Sediments, Harbors, Dikes, Channels (waterways), Excavation, Spoil, Waterways (watercourses), Channel stabilization	Landfills	13B 68C

18. DISTRIBUTION STATEMENT Release to public	**19. SECURITY CLASS** *(This Report)* UNCLASSIFIED	**21. NO. OF PAGES** 356
	20. SECURITY CLASS *(This page)* UNCLASSIFIED	**22. PRICE** A16-A01

EPA Form 2220-1 (9-73)

REPRODUCED BY
NATIONAL TECHNICAL
INFORMATION SERVICE
U. S. DEPARTMENT OF COMMERCE
SPRINGFIELD, VA. 22161

BEGIN FIRST LINE OF TEXT HERE
TYPING GUIDE SHEET
CENTER OF PAGE
TOP OF IMAGE AREA
DROPPED HEAD: BEGIN SECTIONS HERE

EPA-600/2-78-088b
May 1978

USE OF DREDGINGS FOR LANDFILL

Technical Report No. 1
Engineering Characteristics of Polluted Dredgings

by

Raymond J. Krizek
The Technological Institute
Northwestern University
Evanston, Illinois 60201

Gabor M. Karadi
University of Wisconsin-Milwaukee
Milwaukee, Wisconsin 53201

Paul L. Hummel
University of Hawaii
Honolulu, Hawaii 96822

Grant No. R-800948 (15070-GCK)

Project Officers

Clifford Risley
U.S. Environmental Protection Agency
Region V
Chicago, Illinois 60604

Richard Traver
Storm and Combined Sewer Section
Wastewater Research Division
Municipal Environmental Research Laboratory (Cincinnati)
Edison, New Jersey 08817

MUNICIPAL ENVIRONMENTAL RESEARCH LABORATORY
OFFICE OF RESEARCH AND DEVELOPMENT
U.S. ENVIRONMENTAL PROTECTION AGENCY
CINCINNATI, OHIO 45268

6-1/2"
9-1/8"
BEGIN LAST LINE OF TEXT
BOTTOM OF IMAGE AREA OUTSIDE DIMENSION FOR TABLES AND ILLUSTRATIONS
3/8"
PAGE NUMBER
EPA-287 (Cin.)
(4-76)

TYPING GUIDE SHEET
BEGIN FIRST LINE OF TEXT HERE
CENTER OF PAGE
TOP OF IMAGE AREA
DROPPED HEAD: BEGIN SECTIONS HERE

DISCLAIMER

This report has been reviewed by the Municipal Environmental Research Laboratory, U.S. Environmental Protection Agency, and approved for publication. Approval does not signify that the contents necessarily reflect the views and policies of the U.S. Environmental Protection Agency, nor does mention of trade names or commercial products constitute endorsement or recommendation for use.

6-1/2"
9-1/8"
BEGIN LAST LINE OF TEXT
BOTTOM OF IMAGE AREA; OUTSIDE DIMENSION FOR TABLES AND ILLUSTRATIONS
3/8"

PAGE NUMBER
EPA-287 (Cin.)
(4-76)

FOREWORD

The Environmental Protection Agency was created because of increasing public and government concern about the dangers of pollution to the health and welfare of the American people. Noxious air, foul water, and spoiled land are tragic testimony to the deterioration of our natural environment. The complexity of that environment and the interplay between its components require a concentrated and integrated attack on the problem.

Research and development is that necessary first step in problem solution and it involves defining the problem, measuring its impact, and searching for solutions. The Municipal Environmental Research Laboratory develops new and improved technology and systems for the prevention, treatment, and management of wastewater and solid and hazardous waste pollutant discharges from municipal and community sources, for the preservation and treatment of public drinking water supplies, and to minimize the adverse economic, social, health, and aesthetic effects of pollution. This publication is one of the products of that research; a most vital communications link between the researcher and the user community.

The need to protect the ecology of the Great Lakes and the other waterways of the United States has led to a variety of problems concerned with the dredging and disposal of increasing volumes of polluted dredge spoil in areas of high population density and industrial development. One commonly used alternative to open water disposal is to place these polluted sediments in diked containment areas to form landfills of marginal value. However, due to the high costs involved, the scarcity of land, and other environmental and economic considerations, these landfills should desirably serve some useful purpose. Accordingly, this study was directed toward evaluating quantitatively the engineering characteristics of dredged materials as they affect their potential usefulness in a landfill.

Francis T. Mayo, Director
Municipal Environmental Research
Laboratory

SUMMARY

Prompted by a need to protect the ecology of the Great Lakes and other waterways of the United States, there is much anxiety concerning the deposition of polluted maintenance dredgings in the open waters, and this leads to a consideration of other means of disposal. One common alternative is to place these dredgings within diked enclosures to form landfills; however, these landfills should desirably serve some useful purpose within the community, rather than add to its environmental degradation by providing unsightly and worthless disposal areas. Toward this end the engineering properties of polluted maintenance dredgings from several harbors along the Great Lakes were examined to evaluate their usefulness as landfill materials.

Included in this study are the sampling and testing techniques employed, the results obtained, and the interpretations advanced. Samples were taken from bottom sediments, dredge hoppers, discharge pipes, fill areas, overflow weirs, and nearby waters, and these samples were tested for chemical composition, biological factors, and routine and special engineering parameters. The field testing program consisted of electrical resistivity soundings, seismic refraction surveys, and vane shear determinations; in addition, undisturbed tube samples and selected disturbed samples were taken for subsequent laboratory tests. Besides the classification tests, mineralogical analyses, and organic content determinations, the laboratory testing program included strength determinations by a miniature vane and by unconfined and triaxial compression tests, compaction tests, and studies of dewatering by electro-

osmosis, gravity drainage, vacuum drainage, and slurry consolidation. The reported engineering properties include density, water content, Atterberg limits, effective grain size, gradation, specific gravity, mineralogy, shear strength, consolidation response, permeability, compressibility, and compaction characteristics.

The engineering properties of most dredgings were found to be quite similar to those of fine-grained, organic soils, and the general notion that maintenance dredgings are soft and weak is only partially due to their inherent nature; the primary reason for this condition seems to be attributable to the environmental circumstances under which they are frequently placed, namely, in low lying swampy areas with poor drainage. Although the chemical composition of polluted maintenance dredgings is often quite unique compared to that of most soils, the influence of other major factors, such as water content and density, tends to control their engineering behavior, and the unique chemical nature of the dredgings is usually subjugated to a somewhat minor role. Despite the low bearing capacity of many existing landfills, experience has proven that they can be successfully sampled and tested in situ by the use of lightweight, manually-operated equipment.

Perhaps the most important parameter in determining the usefulness of dredging spoil is its water content and the associated value of dry density. Hence, dewatering is one of the most significant factors in conditioning the dredgings for subsequent use. Based on a limited laboratory investigation, several techniques of dewatering were found to be technically feasible, but their practical applicability will depend on an appropriate economical study. Field experience suggests that evaporation is probably one of the most useful means for dewatering thin lifts of dredgings, and further attention should be directed toward a quantitative evaluation of this procedure.

Subject to appropriate handling, it appears that dewatered dredgings can be compacted to form a medium-density landfill which may be used for parking lots or residential construction. Although landfills of hydraulically-placed materials may ultimately serve this same purpose after suitable treatment, the time required would normally be much longer; however, proper planning during the fill process can enhance the quality of the fill and accelerate the time at which it can be used, thus increasing its economic value. In addition, the chemistry of the fluids and solids reveals that these dredgings are rich in plant nutrients, and this is further substantiated by the rapid growth of dense vegetation at all fill sites studied; hence, the possible use of polluted dredgings to increase food production is suggested. Additional experience indicates that landfills of dredged spoil may be readily used for wild life refuges or recreational parks.

TABLE OF CONTENTS

Page

SUMMARY iv
LIST OF FIGURES xii
LIST OF TABLES. xvii
ACKNOWLDEGMENTS xix
CHAPTER 1 INTRODUCTION 1
CHAPTER 2 BACKGROUND OF RELATED WORK 6
HYDRAULIC FILL 7
POLLUTION ASPECTS 9
Water Quality 10
Pollution of Sediments 14
Special Processing and Use 16
CONCLUSIONS 18
CHAPTER 3 SAMPLING 20
SAMPLING PHILOSOPHY 20
EQUIPMENT 21
LOCATION AND NOTATION 31
STORAGE AND HANDLING 50
CONCLUSIONS 50
CHAPTER 4 CHEMICAL ANALYSES .52
SCOPE OF TEST PROGRAM 52
TESTING METHODS .53
Total Solids, Total Volatile Solids, and Silica 53
Total Phosphate 54
Metals 55
Ammonia Nitrogen and Total Organic Nitrogen 56
Nitrite Nitrogen 56
Nitrate Nitrogen 56
Sulfide 57
Oil and Grease Hydrocarbons 57
Phenols 57
Chemical Oxygen Demand 57

Biological Oxygen Demand 58
Hydrogen Ion Concentration and Oxidation-Reduction Potential 58
Turbidity 58
TEST RESULTS 58
Northwestern University Test Program 59
Sample Variations 59
Precision of Data 59
Units Employed 59
University of Wisconsin-Milwaukee Test Program . . .65
Carbonates 65
Organic Carbon 65
Cation Exchange Capacity 67
Exchangeable Ions 67
Clay Mineralogy 67
Field Test Program at Toledo, Ohio 67
Pesticide Tests at EPA Laboratory 67
INTERPRETATION OF RESULTS 69
Water Quality as a Function of Distance from Outflow Weir 72
Constituent Concentrations of Water from River, Hopper, and Outflow Weir 73
Composition of Bottom Sediments as a Function of Depth 73
Constituent Concentration as a Function of Dredging Cycle Phase 74
RECOMMENDATIONS 75

CHAPTER 5 ORGANIC CONTENT 76
DEFINITIONS 77
TESTING METHODS 79
Dry Combustion .80
Wet Combustion .81
EXPERIMENTAL RESULTS 85
CONCLUSIONS AND RECOMMENDATIONS 91

CHAPTER 6 DEWATERING 97
SLURRY CONSOLIDATION 97
Test Equipment and Procedures 98
Analysis of Results 103

Conclusions and Recommendations 109
DRAINAGE 111
Equipment and Procedures 111
Results 113
Analysis of Results 113
Conclusions and Recommendations 118

CHAPTER 7 ELECTRO-OSMOSIS 120
ELECTRO-KINETIC PHENOMENA 120
EXPERIMENTAL PROGRAM 122
Apparatus 122
Testing Procedure 126
RESULTS AND INTERPRETATION 127
Energy Relationships 127
Chemical Effects 130
Effects on Engineering Properties 135
CONCLUSIONS .150
RECOMMENDATIONS 150

CHAPTER 8 ELECTRICAL SOUNDING 152
EQUIPMENT AND MEASURING TECHNIQUE 152
METHOD OF INTERPRETATION 153
Barnes Layer Resistivity Method 154
Moore Cumulative Method 155
FIELD WORK 155
ANALYSIS OF DATA 157
Island Site .158
Riverside Site 161
CONCLUSIONS .165

CHAPTER 9 SEISMIC SURVEY 166
OBJECTIVES 167
PRESENTATION OF THE DATA 168
Test Procedure 168
Data 170
Theoretical Response for Constant Velocity Profile 172
General Trends of Actual Response 173
Air Waves .174
Cap Delays 174

Variation of Velocity with Depth 175

METHOD OF ANALYSIS 176

Propagation of Pressure Waves in a Continuum . . 176

Medium with Uni-directional Variation of Velocity 176

Graphical Determination of Time-Distance Plot . .179

Layer of Finite Thickness with a Linear Variation of Velocity 182

Ray Paths 183

Isochrones 184

Time Associated with Each Wave Front 184

Time-Distance Plot 186

Some Features of the Solution 187

Bottom Waves 188

Air Waves 191

Shape of the Response 192

Interpretation Procedure 194

INTERPRETATION OF RESPONSE 199

Penn 7 Site 200

Riverside Site 203

Transverse Base Line 203

First Part of Longitudinal Base Line 206

Second Part of Longitudinal Base Line 210

Third Part of Longitudinal Base Line 210

Fourth Part of Longitudinal Base Line 212

Region Near Inlet Pipe 213

DISCUSSION OF RESULTS 214

Response of the Unfilled Area at Penn 7 214

Response of the Filled Area at Riverside Site . .216

Testing Procedure 218

Embedment 218

Spacing 219

Energy Input 219

Air Wave Control 219

Cap Delays 219

CONCLUSIONS 220

CHAPTER 10 ENGINEERING PROPERTIES SOIL TESTS 221

CLASSIFICATION TESTS 222

MINERALOGICAL ANALYSES 223
STRENGTH 223
Testing Equipment and Procedures 226
Swedish Vane 226
Laboratory Vane 227
Pilcon Vane 228
Compression Tests 228
Results 228
CONVENTIONAL CONSOLIDATION 243
COMPACTION 255
COMPRESSIBILITY 263
PERMEABILITY 263
Electro-osmosis 265
Direct Permeability 265
Drainage Tests 267
Conventional Consolidation 269
CHAPTER 11 INTERPRETATION AND SYNTHESIS 272
FRAMEWORK OF TEST PROGRAM 272
CLASSIFICATION 274
Particle Size and Gradation 274
Mineralogy and Chemistry 275
Water Content and Density 276
Plasticity and Organic Content 279
STRENGTH 285
COMPRESSIBILITY AND CONSOLIDATION 294
COMPACTION 300
PERMEABILITY 301
DEWATERING OF DREDGINGS 307
Evaporation 307
Gravity and Vacuum 314
Electro-osmotic Dewatering 315
Suggested Dewatering Scheme 319
USEFULNESS OF DREDGINGS FOR LANDFILL 321
New Fills 322
Existing Fills 324
Potential Uses of Resulting Landfills 325
CHAPTER 12 CONCLUSIONS AND RECOMMENDATIONS 327
REFERENCES 331

LIST OF FIGURES

Figure		Page
3-1	Flap Valve Sampler	23
3-2	Five-inch Piston Sampler	26
3-3	Three-inch Piston Sampler	27
3-4	Field Frame for Piston Sampler	30
3-5	Milwaukee Harbor Area	46
3-6	Green Bay Disposal Area	46
3-7	Calumet Disposal Area	46
3-8	Monroe Disposal Area	46
3-9	Grassy Island Disposal Area	47
3-10	Fordson Island Disposal Area	47
3-11	Cleveland Harbor Disposal Area	47
3-12	Cuyahoga River Disposal Area	47
3-13	Locations of Toledo Disposal Areas	48
3-14	Riverside Disposal Area	48
3-15	Vicinity of Discharge Pipe at Riverside Site	48
3-16	Penn 7 Disposal Area	49
3-17	Penn 8 Disposal Area	49
3-18	Island Disposal Area	49
5-1	Test Apparatus for Carbon Content Determinations	83
5-2	Organic Content or Loss on Ignition versus Depth	93
5-3	Organic Carbon versus Depth at Different Locations	94
6-1	Slurry Consolidation Apparatus	99
6-2	Cross-section of Slurry Consolidometer	100
6-3	Typical Distribution of Excess Pore Water Pressure	101
6-4	Slurry Consolidometer Sample Removal System	104

Figure Page

6-5 Typical Void Ratio versus Time Plots for Slurry Consolidation Test 105

6-6 Relationships between Void Ratio and Pressure 106

6-7 Rates of Drainage by Gravity and Vacuum Methods 114

6-8 Data from Gravity Drainage Tests 115

7-1 Particle Size Distribution Curves 124

7-2 Outline of Experimental Program 128

7-3 Power Requirements versus Time 129

7-4 Temperature Variations versus Time 131

7-5 Electro-osmotic Dewatering Data for Sample C22TO 136

7-6 Electro-osmotic Dewatering Data for Sample C27MM 137

7-7 Electro-osmotic Dewatering Data for Sample D1DM 138

7-8 Electro-osmotic Dewatering Data for Sample D4CO 139

7-9 Electro-osmotic Flow Rate versus Current 142

7-10 Variation of Moisture Content with Depth 144

7-11 Void Ratio versus Pressure Curves 147

8-1 Wenner Electrode Configuration 153

8-2 Resistivity Profile and Supplemental Data from Island Site 159

8-3 Resistivity Profile and Supplemental Data from Riverside Site 162

8-4 Average Apparent Layer Resistivites 163

8-5 Cumulative Resistivity Curves 164

9-1 Diagrammatic Description of the Seismic Refraction Method 170

9-2 Lay-out of the Seismic Tests at Riverside Site 171

9-3 Theoretical Response for Two Layers with Constant Velocity 173

9-4 Geometrical Interpretation of Snell's Law 179

9-5 Graphical Determination of Seismic Response 180

Figure Page

9-6 Model with Piece-wise Linear Velocity Profile 182

9-7 Path of Integration to Determine Arrival Times 185

9-8 Refraction at the Bottom of the Fill 189

9-9 Refraction at the Surface of the Fill 192

9-10 Typical Shapes of Time-Distance Plots 193

9-11 Seismic Response Curves for Horizontal Distances of 0 and 5 Feet 195

9-12 Seismic Response Curves for Horizontal Distance of 10 Feet 196

9-13 Seismic Response Curves for Horizontal Distance of 30 Feet 197

9-14 Seismic Response Curves for Bottom Waves 198

9-15 Velocity Profile at Penn 7 Site 202

9-16 Comparison of the Seismic Response at Penn 7 and Riverside Site 205

9-17 Velocity and Shear Strength Profiles at Riverside Site 207

9-18 Explanation of Anomalous Response at Riverside Site . . . 209

9-19 Velocity-Confining Stress-Shear Strength Relationships . .216

9-20 Seismic Response Zones at Riverside Site 217

10-1 Field and Laboratory Test Data from BH-1 at Riverside Site 229

10-2 Field and Laboratory Test Data from BH-2 at Riverside Site 230

10-3 Field and Laboratory Test Data from BH-3 at Riverside Site 231

10-4 Field and Laboratory Test Data from BH-4 at Riverside Site 232

10-5 Field and Laboratory Test Data from BH-5 at Riverside Site 233

10-6 Field and Laboratory Test Data from BH-6 at Riverside Site 234

10-7 Field and Laboratory Test Data from BH-7 at Riverside Site 235

Figure Page

10-8 Field and Laboratory Test Data from BH-8 at Riverside Site . . . 236

10-9 Field and Laboratory Test Data from BH-9 at Riverside Site . . . 237

10-10 Longitudinal Profile of Test Data from Riverside Site at Depth of Five Feet . . . 238

10-11 Longitudinal Profile of Test Data from Riverside Site at Depth of Eight to Ten Feet . . . 239

10-12 Field and Laboratory Test Data on Samples from Island Site near Overflow Weir . . . 240

10-13 Field Shear Strength versus Depth from BH-1 through BH-3 at Island Site . . . 241

10-14 Field Shear Strength versus Depth from BH-4 through BH-7 at Island Site . . . 242

10-15 Field and Laboratory Test Data from BH-10 at Riverside Site . . . 244

10-16 Field and Laboratory Test Data from BH-16 at Riverside Site . . . 245

10-17 Field and Laboratory Test Data from BH-18 at Riverside Site . . . 246

10-18 Field Shear Strength versus Depth from BH-14, BH-15, and BH-17 at Riverside Site . . . 247

10-19 Comparative Plots of Field Shear Strength at Riverside Site in 1971 and 1972 . . . 248

10-20 Laboratory Shear Strength and Water Content versus Depth in Gravity Drained Specimens . . . 249

10-21 Laboratory Shear Strength and Water Content versus Depth in Gravity Drained Specimens . . . 250

10-22 Laboratory Shear Strength and Water Content versus Depth in Vacuum Drained Specimens . . . 251

10-23 Stress-Strain-Strength Data on Compacted Dredgings from Vicinity of BH-10 . . . 252

10-24 Stress-Strain-Strength Data on Compacted Dredgings from Vicinity of BH-16 . . . 253

10-25 Stress-Strain-Strength Data on Compacted Dredgings from Vicinity of BH-18 . . . 254

10-26 Standard Proctor Compaction Curves . . . 257

10-27 Harvard Miniature Compaction Curves . . . 258

Figure Page

10-28 Cross-section of Split Ring Compaction Mold 260

10-29 Maximum Dry Density versus Compactive Effort for Three Different Dredgings 261

10-30 Dry Density at Different Locations wtihin the Mold 262

10-31 Compressibility of Various Soils and Dredgings 264

10-32 Permeability as a Function of Void Ratio or Water Content.270

11-1 Influence of Organic Content on Atterberg Limits 283

11-2 Plasticity Index versus Liquid Limit for Soils with Different Organic Contents 284

11-3 Atterberg Limits versus Organic Content for Various Dredgings 286

11-4 Unconfined Compressive Strength versus Organic Content (after Orozco, 1972) 289

11-5 Theoretical Settlement versus Time Curves 296

11-6 Typical Void Ratio versus Consolidation Pressure Curves . 297

11-7 Maximum Dry Density versus Organic Content (after Orozco, 1972) 302

11-8 Comparisons Between Oven-dried and Air-dried Samples (after Orozco, 1972) 303

11-9 Field Study of Evaporation Losses (after Garve and Jeno, 1968) 309

11-10 Laboratory Study of Evaporation Losses (after Greeley and Hansen, 1969) 311

11-11 Proposed Scheme of Drying Beds for Dredgings (after Greeley and Hansen, 1969) 312

11-12 Suggested Dewatering Bin for Dredgings 320

LIST OF TABLES

Table		Page
2-1	Guidelines for Limiting Concentrations of Various Pollutants in Bottom Sediments.	16
3-1	Sample Notation	32
3-2	Summary of "A" Samples.	33
3-3	Summary of "B" Samples.	34
3-4	Summary of "C" Samples.	35
3-5	Summary of "D" Samples.	37
3-6	Summary of "E" Samples.	38
4-1	Chemical Analyses of "A" Samples.	60
4-2	Chemical Analyses of "B" Samples.	61
4-3	Chemical Analyses of "C" Samples.	62
4-4	Chemical Analyses of "D" Samples.	63
4-5	Chemical Analyses of "E" Samples.	64
4-6	Chemical and Mineralogical Analyses of Several Dredgings . . . . . , ...	66
4-7	Chemical Characterization of Field Samples at Toledo. .	68
4-8	Pesticide Analyses of Bottom Sediments.	70
4-9	Pesticide Analyses of Liquids from Bottom Sediments . .	71
5-1	Organic Carbon and Loss on Ignition for Various Dredgings	86
5-2	Organic Carbon Content of Different Dredgings	87
5-3	Effect of Electro-osmosis on Organic Content Determinations	90
5-4	Comparison of Organic Content Determinations by Various Methods	92
6-1	Chemical Analyses of Liquids from Slurry Consolidation Tests	110

Table		Page
6-2	Chemical Analyses of Liquids from Drainage Tests. . . .	117
7-1	Engineering Characteristics of Samples Tested	123
7-2	Chemical Analyses of Samples Tested	132
7-3	Chemical Analyses of Effluents from Samples Tested. . .	133
7-4	Effect of Electro-osmotic Treatment on Engineering Characteristics	145
7-5	Average Shear Strength Determinations	148
7-6	Summary of Test Parameters.	149
9-1	Summary of Data from Seismic Survey	169
10-1	Quantitative Mineralogical Analyses	224
10-2	Qualitative Mineralogical Analyses.	225
10-3	Average Electro-osmotic Coefficient of Permeability . .	266
10-4	Instantaneous Electro-osmotic Coefficient of Permeability.	266
10-5	Coefficient of Permeability from Direct Tests	267
10-6	Coefficient of Permeability from Short-Term Drainage Tests	268
10-7	Coefficient of Permeability from Single-Load Consolidation Tests.	271
11-1	Engineering Properties of Typical Dredgings (after Corps of Engineers, Philadelphia District, 1969). . .	278
11-2	Effect of Organic Content on Atterberg Limits of Two Soils	282
11-3	Predicted Field Performance of Drying Beds (after Greeley and Hansen, 1969)	313
11-4	Flow Efficiency for Electro-osmotic Dewatering of Dredgings	317
11-5	Comparison of Dewatering Rates With and Without an Electrical Gradient	318

ACKNOWLEDGMENTS

In every sense of the word, this report represents the combined efforts and genuine cooperation of a multitude of individuals and organizations. With a sincere hope that all appropriate credits will be ennumerated and a humble apology for any omissions, grateful acknowledgments are extended to:

The Environmental Protection Agency for supporting the major portion of the work under Grants 15070-GCK and R-800948

Northwestern University and the University of Wisconsin-Milwaukee for the many ways they have cost-shared in this effort

John Mulhern, EPA Office of Research and Monitoring in Washington D.C., for his administrative assistance and advice

Clifford Risley and Stephen Poloncsik, Region V Office of EPA, for their role in monitoring this project

Various offices and personnel of the Corps of Engineers, but particularly the personnel of the Toledo Field Office, for their whole-hearted cooperation in almost every request made of them

Several consulting and industrial firms, particularly Dames and Moore, Greeley and Hansen, Soil Testing Services, Inland Steel, and Ace Scavenger Company, for freely sharing their experience relative to dredging disposal problems

Soil Testing Services for the loan of their seismograph and several other items of field equipment

Dr. Jorj O. Osterberg for his advice on various aspects of the sampling and testing program

Dr. Arley G. Franklin for his work on the electrical sounding and seismic surveys

Dr. Edward R. Hermann for his guidance in regard to the chemical sampling and testing program

Dr. Frederic D. Fuller, Illinois District Office of EPA, for analyzing four samples to determine their pesticide content

Dr. Gilbert L. Roderick for his technical guidance regarding the use of additives to improve the engineering properties of dredgings and for conducting many of the tests to characterize the dredgings

Dr. Leo A. Raphaelian, Bernice Katz, and Berrin Edil for their untiring efforts in performing the multitude of chemical analyses

Dr. Antonio Soriano for his evaluation of the data from the seismic survey

Dr. Marshal Silver for his advice concerning the handling and storage of dredging samples

Dr. Emil Mosonyi for his valuable discussions regarding water quality problems associated with dredgings disposal

Dr. J. Neil Kay for his help in designing the sampling equipment and his role in organizing the initial phases of the laboratory and field testing programs

Dr. Donald E. Sheeran and Tuncer B. Edil for their assistance and advice regarding the use of the slurry consolidometers

Abdelsalam M. Salem for his tremendous help in systematizing the voluminous amounts of data and for conducting many of the slurry consolidation tests

Max W. Giger for his interpretation of the data from the electrical sounding survey and for his organization and supervision of the engineering properties testing program

Francis B. Gularte for evaluating the effectiveness of dewatering by electro-osmosis

Jau Scott Jin for performing some of the drainage tests and particle size analyses

Jose L. Monte for his computer programming assistance to aid in reducing the data

Kanwarjit S. Chawla for conducting some of the mineralogical analyses and the material characterization tests

Sheshadri Gupta for his work in performing the tests for organic content

Dominic M. Delle Grazie and Theophille Felten for their ever-ready assistance and advice in constructing the various pieces of equipment needed for this work

Hugo K. Koller for his conscientious help in building and testing the flap valve sampler and the drainage cylinders

Dr. Enrique Castillo, Dr. Antonio Santos-Moreno, Salah Abdelhamid, Manolo Casteleiro, Enrique De Miguel, Dinesh C. Gupta, Roger Kamm, Andras Karadi, Manuel Melis, Luis F. Orozco, Kutay I. Ozaydin, Rudolfo Semrau, Enrique Socias, and John R. Wiesneth, as well as many of the previously mentioned persons, for their conscientious attitudes and whole-hearted efforts in performing the many laborious tasks associated with the laboratory and field phases of this work.

CHAPTER 1

INTRODUCTION

The development and maintenance of the navigable waterways in the United States has been assigned by Congress to the United States Army Corps of Engineers. The magnitude of this task is suggested by the fact that approximately 19,000 miles of waterways and 1,000 harbors must be kept open to support our nation's waterborne commerce. To fulfill this assignment, about 300,000,000 cubic yards of bottom materials are dredged annually to maintain the waterways in the United States, and an additional average of 80,000,000 cubic yards are dredged to develop new projects or or to increase the capacity of existing systems. Current (1972) annual costs for these operations are approximately $150,000,000; hence, the average cost of dredging is about 40 cents per cubic yard with the range varying from about 20 cents to several dollars per cubic yard.

More specifically, about 10,800,000 cubic yards of spoil are dredged annually from approximately 115 Great Lakes harbors. The streams leading into these harbors carry heavy sediment loads of soil, which has eroded from the surrounding region, and of wastes, which have been discharged from urban and industrial areas, into the channels of the harbor, where the water velocities drop to lower values and thereby deposit these materials. With the population growth and the industrial development of a given region, the sediments dredged from the harbors and channels have become increasingly polluted. Until recently, most of these dredged materials were deposited in the lakes at selected disposal areas located sufficiently near the harbors to minimize dredging costs, but far enough away to avoid interference with water intakes, beaches, and other facilities. However, the current concern for protection of the environment has been expressed publicly by political and community leaders through their appeals to the President of the United States to halt the open lake disposal of polluted dredgings.

The Environmental Protection Agency is charged with the tasks of protecting the health and welfare of the people through the use of appropriate controls on waste disposal and of encouraging industry, communities, and individual citizens to safeguard and improve the quality of the environment. Unfortunately, the requirement to avoid open lake disposal of polluted dredgings is usually met with the lack of any practical and economical alternate means of disposal. Accordingly, the research reported herein is part of a program by the Environmental Protection Agency to explore new methods and ideas for enhancing the quality of the environment by using polluted dredging spoil to construct useful landfills.

The true spirit of public service has been exemplified in this regard by the far-sighted leadership of the Corps of Engineers; their anticipation of the need for alternate methods of dredging disposal has led to pioneering developments of diked disposal procedures. In an effort to address the numerous problems associated with such a practice, the Corps has conducted and participated in numerous studies to evaluate the pollutional effects of dredging operations and disposal. As a result of these studies and their experience with dredging, the Corps acknowledges the need to constrain the practice of open water disposal of polluted maintenance dredgings. However, they simultaneously express a strong concern that proper balance and perspective be retained by careful study, research, and development to allow safe and economical solutions of these problems to be obtained.

Although several alternative methods for the disposal of polluted maintenance dredgings are possible, the currently used major alternative to open lake disposal is to deposit the dredgings behind dikes in areas near the harbor. Such a procedure has been found to satisfactorily prevent the polluted sediments from reaching the open lake waters, and, although very costly, it is generally more economical than any other means of handling the dredgings, except lake disposal. The placement of dredging wastes in diked areas has the potential to serve two useful purposes at the same time -- disposal of the dredgings and creation of needed landfill for community development projects. Hence, the desirability of using diked areas to dispose of polluted dredgings is reasonably well established, but there is a need to study the details associated with such operations and to evaluate the potential benefits to be derived.

Since dredging wastes usually contain a substantial amount of clay-like and/or organic materials with high water content, the effectiveness and economy of associated landfill operations are often hampered by the time-consuming process of consolidation, and the resulting man-made land is usually of very low quality. These latter considerations are most significant because the feasibility of using diked disposal areas on a long-term basis is strongly dependent on the cost benefits derived from the created land. Since land in the urban areas surrounding most harbors is usually very expensive, as well as difficult to locate, landfills of sufficiently high quality to play a positive role in the forthcoming systems of urban and regional development would certainly be extremely valuable. By the same token, worthless waste land created by the disposal of polluted dredging spoil simply cannot be tolerated economically. Hence, there is a vital need to investigate methods by which dredging wastes can be used to produce useable land of economic value.

In general, the use of landfill for industrial or residential construction involves consideration of both settlement and stability, both with respect to time. Since dredging wastes are known to be very compressible and very weak in their natural state, methods must be sought to improve the engineering properties of these materials. Also, since consolidation of these materials often requires appreciable periods of time, it is desirable to investigate techniques whereby this process can be predictably accelerated. Although the preceding problems can be readily isolated, the solutions are, unfortunately, not so readily available. Since relatively little is known about the behavioral characteristics of dredging wastes, the major thrust of the research reported herein is a study of their fundamental nature, their basic physical and chemical characteristics, and their associated engineering behavior.

To accomplish these goals, the background information outlined in Chapter 2 was studied, samples were taken as described in Chapter 3, and the results of analyses for chemical constituents and organic content are reported in Chapters 4 and 5, respectively. In addition, special and conventional engineering tests were conducted on these materials in the field and in the laboratory. The special laboratory studies described in Chapters 6 and 7 include dewatering by gravity, vacuum drainage, and the use of slurry consolidometers, and dewatering by electro-osmosis. The results of electrical resistivity and seismic refraction surveys conducted in the field are reported in Chapters 8 and 9. Chapter

10 gives a summary of additional laboratory and field test data concerned with the fundamental properties and indices (such as density, moisture content, specific gravity, Atterberg limits, mineralogy, and grain size distribution) and the engineering properties (such as shear strength, consolidation, compaction, and permeability) of the dredgings. The data are analyzed and interpreted in Chapter 11, and alternative solutions to spoil disposal are discussed. Detailed conclusions regarding each phase of the study are listed at the end of each chapter, and the general conclusions which can be deduced from the overall investigation are presented in Chapter 12.

CHAPTER 2

BACKGROUND OF RELATED WORK

Although various aspects of the problems associated with the disposal of polluted dredgings have been investigated and reported in the literature, relatively little has been done on the use of dredgings for landfill. In general, when "made" land is to be created, the highest quality material consistent with overall economy is sought; this usually results in the use of sand or other granular materials, but silts and clays are used occasionally. The other major aspect of the general problem is that of pollution, usually involving air or water. In this study, however, air pollution is not considered as being significantly related to the use of polluted dredging for landfill; nevertheless, an investigation of the pollutants washed directly from the air during rains or settling from the air into the water, as well as the polluted gas balance between the atmosphere and the water, may add meaningful knowledge to a study of the environmental condition of the Great Lakes.

The potential for water pollution is the motivating factor for the requirement to place polluted dredgings behind dikes, thereby creating a mud hole which can hopefully be used as productive land at some future time. Water quality has been studied extensively to assure the safety of public drinking water and the safe disposal of sanitary and industrial wastes, and certain criteria have been established to evaluate the pollution potential of various maintenance dredgings. Since the main thrust of this research is concerned with the use of dredgings for landfill, only a brief review of the pollution and water quality literature will be considered herein. However, the presence of various pollutants in the dredging spoil does affect the physical and chemical properties of the fill, and thereby its engineering properties.

Included in this chapter will be a brief review of certain general experiences with hydraulically placed landfills and a survey of the pollutional aspects of the water and sediments associated with the disposal of polluted maintenance dredgings behind dikes. Although not explicitly included herein, most of the articles reviewed from the dredging literature were found to contain significant detailed technical information on various aspects of dredging.

HYDRAULIC FILL

Hydraulically placed fill has frequently been used to create new land or to raise low swampy land near waterways and ports so that it may be suitable for various commercial purposes. Although not intended to be comprehensive, this review will illustrate the various aspects of a hydraulic fill operation that are of interest in the placement of polluted maintenance dredgings.

Whitman (1970) discusses the advantages and disadvantages of various types of fill material that may be placed hydraulically for the support of structural loads. Clean sands are considered to be the ideal fill material since they are easily placed and the resulting fill exhibits desirable engineering characteristics. One example of such a fill is an industrial site formed along the west coast of Florida by material dredged to improve the ship channels immediately off shore. Similarly, sand fills were placed for the Newark Airport in New Jersey and for a site at Marsa Brega, Libya, to be used for a petroleum plant, port facility, and associated storage tanks. At Kawasaki, Japan, the harbor sediments consisted of material ranging from fine and medium sands to silts with sand and clay. This particular site was studied intensively by Lambe (1969), and the behavior of the soft foundations underlying the fill indicated the important role that foundation materials have on the use of fills for commercial purposes.

The construction of a dredged-fill island in Lake Maracaibo to accommodate the Lacustre Marine Terminal of the Creole Petroleum Corporation was reported by Whitman (1970). Stiff clay with interspersed sand lenses was dredged to form the shipping channels, and this material was carried through the pipeline and placed as clay lumps with a matrix of clay and sand particles filling the spaces between the lumps. Whereas the clay lumps accumulated near the discharge pipe, the suspended particles carried well beyond and were deposited in accordance with particle size and flow velocity. The resulting mounds of clay lumps required the continual advancement of the end of the discharge pipe, thereby causing a ridge of clay lumps to be formed with other zones of sands, silts, and clays. This type of material and fill placement was also observed at Green Bay, Wisconsin, as part of this research project. However, this type of dredged material is not typical of maintenance dredgings; it is rather associated with new work which requires the deepening of channels into stiff clay bottom materials.

Soft cohesive soils have also become useful fills for the Creole Petroleum Company refinery at Amuay, Venezuela (Whitman, 1970), and for tanks constructed on a soft hydraulic fill (Penman and Watson, 1967). The filling of low-lying land in the vicinity of coastal cities has been proceeding for long periods of time, and Rutledge (1970) discusses the utilization of marginal land for urban development and presents information on the engineering and economic aspects of filled land on soft foundations.

Hartzell (1968) summarized the efforts of the Corps of Engineers at the Philadelphia District in the dredging and disposal of sediments from the Delaware River. These dredgings consist of very fine-grained particles, generally smaller than the #200 sieve and often with a mean size of about 3 microns, with organic contents varying from 7 to 12 percent. A large percentage of the fine-grained material is composed of quartz and feldspar, rather than clay minerals. The Philadelphia District has pioneered in the development of hopper dredging equipment capable of unloading directly into pipes which discharge into diked areas on shore, and their Special Studies Section conducted a Long Range Spoil Disposal Study consisting of seven parts or substudies. Part II of this study was published in June of 1969 and contains information on the engineering properties of the materials and other considerations associated with dredgings disposal.

POLLUTION ASPECTS

Waters are generally defined as polluted when they contain significant amounts of hazardous or undesirable materials. These materials may cause the water to become unsightly or to emit offensive odors, and they may constitute a health hazard to the users of the water. The exact quantities of these materials necessary to cause specific effects are generally not known. In particular, Kramer and Rogers (1968) state:

> One of the major problems in the management of water resources lies in the difficulty of defining valid criteria for water quality.

The complex interaction of various forms of life with components of the environment make the determination of standards extremely difficult. As a result of these difficulties, and yet facing the requirement to improve the deteriorating water quality, responsible government leaders have set various standards according to use for the various waters available. Water Quality Criteria (1968) sets forth standards for public water supplies, fish and wild life, agricultural use, industrial use, recreation, and other specific categories.

Water Quality

The Water Quality Criteria Data Book (1970, 1971) summarizes most of the known information on water quality in three volumes (Volume 1: Organic Chemical Pollution of Freshwater; Volume 2: Inorganic Chemical Pollution of Freshwater; and Volume 3: Effects of Chemicals on Aquatic Life); these volumes will form the basis for a revised Water Quality Criteria in the near future. The complex interrelationships of various materials are noted in the Data Book, and the need for large amounts of careful research is outlined in order that progress may be made in quantitatively correlating specific amounts of pollutants with specific effects on the environment.

The cooperation between the United States and Canada for the control of Great Lakes pollution dates back to the Boundary Waters Treaty signed on January 11, 1909. The original goal to minimize pollution of the boundary waters is expanded in greater detail in the more recent agreements between the two countries; the most recent document, dated March 17, 1972, and revised to April 5, 1972, is entitled Agreement Between Canada and the United States of America on Great Lakes Water Quality. These documents have established the International Joint

Commission [Canada and United States] (IJC) to implement the goals set forth in the agreements; as an aid in the implementation of the program, the IJC has conducted and published research on the nature and location of the pollution in Pollution of Lake Erie, Lake Ontario, and the International Section of the St. Lawrence River, 1969 (Volume 1, Summary; Volume 2, Lake Erie; and Volume 3, Lake Ontario and the International Section of the St. Lawrence River); this study was updated to 1970 by the inclusion of an additional document.

The Proceedings of the Great Lakes Water Resources Conference (1968) presents numerous articles related to such topics as water use conflicts, regulation of the lakes, and water quality in the lakes. Specifically, Dominguez and Basco (1968) consider the difficulty of applying the EPA standards for turbidity due to instrument errors at relatively high turbidity levels. O'Neal and Sceva (1971) consider the effects of dredging on water quality in an EPA report from Region X; this report summarizes many of the initial pilot programs for the containment of dredgings in diked areas, such as the Calumet River Project, the Inland Steel Landfill Lagoon, the Green Bay Study, the Cleveland Harbor Dredging Effects Study, the Rouge River Study, and the Great Sodas Bay Study. Water quality studies were also made on the effects of dredging in the Chesapeake Bay and in the ocean water near the sludge and waste disposal site in the vicinity of New York City. The detrimental effects of dredging on water quality and/or aquatic life in the Pacific Northwest were also noted. The following is quoted from their Appendix A on the criteria for determining the acceptability of dredged spoil disposal to the nation's waters:

The decision whether to oppose plans for disposal of dredged spoil in U.S. waters must be made on a case-by-case basis after considering all appropriate factors, including the following:

(a) Volume of dredged material.
(b) Existing and potential quality and use of the water in the disposal area.
(c) Other conditions at the disposal site such as depth and currents.
(d) Time of year of disposal (in relation to fish migration and spawning, etc.).
(e) Method of disposal and alternatives.
(f) Physical, chemical, and biological characteristics of the dredged material.
(g) Likely recurrence and total number of disposal requests in a receiving water area.
(h) Predicted long and short term effects on receiving water quality.

When concentrations, in sediments, of one or more of the following pollution parameters exceed the limits expressed below, the sediment will be considered polluted in all cases and, therefore, unacceptable for open water disposal.

Chemical Comparison of Highly and Relatively Unpolluted Bottom Samples

Parameter	Units	Lightly Polluted		Heavily Polluted	
		Mean	Range	Mean	Range
Total Volatile Solids	%	2.9	0.7-5.0	19.6	10.2-49.3
Chemical Oxygen Demand	g/kg	21	3-48	177	39-395
Kjehldal Nitrogen	g/kg	0.55	0.01-1.31	2.64	0.58-6.80
Total Phosphorus	g/kg	0.58	0.24-0.95	1.06	0.59-2.55
Grease and Oil	g/kg	0.56	0.11-1.31	7.15	1.38-32.1
Initial Oxygen Demand	g/kg	0.50	0.08-1.24	2.07	0.28-4.65
Oxygen Uptake	g/kg				
Sulfides[a]	g/kg	0.14	0.03-0.51	1.70	0.10-3.77
Oxidation-Reduction Potential	mv	+0.05	(-0.18)-(+0.41)	-0.13	+.11 to -.22

[a] Values are conservative due to preservation method used.

Nedved (1969) reports the development of an outfall sampler that may be used to accurately calculate the sediment and pollution contributed by an outfall discharging into a waterway. Research conducted by the Illinois Institute of Technology Research Institute found a complex time-dependent variation of sediment load over the cross-section of the outfall. To obtain accurate results, a complicated system of sampling tubes and monitoring devices was assembled and tested, and the results were found to be very good. This system may be used to monitor industrial waste outfalls in order that the sediment load due to each of several outfalls contributing to a drainage system may be analyzed. In addition to the development of this special outfall sampler, valuable information was obtained on the density and distribution of the shoal material formed by the sedimentation of the suspended solids in the Calumet River.

The Buffalo District of the U.S. Army Corps of Engineers conducted a major study of the interrelationship between dredging and water quality, and the results are published in a twelve-volume report, dated June, 1969, and entitled Dredging and Water Quality Problems in the Great Lakes. Research for this study included numerous water samples and some sediment samples from many harbors along the Great Lakes, and the conditions before, during, and after dredging were analyzed. The effects of maintenance dredging on the harbor environment is summarized in this report (page 9.64) as follows:

> The effects of maintenance dredging on the harbor environment are generally limited to temporary increases in turbidity and suspended solids. For the most part, no significant lasting changes were noted;...

The report emphasizes the need for widespread pollution abatement practices to be implemented at the sources of the pollutants (page 8.13), and it presents considerable information on various dredging operations and on the water and sediment quality at the various harbors sampled.

Some of this information will be compared with the test results obtained from the current research program. Numerous other reports of interest to the topic of pollution are listed by EPA in Bibliography of Water Quality Research Reports, dated March, 1972.

Pollution of Sediments

Early efforts by the Federal Water Pollution Control Administration (FWPCA) to sample and test bottom sediments are presented in the report entitled Michigan Harbors and Navigation Channels Bottom Sediment Analysis (1967). Samples were obtained from 17 harbors within the Detroit District of the Corps of Engineers. Only the bottom sediments from the samples were tested for total, volatile, and suspended solids, oil and grease, total and soluble phosphates, and iron. Samples tested within 5 to 10 hours from the time of sampling were also tested for dissolved oxygen, biological oxygen demand, chemical oxygen demand, phenolics, and nitrate, nitrite, ammonia, and organic nitrogen. In 1968, the FWPCA published a report entitled A Study to Establish Empirical Criteria for Harbor Sediments, in which various polluting factors are compared with various pollution conditions in an effort to find one or more significant criteria that might be used to establish sediment pollution standards. The factors included in this study were ammonia, nitrate, and organic nitrogen, chemical oxygen demand, oil and grease, phenolics, total phosphates, total iron, lead, copper, chromium, cadmium, nickel, zinc, sulfides, and percent volatile solids, and the pollution indicators were color, odor, particle size, and benthic fauna. This effort was only partially successful, as evidenced by the statement that

> No single parameter was found that can be used as a sediment quality indicator by itself.

Of all the factors considered, oil and grease was found to be the most reliable parameter.

The report entitled Dredging and Water Quality Problems in the Great Lakes (1969) includes considerable information on the pollutional characteristics of the bottom sediments from various harbors. Motivated by an increasing interest in the characteristics of bottom sediments and dredgings, the various testing laboratories developed the methods necessary to determine the quantities of pollutants present. As an aid in comparing results, representatives of the various laboratories met to standardize methods, and this led to the publication of the Chemistry Laboratory Manual for Bottom Sediments compiled by Great Lakes Region Committee on Analytical Methods (1969).

Hutton, Hann, and Smith (1970) report on the pollutional significance of benthal deposits contained in the Houston Ship Channel. From a study of bottom conditions, dredging records, outfall contributions, and urban runoff records, they were able to calculate the mass balance for the entire channel as an aid in evaluating the benthal deposits. Their testing program included biochemical oxygen demand, chemical oxygen demand, volatile solids, and oil and grease content. It was determined that about 32 percent of the total wastes had reached the bottom, and this varied from about 24 percent in the upper channel to about 52 percent in the lower channel.

Brown and Keffer (1971) considered the pollution potential of sediments, and they indicate that, due to the wide scope that standards must cover and the paucity of knowledge of specific contaminant levels which cause detrimental effects, the criteria are necessarily somewhat vague and subject to interpretation. They further report that there is not available an adequate set of criteria which are reasonably applicable to the majority of problem situations encountered with waste water discharges, and procedures that will eventually lead to the establishment of better standards are outlined. They also reported the results of some detailed studies conducted by the Kansas City office of EPA and published the following table of pollution parameters with limiting concentrations which were established by EPA as a guideline for judging the state of pollution of a given sediment.

Table 2-1

Guidelines for Limiting Concentrations of Various Pollutants in Bottom Sediments

Sediments in Fresh and Marine Waters	Concentration Percent (Dry Weight Basis)
Volatile Solids	6.0
Chemical Oxygen Demand (COD)	5.0
Total Kjeldahl Nitrogen	0.10
Oil and Grease	0.15
Mercury	0.0001
Lead	0.005
Zinc	0.005

Special Processing and Use

Heller and Thelen (1971) conducted a novel research program for the Philadelphia District of the Corps of Engineers. They found it possible to take dredgings which have been previously dried to some desired water content, and, with the use of certain additives and considerable heat, to compress them into brick. Although the feasibility of employing this technique on a large scale awaits further study and research, the study illustrates one of numerous potential uses that may be made of dredgings. Greeley and Hansen (1969) studied the feasibility of drying material dredged from the Chicago area, and they found that it could be accomplished at a reasonable cost, which was estimated to be in the range of $0.85 to $1.28 per cubic yard. In locations generating relatively large quantities of spoil on a regular basis, the drying of dredgings and their subsequent removal to another site for use is a feasible alternative to other methods of disposal.

Another approach to the dewatering of dredgings is being studied at Oklahoma State University, where the hydrocyclone is being model-tested as a tool for densifying the dredgings. The Italian Vortex Hydra Company uses the hydrocyclone for this purpose in Europe.

Based on some field experience in which the presence of a ditch accelerated greatly the rate of drainage, the Philadelphia District of the Corps of Engineers (1969) projected that considerable benefit could be obtained by placing deep parallel trenches about 200 feet apart in a spoil fill to aid in the dewatering process. Engineers at Dames and Moore described several experiences with the use of dredgings for landfill; although most of their experience relates to the use of San Francisco Bay Mud as a fill, the physical-chemical characteristics of the Bay Mud is quite similar to many of the dredgings from harbors around the Great Lakes. McNely (1966) discussed some early experiences accumulated by placing a three foot lift of mud at a dry density of about 22 pounds per cubic foot; as a consequence of evaporation only, the material went to about half the height and twice the density in about seven months. Garbe and Jeno (1968) reported the rapid drying of Bay Mud by placing thin lifts of about one and a half feet and by using mechanical equipment to turn the material. Nichols (1972) summarizes the Dames and Moore experience and indicates that (a) although vacuum drainage has been used as a method of consolidation, it has drawbacks in practical application, and (b) drainage by evaporation from the surface is very effective.

Soil Testing Services (1968) reported the results of a testing program for Inland Steel Company of East Chicago, Indiana, concerned with the proposed use of dredgings mixed with slag, a waste product from the production of steel, for landfill. Considerable lake area had already been filled to provide locations for expanded production facilities and to develop a profitable use for the slag. It was found that the dredgings could be mixed with the slag to occupy the void space otherwise existing within the slag, but that the process would be prohibitively expensive. When slag was end-dumped into a previously used dredgings disposal area, it was found that the dredgings were forced ahead of the slag as a mud wave, thereby causing large concentrations of soft dredgings.

Additional literature on the use and disposal of materials, which are in many respects similar to dried processed dredging spoil, can be found on sludge ash, bottom ash, fly ash, mine tailings, and other solid waste materials.

CONCLUSIONS

Based on a brief review of the literature related to water quality, harbor sediments, dredging operations, pollution criteria, and the use of dredgings for landfill, the following conclusions can be advanced:

1. Water pollution in the Great Lakes, as well as all the waters of the world, is a serious problem that will require the concerted effort of everyone to bring about the desired results.
2. The exact relationship between pollutional effects and pollutional factors is very complicated and will require extensive research before it can be identified and quantified.
3. Based on current knowledge, programs have been and are being implemented to decrease the level of pollutants in the Great Lakes.
4. Many harbor sediments are highly polluted,.and, when dredged, should not be deposited in the lake water.

5. Pilot programs for the containment of polluted dredgings in diked areas have been successful as far as retaining the major portion of the solids is concerned, but their role in reducing the total effect of pollution is largely unknown.

6. The drying of dredging spoil by evaporation or drainage is feasible, thereby allowing the possibility for its use as landfill.

7. Due to the environmental impact of dredging operations, additional research is justified to determine intelligent and economical solutions for the disposal of these materials.

CHAPTER 3

SAMPLING

Representative samples of dredgings were obtained under various conditions at different stages of the dredging and disposal operation. Several unique sampling problems were encountered, and the details of their solution are discussed in this chapter; included are the philosophy of sampling, the development and use of special equipment, a description of the samples and the locations from which they were obtained, and the storage and handling procedures.

SAMPLING PHILOSOPHY

Other research and testing programs have established the variability of dredging materials from site to site, as well as within the confines of a particular site. The major objective of this sampling effort was to obtain representative dredging samples which could be used to determine the significant engineering properties of the material. As can readily be appreciated, it was neither possible nor necessary to sample every variety of dredging spoil at a given site, much less the multitude of dredgings at different sites. Accordingly, a planned program of selective sampling was undertaken to obtain typical dredging samples from several different harbors and at several different stages of the dredging cycle. It was considered necessary to study the material (a) before and during dredging, and (b) during and after placement. Hence, samples were typically obtained from bottom sediments, hoppers of dredges, discharge pipes, and the fill area itself. In general, it was not possible to coordinate all phases of the sampling operation at a given site, and, with the exception of an attempt at Toledo, Ohio, to get bottom, hopper, and discharge pipe samples from a specific location in the channel, all samples represent different materials. Consequently, the conclusions derived from this program must be tempered with this limitation.

To adequately examine the usefulness of dredgings for landfill, it is necessary to study existing spoil areas in some detail; furthermore, it is desirable to know as much as possible about the virgin sites before deposition of the spoil and the history of the spoil placement. After an extensive search for locations which meet these criteria, it was decided to concentrate the major research effort at Toledo, Ohio, where typical dredging operations were being conducted and where several recently filled areas were readily available for testing. In order to obtain the information desired, the fills were tested in several ways. Overall patterns were examined by use of electrical resistivity and seismic methods. Other field tests included in-situ vane shear tests and in-place density determinations. Undisturbed and remolded samples were obtained for laboratory tests to determine the chemical and engineering properties. Water samples were obtained from the harbor surface, the top of the hopper, and the overflow weir, and these were tested to evaluate their pollutional aspects and the general disposition of the soluble constituents.

EQUIPMENT

Sampling of dredgings presented several difficult problems, virtually all of which are based on the desire to obtain the most information at the least cost. There is very little experience on the techniques of obtaining samples from soft fills, dredge hoppers, or discharge pipes, and considerable ingenuity was required to find adequate solutions. The equipment designed and built specifically for this operation is described in this section, and, where appropriate, suggestions are made for improvements.

The usual approach for sampling a soft fill involves the use of either a mat or a raft foundation or some type of floating platform to support the commonly used heavy testing equipment. However, a study of these options led to the conclusion that they were too expensive for this research program, and it was decided to use light-weight, hand-operated equipment. Since nearly all available sampling equipment is designed for use with powerful engines and heavy drill rod, it is too heavy and awkward for manual operation. Therefore, it was necessary to design and build the type of sampling equipment which was needed.

The sampling of soft bottom sediments and hopper sediments was accomplished by use of either an Ekman dredge or a flap valve sediment sampler, each of which had a special role in the sampling operation. Whereas the Ekman dredge was fast and easy to operate, even from small boats, it sampled only the very soft, watery top zone of the bottom sediments; on the other hand, the long tubular flap valve sampler, shown in Figure 3-1, allowed deeper penetration into the thicker bottom sediments. The flap valve sampler was capable of sampling materials ranging from water to quite thick slurries, but not stiff or hard materials. However, due to handling of the rod and pushing the sampler into place, it was necessary to work from a substantial platform;

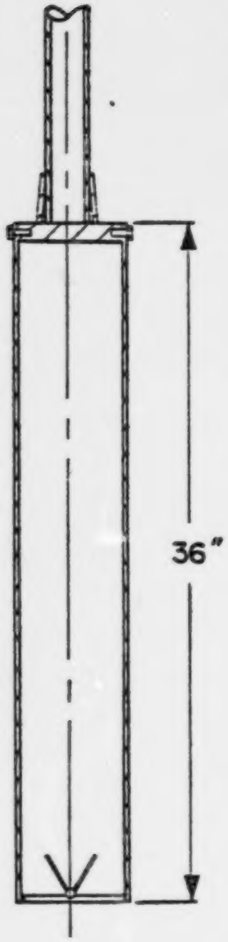

Figure 3-1. Flap Valve Sampler

although the flap valve sampler could be operated very well from a tug boat, barge, or hopper dredge, it was awkward to use from a small boat.

The operating principle of the flap valve sampler is to press the sampling tube downward by use of light-weight aluminum rod through any overlaying water to the sediment to be sampled. The bottom flap valve opens on the downward thrust, thereby allowing water and sediment to enter the tube. Vent holes in the top cover plate of the tube allow the trapped water to escape as the sediment is forced into the tube. The sampling depth can be adjusted by the length of rod used. Upon raising the sampler, the hinged bottom flap valve closes and forms a nearly watertight seal against its seating ring, thus allowing sample retrieval. When the tube with the sample is placed on the working platform, the top plate is removed and the sample is emptied into a container.

The Ekman dredge is operated by lowering it on a line to the harbor bottom; during this lowering maneuver, the spring-loaded doors are locked open. When the slack in the line indicates that bottom contact has been made, a weight is released from the surface; this weight slides down the line and actuates a trigger which releases the locking mechanism, and the spring-loaded doors snap shut. The dredge is then raised to the surface, and the sample is released into the container by reopening the bottom doors. The depth to which the sampler penetrates the bottom sediment can be adjusted to some degree by adding weights to the dredge.

In order to conduct strength, density, and consolidation tests, undisturbed samples are needed, and the requirement to obtain undisturbed samples from soft fills dictated the need for special equipment. Although the 3-inch Osterberg piston sampler does an excellent job of sampling such materials, it is designed for use with heavy, powerful equipment. Despite this limitation, it was employed in this work; several men were able to press it into position and, in many cases, remove it.from the hole, and a tripod with a block-and-tackle system was used to extract the sampler from holes where hand-pulling was too difficult. Another requirement of the Osterberg piston is a water supply and a hydraulic pump to actuate the system during sampling; this added to the overall difficulty in its use, especially on the Island Site at Toledo where water was carried for some distance for this purpose.

Due to these difficulties, it was decided to build a special, lightweight piston sampler for hand operation in soft fill materials. The feasibility of such a sampler was demonstrated by first building and using a 5-inch piston sampler (Figure 3-2) in a trial test at Riverside Site in Toledo on July 1, 1971. The sampler was easily pressed by hand into the soft fill materials and retrieved; excellent samples were obtained, but suitable containers were not available to receive and preserve the samples in an undisturbed condition. Nevertheless, this performance was very encouraging and led to the development of the 3-inch piston sampler (Figure 3-3).

An interesting feature of the original 5-inch piston sampler was the use of available stainless steel tubing, even though it was not perfectly round; the piston was circular with O-ring grooves cut the width of the O-ring, but deeper (by trial and error) than usual. The O-rings were slightly oversized, and this allowed them to adjust to the uneven interior surface of the tube and provide an adequate seal with minimum wall friction.

Due to the suction developed in the soft soil, considerable effort

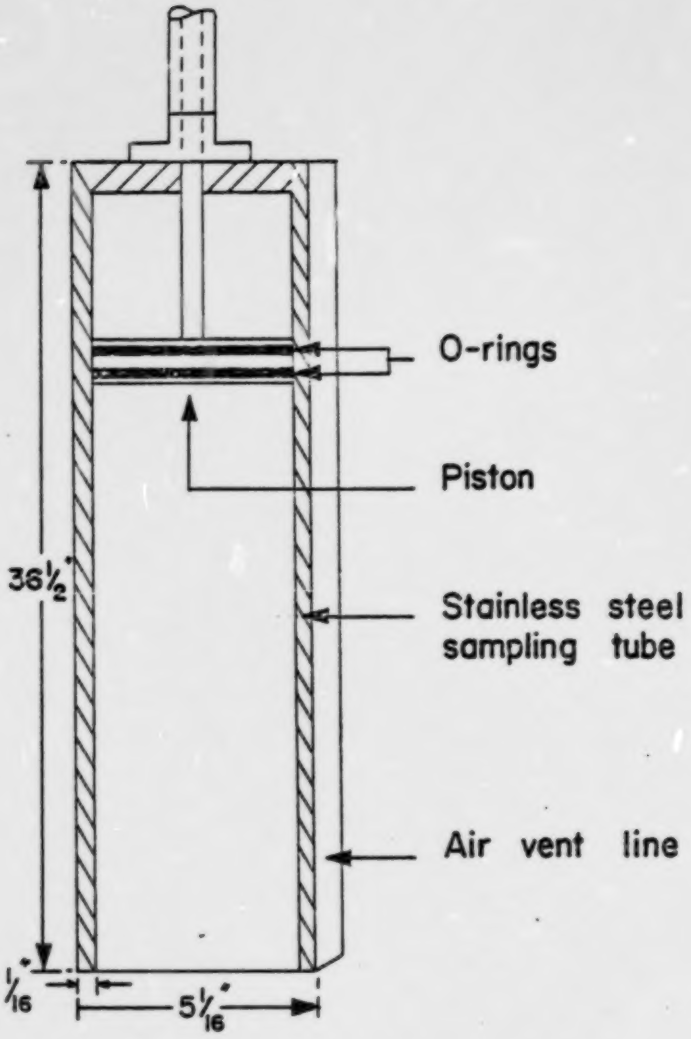
O-rings
Piston
36½"
Stainless steel sampling tube
Air vent line
1/16"
5 1/16"

Figure 3-2. Five-inch Piston Sampler

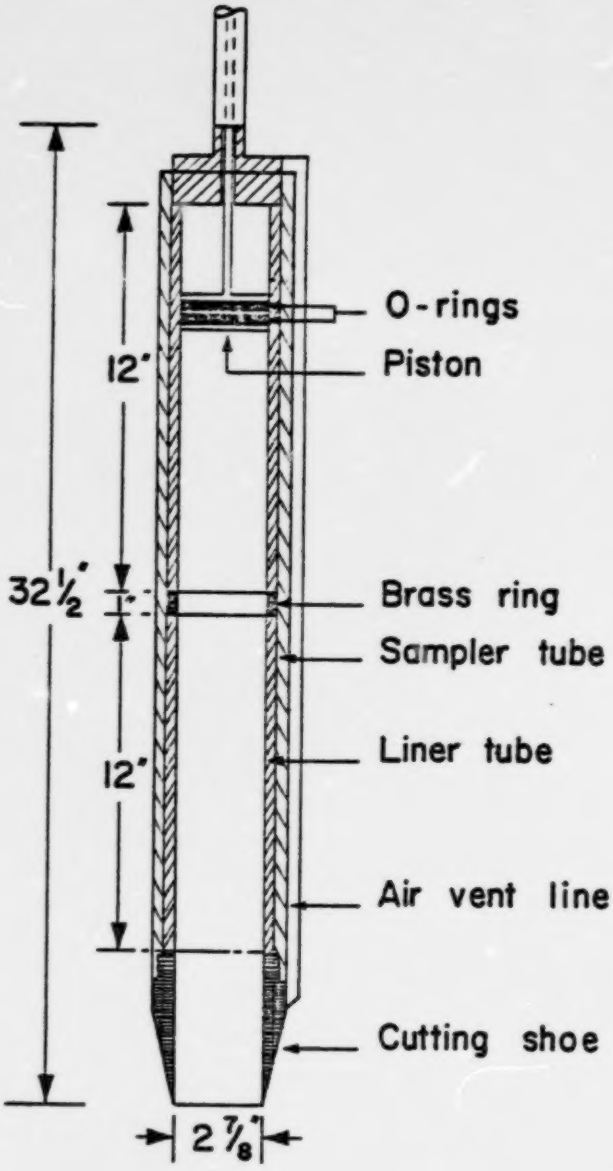
O-rings
Piston
12"
32½"
Brass ring
Sampler tube
Liner tube
12"
Air vent line
Cutting shoe
2 7/8"

Figure 3-3. Three-inch Piston Sampler

was required to retrieve the 5-inch piston sampler. In an attempt to enhance sample recovery and to facilitate sampler retrieval, the 3-inch piston sampler was designed with an air vent connecting the hollow stem of the rod to the cutting tip; this allowed air to pass from the atmosphere into the zone between the lower end of the sampler and the remaining soil mass as the sampler was raised.

Thin tubing was used as liners in the core barrel of the 3-inch sampler to allow the sampled soil to remain in the container in which it was initially received during the sampling operation and to thereby minimize sample disturbance in extraction, handling, and storage. However, since the space between the liner and the sampler wall necessary to allow placement and extraction of the liners also allowed some leakage of air during the sampling operation, the 3-inch sampler did not exhibit as tight a seal or as high a degree of suction above the sample and under the piston during sample recovery as the 5-inch sampler.

In addition, the frictional drag of the sample did not always allow the sampling depth to fill both liners with soil; therefore, the depth of sampler penetration had to be varied with soil consistency, and this means that a truly undisturbed sample was not obtained. It was found that the stiffer soils did not fill both tubes, but the soft materials easily filled both tubes, and good recovery was achieved. As a comparison, thin steel liner tubes pressed by hand into the stiff surface materials at Riverside Site yielded about 6 inches of sample for a 12-inch drive; this demonstrated the effect of interior wall friction in limiting the amount of sample recovered, and a tube with a lower coefficient of friction is needed to improve sample recovery and decrease sample disturbance. A tube pressed into the surface at BH-19 received 11 inches of sample for a 12-inch thrust; the material at this location was more silty and sandy than the materials at other locations. Despite the limitations indicated, the piston sampler performed very well and allowed the collection of samples from various depths within the fill.

The operation of the 3-inch piston sampler is similar to that of any other fixed-rod piston sampler. When the operation is begun, the liners are in place within the tube, the piston is positioned at the lower end of the tube, and the 3-inch channel (snug against the end of the pipe) is tightened onto the piston rod by means of the center locking bolt (Figure 3-4). While in this position, the unit is lowered to the sampling depth without allowing the piston to move relative to the tube. Once the sampling depth is reached, the other two locking bolts are tightened to the rods of the field frame (Figure 3-4), thereby fixing the position of the piston relative to the ground surface. With all three bolts locked, the pipe attached to the sampling tube is pressed downward, and soil enters the tube. In soft soil the end of the stroke required to fill the tube is easily noticed, because the downward resistance increases considerably when the tube is filled. At the end of the downward thrust, the thrust length is recorded as the distance between the 3-inch channel and the top of the pipe. Then the locking bolts are released, the sample is twisted at least one revolution, the channel is lowered to the pipe, and the center bolt is tightened, again fixing the piston relative to the sampler. Next, the entire unit is raised to the ground surface, and the samples are recovered by unscrewing the cutting shoe and sliding the sample tubes out of the barrel. The tubes are labeled, sealed at the ends, and placed in containers for shipment.

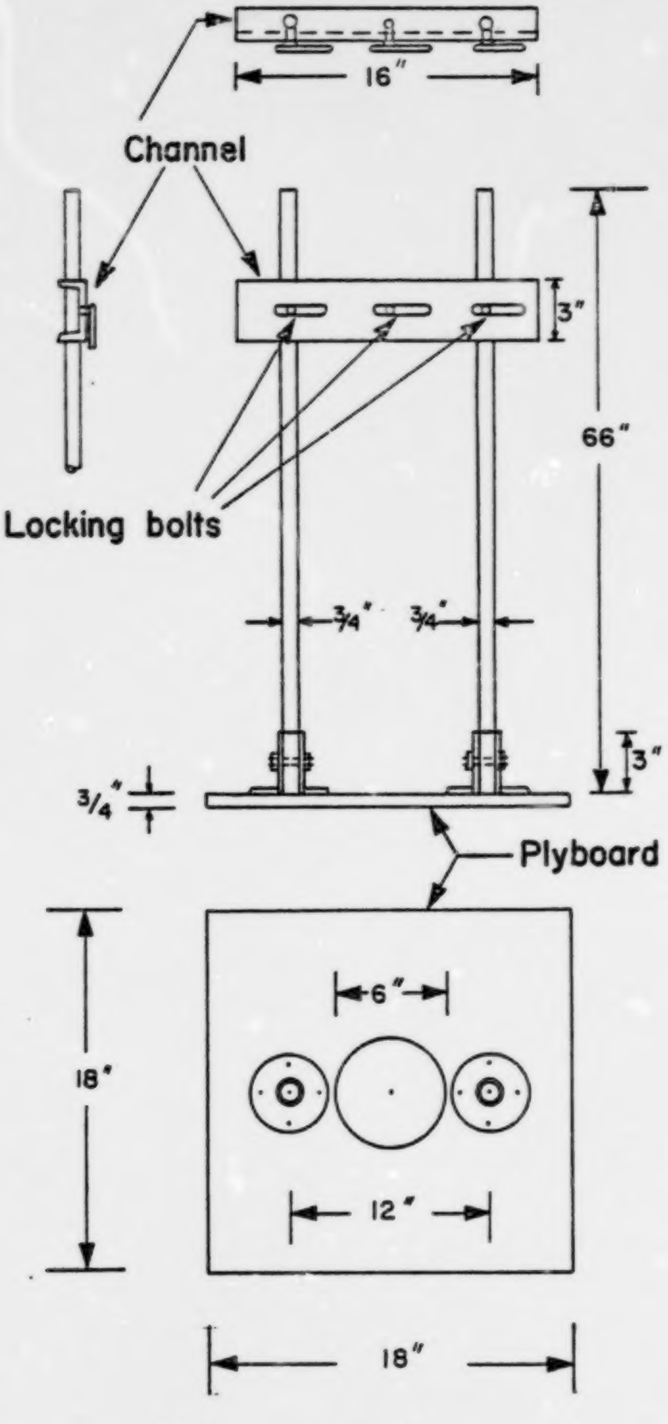
16"
Channel
3"
Locking bolts
66"
3/4"
3/4"
3"
3/4"
Plyboard
6"
18"
12"
18"

Figure 3-4. Field Frame for Piston Sampler

The problem of sampling the material emanating from a discharge pipe was handled very simply. In cases where the pipe diameter was small and/or the flow velocity was low, samples were obtained by the use of a bucket which was held manually near the outflow end of the pipe. However, for larger diameter pipes where the flow velocity was about 12 to 15 feet per second, this method of sampling was dangerous and ineffective. The impact force of the flow caused the bucket to be pulled away or the material to splash into and back out of the bucket. Sampling under such conditions was accomplished by using a section of down-spout with an elbow; this device was positioned several feet from the end of the pipe, and a rope tie-line allowed it to be maneuvered into the pipe discharge. The elbow intercepted a portion of the flow and directed it into the down-spout, where the material was accumulated in 5-gallon buckets and transferred into 30-gallon containers for shipment and storage. Leakage was prevented by the use of a double set of plastic liners.

LOCATION AND NOTATION

Samples with consistencies varying from water to solid were obtained from seven cities, and these were numbered systematically according to the scheme described in Table 3-1. Although the first letter and subsequent numbers completely identify any given sample, the last two letters are used for convenience to aid in immediately locating the city and state from which the sample was obtained. The consistency indices were assigned in the field at the time of sampling, and they are based on the judgment which the field personnel exercised at that time; although subsequent laboratory results indicated that this index should have been different (based on relative amounts of solids present) in a few cases, no changes were made. Tables 3-2 to 3-6 summarize the samples

Table 3.1

Sample Notation

Typical Sample Designation:

B 7 T O

Letter which designates the consistency of the sample → B
Number of sample within given consistency group → 7
First letter of city from which sample was obtained → T
First letter of state from which sample was obtained → O

Consistency Indices:

A -- Essentially water
B -- Water with noticeable amount of suspended solids
C -- Slurry with the consistency of muddy water (10 to 25% solids)
D -- Material with the consistency of thick mud
E -- Solid material capable of maintaining given shape

Locations of Samples:

CI -- Chicago, Illinois
CO -- Cleveland, Ohio
DM -- Detroit, Michigan
GW -- Green Bay, Wisconsin
MM -- Monroe, Michigan
MW -- Milwaukee, Wisconsin
TO -- Toledo, Ohio

Table 3-2

Summary of "A" Samples

Sample Number	Date Obtained	Brief Description
A1TO	12/9/70	Water from inside Penn 8
A2TO	12/9/70	Water from Maumee River
A3TO	12/9/70	Water from east weir of Penn 8
A4TO	12/9/70	Water from west weir of Penn 8
A5TO	12/9/70	Water from east end of Penn 8
A6TO	12/9/70	Water from west end of Penn 8
A7TO	12/9/70	Water from coal yard discharge pipe near Penn 8 weir
A8CO	12/11/70	Water from inside diked area
A9CO	12/11/70	Water from Cuyahoga River
A10MW	6/ 8/71	Water from Station M1 on Menomohee River
A11MW	6/ 8/71	Water from Station M2 in harbor near sewer outfall
A12MW	6/ 8/71	Water from Station M3 in harbor near War Memorial
A13TO	6/30/71	Water from Station E-55
A14TO	6/30/71	Water from Station E-50
A15TO	6/30/71	Water from Station E20N
A16TO	6/30/71	Water from Station E30N
A17TO	6/30/71	Water from Station E30S
A18TO	6/30/71	Water from Station E40
A19TO	7/27/71	Surface water at weir outlet at Island Site
A20TO	7/27/71	Surface water at 100 feet from weir outlet at Island Site
A21TO	7/27/71	Surface water at 200 feet from weir outlet at Island Site
A22TO	7/27/71	Ambient surface water in vicinity of Island Site

Table 3-3

Summary of "B" Samples

Sample Number	Date Obtained	Brief Description
B1DM	12/7/70	Fluid from top of hopper of dredge Hoffman with the hopper full
B2TO	12/9/70	Fluid from top of hopper of dredge Markham at the end of the fill
B3TO	12/9/70	Fluid from top of hopper of dredge Markham just prior to pump out
B4GW	10/15/70	Fluid from top of hopper of dredge Markham at the end of the fill cycle
B5TO	7/ 2/71	Hopper sample from dredge Hoffman with flap valve sampler
B6TO	7/ 2/71	Hopper sample from dredge Hoffman with flap valve sampler
B7TO	7/ 2/71	Hopper sample from overflow weir of dredge Hoffman
B8TO	7/27/71	Turbid water from weir at Island Site
B9TO	7/27/71	Turbid water from vicinity of discharge pipe at Island Site

Table 3-4

Summary of "C" Samples

Sample Number	Date Obtained	Brief Description
C1DM	12/7/70	Material from bottom of hopper of dredge Hoffman by sampler
C2DM	12/7/70	Material from discharge pipe at Grassy Island
C3TO	12/10/70	Material from discharge pipe at Penn 8
C4TO	12/ 9/70	Material from bottom of hopper of dredge Markham by sampler
C5CO	12/11/70	Material from discharge pipe at diked area
C6GW	10/15/70	Material from discharge pipe at diked area
C7MW	6/ 8/71	Bottom sediments from Station M1 on Menomohee River
C8MW	6/ 8/71	Bottom sediments from Station M2 in harbor near sewer outlet
C9MW	6/ 8/71	Bottom sediments from Station M3 in harbor near War Memorial
C10TO	6/29/71	Bottom sediments by Ekman dredge (Field Station E55)
C11TO	6/29/71	Bottom sediments by Ekman dredge (Field Station E50)
C12TO	6/29/71	Bottom sediments by Ekman dredge (Field Station E40N)
C13TO	6/29/71	Bottom sediments by Ekman dredge (Field Station E30N)
C14TO	6/29/71	Bottom sediments by Ekman dredge (Field Station E20N)
C15TO	6/29/71	Bottom sediments by Ekman dredge (Field Station E30S)
C16TO	6/29/71	Bottom sediments by Ekman dredge (Field Station E30C)
C17TO	6/29/71	Bottom sediments by Ekman dredge (Field Station E40S)
C18TO	6/29/71	Bottom sediments by Ekman dredge (Field Station E20S)
C19TO	7/ 2/71	Material from hopper of dredge Hoffman by Ekman dredge
C20TO	7/ 2/71	Material from hopper of dredge Hoffman by Ekman dredge

Table 3-4 (cont.)

Summary of "C" Samples

Sample Number	Date Obtained	Brief Description
C21TO	7/ 2/71	Material from hopper of dredge Hoffman by flap valve sampler
C22TO	7/ 2/71	Material from discharge pipe at Island Site
C23TO	7/27/71	Material from vicinity of discharge pipe at Island Site
C24MM	11/11/71	Material from discharge pipe
C25MM	11/11/71	Material from discharge pipe
C26MM	11/11/71	Material from discharge pipe
C27MM	11/11/71	Material from discharge pipe
C28CI	7/13/71	Material from discharge pipe

Table 3-5

Summary of "D" Samples

Sample Number	Date Obtained	Brief Description
D1DM	12/8/70	Bottom sediments from Rouge River by flap valve sampler
D2DM	12/7/70	Soft sediments from Grassy Island by shovel
D3TO	12/9/70	Soft sediments from Riverside Site by shovel
D4CO	12/11/70	Bottom sediments from Cuyahoga River by shovel from scow
D5DM	12/7/70	Coarse-grained sediments from Grassy Island by shovel
D6TO	12/9/70	Mixed coarse- and fine-grained materials from top of beam in hopper of dredge Markham by shovel
D7GW	10/15/70	Material from pond at end of discharge pipe while pipe was discharging
D8TO	6/29/71	Bottom sediments by flap valve sampler (Field Station V40N)
D9TO	6/29/71	Bottom sediments by flap valve sampler (Field Station V30N)
D10TO	6/29/71	Bottom sediments by flap valve sampler (Field Station V20N)

Table 3-6

Summary of "E" Samples

Sample Number	Date Obtained	Brief Description
E1GW	10/15/70	Clayey-sand from fill near end of discharge pipe
E2GW	10/15/70	Sandy-clay lump from cutter head of dredge
E3GW	10/15/70	Sandy-clay and clay lumps from pile near end of discharge pipe
E4TO	6/29/71	Undisturbed sample from BH-1 at 3' to 6' at Island Site by Osterberg piston sampler
E5TO	6/29/71	Undisturbed sample from BH-2 at 3' to 6' at Island Site by Osterberg piston sampler
E6TO	6/29/71	Undisturbed sample from BH-4 at 3' to 6' at Island Site by Osterberg piston sampler
E7TO	6/29/71	Undisturbed sample from BH-4 at 6' to 9' at Island Site by Osterberg piston sampler
E8TO	6/29/71	Undisturbed sample from BH-4 at 9½' to 12½' at Island Site by Osterberg piston sampler
E9TO	6/30/71	Undisturbed sample from BH-12 at 0' to 3' at Riverside Site by Osterberg piston sampler
E10TO	6/30/71	Undisturbed sample from BH-12 at 3' to 6' at Riverside Site by Osterberg piston sampler
E11TO	6/30/71	Undisturbed sample from BH-12 at 6' to 9' at Riverside Site by Osterberg piston sampler
E12TO	6/30/71	Undisturbed sample from BH-12 at 9' to 12' at Riverside Site by Osterberg piston sampler
E13TO	6/29/71	Disturbed sample from BH-3 at 3/4' at Island Site by shovel
E14TO	6/29/71	Disturbed sample from BH-3 at 3' at Island Site by auger
E15TO	6/29/71	Disturbed sample from BH-5 at ½' at Island Site by shovel
E16TO	6/29/71	Disturbed sample from BH-5 at 3' at Island Site by auger
E17TO	6/29/71	Disturbed sample from BH-6 at 3/4' at Island Site by shovel
E18TO	6/29/71	Disturbed sample from BH-6 at 3' at Island Site by auger
E19TO	6/29/71	Disturbed sample from BH-7 at 1' at Island Site by shovel
E20TO	6/29/71	Disturbed sample from BH-7 at 3' at Island Site by auger

Table 3-6 (cont.)

Summary of "E" Samples

Sample Number	Date Obtained	Brief Description
E21TO	6/29/71	Disturbed sample from BH-8 at 3/4' at Island Site by auger
E22TO	6/29/71	Disturbed sample from BH-8 at 3' at Island Site by auger
E23TO	6/29/71	Disturbed sample from BH-9 at 3/4' at Island Site by auger
E24TO	6/29/71	Disturbed sample from BH-9 at 3' at Island Site by auger
E25TO	7/ 1/71	Sample from BH-13 at 0' to 1' at Riverside Site by 5-inch piston sampler
E26TO	7/ 1/71	Sample from BH-13 at 1' to 2' at Riverside Site by 5-inch piston sampler
E27TO	7/ 1/71	Sample from BH-13 at 2' to 3' at Riverside Site by 5-inch piston sampler
E28TO	7/ 1/71	Sample from BH-13 at 3' to 4' at Riverside Site by 5-inch piston sampler
E29TO	7/ 1/71	Sample from BH-13 at 4' to 5' at Riverside Site by 5-inch piston sampler
E30TO	7/ 1/71	Sample from BH-13 at 5' to 6' at Riverside Site by 5-inch piston sampler
E31TO	7/28/71	Tube sample from BH-2 at 0.5' at Riverside Site
E32TO	7/28/71	Tube sample from BH-2 at 1' to 2' at Riverside Site
E33TO	7/28/71	Tube sample from BH-2 at 2' at Riverside Site
E34TO	7/28/71	Tube sample from BH-2 at 2' to 3' at Riverside Site
E35TO	7/28/71	Tube sample from BH-2 at 3.5' to 4.5' at Riverside Site
E36TO	7/28/71	Tube sample from BH-2 at 5' to 6' at Riverside Site
E37TO	7/28/71	Tube sample from BH-2 at 6' to 7' at Riverside Site
E38TO	7/28/71	Tube sample from BH-2 at 7.5' to 8.5' at Riverside Site
E39TO	7/28/71	Tube sample from BH-2 at 8.5' to 9.5' at Riverside Site
E40TO	7/28/71	Tube sample from BH-3 at 0.5' at Riverside Site

Table 3-6 (cont.)

Summary of "E" Samples

Sample Number	Date Obtained	Brief Description
E41TO	7/28/71	Tube sample from BH-3 at 2' at Riverside Site
E42TO	7/28/71	Tube sample from BH-3 at 4' to 5' at Riverside Site
E43TO	7/28/71	Tube sample from BH-3 at 5' to 6' at Riverside Site
E44TO	7/28/71	Tube sample from BH-3 at 6.5' to 7.5' at Riverside Site
E45TO	7/28/71	Tube sample from BH-3 at 7.5' to 8.5' at Riverside Site
E46TO	7/28/71	Tube sample from BH-3 at 8.25' to 9.25' at Riverside Site
E47TO	7/28/71	Tube sample from BH-3 at 9.25' to 10.25' at Riverside Site
E48TO	7/28/71	Tube sample from BH-4 at 0.5' at Riverside Site
E49TO	7/28/71	Tube sample from BH-4 at 2' at Riverside Site
E50TO	7/28/71	Tube sample from BH-4 at 2' to 3' at Riverside Site
E51TO	7/28/71	Tube sample from BH-4 at 6' to 7' at Riverside Site
E52TO	7/28/71	Tube sample from BH-4 at 7.75' to 8.25' at Riverside Site
E53TO	7/28/71	Tube sample from BH-4 at 8.25' to 9.25' at Riverside Site
E54TO	7/28/71	Tube sample from BH-5 at 0.5' at Riverside Site
E55TO	7/28/71	Tube sample from BH-5 at 2' at Riverside Site
E56TO	7/28/71	Tube sample from BH-5 at 2.25' to 3' at Riverside Site
E57TO	7/28/71	Tube sample from BH-5 at 3' to 5.5' at Riverside Site
E58TO	7/28/71	Tube sample from BH-5 at 5.5' to 6.25' at Riverside Site
E59TO	7/28/71	Tube sample from BH-5 at 7' to 8.75' at Riverside Site
E60TO	7/28/71	Tube sample from BH-6 at 0.5' at Riverside Site
E61TO	7/28/71	Tube sample from BH-6 at 2' at Riverside Site

Table 3-6 (cont.)

Summary of "E" Samples

Sample Number	Date Obtained	Brief Description
E62TO	7/28/71	Tube sample from BH-6 at 2.75' to 4.25' at Riverside Site
E63TO	7/28/71	Tube sample from BH-6 at 6' to 7' at Riverside Site
E64TO	7/28/71	Tube sample from BH-6 at 7' to 8' at Riverside Site
E65TO	7/28/71	Tube sample from BH-7 at 0.5' at Riverside Site
E66TO	7/28/71	Tube sample from BH-7 at 2' at Riverside Site
E67TO	7/28/71	Tube sample from BH-7 at 3.75' to 4.5' at Riverside Site
E68TO	7/28/71	Tube sample from BH-7 at 6' to 6.75' at Riverside Site
E69TO	7/28/71	Tube sample from BH-7 at 8.25' at Riverside Site
E70TO	7/28/71	Tube sample from BH-7 at 8.5' to 9.5' at Riverside Site
E71TO	7/28/71	Tube sample from BH-7 at 9.5' to 10.5' at Riverside Site
E72TO	7/28/71	Tube sample from BH-8 at 0.5' at Riverside Site
E73TO	7/28/71	Tube sample from BH-8 at 2' at Riverside Site
E74TO	7/28/71	Tube sample from BH-8 at 3' at Riverside Site
E75TO	7/28/71	Tube sample from BH-8 at 4.25' to 5' at Riverside Site
E76TO	7/28/71	Tube sample from BH-8 at 6.5' at Riverside Site
E77TO	7/28/71	Tube sample from BH-8 at 7' to 7.25' at Riverside Site
E78TO	7/28/71	Tube sample from BH-8 at 7.25' to 8.25' at Riverside Site
E79TO	7/28/71	Tube sample from BH-8 at 9' to 9.25' at Riverside Site
E80TO	7/28/71	Tube sample from BH-8 at 9.25' to 10.25' at Riverside Site
E81TO	7/28/71	Block sample from BH-1 at Riverside Site
E82TO	7/28/71	Block sample from BH-2 at Riverside Site
E83TO	7/28/71	Block sample from BH-3 at Riverside Site

Table 3-6 (cont.)

Summary of "E" Samples

Sample Number	Date Obtained	Brief Description
E84TO	7/28/71	Block sample from BH-4 at Riverside Site
E85TO	7/28/71	Block sample from BH-5 at Riverside Site
E86TO	7/28/71	Block sample from BH-5 at Riverside Site
E87TO	7/28/71	Block sample from BH-6 at Riverside Site
E88TO	7/28/71	Block sample from BH-6 at Riverside Site
E89TO	7/28/71	Block sample from BH-7 at Riverside Site
E90TO	7/28/71	Block sample from BH-7 at Riverside Site
E91TO	7/28/71	Block sample from BH-8 at Riverside Site
E92TO	7/28/71	Block sample from BH-8 at Riverside Site
E93TO	7/28/71	Block sample from BH-9 at Riverside Site
E94TO	7/28/71	Shovel sample from Station 1 at Riverside Site
E95TO	7/28/71	Shovel sample from Station 2 at Riverside Site
E96TO	7/28/71	Shovel sample from Station 3 at Riverside Site
E97TO	7/28/71	Shovel sample from Station 4 at Riverside Site
E98TO	7/28/71	Shovel sample from Station 5 at Riverside Site
E99TO	7/28/71	Shovel sample from Station 6 at Riverside Site
E100TO	7/28/71	Shovel sample from Station 7 at Riverside Site
E101TO	7/28/71	Shovel sample from Station 8 at Riverside Site
E102TO	7/28/71	Shovel sample from Station 9 at Riverside Site
E103TO	7/28/71	Shovel sample from Station 10 at Riverside Site
E104TO	7/28/71	Shovel sample from Station 11 at Riverside Site
E105TO	7/28/71	Shovel sample from Station 12 at Riverside Site
E106TO	7/28/71	Shovel sample from Station 13 at Riverside Site
E107TO	7/28/71	Shovel sample from Station 14 at Riverside Site
E108TO	7/28/71	Shovel sample from Station 15 at Riverside Site
E109TO	7/28/71	Shovel sample from Station 16 at Riverside Site
E110TO	7/28/71	Auger sample from Station P1 at 1' depth at Penn 7
E111TO	7/28/71	Auger sample from Station P1 at 2' depth at Penn 7
E112TO	7/28/71	Auger sample from Station P1 at 3' depth at Penn 7

Table 3-6 (cont.)

Summary of "E" Samples

Sample Number	Date Obtained	Brief Description
E113TO	7/28/71	Auger sample from Station P2 at 1' depth at Penn 7
E114TO	7/28/71	Auger sample from Station P2 at 2.5' depth at Penn 7
E115TO	6/27/72	Tube sample from BH-10 at 0' at Riverside Site
E116TO	6/27/72	Tube sample from BH-10 at 3.8' at Riverside Site
E117TO	6/27/72	Tube sample from BH-10 at 6.1' at Riverside Site
E118TO	6/27/72	Tube sample from BH-10 at 8.5' at Riverside Site
E119TO	6/27/72	Tube sample from BH-10 at 11.0' at Riverside Site
E120TO	6/27/72	Tube sample from BH-10 at 13.5' at Riverside Site
E121TO	6/27/72	Tube sample from BH-10 at 14.3' at Riverside Site
E122TO	6/27/72	Tube sample from BH-11 at 3.9' at Riverside Site
E123TO	6/27/72	Tube sample from BH-11 at 6.1' at Riverside Site
E124TO	6/27/72	Tube sample from BH-14 at 0' at Riverside Site
E125TO	6/27/72	Tube sample from BH-14 at 3.9' at Riverside Site
E126TO	6/27/72	Tube sample from BH-14 at 6.1' at Riverside Site
E127TO	6/27/72	Tube sample from BH-14 at 8.6' at Riverside Site
E128TO	6/27/72	Tube sample from BH-14 at 9.6' at Riverside Site
E129TO	6/27/72	Tube sample from BH-15 at 0' at Riverside Site
E130TO	6/27/72	Tube sample from BH-15 at 3.1' at Riverside Site
E131TO	6/27/72	Tube sample from BH-15 at 5.7' at Riverside Site
E132TO	6/27/72	Tube sample from BH-15 at 7.8' at Riverside Site
E133TO	6/27/72	Tube sample from BH-15 at 9.3' at Riverside Site
E134TO	6/28/72	Tube sample from BH-16 at 0' at Riverside Site
E135TO	6/28/72	Tube sample from BH-16 at 3.1' at Riverside Site
E136TO	6/28/72	Tube sample from BH-16 at 3.9' at Riverside Site
E137TO	6/28/72	Tube sample from BH-16 at 7.8' at Riverside Site
E138TO	6/28/72	Tube sample from BH-16 at 10.1' at Riverside Site
E139TO	6/28/72	Tube sample from BH-16 at 11.4' at Riverside Site
E140TO	6/28/72	Tube sample from BH-17 at 0' at Riverside Site
E141TO	6/28/72	Tube sample from BH-17 at 3.9' at Riverside Site

Table 3-6 (cont.)

Summary of "E" Samples

Sample Number	Date Obtained	Brief Description
E142TO	6/28/72	Tube sample from BH-17 at 5.9' at Riverside Site
E143TO	6/28/72	Tube sample from BH-17 at 8.1' at Riverside Site
E144TO	6/28/72	Tube sample from BH-17 at 10.3' at Riverside Site
E145TO	6/28/72	Tube sample from BH-17 at 11.9' at Riverside Site
E146TO	6/28/72	Tube sample from BH-18 at 0' at Riverside Site
E147TO	6/28/72	Tube sample from BH-18 at 3.7' at Riverside Site
E148TO	6/28/72	Tube sample from BH-18 at 5.3' at Riverside Site
E149TO	6/28/72	Tube sample from BH-18 at 6.3' at Riverside Site
E150TO	6/28/72	Tube sample from BH-18 at 8.7' at Riverside Site
E151TO	6/28/72	Tube sample from BH-18 at 10.8' at Riverside Site
E152TO	6/28/72	Tube sample from BH-19 at 0' at Riverside Site

obtained, the dates on which they were taken, brief sample descriptions, and the type of sampling equipment and method used; the general locations from which the samples were taken are given in Figures 3-5 through 3-18. Although it is impossible to show exact locations for all samples, the location of each sample can be adequately found by reference to the maps in Figures 3-5 through 3-18. Samples taken from the hoppers of dredges are suitably described in Tables 3-2 to 3-6, and Samples A13 to A18, C10 to C18, and D8 to D10 may be located in Figure 3-13 by reference to the coordinate system used by the Corps of Engineers to set stations along the shipping channel in the Maumee River. The various samples were taken at the stations indicated either at the center of the channel or near the north or south edge of the channel, as indicated in the description of the sample location by the suffix of C, N, or S, respectively. The prefix E or V indicates that the sample was taken either by an Ekman dredge or a flap valve sampler, respectively. For example, sample C17T0 was taken from the south edge of the channel at Station 40, by using the Ekman dredge, and this location is denoted as Field Station E40S.

At Riverside Site in Toledo, Ohio, the 5-inch piston sampler was used at BH-13 while the 3-inch piston sampler was used for BH-1 through BH-12 and BH-14 through BH-19. Samples E81 through E93 (block samples) were taken from the immediate vicinity of BH-1 through BH-9. Samples E115 through E152 were taken from BH-10, BH-11, and BH-14 through BH-19, with BH-10, BH-12, and BH-13 being in the immediate vicinity of each other and with BH-11 near BH-1, BH-14 near BH-4, etc., as shown in Figure 3-14.

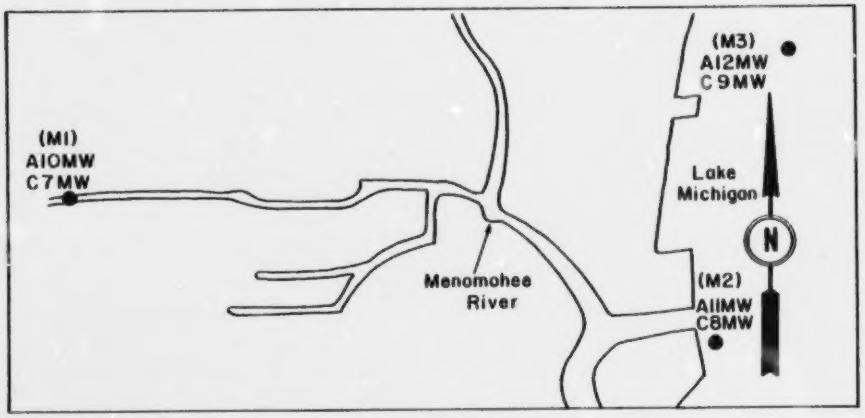
(M1)
A10MW
C7MW
Menomohee
River
Lake
Michigan
(M3)
A12MW
C9MW
(M2)
A11MW
C8MW
N

Figure 3-5. Milwaukee Harbor Area

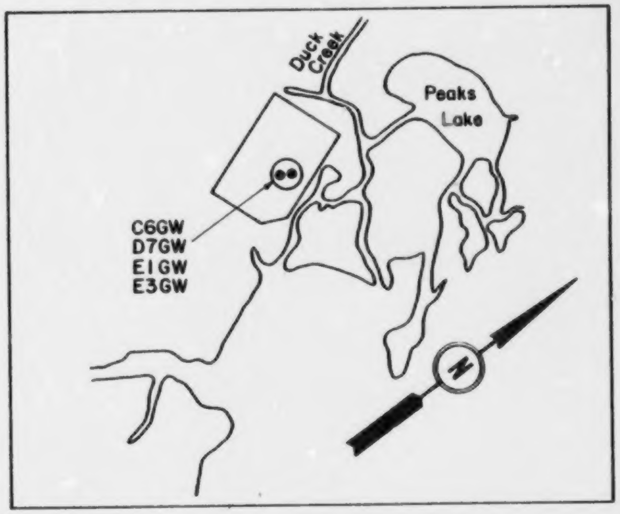
Duck
Creek
Peaks
Lake
C6GW
D7GW
E1GW
E3GW
N

Figure 3-6. Green Bay Disposal Area

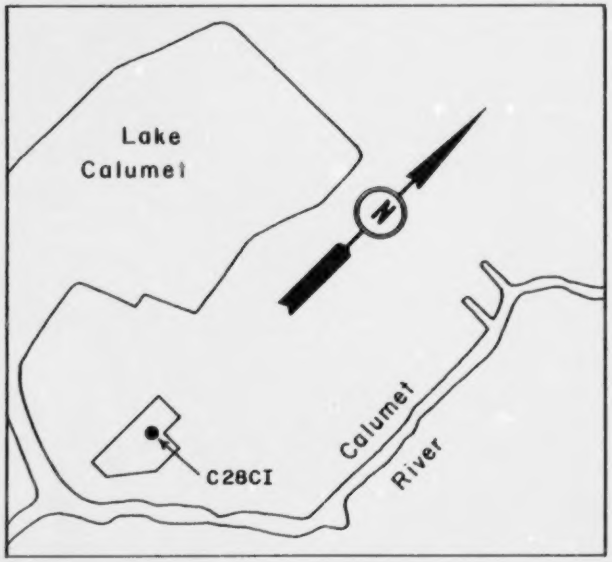
Lake
Calumet
N
C28CI
Calumet
River

Figure 3-7. Calumet Disposal Area

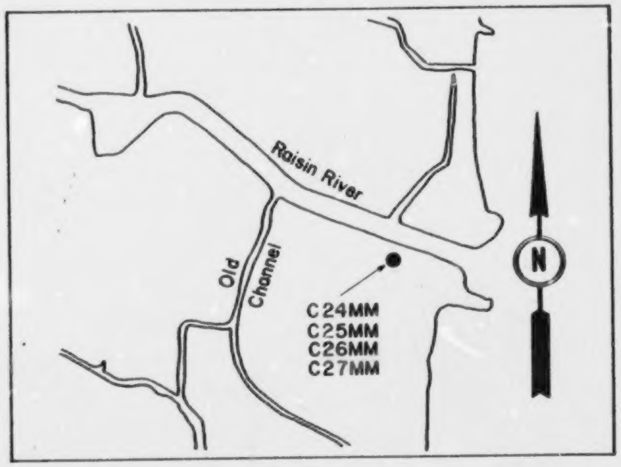
Raisin River
Old
Channel
C24MM
C25MM
C26MM
C27MM
N

Figure 3-8. Monroe Disposal Area

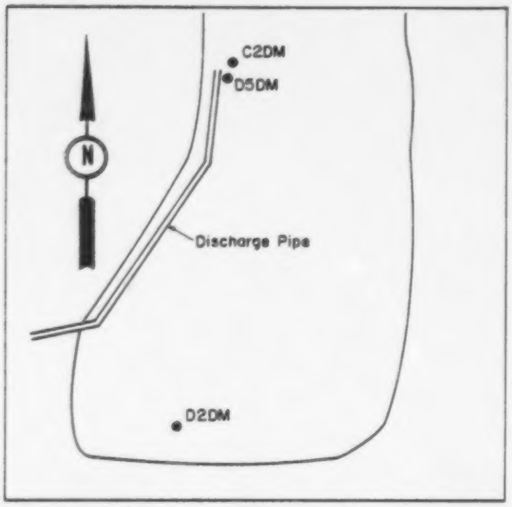
C2DM
D5DM
N
Discharge Pipe
D2DM

Figure 3-9. Grassy Island Disposal Area

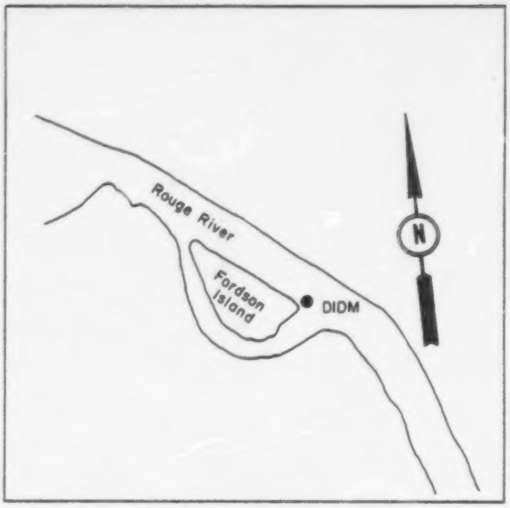
Rouge River
Fordson Island
D1DM
N

Figure 3-10. Fordson Island Disposal Area

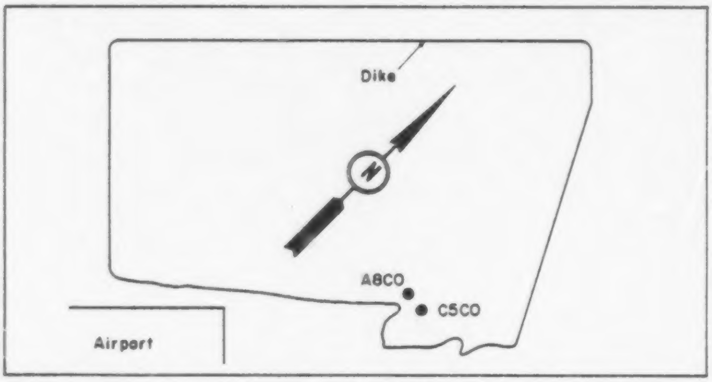
Dike
N
A8CO
C5CO
Airport

Figure 3-11. Cleveland Harbor Disposal Area

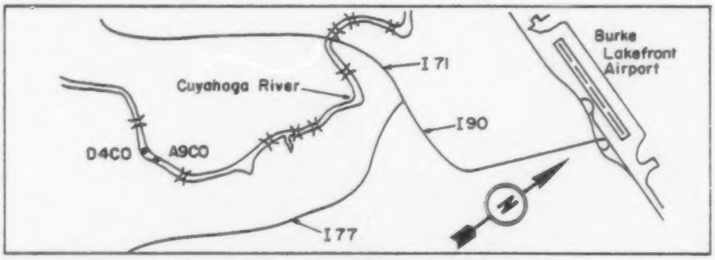
Burke Lakefront Airport
I 71
Cuyahoga River
I90
D4CO
A9CO
N
I77

Figure 3-12. Cuyahoga River Disposal Area

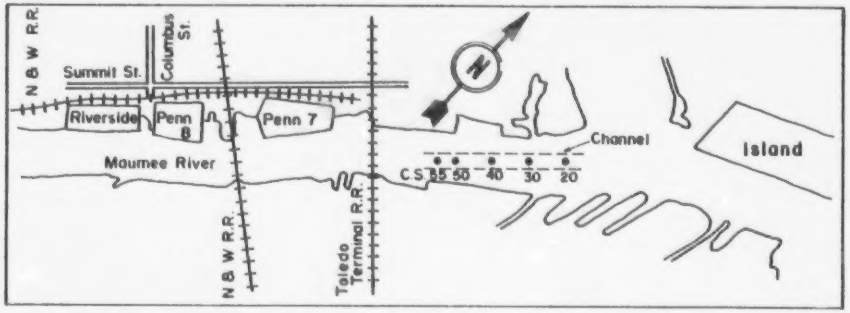
N & W R.R.
Summit St.
Columbus St.
Riverside
Penn 8
Penn 7
Maumee River
N & W R.R.
Toledo Terminal R.R.
N
C.S. 55 50 40 30 20
Channel
Island

Figure 3-13. Locations of Toledo Disposal Areas

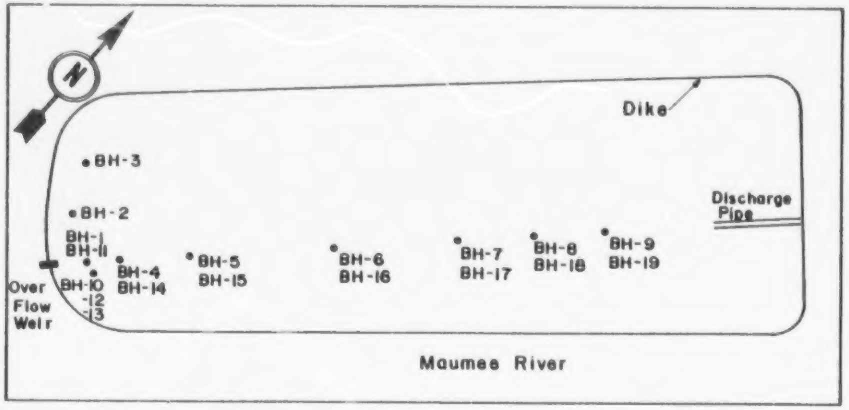
N
Dike
BH-3
BH-2
BH-1
BH-11
BH-10
-12
-13
BH-4
BH-14
BH-5
BH-15
BH-6
BH-16
BH-7
BH-17
BH-8
BH-18
BH-9
BH-19
Discharge Pipe
Over Flow Weir
Maumee River

Figure 3-14. Riverside Disposal Area

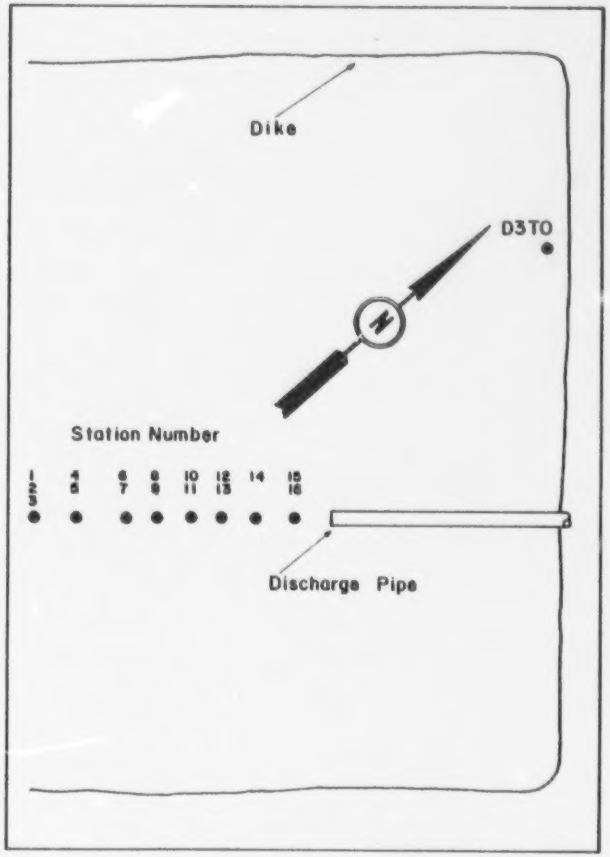
Dike
D3TO
N
Station Number
1 2 3
4 5
6 7
8 9
10 11
12 13
14
15 16
Discharge Pipe

Figure 3-15. Vicinity of Discharge Pipe at Riverside Site

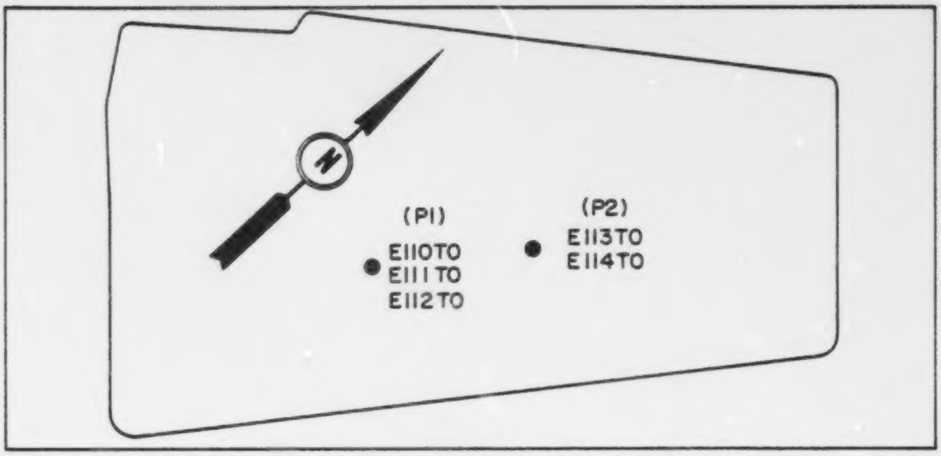
N
(P1)
E110TO
E111TO
E112TO
(P2)
E113TO
E114TO

Figure 3-16. Penn 7 Disposal Area

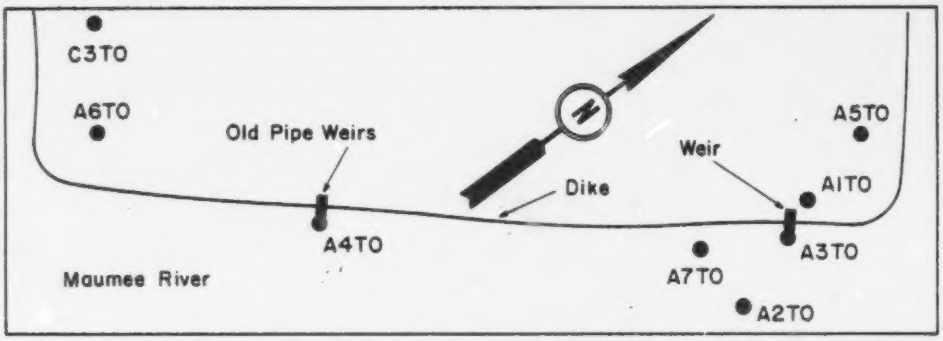
C3TO
A6TO
Old Pipe Weirs
N
A5TO
Weir
A1TO
Dike
A4TO
A3TO
A7TO
Maumee River
A2TO

Figure 3-17. Penn 8 Disposal Area

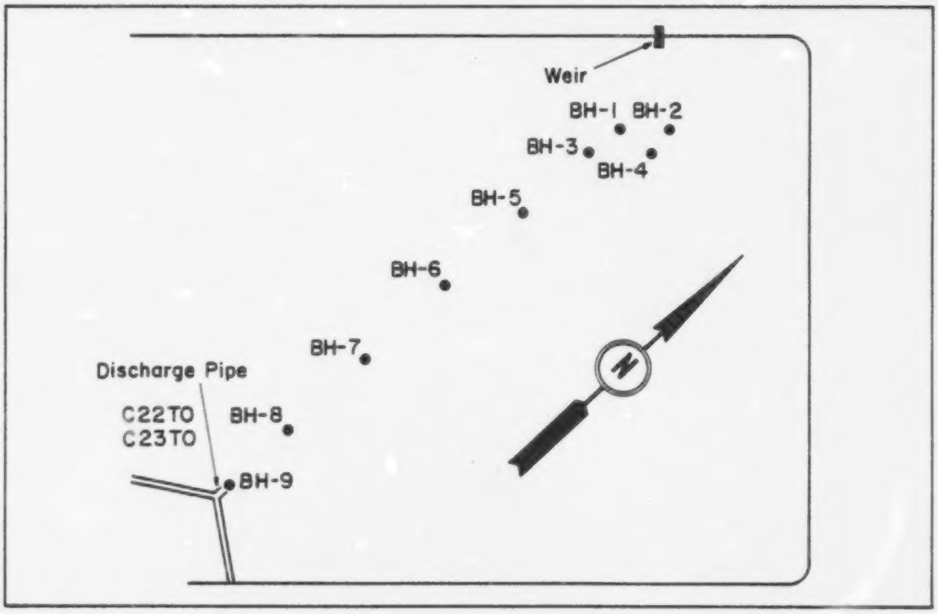
Weir
BH-1
BH-2
BH-3
BH-4
BH-5
BH-6
BH-7
N
Discharge Pipe
C22TO
C23TO
BH-8
BH-9

Figure 3-18. Island Disposal Area

STORAGE AND HANDLING

On the initial major sampling expedition in December of 1970 to Detroit, Toledo, and Cleveland, the cold winter temperatures kept the samples cool during sampling and transportation. Upon arrival at Northwestern University, the samples were placed in a large (10 feet by 10 feet by 10 feet) cold storage room, and temperatures were maintained between $2^{o}C$ and $4^{o}C$. For convenience in later obtaining small representative samples for testing, large samples were thoroughly mixed, and a portion was placed into one-gallon plastic bottles.

On the next major sampling trip, the major effort was directed toward obtaining samples from the Island Site at Toledo, Ohio. The samples accumulated during the first two days were taken to Northwestern University by car, and the remainder were shipped by truck at the end of the sampling expedition. The Osterberg tube samples were immediately sealed at Toledo with wax on the ends as a moisture seal; these samples were then stored in a humid room, whereas all other samples were stored in the cold room.

On the third major sampling trip, samples were obtained from Riverside Site, the shipping channel to be dredged, and the hopper of the dredge; some of these samples were tested on the site for parameters that are time sensitive; other samples were iced and promptly returned by car to Northwestern University for additional testing.

CONCLUSIONS

As a result of the experience gained during the sampling operations described, the following conclusions and recommendations are advanced:

1. Soft fill materials can be adequately sampled with hand-operated piston samplers, thereby obviating the need for expensive supporting platforms to accommodate heavy truck-mounted equipment; however, additional modifications to the 3-inch piston sampler should improve the quantity and quality of the sample recovered.

2. The Ekman dredge and the flap valve sediment sampler enabled soft harbor sediments to be recovered successfully with a reasonable amount of effort; however, additional research and development should be directed toward obtaining more representative samples of dredgings from the discharge pipe and from the hopper of the dredge.

3. Newly placed fine-grained materials with very high water contents can be readily sampled with the flap valve sampler; furthermore, a variation of this sampler could be designed and built to allow the sampling of high water content materials at specific depths in a fill.

CHAPTER 4

CHEMICAL ANALYSES

Chemical and biological tests were conducted on numerous samples of water, fluid-like dredgings, soft bottom sediments, and firm fill materials from several locations in the vicinity of the Great Lakes. The principal purpose of these tests was to determine the concentrations of various chemical constituents which are present in maintenance dredgings. These data will be used (a) to evaluate the pollution potential of such materials, (b) to assess the variability in the measured parameters for different locations, (c) to aid in interpreting the engineering behavior of associated landfills, and (d) to provide a basis for selecting appropriate additives to improve the engineering properties of these materials. Some consideration was given to the distribution of the pollutants throughout the dredging cycle, but only general comparisons of this nature are possible due to restrictions in the sampling procedures.

SCOPE OF TEST PROGRAM

Rather complete tests were conducted at Northwestern University on 21 water samples (A and B materials), 22 samples of slurry (C material), 6 mud-like samples (D material), and 26 samples of firm soil from various landfills (E material). In addition, tests were made on the fluids discharged by electro-osmosis (22 samples), gravity and vacuum drainage (9 samples), and slurry consolidation (25 samples). Supplemental tests were conducted at the University of Wisconsin-Milwaukee, in the field at

Toledo, Ohio, and by the EPA laboratory in Chicago, Illinois. The quantitative tests conducted at Northwestern University included:

(a) Metals: aluminum, arsenic, cadmium, calcium, copper, soluble and total iron, lead, mercury, potassium, and sodium.

(b) Inorganics: ammonia-nitrogen, nitrite-nitrogen, nitrate-nitrogen, soluble and total phosphate, sulfide, and cyanide.

(c) Organics: organic nitrogen, hydrocarbon, oil and grease, and phenols.

(d) Biological Tests: chemical oxygen demand, biological oxygen demand, and dissolved oxygen.

(e) Other: hydrogen ion concentration, oxidation-reduction potential, turbidity, acidity, volatile solids, suspended solids, volatile suspended solids, and total solids.

TESTING METHODS

The testing procedures used in this work are generally those outlined in the Thirteenth Edition (1971) of Standard Methods for the Examination of Water and Wastewater for the more fluid materials and Chemistry Laboratory Manual for Bottom Sediments (December 1969) for the more viscous and stiffer materials. However, due to the high concentration of interfering compounds in certain cases, modifications of the standard test had to be made, and these are described below.

Total Solids, Total Volatile Solids, and Silica

A sample of bottom sediment was dried at $100^{\circ}C$ in a preweighed crucible, and the weight of the remaining solid is a measure of the total solids; this may be expressed as

$$\text{Total Solids } (\%) = \frac{W_{DS} - W_C}{W_S - W_C} \times 100 \qquad (4\text{-}1)$$

where W_C, W_S, and W_{DS} are the respective weights of the crucible alone, the crucible with the sample before drying, and the crucible with the sample after drying. The dried sample was then ignited at 600°C for one hour, and the loss in weight is a measure of the total volatile solids; this may be written as

$$\text{Total Volatile Solids (\%)} = \frac{W_I - W_{DS}}{W_S - W_C} \times 100 \qquad (4\text{-}2)$$

where W_I is the weight of the crucible with the sample after ignition. The ignited sample was digested for one-half hour at 100°C in concentrated hydrochloric acid and concentrated nitric acid (10:1); then, it was filtered into a preweighed gooch crucible, and the filtrate was used for total phosphate and metal analyses. After drying at 600°C for one hour, the weight of the remaining solid is a measure of the silica content in the original sample; the percent silica may be determined from the relationship

$$\text{Silica (\%)} = \frac{W_{DS} - W_G}{W_{TS}} \times 100 \qquad (4\text{-}3)$$

where W_G, W_{DS}, and W_{TS} are the respective weights of the gooch crucible alone, the gooch crucible with the sample after drying, and the total solids.

Total Phosphate

The filtrate from the silica determination was treated with ammonium molybdate reagent and stannous chloride and measured photometrically at a wavelength of 690 millimicrons, according to the procedure outlined in Standard Methods. This method was reliable for waters containing sewage, sludge effluents, and detergents, and complete recovery of the organophospholypids could be attained.

Metals

The filtrate from the silica test was also used to determine by atomic absorption on a Jarrell-Ash Atomic Absorption Spectrophotometer (Model 82-500) the concentrations of aluminum, cadmium, calcium, copper, total iron, lead, potassium, and sodium. In the calcium determination, a lanthanum chloride-ethylene diamine tetraacetic acid (EDTA) solution was added to prevent interferences from phosphates, sulfates, and aluminum.

Mercury and arsenic could not be determined by the above method, because these metals are lost during ignition in the total volatile solids determination. The normal procedure of treating the sample with strong oxidizing agents over a sand bath was found to be too time-consuming. With mercury, it was found that the sample could be digested at 121°C for one-half hour with concentrated nitric acid in a pressure bottle and reduced to the ground state with stannous chloride. The mercury was then vaporized with nitrogen gas as a carrier into the atomic absorption spectrophotometer. Similarly, with arsenic, the sample was digested at 121°C for one-half hour with a solution of potassium permanganate-sulfuric acid in a pressure bottle, filtered, diluted, and determined by atomic absorption spectrophotometry.

To determine the concentration of soluble iron, the sample of bottom sediment was mixed in boiling water and cooled to room temperature with nitrogen. This was then filtered by bubbling nitrogen through it into a 100 ml volumetric flask, and the iron in the filtrate was determined by atomic absorption. With all the precautions taken to avoid air, a precipitate still formed with the deeper bottom sediments. This precipitate was formed by the oxidation of soluble ferrous ions to insoluble ferric ions. For the E-series the soluble iron was taken to be the sum of the ferrous iron and the iron that precipitated.

Ammonia Nitrogen and Total Organic Nitrogen

For ammonia nitrogen, after the sample was made basic, the ammonia was distilled into a boric acid solution, titrated with 0.20N hydrochloric acid or dilute solutions, and measured photometrically with Nesslar's reagent according to the procedure described in Standard Methods.

The total nitrogen was determined by the Federal Water Pollution Control Administration (FWPCA) method. The residue from the ammonia distillation, together with a potassium sulfate-mercuric sulfate-sulfuric acid solution, was heated to a high temperature, diluted with water, and made alkaline with a sodium hydroxide-sodium thiosulfate solution. Then, as in the ammonia nitrogen determination, the ammonia was distilled into a boric acid solution, titrated with 0.20N hydrochloric acid or dilute solutions, and measured photometrically with Nesslar's reagent.

Nitrite Nitrogen

The nitrite nitrogen was determined according to the procedure outlined in Standard Methods, whereby nitrites react with sulfanilic acid to form diazotized sulfanilic acid, which couples with naphthylamine hydrochloride to a reddish-purple azo dye which can be measured photometrically at a wavelength of 520 millimicrons.

Nitrate Nitrogen

Of the procedures described in Standard Methods, the zinc reduction method did not work at all, and the cadmium amalgam reduction, although sensitive, was quite lengthy and space consuming. After considerable study, the technique of West and Lyles (1960) was found to be the easiest and most effective. In this method, chromotropic acid dissolved in concentrated sulfuric acid was added to 0.2 to 1.0 ppm of nitrate contained in the sample and diluted to 10 cc; not more than 3 percent water should be present. This was then compared to a standard curve, and the yellow color was read photometrically at a wavelength of 420 millimicrons.

Sulfide

The sulfide content was determined according to the Standard Methods-Titrimetric Method, whereby a sample is treated with sulfuric acid and the resulting hydrogen sulfide is carried over with carbon dioxide into a second flask containing a zinc acetate solution. The zinc acetate-hydrogen sulfide solution is then reacted with an excess of standard 0.025N iodine solution and back titrated with standard 0.025N sodium thiosulfate solution.

Oil and Grease and Hydrocarbons

The oil and grease content was determined according to the procedure described in Standard Methods, whereby the sample is acidified with hydrochloric acid, dried to a powder with anhydrous magnesium sulfate, and extracted with hexane in a Soxhlet extractor. The oil and grease was recovered by evaporating the hexane, and the hydrocarbon content was determined by chromatography on alumina.

Phenols

The phenolic content of the sample was determined according to the technique outlined in Standard Methods, whereby the sample was acidified, the phenols steam distilled, and the distillate reacted with aminoantipyrine to give a dye which was measured photometrically at a wavelength of 460 millimicrons.

Chemical Oxygen Demand

A suitable aliquot, predetermined from total volatile solids, was refluxed for two hours in a concentrated sulfuric acid-potassium permanganate solution. This was then titrated with standard ferrous ammonium sulfate, and the difference between a blank and this mixture was used to calculate the chemical oxygen demand.

Biological Oxygen Demand

Exceptionally pure ion exchange treated water was used for the dilution water. In addition, a small amount of sample was aerated overnight with the sewage to be used for seeding in order to acclimate the bacteria. It was hoped that these extra precautions would give a representative biological oxygen demand in a substance as diverse as these bottom sediments and containing so many metals, which could be toxic to the bacteria. Two different dilutions and two samples from each dilution were made for each sample tested, and the standard sodium thiosulfate was checked before each set of titrations.

Hydrogen Ion Concentration and Oxidation-Reduction Potential

The hydrogen ion concentration, pH, was measured by means of a Beckman pH meter on the regular scale. Oxidation-reduction potential, Eh, was measured by use of the same instrument on the expandomatic scale with a platinum electrode.

Turbidity

Turbidity readings were taken on a Hach turbidimeter and read in JTU units.

TEST RESULTS

The test results from the chemical and biological testing programs conducted at Northwestern University, at the University of Wisconsin-Milwaukee, in the field at Toledo, Ohio, and in the EPA laboratories in

Chicago, Illinois, are presented in the following sections. Interpretation of the data on the fluids discharged from the test specimens are included with the discussions to which they are related.

Northwestern University Test Program

The results of the chemical and biological test program conducted at Northwestern University are summarized in Tables 4-1 through 4-5. Brief discussions of sample variations, precision of data, and units employed are given below to aid in interpreting these results.

Sample Variations.--It is well recognized that the constituents of harbor sediments vary considerably over the area of a harbor, as well as with depth at a specific location. Additional sampling problems arise in the laboratory when the small representative portions required for particular tests are taken from the large sample obtained in the field. Although extensive care was exercised to minimize any error associated with sampling procedures, there appears to be a need for improved techniques for sampling materials with varying degrees of consistency.

Precision of Data.--For any given test, the precision of the results depends on the procedure used, the concentration of the constituent investigated, and interferences from other compounds present. The precision of any particular test is generally stated in Standard Methods together with the testing procedure, and it varies from test to test. Due to many factors, it is considered that two significant figures can generally be reliably used for most test results. In Tables 4-1 through 4-5, an attempt was made to establish columns of data according to a consistent decimal format, and this procedure sometimes caused the number of significant figures to vary within that column.

Units Employed.--Insofar as possible, units were selected to maintain

Table 4-1

Chemical Analyses of "A" Samples

Sample	Total Solids	Total Volatile Solids	Total Suspended Solids	Total Volatile Suspended Solids	Turbidity	Acidity	Hydrogen Ion Concentration (pH)	Oxidation-Reduction Potential (Eh)	Dissolved Oxygen (DO)	Biological Oxygen Demand (BOD)	Chemical Oxygen Demand (COD)	Organic Nitrogen (N)	Ammonia (NH_3) Nitrogen (N)	Nitrite (NO_2) Nitrogen (N)	Nitrate (NO_3) Nitrogen (N)	Total Phosphate (PO_4)	Soluble Phosphate (PO_4)
	%	%	%	%	JTU	mg/gm		mv	mg/gm	mg/gm	mg/gm	mg/gm	mg/gm	mg/gm	mg/gm	mg/gm	mg/gm
A6	0.0620	34.24	0.03	0	0.65	324	7.4		13.6	7.1			0.04	1.23	24.67	2.32	0.39
A8	0.0909	9.40	0.34	0	1.10	125	7.3		0.2	18.7			10.78	2.02	33.12	3.30	0.18
A9	0.0583	20.98	0.46	0	0.79	129	7.2		14.3	34.8			0.07	1.27	7.50	10.38	1.03
A10	0.0934	10.88	3.36	1.50	4.3	209	7.4		8.3		17.5	3.64	0.60	0	0.02	2.36	0.99
A11	0.0353	23.04	3.54	2.55	3.4	413	7.5		28.0		34.8	6.79	0.68	0.04	0.34	2.41	1.47
A12	0.0144	21.21	10.57	5.04	4.0	821	7.9		84.4		0	5.22	0	0.03	0	4.52	2.78
A13	0.0432	37.87	5.49	1.22	18.0	273	7.6		30.3		79.1	3.36		0.90	5.93	3.12	1.06
A14	0.0450	36.89	5.11	1.06	19.0	300	7.8		24.9			3.36		0.70	8.29	1.78	1.07
A15	0.0419	15.99	7.64	2.15	22.0	318	7.7				66.3					4.65	
A16	0.0402	35.32	4.73	1.62	15.0	341	7.6		31.8		53.0	3.92	0.70	1.22	10.02	3.11	1.19
A17	0.0431	39.44	3.36	0.81	13.0		7.6				29.7		0.97			4.52	1.16
A18	0.0438	34.25	5.96	1.37	20.0	311	7.8		28.1		45.5	3.71	0.09	0.84	6.92	3.42	0.01
A19	0.0433	32.22	14.09	3.28	27.0	307	9.3		25.8		0.9	2.84	1.94	1.32	0	3.46	2.24
A20	0.0420	28.96	12.63	3.81	34.0	311	10.2		30.5		1.2	3.03	0	1.32	0	2.14	3.22
A21	0.0402	30.74	9.83	4.23	24.0	324	8.9		28.1		0.7	3.90	0	1.49	0	3.73	2.86
A22	0.0390	28.68	6.42	2.18	19.0	336	9.0		27.7		0.3	3.42	0	1.42	0	3.34	2.95

Sample	Grease	Hydrocarbons	Aluminum (Al)	Arsenic (As)	Calcium (Ca)	Copper (Cu)	Total Iron (Fe)	Soluble Iron (Fe)	Potassium (K)	Silica (SiO_2)	Sodium (Na)	Sulfide (S)	Cadmium (Cd)	Cyanide (CN)	Lead (Pb)	Mercury (Hg)	Phenolics
	mg/gm	mg/gm	mg/gm	mg/gm	mg/gm	mg/gm	mg/gm	mg/gm	mg/gm	mg/gm	mg/gm	mg/gm	µg/gm	µg/gm	µg/gm	µg/gm	µg/gm
A6			0	0	144	0	0.40		25.8		53.2		0		855	0.002	
A8			0	0	73	0	0		11.0		46.7		0		583	0.001	
A9			0	0	129	0	0.86		30.0		128.6		0		909	0.008	
A10			0		11	26.77	4.07	0.03	3.2		11.5		0		0	0.003	0
A11			0		29	104.73	3.20	0.07	7.6		56.6		0		0	0.013	0
A12			0		70	312.94	15.30	0	11.6		34.7		0		0	0.013	0
A13			0		238	3.70	8.80	0	12.5	0	41.7		0	0	[illegible]	0.001	3.7
A14			0		236	2.89	8.44	0	11.8	0	40.0		0	0	0	0.002	2.2
A15			0		263	2.15	8.12	0	14.6	0	52.5		0		0	0.001	
A16			0		274	3.23	17.41	0	14.2	0	54.7		0	0	0	0.001	4.0
A17			0		232	3.02	17.17	0	10.7	0	51.0		0		0	0.001	
A18			0		242	1.00	11.87	0	11.2	0	45.7		0	0	0	0.002	5.7
A19			11.55		370	0.51	12.01	1.16	11.1	0	76.2		0		0	0	0
A20			7.15		417	0.52	8.82	1.19	10.7	0	48.9		0	0	0	0.003	0
A21			0		448	0.82	3.73	1.24	11.7	0	57.3		0		0	0.002	62.2
A22			0		411	0.50	3.34	1.28	12.1	0	57.8		0		0	0.011	0

Table 4-2

Chemical Analyses of "B" Samples

Sample	Total Solids	Total Volatile Solids	Total Suspended Solids	Total Volatile Suspended Solids	Turbidity	Acidity	Hydrogen Ion Concentration (pH)	Oxidation-Reduction Potential (Eh)	Dissolved Oxygen (DO)	Biological Oxygen Demand (BOD)	Chemical Oxygen Demand (COD)	Organic Nitrogen (N)	Ammonia (NH_3) Nitrogen (N)	Nitrite (NO_2) Nitrogen (N)	Nitrate (NO_3) Nitrogen (N)	Total Phosphate (PO_4)	Soluble Phosphate (PO_4)
	%	%	%	%	JTU	mg/gm		mv	mg/gm	mg/gm	mg/gm	mg/gm	mg/gm	mg/gm	mg/gm	mg/gm	mg/gm
B5	3.76	10.15					7.3				206.0	1.06	1.64			0.067	
B6	11.93	11.77					7.0				206.0	0.05	1.45			0.132	
B7	6.26	12.18					7.1				431.0	0.17	1.79			0.133	
B8	0.767	1.6	8.9	0.93		35.2	8.8				2.6	0.3	2.65			0.65	0.06
B9	0.070	17.7	51.9	3.90	250	198.8	8.9		15.7		0.6	1.8	3.56	0.53	0	1.63	1.00

Sample	Grease	Hydrocarbons	Aluminum (Al)	Arsenic (As)	Calcium (Ca)	Copper (Cu)	Total Iron (Fe)	Soluble Iron (Fe)	Potassium (K)	Silica (SiO_2)	Sodium (Na)	Sulfide (S)	Cadmium (Cd)	Cyanide (CN)	Lead (Pb)	Mercury (Hg)	Phenolics
	mg/gm	mg/gm	mg/gm	mg/gm	mg/gm	mg/gm	mg/gm	mg/gm	mg/gm	mg/gm	mg/gm	mg/gm	µg/gm	µg/gm	µg/gm	µg/gm	µg/gm
B5	1.02	0.368	2.27		337.0	0.17	161.20		5.0	686	0.84	480	12.6	9.85	1340		
B6	0.21	0.070	16.09		380.0	0.11	31.51		4.6	825	0.66	594	16.0	8.13	106		
B7	5.71	2.300	17.90		625.0	0.11	196.00		4.5	646	1.01		14.9	18.55	161		4.16
B8			30.00		96.5	0.08	45.8	0.30	3.5	600	8.08		0		0		0
B9			23.00		186.5	0.60	14.3	7.17	11.5	340	28.00		0		0	2.65	0.71

Table 4-3

Chemical Analyses of "C" Samples

Sample	Total Solids	Total Volatile Solids	Total Suspended Solids	Total Volatile Suspended Solids	Turbidity	Acidity	Hydrogen Ion Concentration (pH)	Oxidation-Reduction Potential (Eh)	Dissolved Oxygen (DO)	Biological Oxygen Demand (BOD)	Chemical Oxygen Demand (COD)	Organic Nitrogen (N)	Ammonia (NH_3) Nitrogen (N)	Nitrite (NO_2) Nitrogen (N)	Nitrate (NO_3) Nitrogen (N)	Total Phosphate (PO_4)	Soluble Phosphate (PO_4)
	%	%	%	%	JTU	mg/gm		mv	mg/gm	mg/gm	mg/gm	mg/gm	mg/gm	mg/gm	mg/gm	mg/gm	mg/gm
C5	25.23	11.13															
C7	0:29	11.31								301.6		2.37	5.12			81.49	
C8	4.18	24.08								48.9		0.33	1.19			28.13	
C9	1.94	9.29								27.1	72.2	1.97	0.27			8.19	
C10	18.10	14.61									184.5	5.25	1.44			6.54	
C11	14.51	14.44									116.4	3.36	1.67			13.86	
C12	20.24	12.12									180.8	3.46	1.23			11.62	
C13	18.79	10.56									67.4	1.77	0.40			8.37	
C14	14.23	17.34									97.0	3.17	0.47			7.69	
C15	18.07	10.08									85.8	2.33				7.03	
C16	28.61	10.71									105.2	3.71	0.37			7.82	
C17	12.04	10.61									79.8	4.10	0.84			9.71	
C18	20.00	9.72									94.5	3.18	0.49			6.38	
C19	20.83	9.39									86.5	3.38	0.85			6.97	
C20	25.67	10.21									88.0	4.00	0.59			14.19	
C21	19.10	10.32									141.4	3.18	0.52			8.19	
C22	17.33	9.03									116.0	4.10	0.94			6.42	
C23	60.65	6.55															
C24	13.77	13.26															
C25	3.91	4.37															
C26	13.07	14.16															
C27	12.38	12.63															

Sample	Grease	Hydrocarbons	Aluminum (Al)	Arsenic (As)	Calcium (Ca)	Copper (Cu)	Total Iron (Fe)	Soluble Iron (Fe)	Potassium (K)	Silica (SiO_2)	Sodium (Na)	Sulfide (S)	Cadmium (Cd)	Cyanide (CN)	Lead (Pb)	Mercury (Hg)	Phenolics
	mg/gm	mg/gm	mg/gm	mg/gm	mg/gm	mg/gm	mg/gm	mg/gm	mg/gm	mg/gm	mg/gm	mg/gm	μg/gm	μg/gm	μg/gm	μg/gm	μg/gm
C5			18.46		0.77	0.231	0.36		3.33	560.9	0.81		26.3		72		
C7	169.90		2.12		131.10	1.380	47.57		8.13	226.1	147.13		0	11.69	1613		
C8	11.40		12.23		43.59	0.781	44.24		1.57	351.1	10.66		0	5.97	428		
C9	25.00		14.22		62.18	0.485	23.91		4.03	237.7	13.34		77.4		191		
C10			14.61		19.72	0.155	29.44		3.77	634.4	0.53		9.7	11.82	144		
C11			19.34		23.88	1.061	29.97		4.28	634.3	0.62		10.2	4.06	150		
C12			18.62		15.44	0.850	28.51		4.99	661.4	0.60		10.7	3.26	161		
C13			18.88			0.639	26.45		4.52	677.3	0.63		8.6	1.12	101		
C14			17.30		21.47	0.058	25.98		4.39	682.9	6.76		9.6		145		
C15			17.85		32.79	0.053	26.12		5.11	685.5	0.65		6.1	1.11	81		
C16	4.26	1.36	16.09		21.09	0.049	25.45		4.61	689.0	0.47	63.4	5.3	3.84	84		
C17	0.83	0.24	18.86		29.09	0.068	27.85		4.95	673.6	0.62	240.3	7.3	3.41	129		
C18	4.42		17.82		22.31	0.064	30.57		4.83	693.5	0.58	19.6	3.6	0.95	99		
C19	1.17	0.44	16.89		26.13	0.052	28.08		5.06	687.1	0.50	54.8	7.0	2.30	87		
C20	11.90	6.81	16.77		24.13	0.042	31.83		5.03	521.4	0.53	14.6	9.7	2.82	105		
C21	1.36	0.84	15.88		23.09	0.061	29.63		5.44	679.9	0.50	92.8	9.1	5.76	102		
C22	11.48	5.71	16.28		28.99	0.051	30.94		5.34	686.7	0.55	28.1	9.0	1.15	73		
C23			8.82		0.78	0.039	22.94		1.29	803.1	3.46		16.6		89		
C24	5.30	2.86	18.23		36.98	0.356	15.84			624.5		294.2	0	5.32	178		
C25	11.10	6.39				0.677				844.7		191.6	0	10.98	161		
C26	9.16	4.94	19.63		35.50	0.384	15.84			612.4		316.0	0	7.50	181		
C27			24.15			0.443	19.47			597.0			0		181		

Table 4-4

Chemical Analyses of "D" Samples

Sample	Total Solids	Total Volatile Solids	Total Suspended Solids	Total Volatile Suspended Solids	Turbidity	Acidity	Hydrogen Ion Concentration (pH)	Oxidation-Reduction Potential (Eh)	Dissolved Oxygen (DO)	Biological Oxygen Demand (BOD)	Chemical Oxygen Demand (COD)	Organic Nitrogen (N)	Ammonia (NH_3) Nitrogen (N)	Nitrite (NO_2) Nitrogen (N)	Nitrate (NO_3) Nitrogen (N)	Total Phosphate (PO_4)	Soluble Phosphate (PO_4)
	%	%	%	%	JTU	mg/gm		mv	mg/gm	mg/gm	mg/gm	mg/gm	mg/gm	mg/gm	mg/gm	mg/gm	mg/gm
D1	51.91	12.16		13.27													
D3	43.43	6.96		6.76													
D4	47.22	10.53		8.96													
D8	40.21	9.33										0.70	0.82			0.054	
D9	37.81	8.81										0.68	0.68			0.032	
D10	38.68	8.91										0.41	0.70			0.047	

Sample	Grease	Hydrocarbons	Aluminum (Al)	Arsenic (As)	Calcium (Ca)	Copper (Cu)	Total Iron (Fe)	Soluble Iron (Fe)	Potassium (K)	Silica (SiO_2)	Sodium (Na)	Sulfide (S)	Cadmium (Cd)	Cyanide (CN)	Lead (Pb)	Mercury (Hg)	Phenolics
	mg/gm	mg/gm	mg/gm	mg/gm	mg/gm	mg/gm	mg/gm	mg/gm	mg/gm	mg/gm	mg/gm	mg/gm	µg/gm	µg/gm	µg/gm	µg/gm	µg/gm
D1	36.40		4.01			0.106	0.52		0.38	502.9	0.73		9.0		61	0.853	2.7
D3	2.12		8.56		0.14	0.003	0.34		0.65	498.9	5.69		6.7		50	0.423	
D4	29.00		7.91		0.11	0.195	0.79		0.71	503.8	1.31		32.7		115	1.378	
D8	14.80	12.2	12.80			0.037	18.10		3.65	743.0	0.38	63.9	5.2	1.14	68		
D9	6.61	3.7	10.44			0.033	20.20		4.26	746.4	0.44	43.4	5.3	1.47	70		
D10	5.42	6.1	10.24			0.038	22.25		3.63	743.3	0.41	34.1	5.0	0.78	89		

Reproduced from
best available copy.

Table 4-5

Chemical Analyses of "E" Samples

Sample	Total Solids	Total Volatile Solids	Total Suspended Solids	Total Volatile Suspended Solids	Turbidity	Acidity	Hydrogen Ion Concentration (pH)	Oxidation-Reduction Potential (Eh)	Dissolved Oxygen (DO)	Biological Oxygen Demand (BOD)	Chemical Oxygen Demand (COD)	Organic Nitrogen (N)	Ammonia (NH_3) Nitrogen (N)	Nitrite (NO_2) Nitrogen (N)	Nitrate (NO_3) Nitrogen (N)	Total Phosphate (PO_4)	Soluble Phosphate (PO_4)
	%	%	%	%	JTU	mg/gm		mv	mg/gm	mg/gm	mg/gm	mg/gm	mg/gm	mg/gm	mg/gm	mg/gm	mg/gm
E31	62.31	7.94									95.7	0	0	0.020	19.26	4.25	0.028
E33	56.48	6.16									100.9	244.1	360.2	0.009	33.40	3.70	0.038
E36	57.72	6.64									102.2		186.6			3.90	
E39	58.87	6.53									89.5	428.9	68.3	0.008	0	3.70	0.050
E40	65.82	9.89									117.8	120.6	0	0.008	0	6.00	0.053
E41	55.16	7.67									103.0	382.1	254.7	0.036	12.70	5.14	0.099
E43	58.17	6.92									69.6	49.4	145.7	0.009	0	3.86	0.060
E45	59.35	6.28									67.7	0	110.8	0.674	1.68	4.10	0.045
E48	65.22	8.78									122.8	235.9	0	0.019	44.54	5.86	0.036
E49	58.15	8.81									84.8	28.6	0	0.034	3.44	4.57	0.051
E52	53.49	7.81										23.2	99.8	0.834	5.56	5.20	0.159
E54	63.26	8.86										16.2	0	0.243	25.09	4.64	0.037
E55	64.90	7.50										81.3	0	0.238	4.62	3.62	0.022
E58	56.13	7.95										15.7	128.3			7.18	0.033
E60	69.19	8.41										108.1	0	0.286	2.51	7.68	0.028
E61	68.18	8.52										62.4	0	0.371	4.36	4.34	0.023
E63	72.31	8.56										27.2	75.5			5.11	
E65	64.47	9.14										56.5	0	0.464	0.37	7.97	0.024
E66	68.65	9.96										7.6	0	0.371	3.66	5.39	0.022
E68	64.16	8.07											116.0			5.41	
E69	55.91	10.56										12.3	383.1	0.797	5.31	5.70	0.066
E72	69.40	8.45										10.0	0	0.662	38.87	6.17	0.023
E73	72.09	8.38										46.8	0	0.620	27.52	4.61	0.021
E74	74.14	8.51										110.4	0	0.533	29.32	4.30	0.025
E75	70.02	8.28										71.5	95.4	0.364	28.22	2.98	0.031
E76	62.39	8.69										58.5	62.6	0.387	0.46	5.53	0.049

Sample	Grease	Hydrocarbons	Aluminum (Al)	Arsenic (As)	Calcium (Ca)	Copper (Cu)	Total Iron (Fe)	Soluble Iron (Fe)	Potassium (K)	Silica (SiO_2)	Sodium (Na)	Sulfide (S)	Cadmium (Cd)	Cyanide (CN)	Lead (Pb)	Mercury (Hg)	Phenolics
	mg/gm	mg/gm	mg/gm	mg/gm	mg/gm	mg/gm	mg/gm	mg/gm	mg/gm	mg/gm	mg/gm	mg/gm	µg/gm	µg/gm	µg/gm	µg/gm	µg/gm
E31	25.30	1.97	16.13	0	23.21	0.152	26.19	0.12	2.89	740.0	1.84	1.6	4.5		45	270	5.60
E33	0.46		13.79	0	25.69	0.194	23.86	0.26	2.62	697.5	1.28	57.5	2.5		41	370	0.20
E36	1.62	1.32	18.91	0	32.03	0.249	24.40		2.68	692.9	1.46	32.0	3.0		31	151	
E39	1.46		12.69	0	25.25	0.143	20.48	0.96	2.07	702.8	1.25	71.5	3.0		30	591	0.40
E40	2.42		20.36	0	20.38	0.270	31.25	0.37	3.06	676.4	1.60	1.8	5.7		44	213	0.40
E41	2.54	1.99	21.56	0	30.37	0.208	29.21	1.63	2.88	665.0	1.70	119.5	7.0		52	138	0.09
E43	3.52	1.02	15.16		22.82	0.076	21.07	0.26	2.62	691.3	2.54	3.6	2.1		31		0
E45	1.77	0.67	15.20	0	21.54	0.108	22.15	0.66	2.86	688.1	1.45	5.9	3.1	0	38	123	0.47
E48	5.07	1.16	21.72	0	14.89	0.202	29.85	0.24	3.78	669.9	1.96	0.9	5.6		65	147	0.48
E49	2.56	0.49	18.33	0	19.37	0.198	25.10	0.36	3.11	683.0	2.04	2.0	3.8		50	127	0.48
E52	3.34	0.75	17.45	0	19.59	0.142	24.91	2.40	3.19	668.6	1.99		4.0		40	163	1.14
E54	2.74	0.63	20.05	0	13.88	0.166	30.06	0.21	2.98	686.4	1.86	1.7	4.7		59	158	0.76
E55	2.62	2.07	13.77	0	9.78	0.139	17.07	0.03	2.16	607.8	0.43	1.2	2.1		33	106	0.15
E58	2.90	2.72	28.44		32.42	0.343	40.93		5.49	661.8	3.80	7.1	7.1		90		0
E60	2.38	2.29	27.96	0	35.59	0.386	40.96	0.18	5.22	633.5	2.72	0.6	6.0		71	306	
E61	1.93	1.72	19.62	0	19.15	0.175	27.48	0.14	3.12	678.6	1.94	6.4	3.0		51	197	0.40
E63	4.20	2.94	19.54	0	20.30	0.157	25.20		3.58	727.0	2.37		2.8		43	180	
E65	3.35	1.91	17.99	0	20.58	0.261	26.48	0.09	2.73	674.8	1.68	1.2	5.5		55	160	0.40
E66	1.66	1.27	18.72	0	15.40	0.214	22.94	0.11	2.78	567.3	1.96	0.6	3.7		45	133	0
E68	1.08	10.93	18.49	0	23.96	0.232	27.39		2.96	666.2	1.96	3.1	3.7	0	51	344	0.40
E69	3.12	0.23	27.97	0	26.89	0.236	34.96	0.26	4.30	663.6	3.39	29.0	5.4		67	250	0.40
E72	2.18	1.51	20.96	0	19.01	0.231	27.60	0.03	2.66	643.4	1.85	0.9	4.7		45	134	0.50
E73	0.96	0.95	18.44	0	19.86	0.137	25.93	0.01	3.12	672.4	1.23	0.8	4.0		56	129	0.40
E74	1.63	1.04	15.00	0	25.19	0.182	23.37	0.02	2.49	677.4	1.14	1.4	3.4		38	239	0.40
E75	1.46		14.51	0	16.69	0.154	19.87	0.16	2.22	664.9	1.27		2.0		30	148	0.40
E76	1.58		17.40			0.212	27.04	0.29	3.09	660.0	1.70	101.6	3.5		48		0.20

consistency. The traditional JTU unit is used for turbidity and millivolts for the oxidation-reduction potential, Eh. The total solids is expressed as a percentage of the weight of the solids to the total wet weight of the sample; all other weight ratios are expressed as the weight of the constituent to the weight of the solids present. Although the constituents in water are often expressed as the weight of the constituent per unit volume of sample (usually a liter), it is felt that comparisons among the various concentrations can be made more readily by expressing all data on a dry weight basis. The conversion to a wet weight basis is accomplished simply by multiplying the dry weight basis for a constituent by the ratio of the total solids to the total sample, taking proper account of the units of each. Note that the concentrations of cadmium, cyanide, lead, mercury, and phenols are expressed in micrograms per gram (μg/gm), whereas those of other constituents have units of milligrams per gram (mg/gm) where one thousand micrograms equal one milligram.

University of Wisconsin-Milwaukee Test Program

The data from the University of Wisconsin-Milwaukee test program are given in Table 4-6. Thirteen materials were tested in one or more of the following test series: (a) clay mineralogy, (b) cation exchange capacity, (c) relative concentrations of seven ions, (d) calcium carbonate analysis with percentages of calcite and dolomite, (e) hydrogen ion concentration, and (f) organic carbon. Listed below are the testing techniques which were employed.

Carbonates.--The Furman (1939) gravimetric method was used to test for carbonates.

Organic Carbon.--The Walkley-Black Method (Black, 1965) was employed in the organic carbon test.

Table 4-6

Chemical and Mineralogical Analyses of Several Dredgings

Sample	Clay Mineral (%)			Carbonates (%)	Calcite (%)	Dolomite (%)	Hydrogen Ion Concentration (pH)	Organic Carbon (%)	Cation Exchange Capacity (meq per 100 grams of dry material)	Ions (meq relative to milliequivalent of Calcium)						
	Illite	Kaolinite	Mixed Layer							Aluminum (Al)	Calcium (Ca)	Magnesium (Mg)	Iron (Fe)	Sodium (Na)	Potassium (K)	Manganese (Mn)
C1DM	70	30	Trace	31.8	22.2	9.6	8.2	9.5	13.6	6.7	1	0.36	0.043	0.230	0.052	Trace
C2DM	60	20	20	29.3	19.0	10.3	7.6	8.8	15.1	3.3	1	0.31	0.008	0.170	0.030	Trace
C3TO	50	15	35	35.6	19.7	15.9	7.4	3.6	18.2	1.7	1	0.17	---	0.060	0.018	Trace
C4TO	50	15	35	36.4	21.8	14.6	7.2	3.7	15.3	2.8	1	0.21	---	0.120	0.033	Trace
C5CO	60	20	20	38.6	--	--	8.0	10.5	15.3	2.8	1	0.21	---	0.050	0.030	Trace
C7MW	--	--	--	39.9	9.9	30.0	6.4	15.1	21.9	3.6	1	0.23	---	0.035	0.019	Trace
C8MW	--	--	--	--	--	--	6.6	--	--	---	-	--	---	---	---	---
C9MW	--	--	--	38.4	9.6	28.8	7.1	7.7	14.8	4.4	1	0.21	---	0.035	0.023	Trace
C27MM	--	--	--	--	--	--	---	8.8	14.4	---	-	--	---	---	---	---
D1DM	65	35	Trace	24.6	--	--	7.2	10.1	14.0	3.7	1	0.15	---	0.060	0.033	Trace
D2DM	60	15	25	27.0	12.2	14.8	7.1	7.9	11.7	2.2	1	0.23	---	0.035	0.013	Trace
D3TO	50	15	35	28.1	16.9	11.2	6.9	5.1	15.8	1.4	1	0.32	---	0.050	0.023	Trace
D4CO	75	25	Trace	39.9	--	--	7.8	8.8	11.9	2.6	1	0.19	---	0.070	0.028	Trace

Cation Exchange Capacity.--The cation exchange capacity was conducted according to ASTM, STP 142 (1952), and it is recorded as milli-equivalents per 100 grams of dry material.

Exchangeable Ions.--The relative amounts of exchangeable ions were determined by use of atomic absorption and flame emission from the extract of the material from the cation exchange capacity test. The ions are given as milli-equivalents relative to calcium.

Clay Mineralogy.--X-ray diffraction analyses were used to identify the clay minerals present. The relative amounts of each mineral in the minus 2 micron fraction are based on integrated peak intensities and mass absorption coefficients, and the percentages of clay mineral represent rough estimates of the fractions of the clay portion, which consists of various clay minerals.

Field Test Program at Toledo, Ohio

On July 2, 1971, a Corps of Engineers tug boat was used to take water and sediment samples from the Maumee River in the vicinity (see Figure 3-13) of the area to be dredged the following day. These samples were tested immediately by use of a Hach Chemical Company Field Test Kit, and the results given in Table 4-7 compare well with those obtained subsequently from tests conducted at Northwestern University.

Pesticide Tests at EPA Laboratory

Pesticide tests on four samples (C2DM, C3TO, C5CO, and D4CO) were conducted at the EPA, Region V, Chicago District Laboratory. As much water as possible was pipetted from each sample without removing any of the bottom sediments, and this fluid was used for the analyses of the water phase. Then, a portion of the bottom sediment was removed from one of the duplicate samples of each material, and the water was allowed

Table 4-7

Chemical Characterization of Field Samples at Toledo

	Parameter	Station[6]					
		55	50	20N	30N	30S	40
		Sample					
		A13	A14	A15	A16	A17	A18
Surface Water	Hydrogen Ion Concentration (pH)	7.40	7.40	7.40	7.50	7.50	7.60
	Turbidity (JTU)	20.00	20.00	25.00	15.00	15.00	23.00
	Nitrogen[1] (ppm)	35.40	38.10	32.80	35.40	34.60	35.40
	Total Alkalinity[2] (ppm)	140.00	138.00	135.00	135.00	135.00	135.00
	Phosphate[3]	0.75	0.72	0.72	0.75	0.85	0.85
	Total Hardness[4]	240.00	235.00	220.00	230.00	210.00	230.00
	Iron	0.05	---	0.05	---	---	0.05
Bottom Sediment	Hydrogen Sulfide	0.45	0.45	0.10	0.35	0.35	0.55
	Odor[5]	Strong	Strong & foul	Nil	Not so strong	Not so strong	Strong & foul

1. Nitrate and nitrite reported as nitrate.
2. Reported as $CaCO_3$, all in the form of bicarbonate alkalinity.
3. Ortho plus poly (meta) phosphate.
4. Reported as $CaCO_3$, EDTA method.
5. Oils and grease were visible on the surface of the sediment samples; all odors can be best described as "sewage" odors, which are typical of anaerobic activity.
6. For locations of stations, see Figure 3-13 and associated description in text.

to drain from the solids; these bottom sediments were placed on aluminum foil and allowed to air-dry at room temperature. The results of these chlorinated pesticide tests are presented on an air-dry basis in Tables 4-8 and 4-9.

INTERPRETATION OF RESULTS

One of the major purposes for this chemical testing program was to provide background information to assist in interpreting and correlating the engineering property tests conducted on the same dredgings and, if possible, to aid in explaining the engineering behavior of the resulting landfill. However, since this type of interpretation is more appropriate to the portions of this report dealing with engineering properties, it will be included in those discussions. In addition, these chemical data will provide a basis for subsequently selecting appropriate additives to improve the engineering properties of dredged spoil.

This testing program was sufficiently broad in scope to allow some interpretation of the interrelationships among the constituents found in the various phases of the dredging operation. Comparisons may be made between the measured concentrations of the various pollutants and the EPA standards, which were presented and discussed in Chapter 2. As a first conclusion, it comes as no surprise that the various dredgings tested herein would be classified as polluted. The degree of pollution varies from harbor to harbor, from sample to sample within a harbor, and in the intensity of the various pollutants for a particular sample. The chemical composition of the water was very consistent with that expected at particular locations. For example, where sewage was emitted, the dissolved oxygen was low and the biological oxygen demand and

Table 4-8

Pesticide Analyses of Bottom Sediments

Pesticide (ng/kg or ppt)	EPA Sample Number 8211	8212	8213	8214
	Northwestern University Sample Number C2DM	C3TO	C5TO	D4CO
Lindane	35,309	33,194	1,819	24,272
Heptachlor	70,955	9,563	24,818	45,048
Aldrin	44,876	32,566	28,959	74,584
Heptachlor Epoxide	98,645	43,335	82,463	148,831
Methoxychlor	<1	<1	<1	<1
Dieldrin	<1	<1	<1	<1
Endrin	16,365	<1	33,862	18,071
o, p-DDE	120,563	47,379	114,583	185,355
p, p'-DDE	110,053	43,127	97,424	196,931
o, p-DDD	68,148	20,964	111,111	111,760
p, p'-DDT	89,293	34,305	145,653	110,637
o, p-DDT	121,637	15,558	32,669	24,417

Note: No separation of pesticides, PCB's, or phthalates was made; therefore, these values may include the above.

Table 4-9

Pesticide Analyses of Liquids from Bottom Sediments

Pesticide (ng/kg or ppt)	EPA Sample Number			
	8211	8212	8213	8214
	Northwestern University Sample Number			
	C2DM	C3TO	C5TO	D4CO
Lindane	76	5	41	559
Heptachlor	113	11	18	244
Aldrin	62	4	66	2569
Heptachlor Epoxide	464	24	201	1180
Methoxychlor	<1	<1	<1	<1
Dieldrin	115	<1	<1	<1
Endrin	<1	<1	18	<1
o, p-DDE	288	23	313	1109
p, p'-DDE	216	9	536	1513
o, p-DDD	62	7	175	380
p, p'-DDT	100	11	110	412
o, p-DDT	82	5	84	436

Note: No separation of pesticides, PCB's, or phthalates was made; therefore, these values may include the above.

nitrogen content were high; this was also true for bottom sediments. However, the chemical oxygen demand depended not only on organic compounds, but also on other materials (such as the nitrite and sulfide anions and the mercurous, cuprous, and ferrous cations) that are found in high concentrations in these dredgings.

Several series of tests were conducted to investigate specific aspects of the dredging and disposal cycle; these include (a) the variation in water quality with distance from the outflow weir into the bay, (b) a comparison of constituent concentrations in the water from the river, dredge hopper, and outflow weir of the fill area, (c) composition of the sediments on the harbor bottom as a function of depth, and (d) the constituent concentrations during various phases of the dredging cycle.

Water Quality as a Function of Distance from Outflow Weir

Water samples were taken near the outflow weir (A19TO), from the surface water 100 feet from the weir (A20TO), from the surface water 200 feet from the weir (A21TO), and from the ambient surface water (A22TO) in the vicinity of the Island Site at Toledo, Ohio. Although firm conclusions cannot be drawn from such a limited sampling and testing program, certain trends are suggested. In general, the various constituents of the samples from the different locations indicated above have the same order of magnitude of concentrations. Slight decreases of concentration with distance from the weir may be noted for some constituents, such as total solids, total suspends solids, total iron, and aluminum; however, most of the other values appear to be randomly mixed. A truly meaningful study of this type would require that numerous samples be taken over a period of time to allow a statistical analysis of the results; in addition, the need for careful sampling and precise testing is emphasized.

Constituent Concentrations of Water from River, Hopper, and Outflow Weir

Samples A13TO through A22TO are water samples from various locations in the Maumee River and near the Island Site at Toledo, Ohio; sample B5TO represents water from the hopper of the dredge, sample B7TO represents water from the outflow weir of the hopper, and sample B8TO represents water from the outflow weir at the Island Site. This very limited sampling and testing program suggests the following tentative conclusions:

1. The percentage of solids in the water from the hopper is much greater than that in the water from the outflow weir of the fill area; the latter, in turn, is greater than its counterpart in the river water.
2. The total volatile solids, total suspended solids, acidity, and concentrations of phosphates, calcium, copper, potassium, and sodium were higher in the river water than in the water from the outflow weir of the fill area.
3. The chemical oxygen demand, total iron, and silica were higher in the water from the outflow weir of the fill area than in the river water.

Composition of Bottom Sediments as a Function of Depth

Based on the results of a very limited test program, the constituent concentrations in the very top surface sediments of the harbor bottom may be compared with those in the sediments several feet below the bottom surface. This comparison is possible because the Ekman dredge sampled only the very top surface of the bottom sediments, whereas the flap valve sampler penetrated about three feet into the bottom sediments and provided a composite sample of all materials over the three-foot depth. During the sampling operation in the shipping channel (see Figure 3-13) of the Maumee River at Toledo, Ohio, three stations (40N, 30N, and 20N) were sampled by both the Ekman dredge and the flap valve sampler. A comparison of the chemical analyses for the samples taken from these stations (D8TO with C12TO for Station E40N, D9TO with C13TO for Station E30N, and D10TO with C14TO for Station E20N) suggests the following general conclusions:

1. The deeper sediments exhibit about twice the amount of solids per unit wet weight of sample.

2. The deeper sediments have a lower percentage of volatile solids and nitrogen and a much lower concentration of phosphates (on the order of one percent of the phosphates in the surface materials).

3. Concentrations of oil and grease, as well as the metals tested, were about the same order of magnitude in both deep and shallow sediments.

Constituent Concentration as a Function of Dredging Cycle Phase

Some tentative conclusions concerning constituent concentrations during various phases of the dredging cycle may be advanced, but these are subject to the following limitations. Although the materials being compared come from the same general location at Toledo, Ohio, they were obtained at different times and from different parts of the harbor area. The A, B, C, and D materials were taken from the same general location during one sampling tour, but the E material from the fill was deposited during previous dredging seasons. Within these limitations, the indicated conclusions are:

1. The percentages of total solids per unit weight of wet sample are on the order of a few hundredths of a percent for the water samples, several percent for the water from the hopper of the dredge, 15 to 20 percent for the material from the discharge pipe and for the soft bottom sediments obtained by the Ekman dredge, 35 to 40 percent for bottom sediments obtained with the flap valve sampler, and 50 to 70 percent for the fill materials.

2. The percentage of total volatile solids per unit weight of total solids decreases from the water to the bottom sediments and decreases further in the fill materials.

3. There was little variation in the chemical oxygen demand of the various materials, except for the water which had a somewhat smaller value.

4. Respective concentrations of organic and ammonia nitrogen were about the same in the A and C materials, but they were significantly higher in the E or fill materials.

5. Concentrations of total phosphates were about the same order of

magnitude in all materials, but they were slightly lower in the water than in the bottom sediments and fill materials.

6. The soluble metal ions, such as sodium and potassium, were found in greater concentrations in the water, whereas greater amounts of the heavy metals were found in the sediments and fill materials.

RECOMMENDATIONS

For subsequent investigations, it is recommended that a test program be established to maximize the amount of useful information obtained for a given expenditure. To accomplish this objective, careful consideration must be given to the specific needs and goals of the research effort, the equipment and personnel available, and the relative costs of the various tests. For example, tests which are easy and inexpensive to conduct might be performed routinely on each sample, whereas complicated, time-consuming and expensive tests would be used with great care and judgment. In addition, it seems very worthwhile to investigate the possible correlations among the results from simple and inexpensive tests with those from the more difficult and expensive ones.

CHAPTER 5

ORGANIC CONTENT

Experience indicates that organic soils have lower shear strength and greater compressibility than inorganic soils. On most construction sites and in most borrow pits, however, organic soils comprise only the top several inches or perhaps the top foot or two of soil, and the usual engineering procedure is to remove and waste this organic soil prior to proceeding with other construction operations. This being the case, there has been little impetus in the past to thoroughly study the effects of organic content on the engineering properties of soils, and there has been little effort to standardize the testing methods. However, since the press for utilization of marginal lands frequently involves soils with high organic content, more interest is presently being shown in the engineering behavior of organic soils. Some current developments involve large areas, and the cost for removal of topsoil is very high; this has served to emphasize (a) the need for more exact information on the cause and effect of organics in soil and (b) the requirement for more accurate and standardized testing procedures.

Several forms of organic matter may appear in dredgings; these include sanitary sewage with varying degrees of treatment, industrial wastes and sewage which often contain various amounts of petroleum products and other hydrocarbon compounds, and sediments containing agricultural wastes and other plant and animal matter which are transported with the run-off of a given watershed. Once the spoil is placed in a diked area and left dormant for a brief period of time, a variety of dense vegetation, including several forms of large plants, begins to grow rapidly. When a new dredging season begins, the newly placed spoil floods the fill area, partially killing and covering the previous growth; hence, a considerable amount of fibrous material is incorporated into the fill at rather distinct levels, thereby providing still another form of organic material in the fill. In this chapter the nature and amount of organic material found in the spoil are presented with a discussion of the testing procedures used. A detailed consideration of the effects of organic content on the engineering properties of the dredgings will be included with the general interpretation of the field and laboratory test results.

DEFINITIONS

A better understanding of the complex nature of organic materials and organic soils may be obtained by examining the following definitions of organic soil, organic matter, and topsoil.

> An organic soil is one that has a sufficient organic content to affect the engineering properties of the material, but does not have the spongy structure of peat or organic muck. (Schmidt, 1965)

According to this definition, a peat would be classified as a highly organic soil, whereas a soil with smaller percentages of organic matter than peat (around 10 to 15 percent as compared with about 50 percent or more for peats) would be classified as an intermediate organic soil.

> The organic fraction of the soil consists of a complex system of substances the dynamics of which are determined by the continuous admission of organic residues of plant and animal origin into the soil and their continual transformation under the action chiefly of biological factors, but also to some extent of chemical and physical factors. (Kononova, 1961)

The complex system mentioned in the above definition is formed, according to Kononova (1961), by the following organic compounds:

1. Fats and similar substances
2. Carbohydrates and related substances (mono and disaccharides, cellulose, hemicelluloses, and pectins, pentosans, mannans, polyuronides of plant and microbial origin)
3. Proteins and their derivatives, albumins of different complexity, amino acids, amides, various bases of the purine and pyridine and pyrimidine series, and other nitrogen-containing organic compounds
4. Lignins and their derivatives (this group includes not only the formed lignins of higher plants and "precursors of lignin", but also the initial products of their decomposition)
5. Tannic substances in simple and condensed forms
6. Resins and terpenes

In addition, soils contain various organic acids, aromatic materials, hydrocarbons, alcohols, and other groups of compounds.

Most published definitions of topsoil are either inadequate or too general to have specific application. In general, although some definitions, several of which are given below, allude to engineering considerations and the economic importance of the problem, none indicates very specifically the effect of organic matter on engineering properties.

> Top soil is a name given to weathered surface materials which are capable of supporting plant life. (Taylor, 1948)

> The surface horizon is topsoil, or a horizon, often with subdivisions A_0, A_1, A_2, etc.... The very top of the A horizon is humus (designation A_0 formed by the mixture of soil with decomposed organic matter). Although valuable in agriculture and gardening, humus generally is wasted in engineering except in irrigation projects or earth (dirt) roads. (Krynine and Judd, 1957).

> The A horizon is the original top layer of soil having the same color and texture. It is usually 10 to 12 inches thick, but may range from 2 inches to 2 feet. Removing native cover of timber by lumbering operations or of grasses by farming may introduce erosion that removes this top layer as well as underlying layers or horizons. The A horizon is also referred to as the topsoil or surface soil when erosion has not taken place. (Soil Primer, 1956)

> Topsoil--As in materials deposits, the usual practice is to remove topsoil from all foundations. Topsoil in this sense is the surface layer of material containing decaying vegetable matter and roots. It is not necessary to remove all the soil containing fine hairlike roots, but only the rather heavy root mat. On prairie soils containing light grass cover, 2 or 3 inches of stripping will usually suffice for topsoil removal. Agricultural lands are stripped to the bottom of the plowed zone, usually 6 to 9 inches. Valley bottom lands and brush-covered land commonly require stripping up to 2 or 3 feet for removal of inadequate material. Forest covered land requires the removal of stumps resulting in stripping requirements between about 2 and 5 or more feet. (Earth Manual, 1963)

TESTING METHODS

The methods presently available to determine organic content can be grouped into two main categories; these are (1) dry combustion and (2) wet combustion with (a) titration methods or (b) gravimetric methods. In the decision of which test to use, several criteria must be considered. First of all, the test should provide the desired information consistently and accurately; secondly, it should be simple and fast -- simple enough to be performed routinely in a soil mechanics laboratory without demanding specially trained personnel and fast enough so that a reasonable number of tests could be conducted in a normal work day. It is important to note that the results from any investigation for organic matter may depend strongly on the methods used in the analysis.

Dry Combustion

Of all the methods available, the dry combustion procedure is the simplest to perform. There is still great controversy concerning the maximum temperature which can be used to burn the organic fraction without causing losses in the mineral fraction. Theoretically, upon heating a soil to high temperatures, all organic material is driven off, and only an inorganic residue is left. However, the separation of the water from the organic material is not easy. Even at room temperatures, microbial action will cause various organic gases and very light petroleum products to be generated and released to the atmosphere. Heating to 105°C (the temperature used to determine the water content of soils) will release additional organic gases. If various clays are present, and they usually are to some degree, not all of the water is released at 105°C. For example, very high temperatures are required to release the interlattice water held in montmorillonite.

Ball (1964) reports that better organic matter recovery is obtained if soil is burned at 375° ± 5°C for 16 hours, as compared with 850°C for a half-hour period, and statistical evidence is presented to support this statement. Based on evidence furnished by thermogravimetric analysis, Skempton and Petley (1970) concluded that a temperature of 550°C for 3 hours was optimal for the soils tested. Results of loss on ignition were corrected by assuming that mineral matter loses 4 percent of its weight when heated at 550°C. Arman (1970) used 440°C for 5 hours, and he recommended that higher temperatures not be used because dehydroxilization (loss of lattice water) of clay minerals occurs at approximately 450°C, and such loss of weight could be attributed to organic matter. The Netherlands Soil Survey Institute implemented an ignition test temperature of 800°C, and the correction for the bound water is taken as 0.1 gr/gr of the clay fraction (< 2 microns). For calcium carbonates, if present, the correction is 0.44 gr/gr of carbonates; this corresponds to the loss of carbon dioxide. The highest temperature that can be reasonably applied to a soil to determine its organic content is a function of its mineralogy, and this is undoubtedly the reason why so many different temperatures are used. The best way to optimize the test temperature is to conduct thermogravimetric analyses (TGA) to obtain the maximum temperature for a particular type of soil.

The only equipment required to conduct an ignition test is an analytic balance and a furnace. As discussed above, test problems include selecting a suitable temperature and an appropriate burn period. For all tests conducted in this program, a furnace temperature of 440°C was used, and weights were recorded after 5 hours and after 24 hours. Prior to the ignition test, the samples were dried at 105°C, and all weight changes are referred to these weights as the original dry weights.

Wet Combustion

Wet combustion methods range from digestion with hydrogen peroxide (H_2O_2) to strong treatments with sulfuric acid (H_2SO_4), and there is great difficulty in determining which of the many test procedures described in the literature is the best for a specific case. A test that works well for one particular soil might yield poor results when applied to a different soil. Various test procedures of the wet combustion type have been reported by Shaw (1959), Walkley and Black (1934), Tinsley (1950), Schollenberger (1927, 1945), and Allison (1935, 1960). All of these testing techniques seem to be very similar, because they use approximately the same chemical compounds and a somewhat similar test procedure; the differences lie primarily in the concentrations of the reactants, the temperatures used, and the times allowed for the chemical reactions to take place.

The organic carbon test used in this test program to determine the organic content of dredgings was developed by Allison (1960) and modified by Grass and Lemert (1971). The same set-up was used to determine the amount of inorganic carbon; this gives an indication of the error associated with the ignition test due to oxidation of inorganic carbon components. The apparatus for the organic carbon test is shown schematically in Figure 5-1. A sample weighing about one-half a gram was used, and about 1 to 2 grams of potassium dichromate ($K_2Cr_2O_7$) was added to the soil; then, 25 ml of digestion acid (a mixture of 60 percent concentrated sulfuric acid and 40 percent concentrated phosphoric acid) was added (A). The system was preaerated, and the air stream was adjusted to accommodate a slow flow rate (one to two bubbles per second). The mixture was then heated to boiling in about 3 minutes and kept boiling for a total of 10 minutes. Finally, the system was aerated with a fast air flow rate (8 bubbles per second) for 10 more minutes.

The potassium dichromate, digestion acid, and elevated temperature combined to produce chromic acid, a strong oxidant which, in turn, oxidized the organic matter, thereby forming carbon dioxide. The gases produced were carried by the air stream through a cooling tower (B) and through three vials (D, E, and F). The first vial (D) contained a 50 percent solution of potassium iodide; therefore, if any chlorides or bromides were present, potassium chloride or bromide was formed, and free iodine was precipitated with the solution turning a dark yellow. The second vial (E) contained a concentrated solution of silver sulfate; this

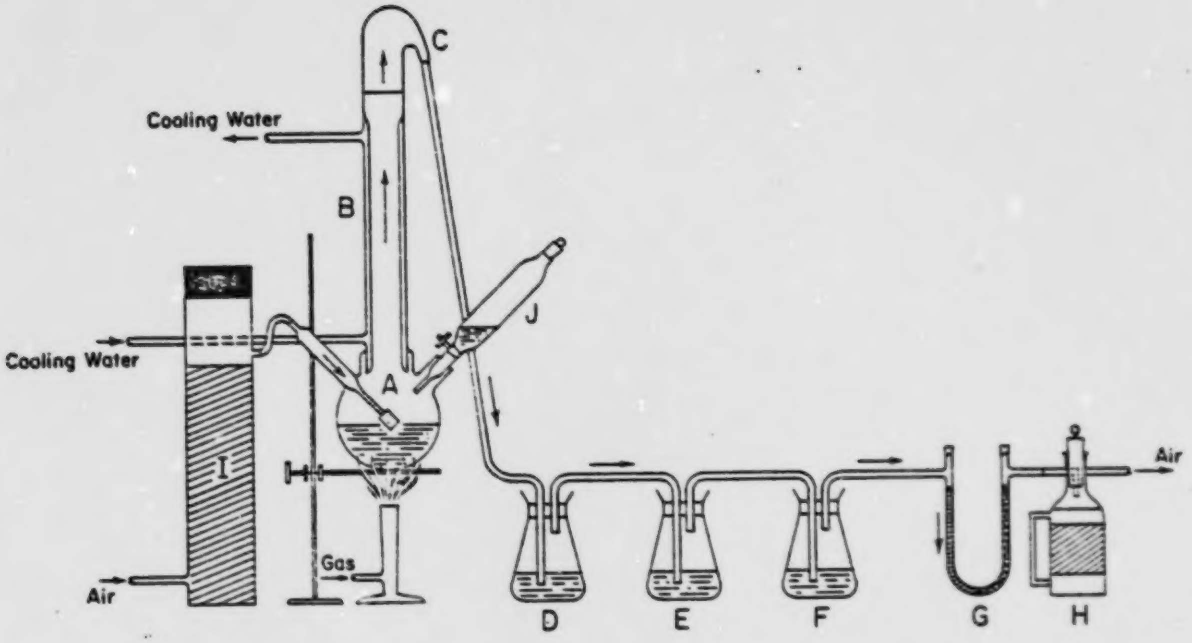
C
Cooling Water
B
J
Cooling Water
A
I
Air
Gas
Air
D
E
F
G
H

Figure 5-1. Test Apparatus for Carbon Content Determinations

solution turned cloudy if any chlorides passed the first vial, and it was used only as an indicator of the effectiveness of the first vial. Concentrated sulfuric acid in the third vial (F) removed water vapors from the air stream. Next was a U-shaped tube (G), one arm of which was filled with zinc granules (minus 30 mesh) and the other with anhydrone (anhydrous magnesium perchlorate). The zinc granules reacted with the acid forms of anions to prevent them from passing through. The anhydrone was a dehumidifier and removed the last traces of any water vapor. The stream then went into a Nesbitt bulb (H), which had been carefully weighed to a tenth of a milligram. At the bottom of the Nesbitt bulb, where the gases entered, was some inert glass wool to distribute the gases evenly; next was a 5-centimeter layer of Mikhobite to absorb the carbon dioxide (potassium carbonate being formed). At the end was a 1-centimeter layer of anhydrone. Finally, the purified air was released to the atmosphere.

The change in the weight of the Nesbitt bulb gave the amount of carbon dioxide released from the oxidation reaction. The amount of carbon released was calculated by multiplying by 0.2727, and this weight divided by the weight of the original sample gave the weight percentage of organic carbon in the sample. To determine the amount of carbon dioxide in the air from the air stream, a blank test was conducted, and the result was used to correct the carbon dioxide indicated by the Nesbitt bulb. If carbonates were present, the sample was pretreated with 3 ml of acid reagent (solution of 57 ml of H_2SO_4 and 92 gr of $FeSO_4.7H_2O$ in 600 ml of H_2O) and boiled gently for one and a half minutes. The inorganic carbon test was very similar to the above described procedure, except that potassium dichromate was not used and the acid reagent (H_2SO_4, $FeSO_4.7H_2O$ and H_2O) was used instead of the digestion acid

(H_2SO_4 and H_3PO_4). Also the boiling time was reduced to 7 minutes.

The only difference between the method used for these tests and the method described by Grass and Lemert (1971) is that a smaller sample (about 0.5 grams) was used for these tests. It was found that larger samples, which were highly organic, gave very low and inaccurate results. Apparently the Mikhobite was not absorbing all of the carbon dioxide generated; in addition, it is possible that the short time of boiling allowed only a portion of the organic matter to be oxidized. When operational, the system was tested with a 0.5-gram sample of dextrose; since it is known that dextrose is 40 percent carbon and a determination of 39.8 percent carbon was obtained from this test, it was judged that the system was satisfactory and the sample size was acceptable. A more complete description of this test has been given by Allison (1960) and Grass and Lemert (1971), and an alternative modification of the same method was reported by Schmidt (1965).

EXPERIMENTAL RESULTS

The results of the organics tests conducted at Northwestern University are summarized in Table 5-1 with the values obtained by wet combustion listed as organic carbon and those obtained by dry combustion listed as loss on ignition. Table 5-2 gives the values of organic carbon obtained from the tests conducted at the University of Wisconsin-Milwaukee by use of the Walkley-Black method. Except for a few instances, the organic carbon content of the samples tested is of the order of 2 to 4 percent. If it is accepted that organic matter consists of 53 to 58 percent organic carbon, the organic matter content for most of the samples will vary from 4 to 8 percent. There are a few exceptions (such

Table 5-1

Organic Carbon and Loss on Ignition for Various Dredgings

Sample	Organic Carbon	After 5 hours at 440°C		After 24 hours at 440°C	
		Loss on Ignition	Carbon Ratio	Loss on Ignition	Carbon Ratio
C22TO	3.72	5.27	0.71	7.60	0.49
C27MM	7.55	11.89	0.63	11.93	0.63
D1DM	12.50	5.97	2.10	12.26	1.02
D2DM	8.96	11.50	0.78	12.25	0.73
D3TO	3.21	5.67	0.57	6.40	0.50
D4CO	8.21	9.00	0.92	10.00	0,82
D6TO	0.79	1.10	0.72	1.25	0.63
D8TO	4.51	7.77	0.58	8.36	0.54
D9TO	3.90	8.27	0.47	8.71	0.45
D10TO	3.69	7.29	0.51	7.93	0.46
E6TO	2.92	5.40	0.54		
E7TO	1.96	4.68	0.42	4.80	0.41
E8TO	2.14	3.90	0.55	4.40	0.48
E10TO	3.12	5.80	0.54		
E13TO	2.35	5.61	0.43	5.93	0.39
E14TO	4.09	7.08	0.58	7.43	0.55
E15TO	2.29	5.27	0.44	6.09	0.38
E16TO	3.12	6.53	0.48	6.65	0.47
E17TO	2.54	5.40	0.47	5.83	0.43
E18TO	2.78	5.70	0.49	6.39	0.43
E19TO	3.33	6.53	0.51	6.65	0.50
E20TO	3.08	6.59	0.47	6.94	0.44
E21TO	2.74	5.35	0.51	5.76	0.47
E22TO	2.17	3.54	0.62	3.84	0.57
E23TO	2.71	5.27	0.52	5.81	0.47
E24TO	2.98	6.13	0.48	6.21	0.48
E25TO	2.60	6.18	0.42	6.40	0.41
E26TO	2.41	5.91	0.41	6.00	0.40
E27TO	2.85	6.02	0.47	6.20	0.46
E28TO	2.95	6.43	0.46	6.70	0.44
E29TO	2.57	6.14	0.42	6.30	0.41
E63TO		5.20		6.20	
E71TO	2.71	5.84	0.46	6.10	0.45
E83TO	1.41	7.39	0.19	7.60	0.19

Table 5-2

Organic Carbon Content of Different Dredgings

Sample	Organic Carbon (%)
C1DM	9.5
C2DM	8.8
C3TO	3.6
C4TO	3.7
C5TO	10.5
C7MW	15.1
C9MW	7.7
C27MM	8.8
D1DM	10.1
D2DM	7.9
D3TO	5.1
D4CO	8.8

as samples C1DM, C2DM, C5TO, C7MW, D1DM, D2DM, and D4CO) where the organic matter content is considerably higher. It was noticed that the samples with high organic contents (especially samples D1DM and D2DM) exhibited a strong oily odor; it is believed that the presence of hydrocarbons accounts for such high organic carbon contents.

In order to check the appropriateness of the dry combustion test for determining organic matter content, the values of organic carbon content were divided by those obtained from loss on ignition tests for 5 hours and 24 hours burning time. Based on the assumption that the results of the wet combustion chemical tests (Grass and Lemert, 1971) are correct, they should be about 0.5 to 0.6 times the results obtained from the dry combustion ignition test. If the carbon ratio is defined as the value of organic carbon content divided by the analogous value from a loss on ignition test, it can be seen in Table 5-1 that such ratios vary over quite a large range for both 5-hour and 24-hour ignition tests; this could be due to several reasons, including the following:

1. Due to the burning temperature used, there may have been a loss of lattice water from the montmorillonite clays in the dredgings; this loss of water would be recorded as organic matter content and may therefore cause a variation in the carbon ratio.
2. Although Allison (1960) recommends that the sample for the chemical test be ground to particle sizes of 0.5 mm or less, samples for these tests were ground to pass the #18 sieve (1 mm); it is known that the recovery ratio (that is, the measured amount of organic carbon divided by the total organic carbon) improves as the sample is ground finer.

3. The volume of the sample used in this type of test influences the results obtained; smaller samples generally yield better results. However, the sample must be large enough to be representative, and it was decided for these particular tests that a sample of approximately 50 grams provided a reasonable compromise between the two conflicting criteria, namely, the sample should be small enough to achieve good test results and it should be large enough to be representative. It is probable that a sample of about 10 grams would give better results.
4. The sample area exposed to direct heat has some effect on the results, but this effect was minimized by placing all samples in the same type of container.
5. The presence of hydrocarbons and other petroleum derivatives in the dredgings could account for the unusually high carbon ratio of certain samples.

The test results in Table 5-3 indicate the variations in the values of organic carbon, loss on ignition, and carbon ratio for four samples (C22TO, C27MM, D1DM, and D4CO) which were subjected to varying degrees of electrical treatment; this phenomenon was investigated in conjunction with the use of electro-osmosis to dewater dredgings. Although the numbers of samples tested in this manner is small (and conclusions deduced therefrom should be weighted accordingly), the following observations can be noted:

1. Organic carbon, as determined by the wet combustion method, varies with the degree of electrical treatment, but the pattern is not meaningful.

2. The loss on ignition values are somewhat greater for the treated samples than for the untreated samples.

3. The carbon ratio varies in a random manner with the degree of electrical treatment.

Table 5-3

Effect of Electro-osmosis on Organic Content Determinations

Sample	Organic Carbon	After 5 hours at 440° C		After 24 hours at 440° C	
		Loss on Ignition	Carbon Ratio	Loss on Ignition	Carbon Ratio
C22TO	3.72	5.27	0.71	7.60	0.49
C22TO(1)	3.38	7.76	0.44	8.15	0.41
C22TO(2)	1.84	7.94	0.23	8.27	0.22
C22TO(3)	3.60	7.93	0.45	8.94	0.40
C27MM	7.55	11.89	0.63	11.93	0.63
C27MM(1)	5.23	11.41	0.46	11.70	0.45
C27MM(2)	6.12	10.98	0.56	11.22	0.54
C27MM(3)	6.45	11.25	0.57	11.35	0.57
D1DM	12.50	5.97	2.10	12.26	1.02
D1DM(1)	13.13	16.46	0.79	17.44	0.75
D1DM(2)	13.49	13.27	1.01	17.98	0.75
D1DM(3)	12.74	16.36	0.78	18.13	0.70
D4CO	8.21	9.00	0.92	10.00	0.82
D4CO(1)	7.87	9.00	0.88	9.20	0.86
D4CO(2)	7.76	9.20	0.84	9.80	0.79
D4CO(3)	7.98	9.03	0.88	10.00	0.80

Table 5-4 gives a comparison of some test results determined by different testing techniques. In general, it is seen that organic carbon values are of the same order of magnitude, with the Walkley-Black (W-B) method giving somewhat higher values than those obtained by the Grass-Lemert (G-L) method. In addition, the test results obtained by the techniques used to determine total volatile solids are compared with those measured by 24-hour loss on ignition tests; in all cases the value for total volatile solids is higher than that for loss on ignition. The percentage of loss on ignition relative to total volatile solids ranges from 73 to 99 percent with an average of about 90 percent. The results of this comparison lend support to the earlier discussion concerning the effects of higher burning temperatures on organic content determinations.

The plots in Figures 5-2 and 5-3 show that organic carbon is almost constant with depth; the samples from BH-4 and BH-13 were obtained in 1971, whereas those from BH-10, BH-16, and BH-18 were taken in 1972. Except for the samples from BH-4, which was located on the Island Site, all samples came from Riverside Site. The low value for the sample at the bottom of BH-18 may be due to the fact that the virgin material below the dredgings was sampled. The remaining scatter is considered representative of testing, sampling, and natural variations in organic carbon content.

CONCLUSIONS AND RECOMMENDATIONS

Within the framework of the organic content study reported herein, the following conclusions and recommendations can be advanced:

1. Although the wet combustion test used in this experimental program is considered adequate for its intended purpose, future tests

Table 5-4

Comparison of Organic Content Determinations by Various Methods

Sample	Total Volatile Solids (%)	Loss on Ignition (24 hours) (%)	Organic Carbon (G - L) (%)	Organic Carbon (W - B) (%)
C22TO	9.03	7.60	3.72	
C27MM	12.63	11.93	7.55	8.8
D3TO	6.96	6.40	3.21	5.1
D4CO	10.53	10.00	8.21	8.8
D8TO	9.33	8.36	4.51	
D9TO	8.81	8.71	3.90	
D10TO	8.91	7.93	3.69	
E63TO	8.56	6.20		

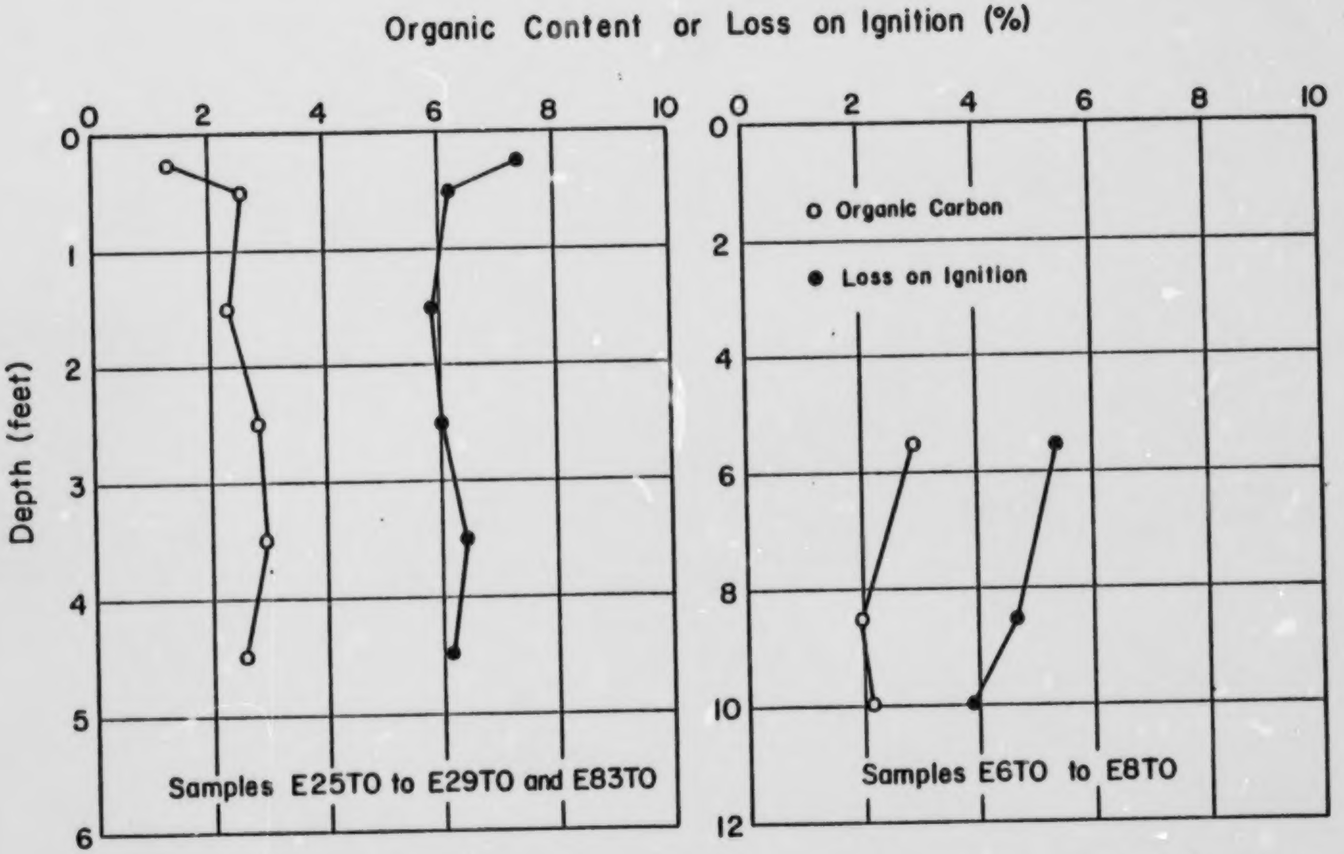

Figure 5-2. Organic Content or Loss on Ignition versus Depth

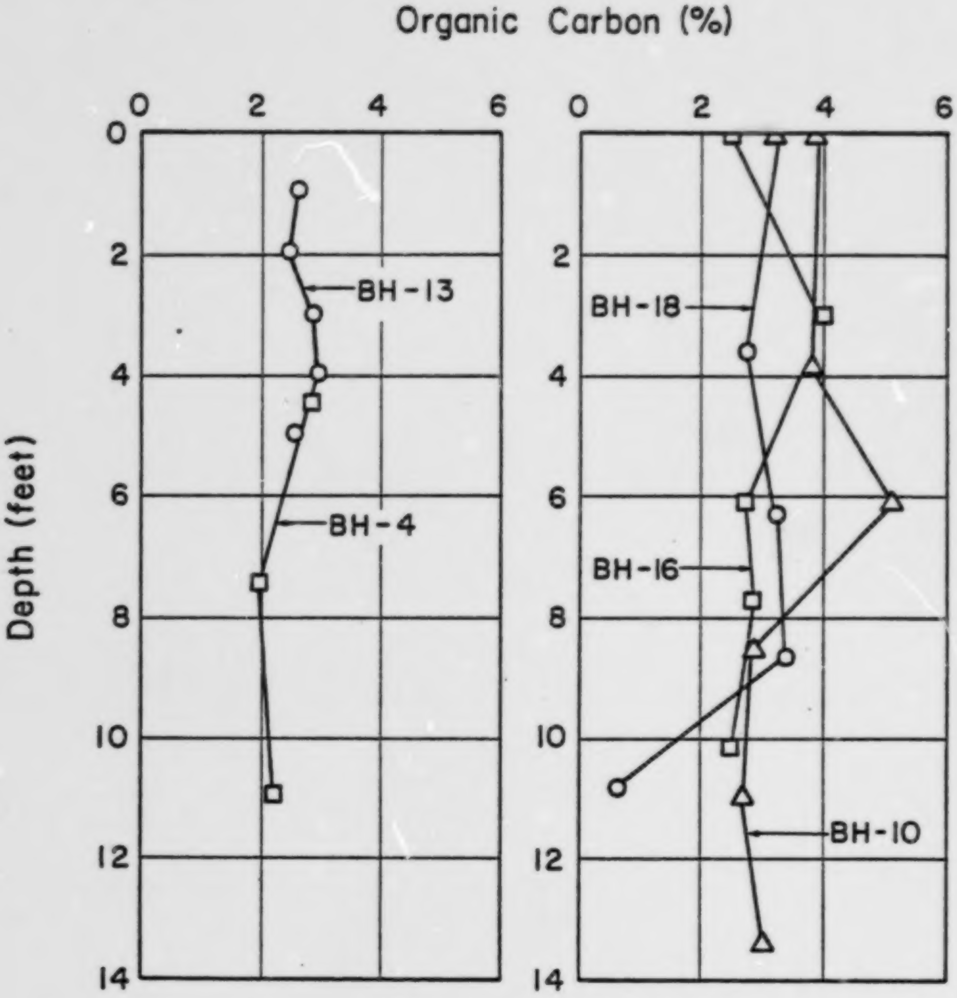

Figure 5-3. Organic Carbon versus Depth at Different Locations

should be performed on samples passing at least the #40 sieve, not the #18 sieve.

2. Mineralogical tests should be conducted to aid in interpreting the test results.

3. In the ignition tests it is considered advisable to use a temperature of 400°C until a constant sample weight is achieved; the temperature of 440°C is probably a little too close to the temperature at which dehydroxylization of montmorillonite begins.

4. The dredgings tested could be classified with respect to their organic content as intermediate organic soils, since the organic content in most cases lies between 4 and 8 percent.

Under various conditions organic and carbon compounds separate into simpler compounds. Although sugars and related compounds and some straight chain hydrocarbons will break down in the Grass-Lemert method, other organic carbon compounds require still more vigorous digestion to achieve the same end result. For instance, calibration tests using the wet method on various known materials yielded 98 percent carbon recovery for dextrose, but only 17 percent for naphthalene and 26 percent for sodium stearate. Therefore, it is possible that, in the test conducted, not all of the organic carbon ions were released into carbon dioxide (CO_2) and measured as organic carbon. Accordingly, future determinations of organic carbon should be made on identical samples by use of several different testing techniques; this will allow an evaluation of the test procedure on the results obtained.

In such a program the following testing procedures may be considered. Various oxidizing agents may be used with titration methods to evaluate the amount of carbon oxidized and thus the carbon content. However, tests should be made to ascertain that other reducing compounds are not also present. For example, it would not be advisable to use such procedures on some of the dredgings tested in this program since ferrous ions were found; the methods discussed above would oxidize these ions to ferric and thus give an erroneous determination of carbon content. The various oxidizing processes include the use of (a) hydrogen peroxide, (b) potassium dichromate, as in the Grass-Lemert method, (c) COD acid (Ag_2SO_4 and H_2SO_4), (d) the Kjeldahl method, which employs elevated temperatures with acid, and (e) a furnace with and without gas composition analyses. The use of hydrogen peroxide or potassium dichromate would be generally acceptable for analyses that involve sugar, but they may not adequately break down the saturated fats or oils and aromatic compounds. The use of COD acid or the Kjeldahl method would break down more of the organic compounds, whereas the furnace would definitely accomplish a complete break-down. However, the furnace has the disadvantage of driving off water vapor and thus causing an error in the carbon content measurement if certain clay minerals are present; this drawback could be overcome by analyzing the discharge gas in a manner similar to that used for the Grass-Lemert method.

CHAPTER 6

DEWATERING

When dredgings are allowed to drain, field experience has established that their density and strength will increase; therefore, considerable attention was given to the procedures by which dewatering can be achieved and the response that is observed for each. In general, dewatering can be accomplished by several different procedures, including evaporation, application of external pressure, gravity, drainage, vacuum drainage, electro-osmosis, use of a centrifuge, heating, etc. Of these, dewatering by use of an external pressure, gravity drainage, and vacuum drainage are studied in this chapter, whereas the application of electro-osmosis is treated in the next chapter; insofar as deemed applicable, the other procedures are discussed in Chapter 11. Dewatering by any method will usually result in the loss of certain soluble ions in the pore water, and this aspect of the problem is addressed briefly herein for the cases considered.

SLURRY CONSOLIDATION

When a high water content slurry with virtually no shear strength is subjected to an external pressure, the liquid is squeezed from the voids between the solid particles; however, since the permeability of most maintenance dredgings is relatively low, this process of dewatering or consolidation usually takes considerable time. The response of several different dredgings to this type of dewatering procedure is investigated by the use of specially designed slurry consolidometers (Sheeran and Krizek, 1971). Following a brief description of the equipment used and the special adaptation of this equipment to the study of dredgings, test results are presented and interpreted, and appropriate conclusions are drawn.

Test Equipment and Procedures

The basic slurry consolidometer apparatus is shown in Figure 6-1. The fundamental unit is the cylindrical chamber into which the slurry is placed, and the supplemental equipment is used to control the conditions under which the test is conducted. After the piston is placed on top of the slurry, the load is applied by use of precisely controlled air pressure on top of the piston. A sensitive pressure transducer is employed to measure the pore water pressure at the top and/or bottom of the sample. The effluent emitted from the slurry is captured by means of an auxiliary tank on the back-pressure line. Back-pressure is used to enhance complete saturation of the test specimen by driving the last vestiges of gas into solution and hopefully preventing the formation of free gas bubbles during the test.

Figure 6-2 shows a cross-sectional view of the consolidometer, including the drainage lines, chamber pressure lines, bleed line from between the two sealing rings on the piston, and the vent line. Porous stones are embedded in the bottom plate and in the base of the piston to transmit the effluent from the slurry to the drainage lines. A typical schematic diagram of the excess pore water pressure distribution for a case of single drainage (top only) is shown in Figure 6-3.

When the slurry consolidometer is used with a load pacer to achieve automatic loading, the lower drainage line is connected to the load pacer, which senses the pore water pressure in the lower stone. With drainage from the upper stone only, the excess pore water pressure in

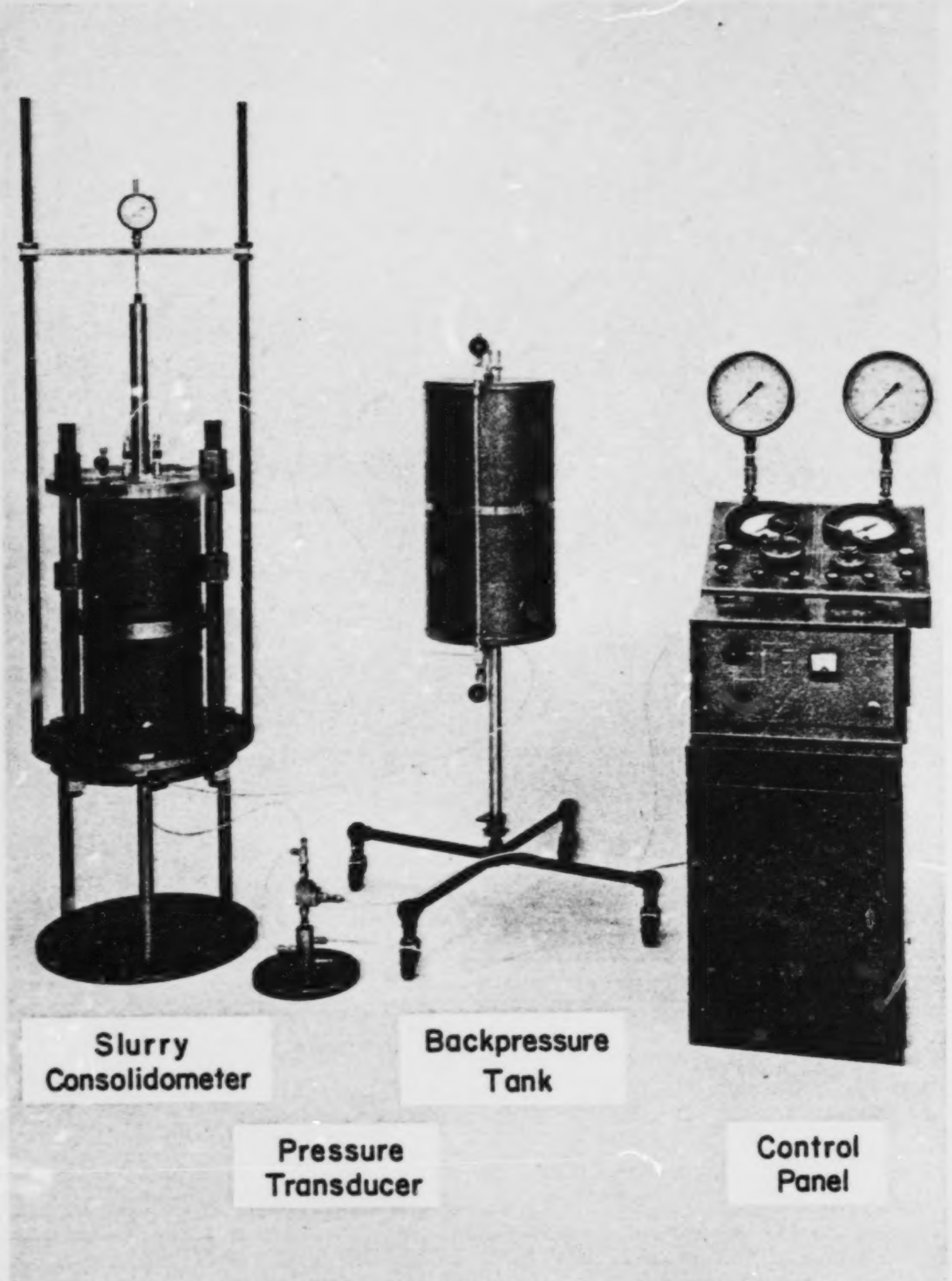
Slurry Consolidometer
Backpressure Tank
Pressure Transducer
Control Panel

Figure 6-1. Slurry Consolidation Apparatus

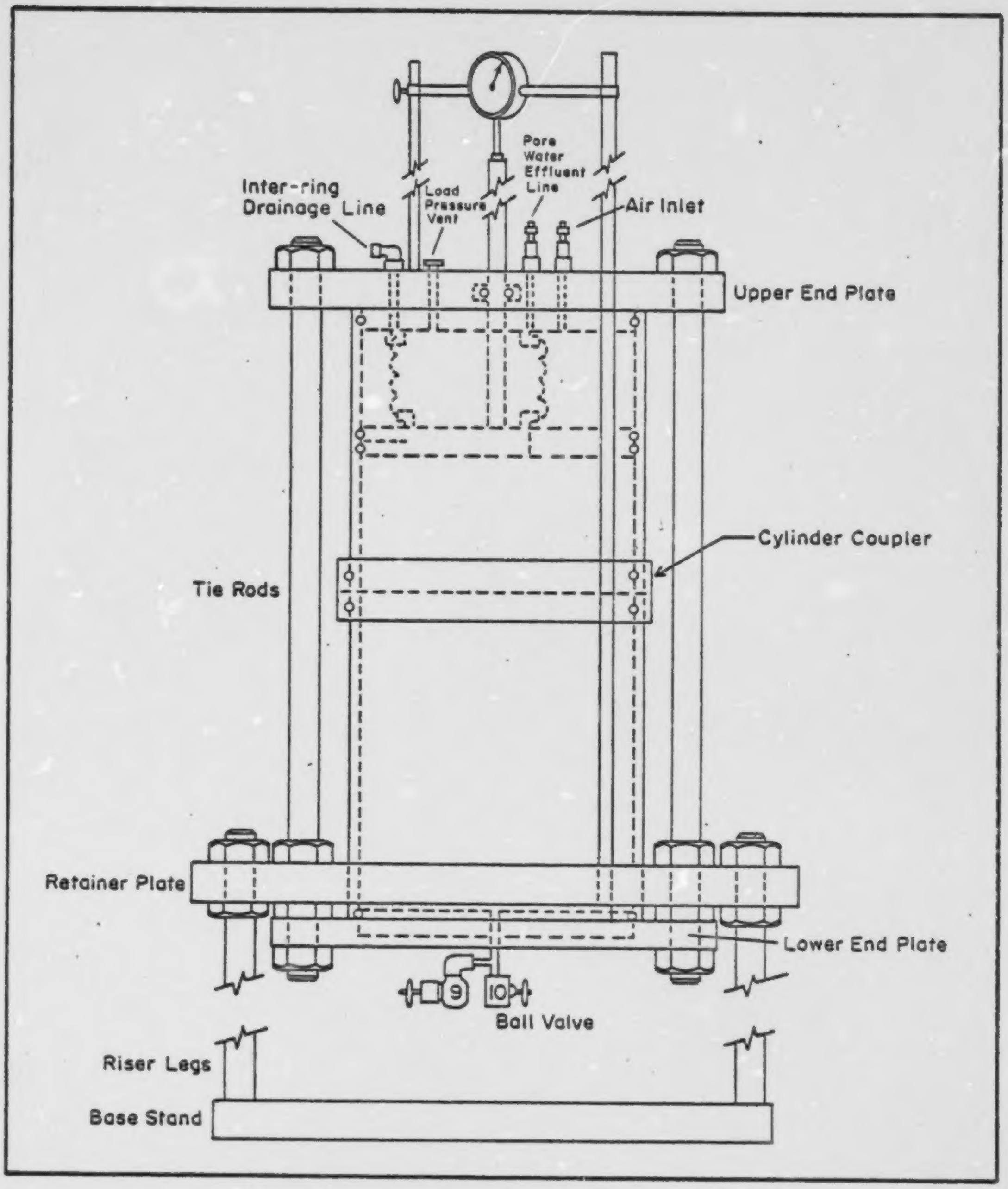
Pore
Water
Effluent
Line
Inter-ring
Drainage Line
Load
Pressure
Vent
Air Inlet
Upper End Plate
Cylinder Coupler
Tie Rods
Retainer Plate
Lower End Plate
9
10
Ball Valve
Riser Legs
Base Stand

Figure 6-2. Cross-section of Slurry Consolidometer

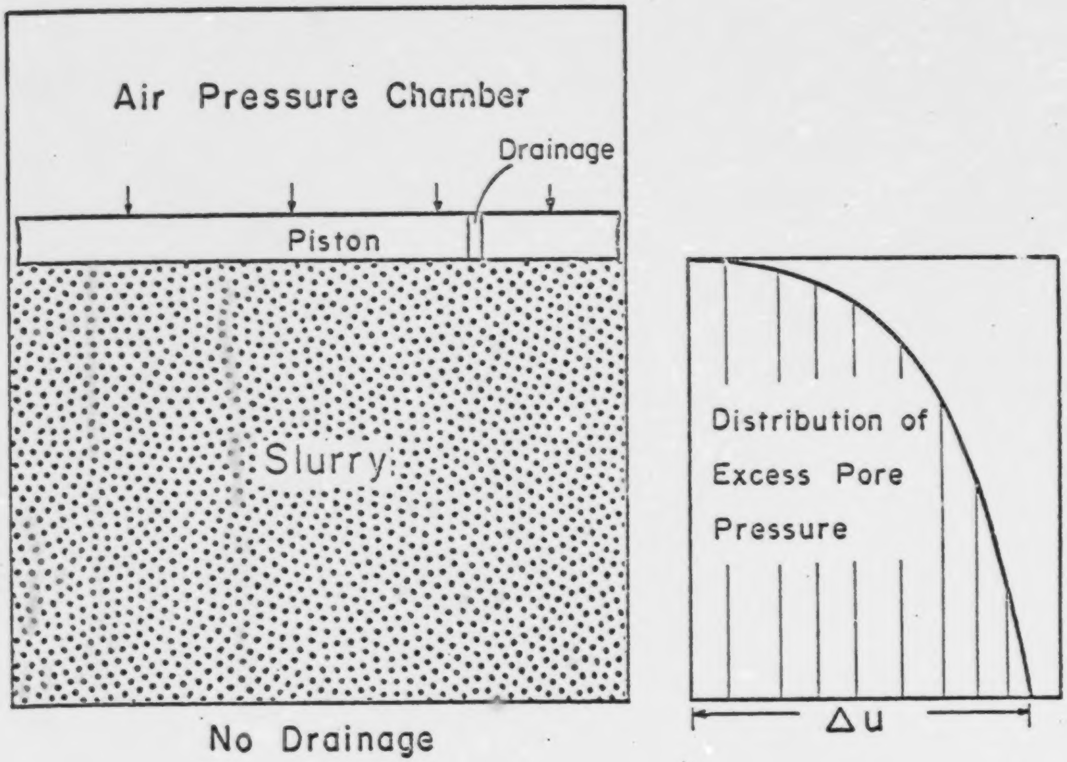
Air Pressure Chamber
Drainage
Piston
Slurry
No Drainage
Distribution of Excess Pore Pressure
Δu

Figure 6-3. Typical Distribution of Excess Pore Water Pressure

the bottom stone is maintained at a preset value, which is greater than that at the upper stone, and the load is continually and automatically increased to maintain the assigned pore pressure difference between the top and bottom stones until the desired total load is reached. During the loading process, the pressure and the movement of the piston are recorded as a function of time. Use of this information and the theory by Lowe, Jonas, and Obrician (1969) allows the coefficients of consolidation and permeability to be calculated; in addition, the compression index may be computed from the relationship between the void ratio, e, and the logarithm of the vertical stress, p.

However, any of several loading schemes may be used with the slurry consolidometer; these include (a) automatic loading, as discussed above, (b) a manually controlled load increment, which is similar to that used for conventional consolidation tests, and (c) a constant rate of strain loading. Based on the results of a preliminary study on one sample of dredgings (D3TO), it was decided to use the manually controlled load increment method for all subsequent tests on dredgings; this decision was made because the gas generating properties of dredgings precluded the use of the load pacer, and the present state of knowledge regarding consolidation theory suggests caution in the use of a constant rate of strain loading procedure. In addition, the load increment method allows a direct association of these test data with those of the conventional consolidation tests reported in Chapter 10.

When the final programmed load was attained in the consolidometer, several options, depending on the information desired, were available for the unloading sequence; for example, one option was to hold the peak load constant for a prolonged period of time to study the secondary consolidation characteristics of the dredgings. Thereafter, the unloading might be either rapid or slow, as desired. Once the loading was removed, the block of consolidated dredgings was removed from the bottom of the test chamber by use of a system shown in Figure 6-4. The piston was secured to the bottom test plate, and both were allowed to move downward as a unit with the sample, thereby minimizing sample disturbance. After the sample was clear of the chamber, the spacer block and nut were adjusted to hold the piston in place, and the block of dredgings was lowered and removed.

Analysis of Results

As shown in Figure 6-5, typical slurry consolidation test data may be plotted directly as the void ratio, e, versus time, t, or the logarithm of time, log t; although the former provides a readily comprehensible demonstration of the measured response, the so-called e-log t curves are usually preferred from an engineering point of view. The selection of one particular point (usually the last one) from each e-log t curve for a given applied stress, p, allows an e-log p curve to be plotted, and representative e-log p curves for each of the twelve samples tested are given in Figure 6-6 with values for the compression indices. Analysis of these data is made with due regard for certain variations in the loading procedure, the unique nature of these materials, and the special features of the test equipment.

A study of the e-log p curves for these materials reveals a nearly linear plot in most cases for the last three load increments. A closer comparison of particular e-log p curves indicates considerable similarities; for example, the points for samples C15TO and C27MM are essentially coincident for the last three load increments, even though the two

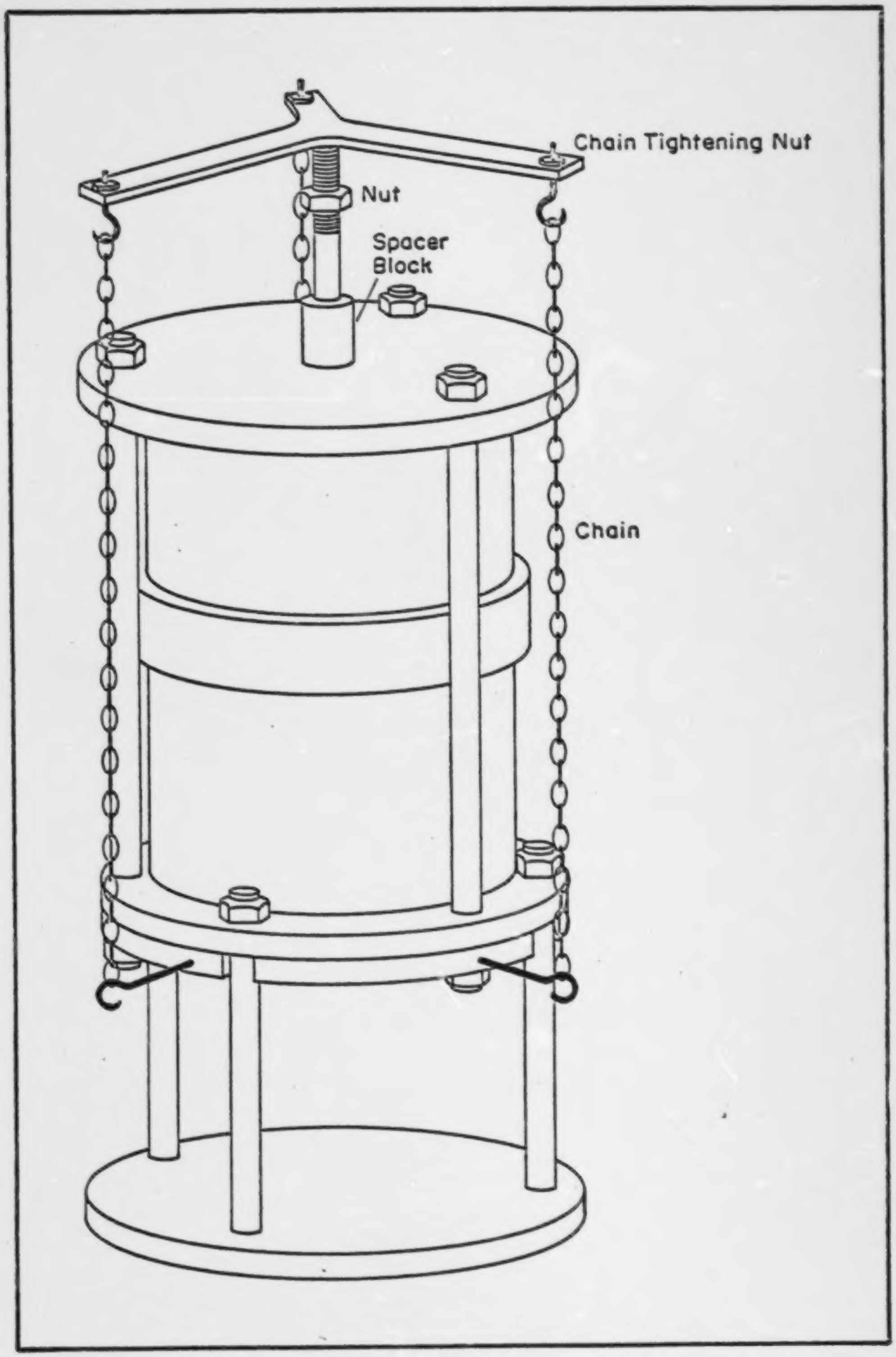
Chain Tightening Nut
Nut
Spacer Block
Chain

Figure 6-4. Slurry Consolidometer Sample Removal System

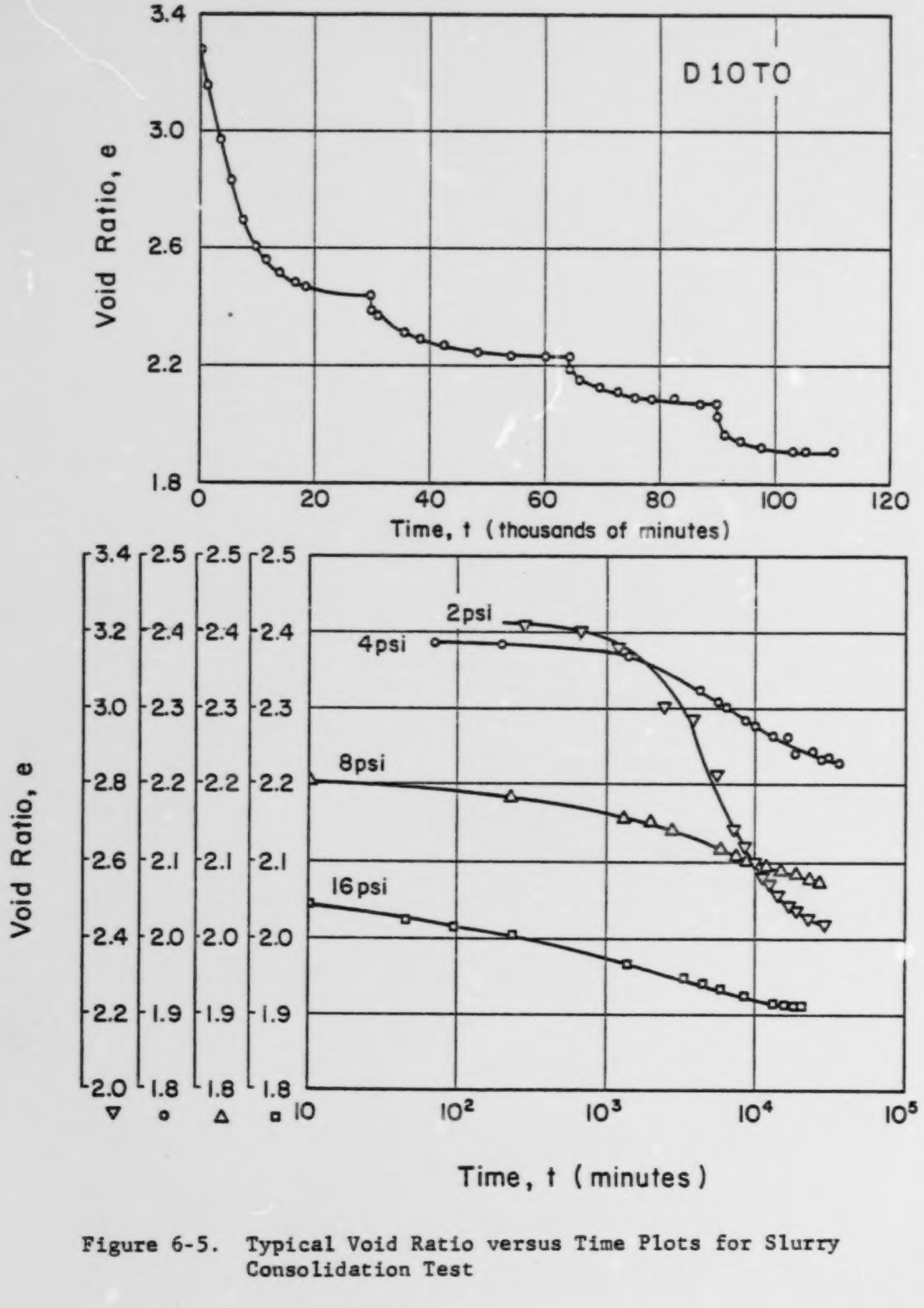

Figure 6-5. Typical Void Ratio versus Time Plots for Slurry Consolidation Test

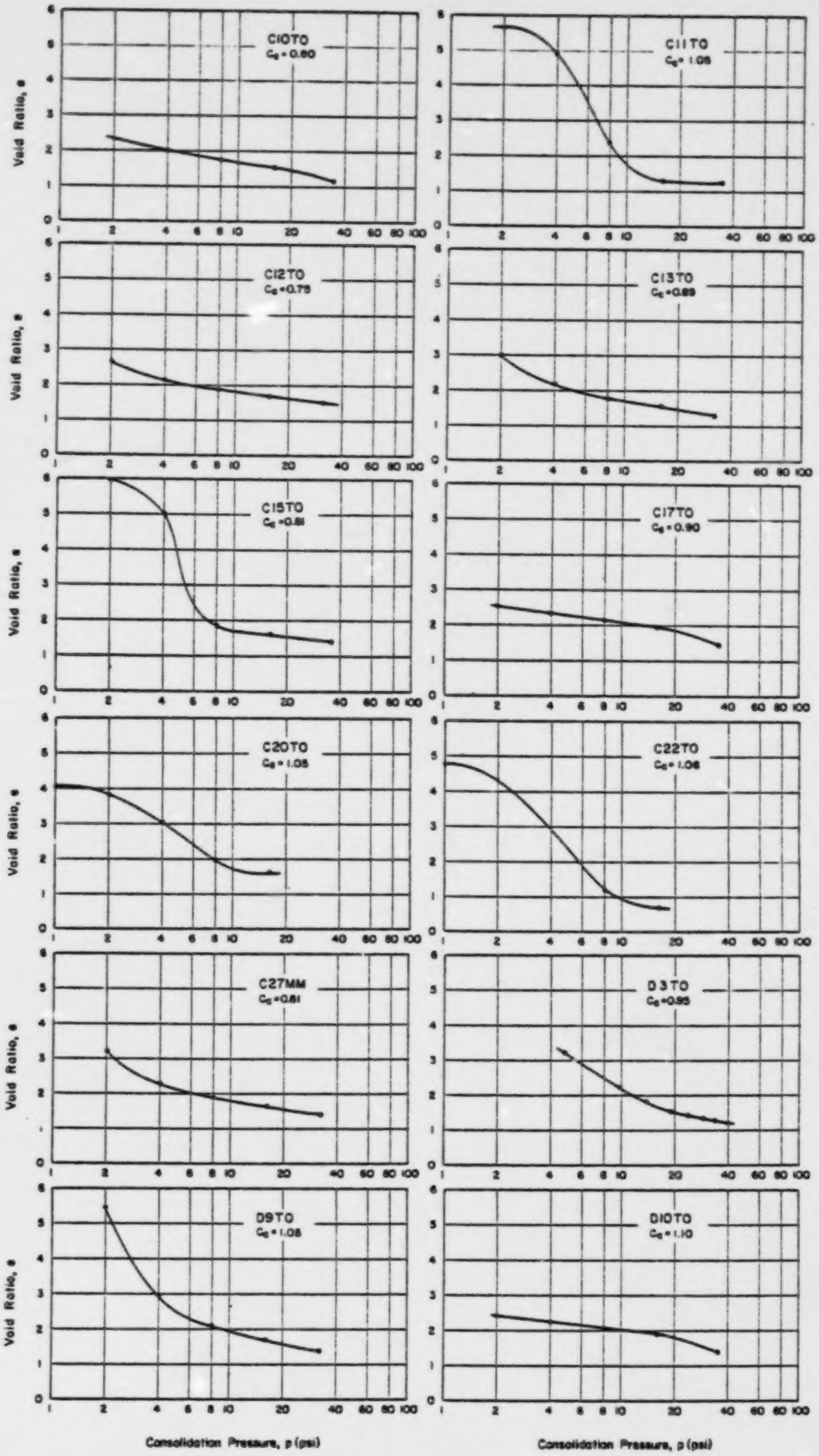

Figure 6-6. Relationships between Void Ratio and Pressure

materials came from different cities and have quite different initial void ratios. In other cases, such as samples C13TO and C27MM or samples C17TO and D10TO, the entire curves are virtually identical. The compression index, C_c, was computed for each material by taking the slope of a "best fit" straight line through the last three or four points (only two points in the case of samples C11TO, C20TO, and C22TO); in the latter two cases (where applied pressures were limited to 16 psi) the values for C_c would probably be lower if additional load increments were applied. The curve for sample D3TO differs from those for the other dredgings due partly to the fact that the load history was dictated by maintaining a constant pore pressure difference across the top and bottom of the specimen, whereas all other specimens were loaded incrementally by doubling the previously applied load, and partly to the fact that it was the first material tested, thereby serving to provide a background of experience. In general, however, the C_c values for virtually all the dredgings tested fall within a fairly narrow range (about 0.91 ± 0.34), even though the samples were taken from bottom sediments with the use of both the flap valve sampler and an Ekman dredge, discharge pipes, the hopper of a dredge, and a fill area.

Perhaps the most striking observations to be made from Figure 6-6 are that (a) most of the test specimens have void ratios of nearly the same magnitude over the final few load increments and (b) the values of the compression index over this loading range are quite close together, even though the initial void ratios varied over a large range. Based on experience with conventional consolidation tests on remolded soils, the compression index usually depends on the material and the initial void ratio, and the void ratio at a particular load increment would be expected to depend on both. In keeping with this experience, the limited test data available suggest that the observed uniformity in consolidation response is related to the relative uniformity in grain size, gradation, and general chemical composition of the different dredgings tested.

The observed e-log p curves for dredgings do differ from those which might be expected from conventional consolidation tests on remolded soils; however, past experience is restricted to soils which possess a lower initial void ratio and sufficient strength and density to retain their shape and volume under a zero applied load condition. One explanation for the initial curved portion of several of the e-log p curves in Figure 6-6 is that the dredgings are simultaneously undergoing drainage due to gravity and drainage due to the applied load. The linear portions of the e-log p curves seem to begin at a void ratio of approximately 2, and this corresponds approximately to the water content obtained by gravity drainage. In addition, the effects of gas generation would probably tend to cause the same type of behavior; as one particular example of the gas generating characteristics of dredgings, a gas sample taken from D3TO was analyzed and found to contain 3.6 percent oxygen, 15.7 percent carbon dioxide, and 16.8 percent methane, with the remainder composed mostly of nitrogen.

A study of the typical e-log t curve shown in Figure 6-5 for the slurry consolidation of sample D10TO reveals a more irregular pattern than usually found for most soils undergoing conventional consolidation. In some cases not illustrated herein the curves for the low intensity of loading indicate an increasing void ratio with time; this behavior is attributed to the gas generation characteristics of the particular material, whereby the pressures developed by the generated gases exceed the applied pressures and cause an expansion of the sample. The curves become more regular at the higher loadings, thus suggesting a combined effect due in part to the inhibition of gas generation at higher loadings and in part to the decrease in gas generation with time. Some of the curves exhibit a tendency toward a flatter slope at the end of the loading period, thereby indicating the completion of primary consolidation and the beginning of secondary consolidation. Most of the loads were held constant for at least a week, and many loads were held constant for several weeks.

An analysis of the chemical constituents of the fluids drained from the dredgings shows a surprising uniformity in the concentrations of certain ions in the fluids during the entire consolidation process. As seen in Table 6-1, the soluble ions of sodium, potassium, and calcium were carried off in the fluid, whereas aluminum, cadmium, lead, and copper were essentially retained with the solids in the consolidometer.

Conclusions and Recommendations

Based on the limited experimental program reported herein for slurry consolidation tests on several samples of dredgings, the following conclusions can be advanced:

1. The slurry consolidation equipment is very useful for studying the consolidation characteristics of materials which are too soft and/or too fluid to test in the conventional manner.
2. The compression index is generally larger than 0.6 and may be considerably larger at high initial void ratios and under light loading.
3. The field consolidation of dredgings is considered to be reasonably well modeled by the test procedure involving the slurry consolidometer; in both cases there will be large strains and gas generation, which violate two of the basic assumptions of classical consolidation theory.

Additional research is needed on the consolidation characteristics of gas generating materials; such research will allow a better interpretation of the data obtained in this test program, and it would lead to

Table 6-1

Chemical Analyses of Liquids from Slurry Consolidation Tests

Sample	Effluent Specimen	Vertical Stress (psi)	Time (min)	Concentration in ppm					
				Pb	Cu	K	Na	Ca	Fe
C11TO	1	1	970	0	0.15	27	22	0	10
	2	4	7,416	0	0.85	27	21	8	--
	3	8	11,090	0	--	32	23	12	10
	4	16	32,603	0	--	27	26	28	--
C13TO	1	2	8,480	0	0.05	27	23	75	4.3
	2	2	11,320	0	0.03	27	21	75	12.2
	3	4	19,100	0.25	0.15	27	23	132	2.5
C15TO	1	4	1,360	0.25	0.03	18	25	95	2.7
C20TO	1	1	970	0	0.05	27	28	22	2.3
	2	8	11,090	0	--	27	--	12	2.5
	3	16	22,585	0	0	27	28	8	2.5
C22TO	1	1	970	0	6	23	30	4	--
	2	4	7,416	0	0	--	--	--	--
	3	8	11,090	0	--	27	--	50	--
	4	16	22,586	0	0	27	25	34	1
C27MM	1	2	1,460	0	0	14	27	50	2.8
	2	2	11,320	--	1	14	25	34	0.3
	3	4	19,100	0	0	14	27	75	2.3
	4	4	19,820	0	0	14	26	56	2.8
D9TO	1	2	8,480	0.25	0.01	18	22	75	2.5
	2	2	11,320	0	0.01	18	23	65	2.5
	3	4	19,100	0.25	0.03	23	23	95	80

improved theories and testing techniques. There is also a need for more comprehensive analyses of the volumes and composition of the gas generated, and a study should be made of the relationship between the applied pressure and the generation of gas.

DRAINAGE

The drainage testing program was designed to study the rate of water loss from several different dredging materials due to (a) gravity only, (b) gravity plus vacuum with the air pressure being directly applied to the surface of the dredgings, and (c) gravity plus vacuum with a membrane between the surface of the dredgings and the atmosphere. This study was conducted in three series of drainage tests. The first and second series used essentially the same equipment and procedures, with the second series incorporating several minor improvements based on the experience gained in the first series. In the third series, only gravity drainage was used. The following sections present the equipment and procedures used, the results obtained, an analysis of these results, and several conclusions.

Equipment and Procedures

The test equipment consisted of a series of plexiglass cylinders with porous stones fitted into the bottom of each cylinder; the effluent was collected in bottles, and the bottle was either vented to the atmosphere for gravity drainage or connected to a vacuum line for vacuum drainage. Two variations of vacuum drainage were used; in the first the air pressure due to the atmosphere was applied directly to the surface of the dredgings, whereas in the second a membrane was placed between the dredgings and the atmosphere. It was found that relatively tall cylinders were preferable to shorter ones; thus, the first and second test series used cylinders 6 inches in diameter and 25 inches high, whereas the third series, in an effort to use a smaller volume of dredgings per test, was conducted in cylinders 3 inches in diameter and 20 inches high.

Due to the expected low rates of drainage, all tests were conducted in a humid room to minimize incidental water losses. However, during the first test series, it was found that significant moisture was still being lost through the top surfaces of the dredgings, even though thin sheets of plastic were draped over the tops of the cylinders. One improvement in the second and third series was to use a smooth fitting plexiglass disk for the top plate; a one-eighth inch brass elbow was fitted into the top to allow equalization of the inner and outer pressures. The adequacy of this arrangement was proven by showing that the water losses from a cylinder filled with only water and with no drainage allowed were insignificant.

The test data also revealed significant losses of water due to evaporation from the collection bottles which were under vacuum, but losses from the bottles vented to the humid room atmosphere were insignificant. Corrections were made for these losses by using the data obtained from weight changes in a bottle of water on the vacuum line, but not connected to a specimen. A plexiglass plug was designed for use with a membrane at the top of several of the cylinders in order to allow atmospheric pressure to act on the dredgings indirectly; the intended purpose was to accelerate the drainage process and hopefully allow the dewatering to continue into the unsaturated range. However, both the initial system and the modified system did not function as hoped due to air losses past the membranes; the slight eccentricity of the plexiglass tubes did not allow the plug to be fitted with suitable tolerances. As a result of these difficulties, the data from the vacuum drainage tests with membranes are not felt to be as good as those from the same type of tests without membranes. Samples of the drainage water were taken for chemical analysis, and these were tested according to the procedures presented in Chapter 4.

Results

Figure 6-7 gives plots of the cumulative weight of the water lost as a function of time for five typical dredgings (C2DM, C5CO, D1DM, D3TO, and D4CO) drained under three different conditions; the C samples are from the first series, whereas the D samples are from the second series. The discontinuity in the drainage rates for the C samples is attributed to a continually worsening leak in the vacuum line; when fixed on the ninth day of the test, the time rate of drainage accelerated greatly for a few days. Figure 6-8 presents the results from six tests in the third series, which employed gravity drainage only; the top part of the figure describing each test gives the changing levels of the sediment and water surfaces as a function of time, and the lower part of each figure gives the weight of the water lost. The results of the chemical tests are summarized in Table 6-2, wherein the symbol M designates vacuum with a membrane; V, vacuum without a membrane; and G, gravity only.

Analysis of Results

A study of the data presented in Figure 6-7 indicates that (a) the use of a vacuum extracted significantly larger quantities of water from the dredgings than did gravity alone and (b) the major effect of the vacuum occurs during the initial time period. For example, the drainage amounts after one day with vacuum were from one and a half to five times the amounts obtained for gravity alone; viewed differently, the amount of drainage

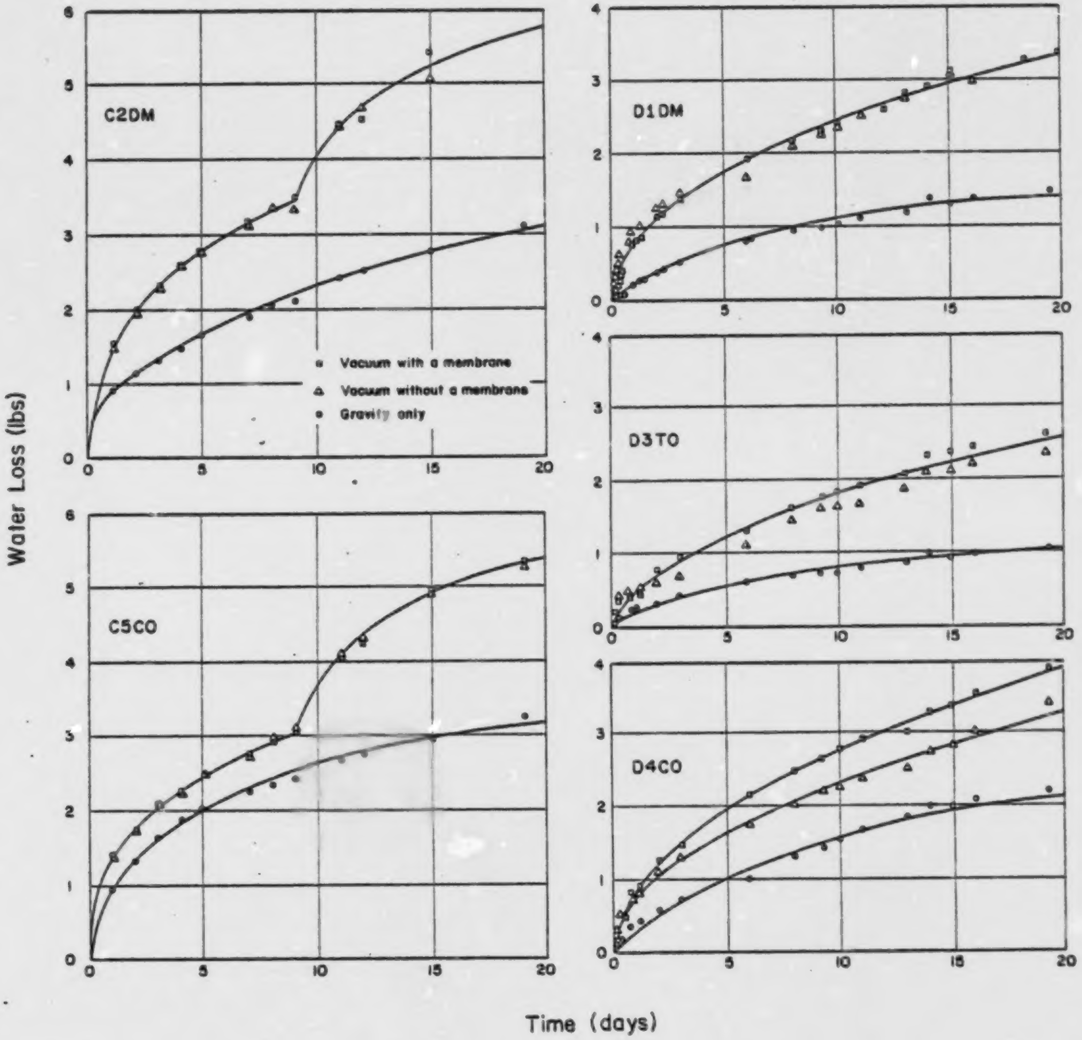

Figure 6-7. Rates of Drainage by Gravity and Vacuum Methods

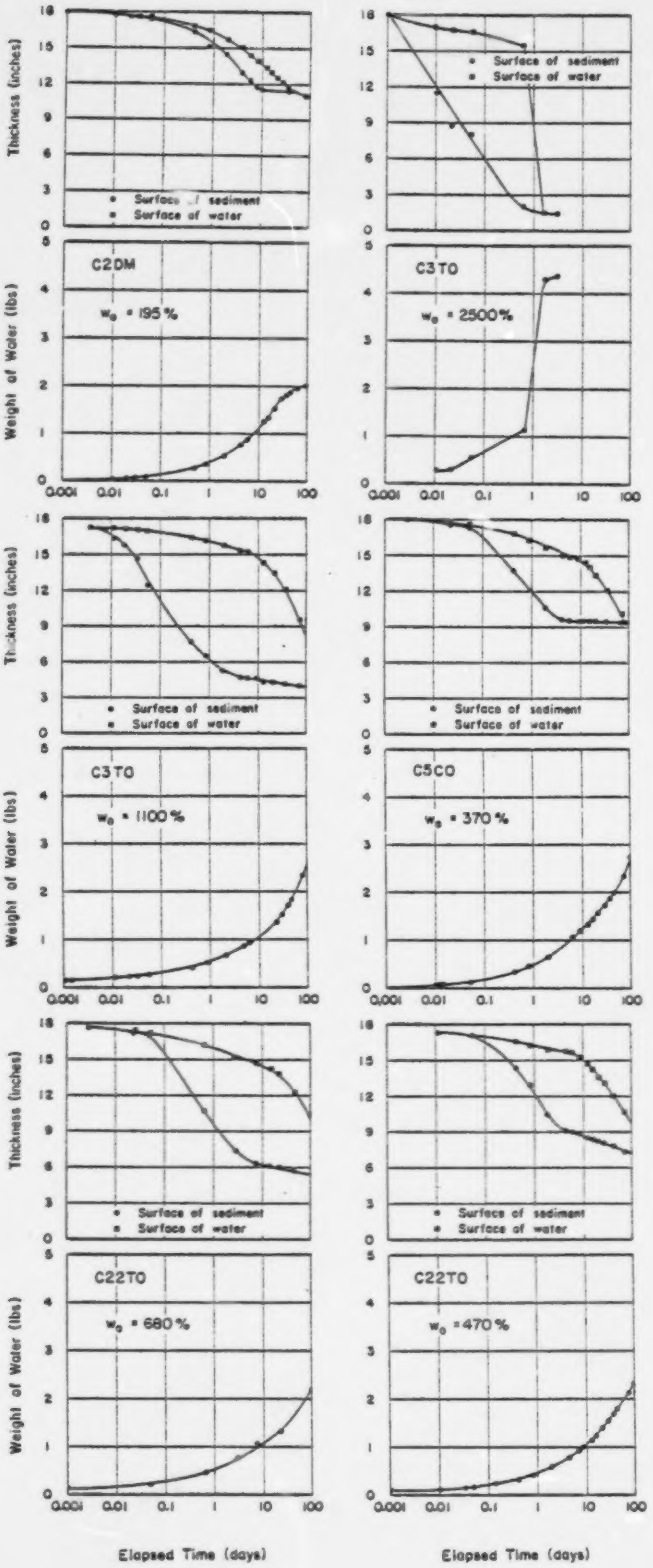

Figure 6-8. Data from Gravity Drainage Tests

with vacuum during the first five hours was about the same as by gravity alone for the first day or two, while the drainage by vacuum for one day was comparable to that by gravity alone for about a week. After three weeks, the amounts of drainage by gravity alone were about one-half of those achieved by vacuum for all samples.

An examination of the height-versus-time curves presented in Figure 6-8 reveals that, shortly after the test was begun, the material settled and left a zone of relatively clear water above it. As drainage occurred, the sediment densified, and its top surface lowered initially more rapidly than the water surface. At a later stage in the drainage process, the surface of the sediment tended to stabilize as the water continued to drain from the specimen, until eventually the water surface reached the sediment surface. All four materials tested in this series had an initial thickness of about 18 inches, but the time for drainage varied considerably for the different materials and with different concentrations of solids for a given material. The drainage times varied from about one day for sample C3TO at a water content of 2500% to periods in excess of 100 days. Several of the tests were concluded before all the free water had drained (Sample C3TO with an initial water content of 1100%, and both tests on Sample C22TO), in which cases the excess free water was syphoned out to allow the vane shear strength determination to be made on the sediment. Specific values of the shear strength are reported in Chapter 10 together with a full presentation of all strength data.

Table 6-2 presents the chemical analysis of the fluids drained from the D1DM, D3TO, and D4CO materials. Note that the values in Table 6-2 are on a wet weight basis, whereas those in the comparable tables in Chapter 4 are on a dry weight basis. A comparison of the concentrations

Reproduced from best available copy.

Table 6-2

Chemical Analyses of Liquids from Drainage Tests

Sample	Total Solids	Total Volatile Solids	Total Suspended Solids	Total Volatile Suspended Solids	Turbidity	Acidity	Hydrogen Ion Concentration (pH)	Oxidation-Reduction Potential (Eh)	Dissolved Oxygen (DO)	Biological Oxygen Demand (BOD)	Chemical Oxygen Demand (COD)	Organic Nitrogen (N)	Ammonia (NH$_3$) Nitrogen (N)	Nitrite (NO$_2$) Nitrogen (N)	Nitrate (NO$_3$) Nitrogen (N)	Total Phosphate (PO$_4$)	Soluble Phosphate (PO$_4$)
	%	%	%	%	JTU	mg/gm		mv	mg/gm	mg/gm	mg/gm	mg/gm	mg/gm	mg/gm	mg/gm	mg/gm	mg/gm
D1DM-H	0.1681	0.0914	0.0126	0.0065	92		9.2	0.030		0.1000	0.672	0.0121	0.0356	0	0.0188	0.0061	0.0061
D1DM-V	0.1726	0.0835	0.0083	0.0054	58		9.1	0.025		0.0662	0.586	0.0157	0.0291	0	0.0131	0.0020	
D1DM-C	0.1318	0.0516	0.0124	0.0072				0.030		0.0409	0.309	0.0330	0.3359	0	0.0097	0.0017	
D3TO-H	0.1256	0.0336	0.05[illegible]		100		8.8			0.0935	0.287			0	0.0073	0.0008	
D3TO-V	0.1076	0.0336	0.0356	0.0091	130		8.5	0.025		0.0850	0.186	0.0011	0	0	0.0072	0.0015	
D3TO-C	0.0731	0.0165	0.0185	0.0035	70		9.2	0.020		0.0505				0	0.0046	0.0002	
D4CO-H	0.1952	0.0540	0.0244	0.0070	55		9.0	0.065		0.0566	0.349	0.0112	0.1337	0	0.0076	0.0033	
D4CO-V	0.1381	0.0423	0.0065	0.0025	36		8.9	0.030		0.0675	0.315	0.0190	0.2532	0	0.0078	0.0061	
D4CO-C	0.1210	0.0352	0.0188	0.0045	45		8.7	0.030		0.0656				0	0.0096	0.0041	

Sample	Grease	Hydrocarbons	Aluminum (Al)	Arsenic (As)	Calcium (Ca)	Copper (Cu)	Total Iron (Fe)	Soluble Iron (Fe)	Potassium (K)	Silica (SiO$_2$)	Sodium (Na)	Sulfide (S)	Cadmium (Cd)	Cyanide (CN)	Lead (Pb)	Mercury (Hg)	Phenolics
	mg/gm	mg/gm	mg/gm	mg/gm	mg/gm	mg/gm	mg/gm	mg/gm	mg/gm	mg/gm	mg/gm	mg/gm	μg/gm	μg/gm	μg/gm	μg/gm	μg/gm
D1DM-H			0.030		0.0737	0.0117	0.185		0.022	0	0.200		0		0	0.0175	
D1DM-V			0.030		0.0652	0.0083	0.185		0.040	0	0.180		0		0	0.0021	
D1DM-C			0.030		0.0997	0.0061	0.115		0.038	0	0.120		0		5.5		
D3TO-H			0.040		0.1000	0.0061	0.280		0.028	0	0.050		0		4.0	0.0037	
D3TO-V			0.040		0.1040	0.0061	0.200		0.020	0	0.034		0		0	0.0016	
D3TO-C			0.030		0.0870	0.0084	0.075		0.012	0	0.034		0		2.0		
D4CO-H			0.040		0.0850	0.0093	0.390		0.063	0	0.240		0		6.0	0.0136	
D4CO-V			0.040		0.0630	0.0150	0.200		0.050	0	0.200		0		3.5	0.0039	
D4CO-C			0.015		0.0720	0.0110	0.280		0.072	0	0.150		0		6.0	0.0095	

of the various constituents may be made with the values found in Chapter 4 for the original D1DM, D3TO, and D4CO materials and for the various water samples analyzed. These comparisons indicate that the fluids from these drainage tests contained about three times more solids than the water samples from the Maumee River. Most of the other parameters, such as turbidity, biological and chemical oxygen demand, nitrogen, phosphates, sodium, potassium, and calcium were also higher. Significant quantities of mercury, copper, aluminum, and iron were found in the drainage effluents, but most of the heavy metals were retained in the sediments.

Conclusions and Recommendations

Subject to the scope of the drainage test program described herein, the following conclusions can be deduced:

1. Vacuum drainage removes water from dredgings much faster than gravity drainage alone, and it allows greater amounts of water to be extracted in a given period of time.
2. The maximum effect of vacuum on the drainage response is achieved during the initial time period, and less significant effects are observed over longer periods of time.
3. Different dredgings drain at different rates and are affected to different degrees by vacuum drainage.
4. The drainage characteristics of a given material depend on the nature of the solids and the fluids, as well as the water content at the time of drainage.

When dewatering is considered for a particular site, it is recommended that a drainage test be conducted on the material to determine the specific effects of vacuum compared to gravity alone, since the results for the seven materials tested indicated significant differences for different materials. If additional tests of the type described herein are to be conducted, a sufficient volume of a suitable chemical should be placed in the vacuum line between the collecting bottle for each sample and the vacuum source to adsorb the moisture from the air. This would allow a better determination of the amount of water emitted from the sample, and it would also be beneficial for the vacuum pump.

CHAPTER 7

ELECTRO-OSMOSIS

As discussed previously, the potential usefulness of a landfill composed of dredging spoil is largely governed by the degree of stability which can be achieved by treatment during and/or after deposition, and the study reported in this chapter is directed toward evaluating the possibility of stabilizing such a land mass by use of electro-osmosis. To achieve this end, four typical dredgings from different locations have been subjected in the laboratory to three different electrical gradients (including a zero electrical gradient), and the effects of this treatment on the strength, compressibility, and time rate of dewatering have been measured. The resulting data provides a preliminary indication of the practical and economical feasibility of applying electro-osmosis to improve the engineering properties of dredging wastes.

ELECTRO-KINETIC PHENOMENA

Electro-osmosis, streaming potential, electro-phoresis, and sedimentation potential are an interrelated family of electro-kinetic phenomena. Electro-osmosis is the process whereby a liquid moves through a matrix of fixed particles in response to an applied electrical field. The opposite phenomenon is termed the streaming potential, and a potential difference is established with respect to a matrix of fixed particles due to the movement of a liquid over the particle surfaces. When the particles are not fixed, they will move in response to an applied electrical field, and this is known as electro-phoresis. In contradistinction, when particles are forced to move through a liquid, a potential is developed, and this condition is known as the sedimentation potential. Since soil is normally considered to be a matrix of fixed particles, the phenomena of electro-osmosis and streaming potential would be expected to occur, and this is indeed the case, as demonstrated by many experiments and applications. There is, in fact, a theoretical relationship between electro-osmosis and the streaming potential, and some research has been directed toward establishing experimental verification of this theory.

In addition, there is a considerable amount of literature dealing with the many differing aspects of electro-osmosis. Early research in the field was confined primarily to the development of equations that could explain and predict the phenomenon. It was not until the 1930's that interest was shown in the possibility of actually using electro-osmosis for field applications. The 1940's and 1950's saw considerably more research and additional applications of electro-osmosis to stabilize slopes, dewater soils, increase the bearing capacity of piles, etc. In the 1960's research was conducted to determine the best theory or combination of theories to describe electro-osmosis in such a way as to be better able to ascertain its applicability to particular field problems and to predict the results that might be expected. Despite this effort, however, there is still no single unifying theory of electro-osmosis; this is due in large part to the many interrelated parameters (such as water content, particle size, particle size distribution, cation exchange capacity, organic content, pH, electrolyte concentration, temperature, ion valence, size of hydrated ion, etc.) which influence the phenomenon.

EXPERIMENTAL PROGRAM

The materials used for this study were samples C[illegible]2TO, C27MM, D1DM, and D4CD. Some characteristics of these samples are summarized in Table 7-1, and the respective grain size curves, as obtained with and without a flocculent (Calgon), are shown in Figure 7-1.

Apparatus

An apparatus was designed and constructed to enable (a) the uniform consolidation of the dredging samples under a pressure of approximately 0.6 kg/cm^2, and (b) the simultaneous application of a potential difference across the ends of the sample. This apparatus consisted of three main parts: three consolidation cells, a loading frame capable of loading three cells simultaneously, and the necessary electrical equipment to apply a voltage difference across two of the cells; no electrical gradient was applied across the third cell.

In order to be non-conductive, the consolidation cells were constructed almost entirely of plexiglass. A thin teflon sheet etched on one side was affixed to the inside surface of a plexiglass cylinder (height of 10 inches, inside diameter of 5.5 inches, and wall thickness of 0.25 inches) to provide more uniform consolidation by minimizing the side wall friction as much as possible. A movable piston with two O-rings was fitted to the inside of the lined plexiglass cylinder with the lowest amount of drag consistent with maintaining an effective seal for the pore water pressures developed due to loading. Carborundum porous stones were attached to the piston and the base, and separate drainage outlets were provided for each. For the cells in which an electrical gradient was to be used, sheets of perforated stainless steel were affixed to the porous stones to serve as electrodes. The cylinder was held in place by means

Table 7-1

Engineering Characteristics of Samples Tested

Sample	Water Content %	Solids Content (gm/cc)	Organic Content %	Specific Gravity	Liquid Limit %	Plasticity Index %	Shrinkage Limit %
C22TO	138.0	0.510	3.7	2.56	69	29	24
C27MM	142.8	0.531	7.6	2.51	59	10	23
D1DM	99.3	0.717	12.5	2.53	56	17	40
D4CO	117.0	0.650	8.2	2.74	50	13	40

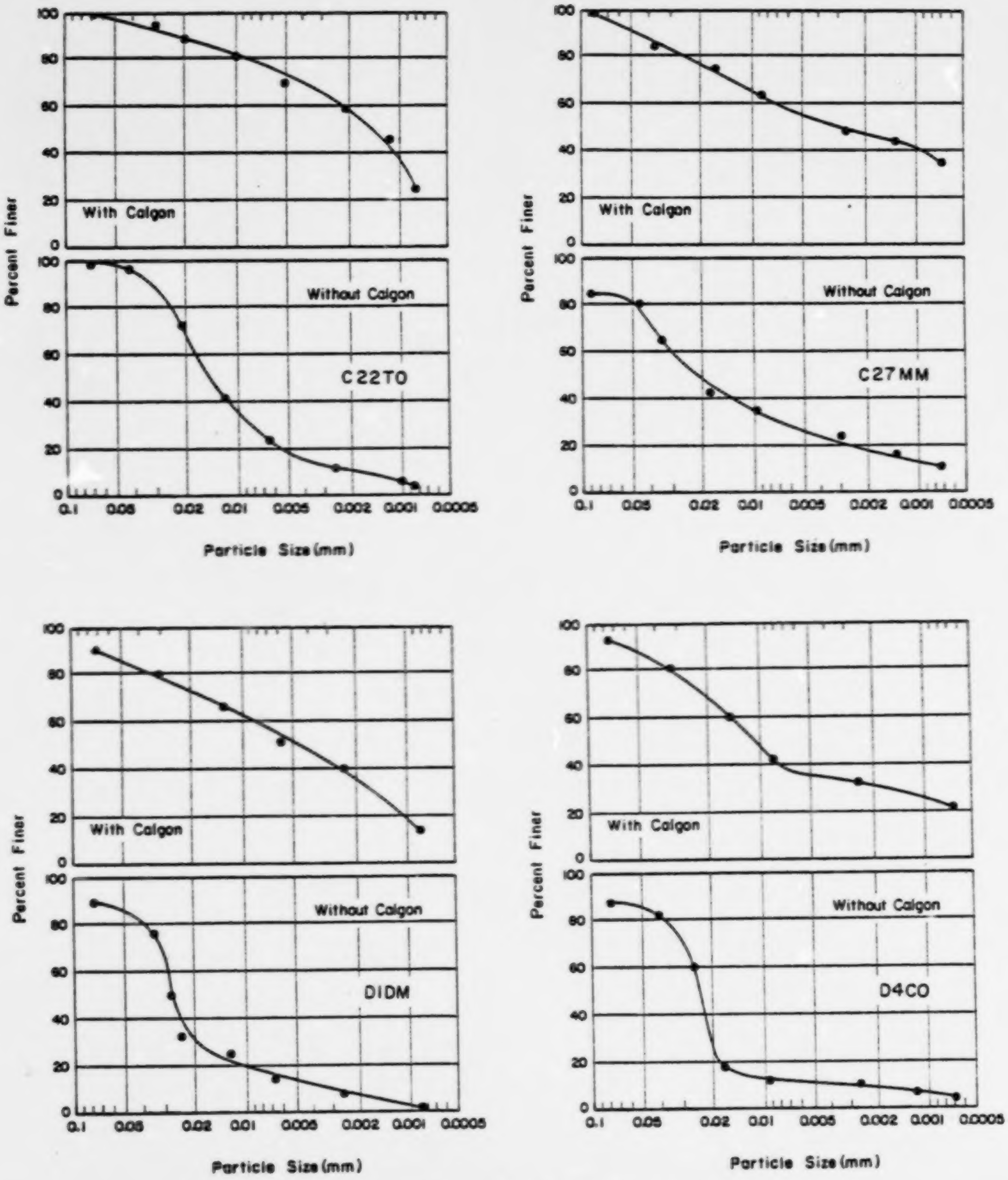

Figure 7-1. Particle Size Distribution Curves

of four assembly rods which connected a top plate to the base.

A fixture for holding a thermometer was attached to the exterior of the plexiglass cylinder at approximately the mid-point of the initial sample height; this permitted the measurement of temperature changes in the samples. Several small holes were drilled into the side of one of the plexiglass cylinders in order to enable the electrical potential to be monitored at several points within the sample by means of a hypodermic needle. Scales were fixed to the outside of the plexiglass cylinders to allow the changes in sample height to be monitored.

The pressure and loading system, which comprised the second part of the testing apparatus, consisted of a structural steel frame with hydraulic cylinders mounted directly over each cell. The hydraulic cylinders were connected to an air-oil interface reservoir, wherein the air pressure was supplied by a constant air pressure source and regulated by a constant bleed air regulator, which controlled the air pressure to within one psi during the test.

The third part of the testing apparatus was the electrical system, which consisted of two power sources and a Wheatstone bridge. The direct current power sources were supplied by a constant voltage regulator to reduce line fluctuations. The cathode and anode of the direct current power supply were connected to the base and top electrodes, respectively, and direct current voltage and current meters were included in each circuit. After two dredging materials were tested, it was noted that a considerable amount of power was being lost through corrosion of the electrodes, the filter paper at the sample ends, and heat generation. In order to obtain an estimate of these losses and the manner in which they varied, a Wheatstone bridge arrangement was devised to measure the potential at the ends of the sample and thereby give an indication of the actual energy reaching the sample. This arrangement was designed and constructed into the system so that it could be switched from one cell to the other. A one-thousand ohm ten-turn potentiometer, combined with a micro-amp meter, provided sufficient sensitivity for measuring the potentials within and at the ends of the sample. The potentiometer was installed between the cathode and the anode, and the variable post was connected to the micro-amp meter, which, in turn, was connected to the probe. The Wheatstone bridge was then balanced by zeroing the micro-amp meter and the potential determined as a percentage of the potentiometer reading.

Testing Procedure

Electrical gradients of one-half and one volt per centimeter of initial sample height were selected as typical of values which have been used successfully in previous field applications of electro-osmosis; in addition, a reference test with zero electrical gradient was conducted on each material. It is significant that the voltage difference across the sample was determined on the basis of the prescribed initial gradient and the initial height of the specimen, and this voltage difference was maintained constant throughout the test; in effect, this means that the actual gradient across the specimen increased with time since the sample height decreased. All samples were drained at both the top and bottom surfaces, but the electrical gradient always induced flow toward the bottom.

The dredgings were loaded into each cell with the occasional use of a small vibrator; the top and bottom porous stones were fully saturated and covered with a sheet of filter paper. The piston was then inserted into the cylinder, the assembly rods were secured, and, after appropriate measurements were recorded, each cell was installed in the loading frame, and the test was started. The testing sequence is outlined briefly in Figure 7-2. In addition to the usual measurements of sample height, temperature, current, and weight of fluid discharged, the Wheatstone bridge was used to record the potential at the cathode and the anode and, whenever possible, the potentials at various probe points. Effluent samples were collected and subjected to chemical analyses.

After the electro-osmosis portion of the test was completed, the cell was disconnected and weighed, and the sample was removed. This consolidated sample was then subjected to a planned series of vane shear tests while supported along the sides. A motor-driven vane, rotated at a rate of one revolution per hour until failure of the soil, was used to perform three vane shear tests at each of three different depths in each sample. The remolded strength was determined by revolving the vane rapidly through ten revolutions and then repeating the test at the same location. A specimen taken from the center of the sample was immediately subjected to a conventional consolidation test. The tests for organic content, Atterberg limits, and chemical constituents were then performed.

RESULTS AND INTERPRETATION

Presented herein are the results of the experimental investigation and interpretations of the observed effects, which include the energy requirements, effects on chemical constituents, and the resulting changes in the engineering properties of the dredgings.

Energy Relationships

The voltage measured at various points along the specimen indicate a generally linear gradient with some variation near the electrodes. Figure 7-3 allows a comparison of the power consumed by the dewatering process

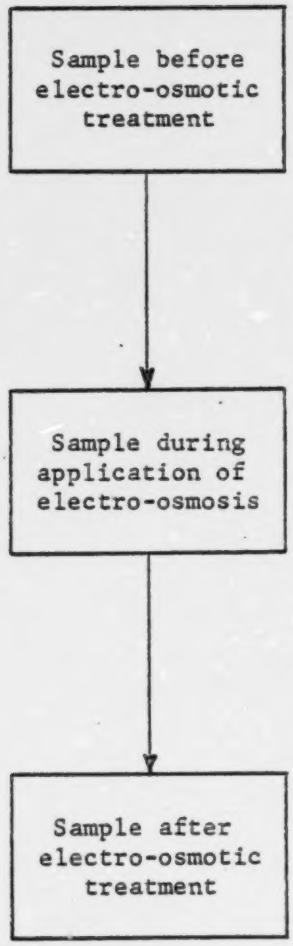
Sample before electro-osmotic treatment
Sample during application of electro-osmosis
Sample after electro-osmotic treatment

1. Moisture content
2. Solids content
3. Hydrometer analysis
4. Organic content
5. Chemical analysis
6. Atterberg limits

1. Time and date
2. Change in sample height
3. Temperature
4. Current and potential difference
5. Effluent samples
6. Chemical analysis of effluent

1. Vane shear
2. Consolidation
3. Moisture content
4. Organic content
5. Atterberg limits
6. Chemical analysis

Figure 7-2. Outline of Experimental Program

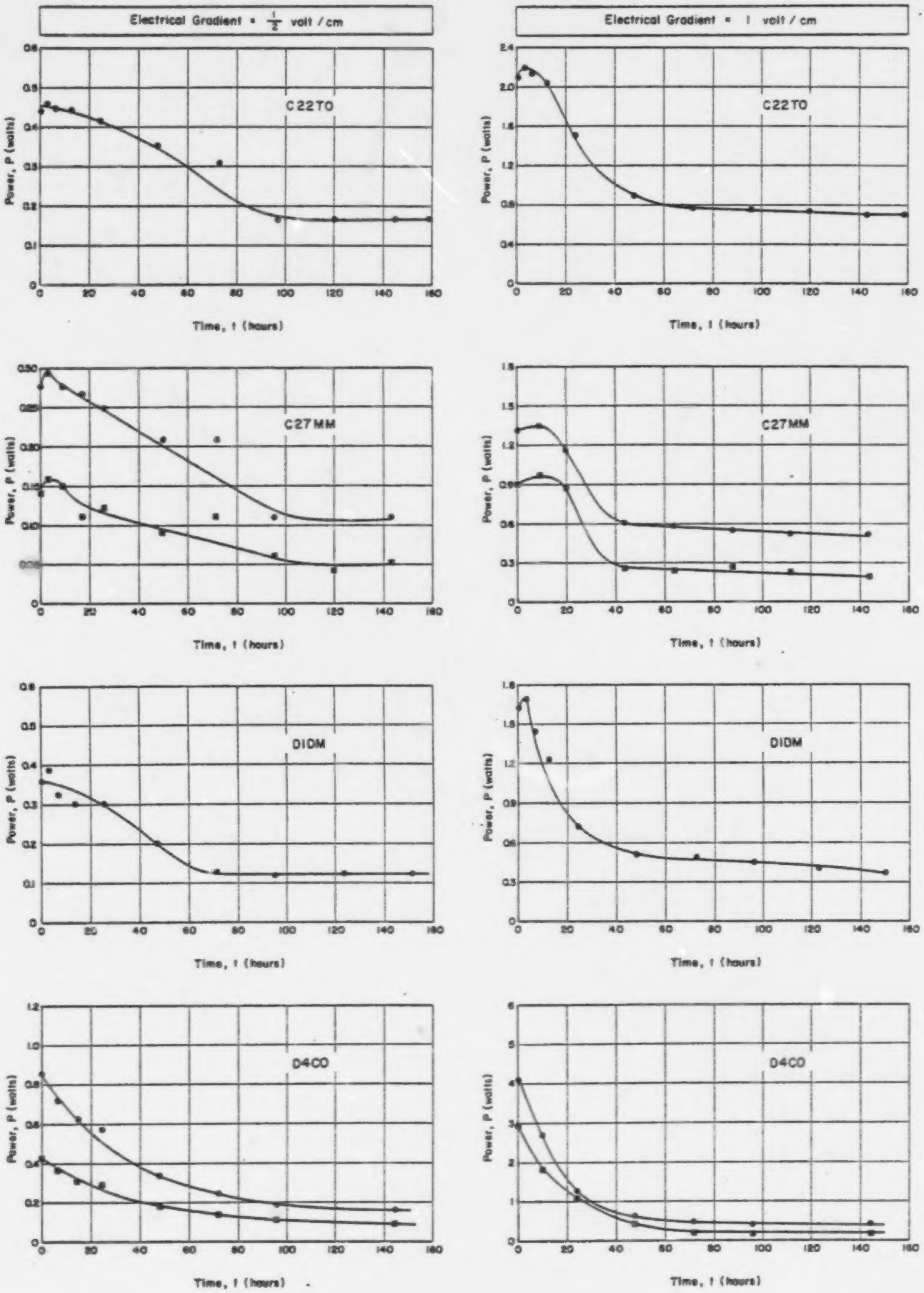

Figure 7-3. Power Requirements versus Time

for the three conditions investigated. Initially the specimens with an electrical gradient of one volt per centimeter used about five times as much power as those subjected to a gradient of one-half volt per centimeter, but this ratio decreased with time to a value of approximately two or three. In the tests on samples C27MM and D4OO the power reaching the soil was determined in addition to the total power used, and it is noted that about half of the total energy was lost in each case. The power loss in the specimens subjected to a gradient of ½ volt/cm was rather consistently about one-half of the total power, whereas the loss for the specimens subjected to a 1 volt/cm gradient varied more with time, with a smaller percentage lost initially and increasing to a larger percentage. In the cases where an electrical gradient of 1 volt/cm was used, the magnitude of the power loss remained nearly constant over the last two-thirds of the test (from about 40 hours to 140 hours). The power losses are attributable primarily to electrode corrosion and heat generation. As an example, the stainless steel electrodes had to be replaced after the second test due to corrosion; in retrospect, it is probable that carbon electrodes would have been superior to the stainless steel ones. However, it was not possible to evaluate the effects of the influx of ions from the corroding electrodes. The temperature variations with time are plotted in Figure 7-4. As can be seen, the greatest temperature increases were recorded shortly after the initial application of the power; as the power consumption decreased, the heat was dissipated and the temperature decreased.

Chemical Effects

The major chemical effects recorded in Tables 7-2 and 7-3 are probably due to two principal causes—the loss of ions into the effluent and

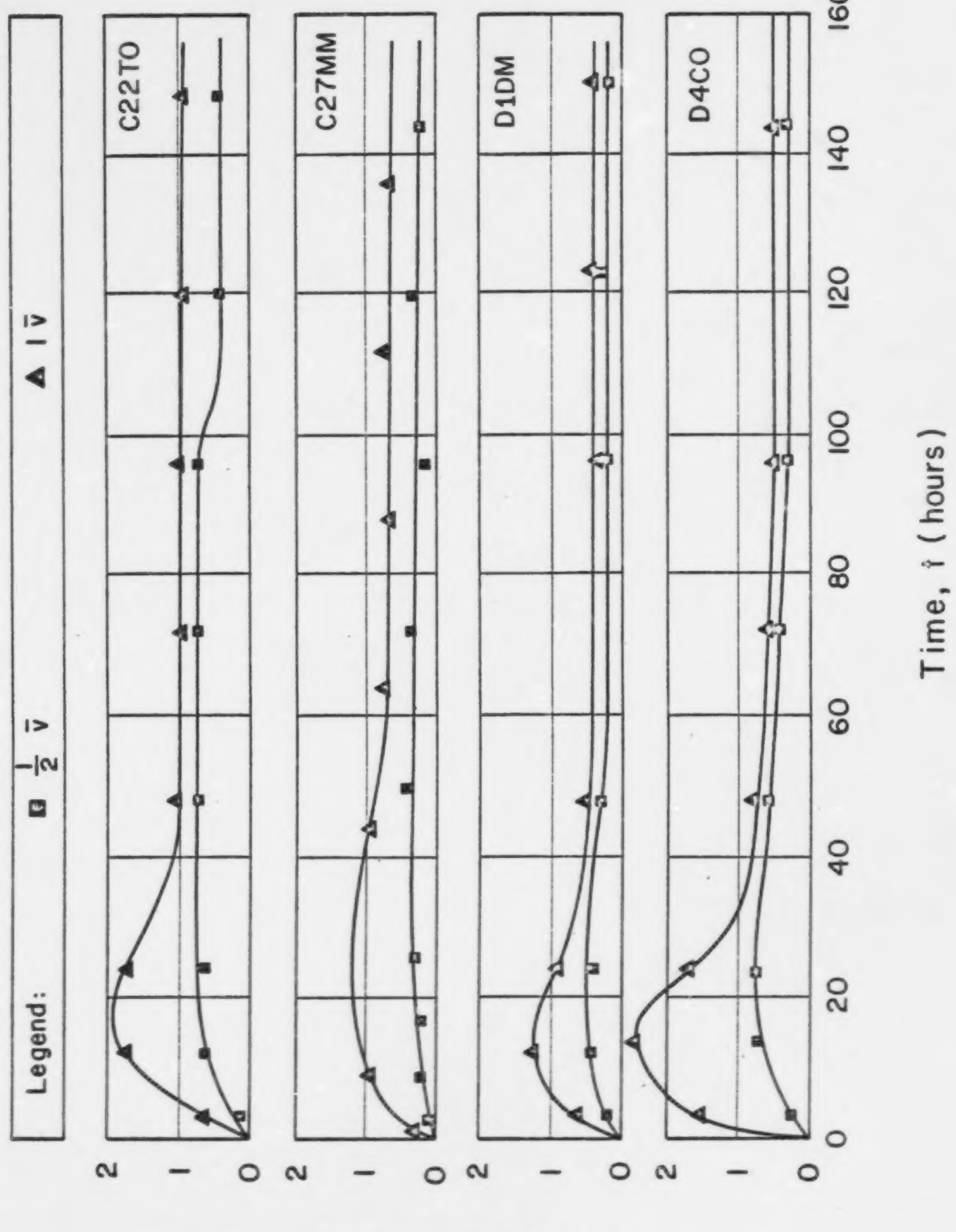

Figure 7-4. Temperature Variations versus Time

Table 7-2

Chemical Analyses of Samples Tested

Sample	Electrical Gradient (volt/cm)	Total Solids %	Total Volatile Solids %	In-Organic Carbon %	Organic Carbon %	pH	NH_3-N (μg/gm)	Organic Nitrogen (μg/gm)	Al (mg/gm)	Ca (mg/gm)
C22TO	Slurry	48.83	4.39	1.43	3.72	7.50	211.06	12.77	7.02	13.20
	0	60.97	5.26	1.36	3.38	8.55	225.72	877.35	8.94	18.30
	½	61.82	6.53	1.14	3.60	7.50	130.92	372.50	10.30	20.90
	1	63.11	5.83	1.37	1.84	8.85	49.46	426.70	7.98	23.20
C27MM	Slurry			1.93	7.55					
	0	62.27	7.82	1.97	5.23	8.06	56.05		8.58	18.20
	½			1.88	6.45					
	1	70.74	8.93	1.86	6.12	7.56	36.12		7.26	17.20
D1DM	Slurry			1.62	12.50		161.68	81.25		
	0	66.99	10.38	1.01	13.13	8.10	144.36		7.46	10.90
	½			1.48	12.74					
	1	70.02	12.06	1.57	13.49	6.95	0		7.57	11.60
D4CO	Slurry	46.72	4.60	0.96	8.21	8.25			6.22	4.80
	0	67.21	6.76	0.90	7.87	8.95	493.40		9.95	8.32
	½			1.01	7.98					
	1	74.98	7.07	1.22	7.76	8.40	44.48		10.30	6.77

Sample	Electrical Gradient (volt/cm)	Cd (mg/gm)	Cu (mg/gm)	Fe (mg/gm)	K (mg/gm)	Na (mg/gm)	Pb (mg/gm)	SiO_2 (%)	CEC Na (mg/gm)	CEC K (mg/gm)	CEC Ca (mg/gm)
C22TO	Slurry	0.003	0.017	[illegible]	0.86	0.122	0.033	31.60			
	0			[illegible]	2.08	0.190		44.90			
	½			[illegible]	2.55	0.162		45.80			
	1			18.70	2.57	0.250		48.50			
C27MM	Slurry										
	0	0.002	0.208	10.70	2.40	0.220	0.095	40.10	0.067	0.140	3.02
	½										
	1	0.001	0.220	12.70	2.21	0.220	0.100	46.05	0.040	0.104	4.82
D1DM	Slurry										
	0	0.006	0.096	90.40	2.22	0.310	0.239	37.20	0.061	0.126	1.63
	½										
	1	0.063	0.105	88.90	2.52	0.370	0.232	38.40	0.016	0.081	2.53
D4CO	Slurry	0.014	0.095	82.60	1.61	0.300	0.160	25.80			
	0	0.022	0.152	131.00	2.62	0.370	0.246	35.70	0.177	0.148	1.88
	½										
	1	0.024	0.158	144.10	2.31	0.270	0.245	41.30	0.016	0.065	1.77

Table 7-3

Chemical Analyses of Effluents from Samples Tested

Sample	Electrical Gradient (volt/cm)	Specimen Number	Total Solids (gm/1)	Total Volatile Solids (gm/1)	NH$_3$-N (mg/1)	pH	Al (mg/1)	Ca (mg/1)	Cu (mg/1)	Fe (mg/1)	K (mg/1)	Na (mg/1)
C22TO	0	1			132	8.9	0	102	0.35	0.19	12	290
		2	0.129		84	8.2	25	2000		14.00	87	260
	½	1	0.561		138	9.9	0	65	0.80	9.20	7	320
		2	1.849		246	12.4	0	550	0.70	8.30	20	530
		3	0.233		320	12.5	0	640		2.50	290	330
	1	1			172	12.1	12	340	0.85	9.30	15	360
		2	2.297		400	12.3	0	678	0.35	2.00	28	630
		3	0.257		456	12.6	26	5800		33.00	160	205
C27MM	0	1	0.607	0.129	46	8.1		13.8			13	39
		2	0.732	0.154	32	8.2		11.0			16	41
	1	1	0.539	0.105	115	11.4		0.5			15	90
		2	2.073	0.125	228	12.4		240			24	38
D1DM	0	1	0.988		132	7.9	0	340		0	120	900
		2			120	9.4						
	1	1	0.107		210	12.0	26	950		101.00	170	1170
		2			384	11.3						
D4CO	0	1 Bottom	0.703	0.252	255	8.6		12.5			18	97
		1 Top	0.760	0.289		8.4		5.8			18	100
		2	0.904	0.329	354	8.9		5.4			21	170
	1	1 Bottom	1.363	0.208	724	12.3		1.2			170	380
		1 Top	2.377	1.179		5.0		68			12	41
		2	1.574	0.109	1117	12.4		2.4			225	420

the loss of compounds in the generated gases. The desired effect of dewatering by electro-osmosis is reflected in Table 7-2 in the noticeable increase in the percentage of total solids with larger electrical gradients. A similar trend in the percentage of total volatile solids is not so well defined; this is probably due to the increased generation of gases with the larger gradients and the difficulty in obtaining a truly representative sample of the specimen for chemical analysis. The inorganic and organic carbon showed minor random variations, which are very likely due to a combination of the minor effects of the electrical treatment and sampling difficulties.

The electrical treatment did, however, have a pronounced effect on the concentrations of ammonia nitrogen. Smaller amounts of ammonia nitrogen remained in the specimens subjected to the larger gradients; this is due to the fact that large amounts were removed with the effluent and probably to the generation and release of gases. The losses of soluble ions from the sediment subjected to electrical treatment are reflected in gains for the same ions in the respective effluents, wherein the concentrations of the soluble ions per unit volume, as well as the quantities of effluent discharged, increased as the gradient increased. In Table 7-3 effluent samples 1, 2, and 3 designate samples which were collected at the beginning, middle, and end, respectively, of the electro-osmotic dewatering process; for cases where a third effluent sample was not taken, sample 2 represents the fluid collected at the end of the test.

As expected, the heavy metals remained in the sediments, regardless of the degree of electrical treatment; observed variations are probably due to testing and sampling variations. A comparison of the test data for potassium and calcium from fluid samples 1, 2, and 3 for the C22TO material indicates a general increase in concentration with the progress of dewatering, but the concentration of sodium reached a maximum for the middle sample and then decreased. In the case of the D400 material, the initial fluids obtained from the top and bottom of the specimens subjected to zero electrical gradient and 1 volt/cm electrical gradient were analyzed separately; it is noted that the concentrations of both the potassium and the sodium ions are much higher in the fluids drained from the bottom compared to those drained from the top for the 1 volt/cm electrical gradient, but there is little change in the ion concentrations of the fluids from the top and bottom for the zero electrical gradient test. The decreases in the cation exchange capacity for sodium and potassium again reflect the loss of these soluble ions to the effluents, but the effects on calcium are not so pronounced. The pH generally increased slightly in the effluent with larger gradients, while it decreased in the remaining sediment.

Effects on Engineering Properties

Previous experience indicates that electro-osmosis would be expected to dewater and consolidate the sample, thereby producing a denser material with increased shear strength. These expectations were met in this testing program, and the detailed effects are reported in this section. Figures 7-5 through 7-8 show the rate of fluid discharged from the sample, the change in sample height, and the current used as a function of time for various electrical gradients. A study of these plots indicates that an increase in the electrical gradient causes a substantial increase in the amount of fluid discharged. The higher gradient produces its major effect in a shorter period of time than the lower gradient; for the thicker material, the major effect caused by the higher gradient occurred in about one day, whereas that for the lower gradient occurred in about

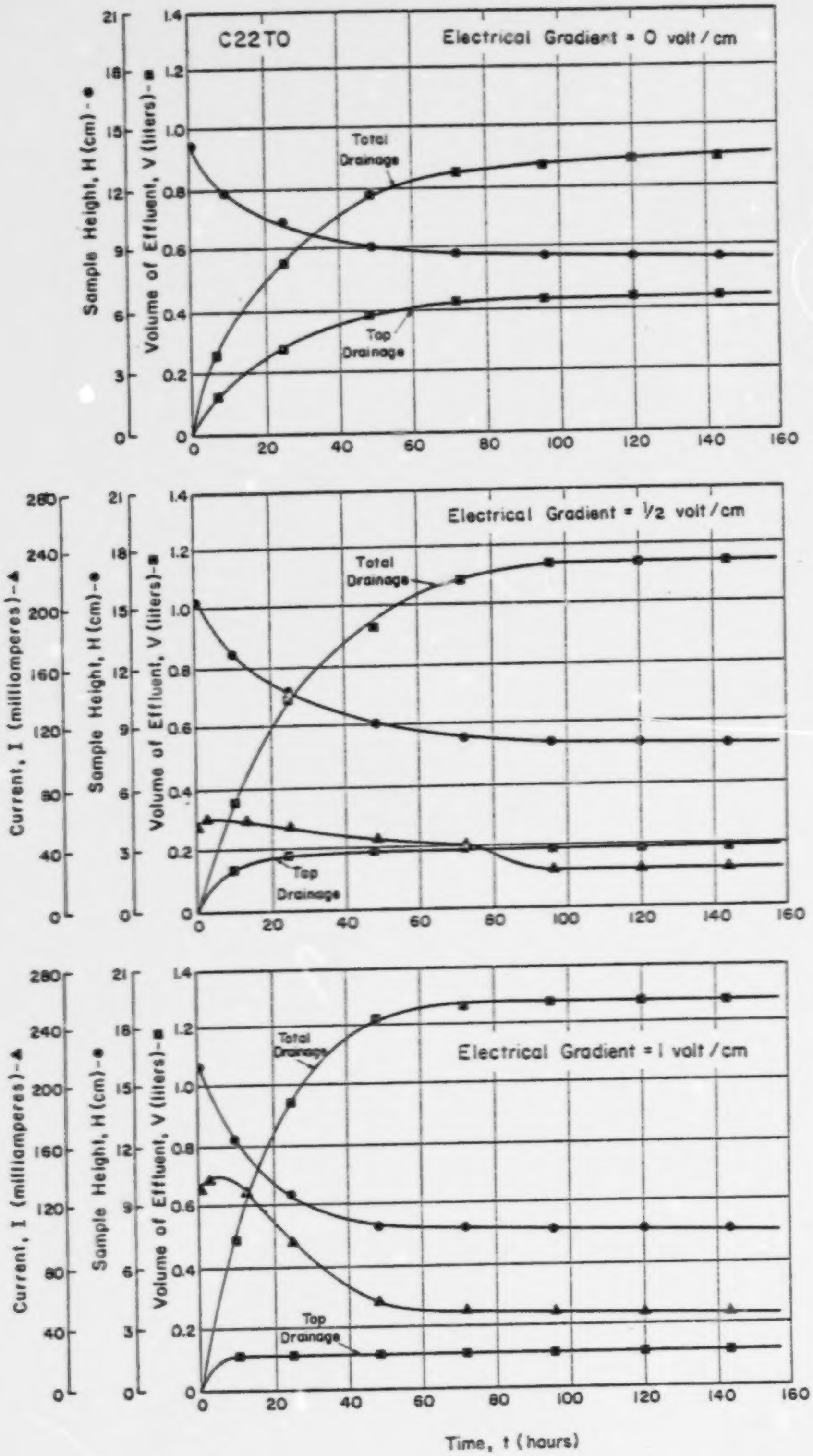

Figure 7-5. Electro-osmotic Dewatering Data for Sample C22TO

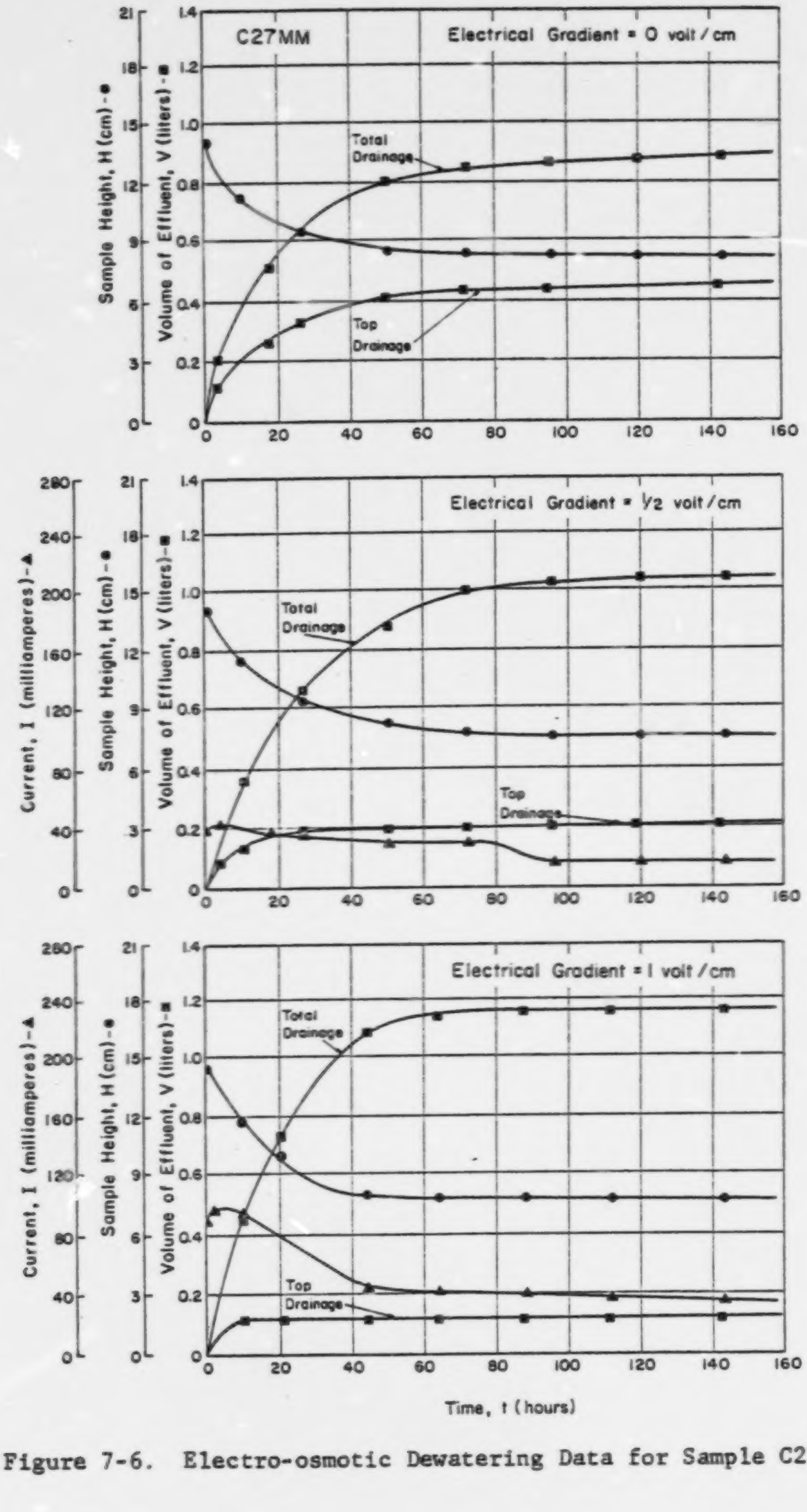

Figure 7-6. Electro-osmotic Dewatering Data for Sample C27MM

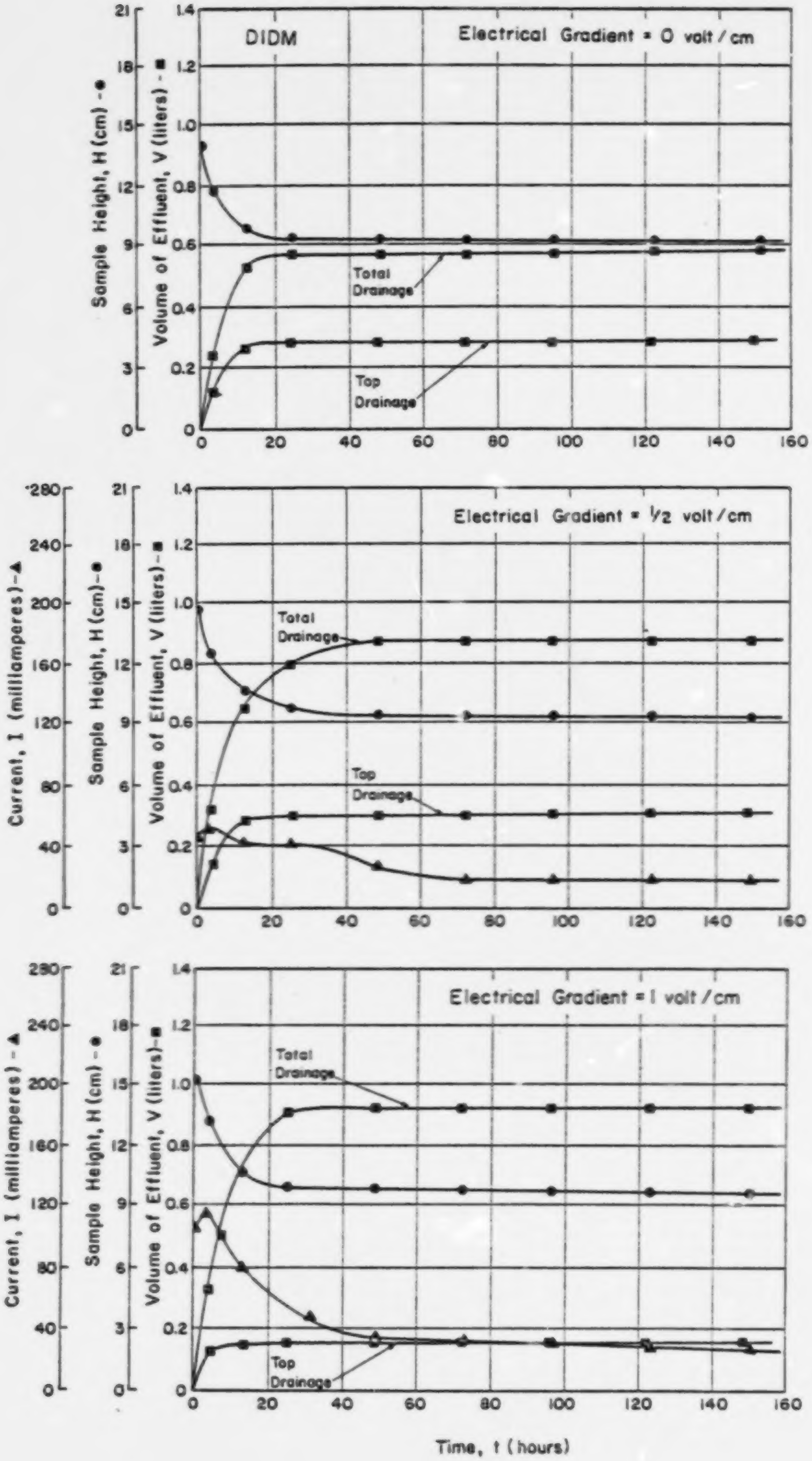

Figure 7-7. Electro-osmotic Dewatering Data for Sample D1DM

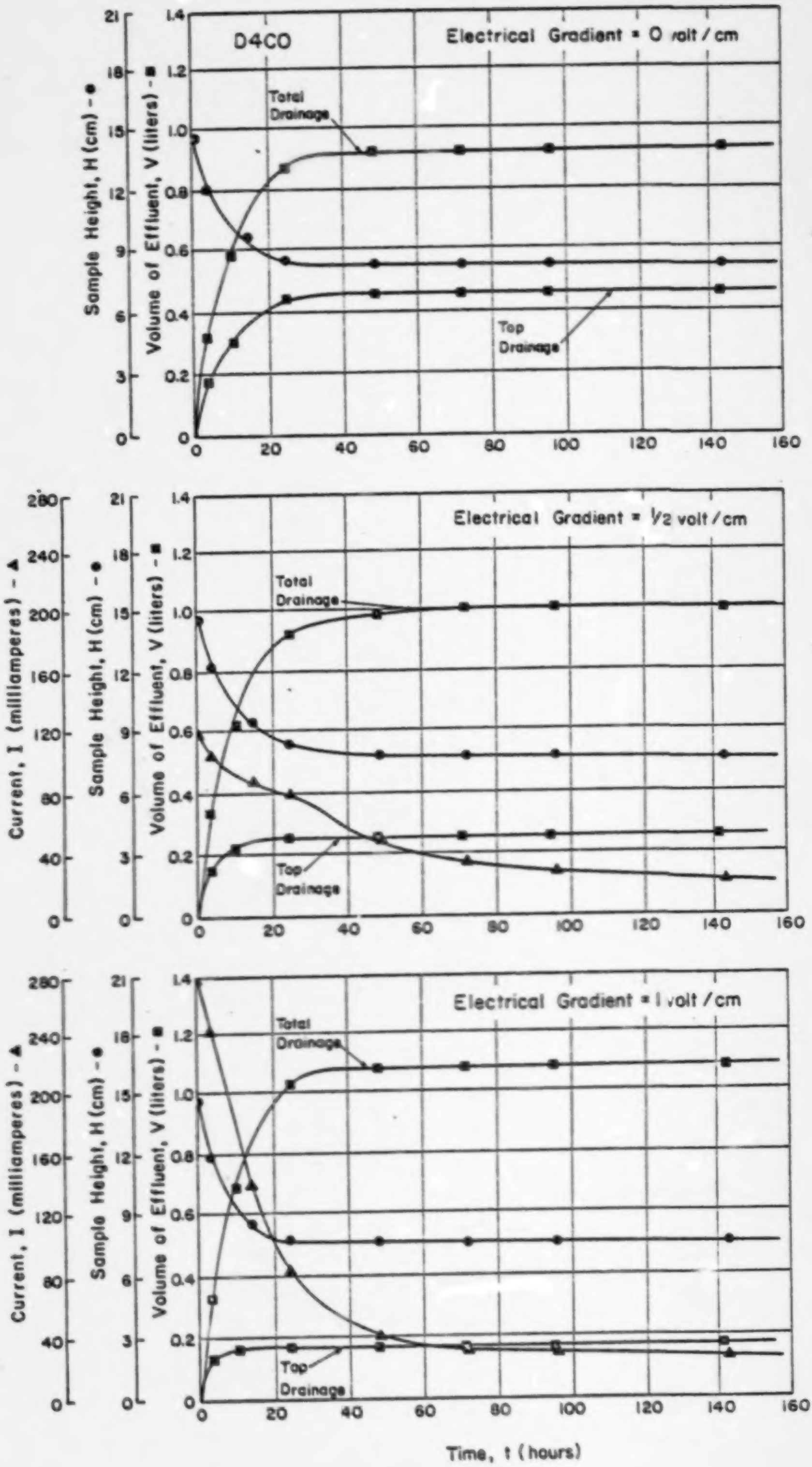

Figure 7-8. Electro-osmotic Dewatering Data for Sample D4CO

two days.

In each case the dewatering process using an electrical gradient is somewhat faster, especially for the C samples, than that associated with a pressure gradient only. However, in making a comparison of the time rates of fluid discharged with and without an electrical gradient, attention must be given to the fact that drainage was allowed from both the top and bottom stones. Under zero electrical gradient, drainage would take place from the center of the sample toward both the upper and lower porous stones. Since the applied electrical gradient tends to drive the water downward, the pressure and electrical gradients oppose each other in the upper half of the specimen; this effect can be noted in Figures 7-5 through 7-8 by observing the smaller proportion of effluent that is discharged through the upper stone. For all practical purposes, gravity effects are essentially negligible compared to the other gradients involved in this phenomenon. The current can also be seen to decrease as the rate of flow decreases. Although the complex nature of these tests (variable gradient with time, drainage conditions, time-dependent changes in material characteristics, etc.) preclude any straightforward simple interpretation of the data, a first-order approximation of the electro-osmotic coefficient of permeability, k_e, can be determined from the information presented in Figures 7-5 through 7-8 and use of the relationship

$$k_e = \frac{Q\ H}{t \Delta V\ A} \quad , \qquad (7\text{-}1)$$

where Q is the total volume of fluid discharged in time, t, from a sample of cross-sectional area, A, and height, H, due to a voltage difference, ΔV. If data associated with the time required to reach approximately one-half the maximum volume of effluent discharged are selected from Figures 7-5 through 7-8 and substituted into Equation (7-1), it is found that values for the electro-osmotic coefficient of permeability, k_e, are of the same order of magnitude as those which characterize a large variety of soils (that is, 5 x 10^{-5} cm/sec per volt/cm). However, additional tests under more controlled conditions should be conducted before attempting to apply these preliminary results to specific field situations.

Plots of the electro-osmotic flow rate versus the current are given in Figure 7-9 for each of the four dredgings. A general pattern of increasing flow rate with increasing current is observed, but the relationship is not linear, as found by Gray and Mitchell (1967) for tests on clays under very well controlled laboratory conditions. If Equation (7-1) is written in an alternate form

$$k_e \rho = \frac{Q}{I\ t} \quad , \qquad (7\text{-}2)$$

where ρ and I are the specific electrical resistance of the material and the current, respectively, the basis for the Gray and Mitchell relationship can be readily appreciated, namely, the product of the material properties, $k_e \rho$, is a constant. However, the complex nature of the chemical constituents in the dredgings tested does not justify the expectation that $k_e \rho$ would be a constant throughout these tests. Rather, the initial portions of the curves in Figure 7-9 generally increase at an increasing rate and exhibit a final very steep slope. The physical explanation for this phenomenon follows from the curves presented in Figures 7-5 through 7-8, where the flow rate is the slope of the volume of effluent versus time curve and the current is read directly. In most cases it takes a short period of time before the current reaches its maximum value, after which it decreases. This slight time lag is probably caused by the

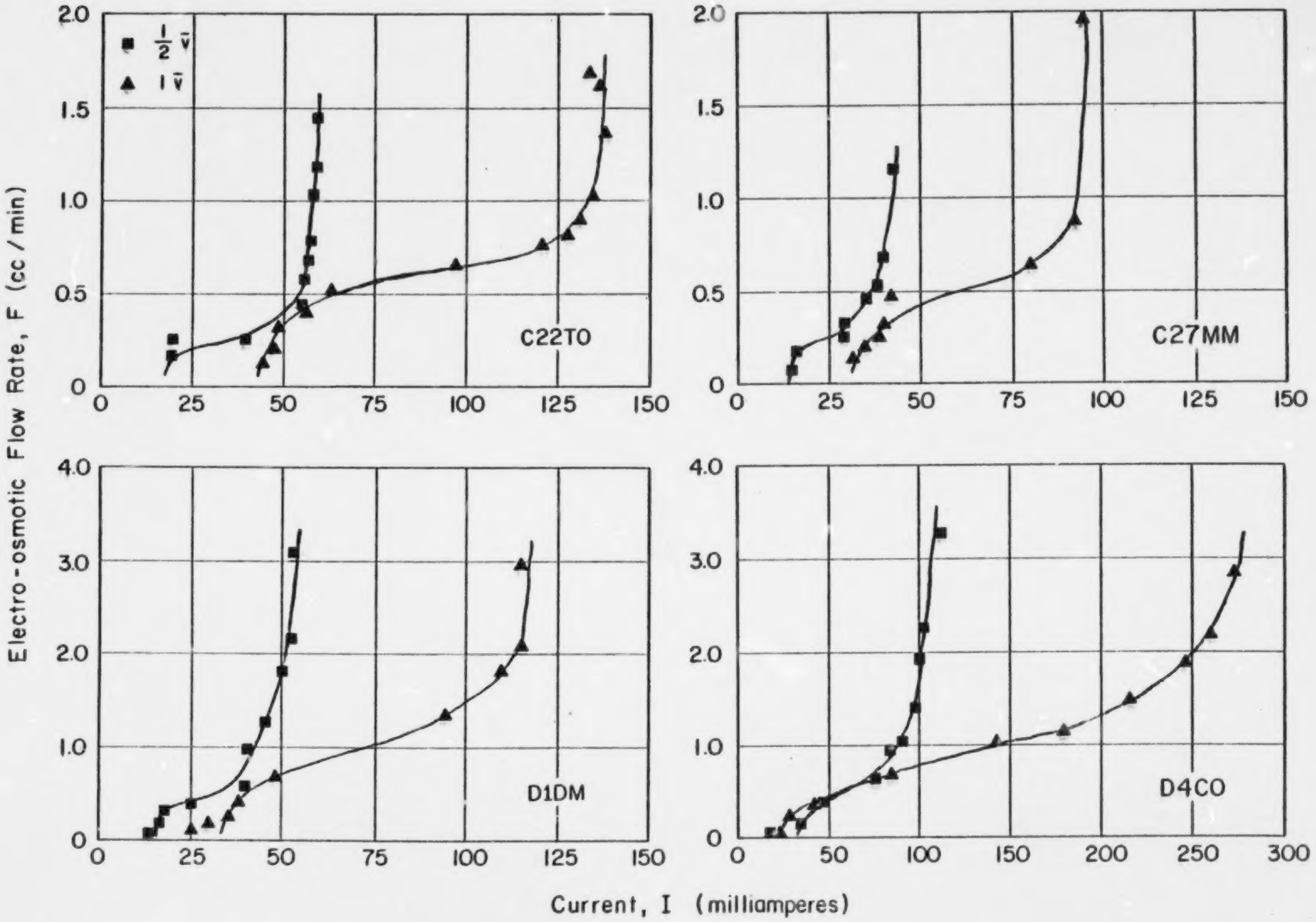

Figure 7-9. Electro-osmotic Flow Rate versus Current

inertia of the ions to movement. At the instant the voltage is applied, the system is static; shortly afterward, it becomes dynamic, and the current reaches a maximum during the early stage of flow, which is represented in Figure 7-9 by the data in the upper right-hand portion of each curve. As time passes, the rate of fluid flow, as well as the current, decreases, and the curves in Figure 7-9 move downward and toward the left. Hence, the dewatering process continues at a decreasing rate for all samples and eventually reaches a condition where very little additional drainage occurs. This condition is indicated by the relatively rapid change in the slope of the curves in Figure 7-9. It is possible that a point is reached where the continuity breaks down between the dredgings sample and the anode, thereby causing a sudden drop in power consumption and flow of current.

Figure 7-10 shows the variation of moisture content with depth in each specimen tested. The specimens subjected to no electrical treatment show essentially no change in moisture content with depth, whereas the electrically treated specimens portray a marked decrease in moisture content at the top of the specimen with relatively larger moisture contents toward the bottom. The larger gradients produced lower water contents in all materials at all depths.

The Atterberg limits and associated indexes presented in Table 7-4 indicate that the electrical treatment produced no noticeable trends. The minor differences observed may be attributed to normal variations in the test results, variations of material properties within the specimen, and the loss of ions from the original sample.

The conventional consolidation test data resulting from tests made on specimens trimmed from the samples consolidated by the electrical and

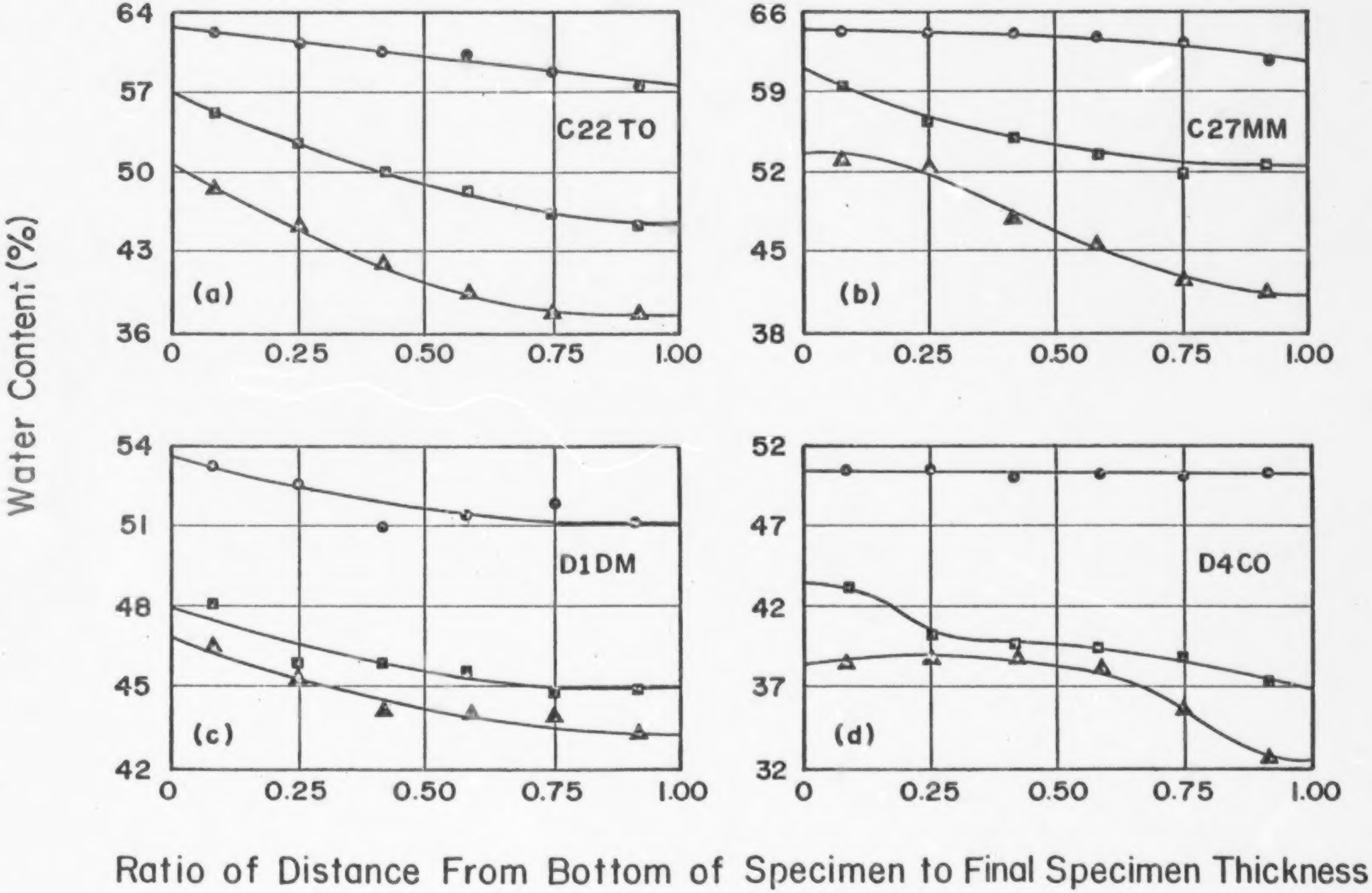

Figure 7-10. Variation of Moisture Content with Depth

Table 7-4

Effect of Electro-osmotic Treatment on Engineering Characteristics

Sample	Electrical Gradient	Moisture Content	Liquid Limit	Plastic Limit	Plasticity Index	Shrinkage Limit	Flow Index	Toughness Index
C22TO	INITIAL	138	69	40	29	24	16	181
	0 volt/cm	60	78	44	34	26	22	154
	½ volt/cm	50	75	45	30	30	20	150
	1 volt/cm	42	70	37	33	21	19	174
C27MM	INITIAL	143	59	49	10	23	14	72
	0 volt/cm	63	87	45	42	24	28	150
	½ volt/cm	55	81	55	26	25	16	163
	1 volt/cm	47	79	51	28	29	21	133
D1DM	INITIAL	99	56	39	17	40	13	128
	0 volt/cm	52	60	51	9	46	11	82
	½ volt/cm	46	58	45	13	53	15	87
	1 volt/cm	45	58	50	8	43	13	62
D4CO	INITIAL	117	50	36	13	40	9	149
	0 volt/cm	50	51	41	10	26	12	83
	½ volt/cm	40	55	44	11	37	14	79
	1 volt/cm	37	52	41	11	31	16	69

pressure gradients are presented in Figure 7-11. The major effect seems to be due to the decreased initial void ratio in the specimens subjected to an electrical gradient. Although the preconsolidation stress generally appears to increase with increasing electrical gradient, this effect is not very well defined in these results. The compression index, C_c, for the different materials, varies from about 0.38 to 0.66, but it is relatively constant for a given material, regardless of the amount of electrical treatment imposed.

In Table 7-5 are tabulated the average shear strengths of the top (anode end), center, and bottom (cathode end) of the sample. General trends of decreasing shear strength with increasing depth and decreasing electrical gradient can be noted. Although the overall shear strength was increased considerably by electrical treatment in all the dredging samples, the sensitivity varied little between the untreated and treated samples.

Table 7-6 lists several of the more important properties of the dredging materials, and specific values are tabulated in order to enable the effects of the electrical treatment to be better evaluated. The greatest percentage change in dry density occurred in Sample C22TO, but somewhat lesser changes were observed for the other materials. A large portion of the percentage change in dry density resulted from the consolidating pressure (0.6 kg/cm^2) applied by the piston, and not the electrical gradient. This table also lists the total energy consumed by the various samples, and a general comparison of its effect on the increased density and shear strength can be made.

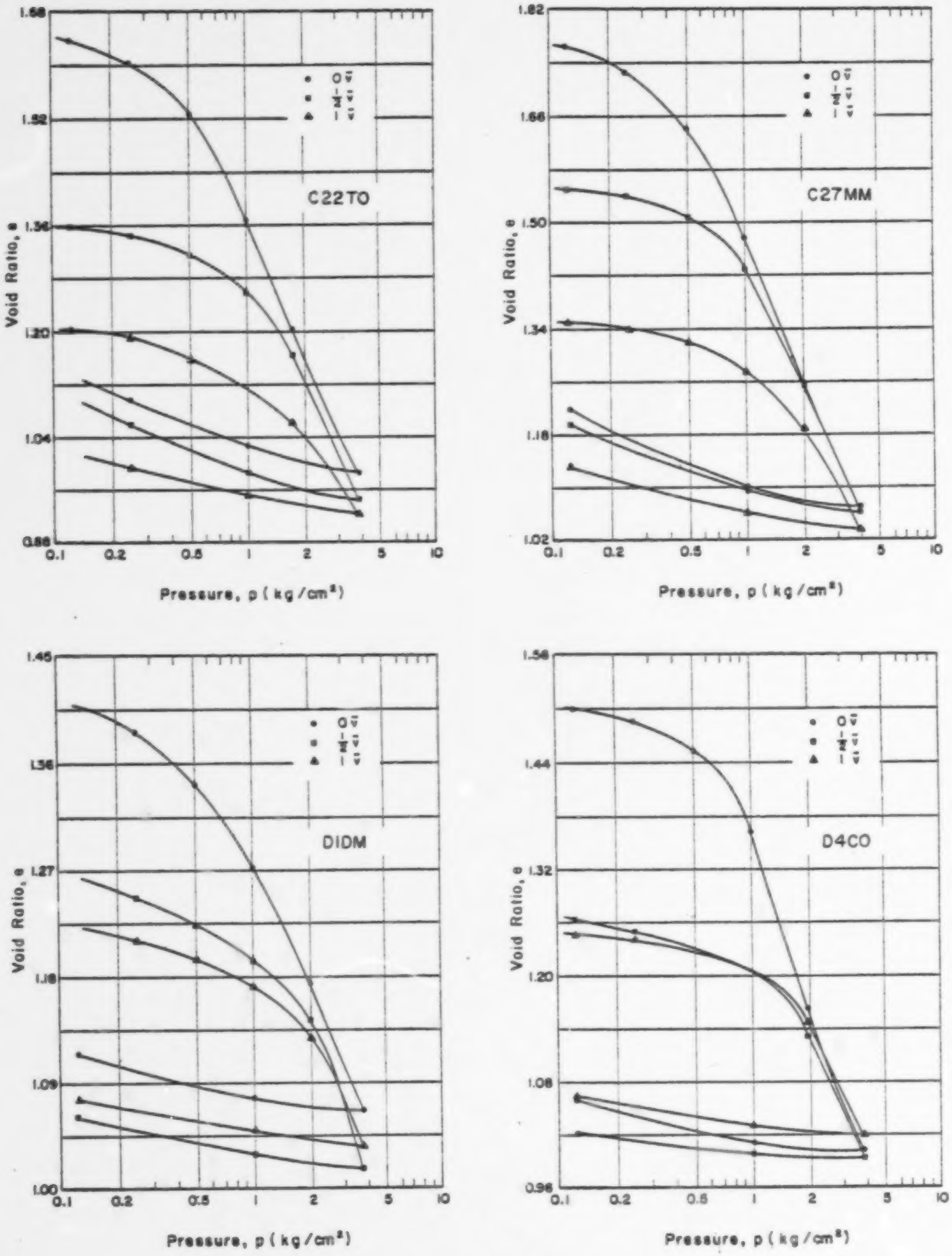

Figure 7-11. Void Ratio versus Pressure Curves

Table 7-5

Average Shear Strength Determinations

Sample	Electrical Gradient (volt/cm)	Location in Sample						Overall	
		Top		Center		Bottom			
		Average Shear Strength (psf)	Sensitivity	Average Shear Strength (psf)	Sensitivity	Average Shear Strength (psf)	Sensitivity	Average Shear Strength (psf)	Sensitivity
C22TO	0	470	3.1	430	2.7	400	2.9	430	2.9
	½	1562	3.7	1006	2.8	811	2.9	1130	3.1
	1	2850	4.7	1720	3.0	1460	3.1	2010	3.6
C27MM	0	980	4.3	830	4.2	840	4.3	880	4.3
	½	2180	4.8	1620	4.2	1320	3.6	1710	4.2
	1	5040	7.5	3200	4.6	2180	3.4	3470	5.2
D1DM	0	550	3.1	550	3.3	480	3.2	530	3.2
	½	1580	4.5	1330	4.7	1270	3.7	1400	4.3
	1	1720	4.1	1500	3.6	1610	3.3	1610	3.7
D4CO	0	550	3.9	550	3.5	580	4.4	560	3.9
	½	2980	15.6	2650	8.4	2320	6.1	2650	6.1
	1	2570	4.4	2460	4.6	2370	4.5	2470	4.5

Table 7-6

Summary of Test Parameters

Sample	Electrical Gradient (volt/cm)	Initial Density (gm/cc)		Final Density (gm/cc)		Final Height / Initial Height	Final Void Ratio	Change in Dry Density %	Total Energy Consumed (watt-hours)	Average Shear Strength (psf)
		Wet	Dry	Wet	Dry					
C22TO	0	1.38	0.58	1.56	0.98	0.61	1.66	69	0	430
	½	1.36	0.57	1.66	1.11	0.53	1.36	95	43	1130
	1	1.33	0.56	1.65	1.15	0.49	1.21	105	154	2010
C27MM	0	1.31	0.54	1.53	0.94	0.58	1.81	74	0	880
	½	1.33	0.55	1.54	1.00	0.54	1.60	82	26	1710
	1	1.36	0.56	1.53	1.04	0.54	1.35	86	97	3470
D1DM	0	1.43	0.72	1.74	1.15	0.66	1.43	60	0	530
	½	1.44	0.72	1.60	1.10	0.64	1.28	53	86	1400
	1	1.47	0.74	1.67	1.16	0.64	1.23	57	114	1610
D4CO	0	1.40	0.65	1.71	1.14	0.57	1.53	75	0	560
	½	1.42	0.65	1.73	1.24	0.53	1.28	91	47	2650
	1	1.41	0.65	1.69	1.23	0.51	1.26	89	115	2470

CONCLUSIONS

Based on the rather limited experimental program described in this chapter, the following conclusions regarding the response of polluted dredging spoil to electro-osmotic treatment can be advanced:

1. Electro-osmosis serves to significantly increase the volume of fluid discharged from the dredgings and to accelerate the rate of dewatering, with the associated decreases in water content and void ratio and increase in shear strength.
2. The Atterberg limits and the conventional consolidation characteristics are not significantly affected by the electrical treatment.
3. The electro-osmotic process carries substantial amounts of soluble ions out of the specimen with the fluid discharged.
4. The chemistry of the sediment and the dewatering process are influenced to some degree by the generation and release of gases.
5. The major effect of the electrical treatment occurs soon after the current is applied, but this response varies with the material.

RECOMMENDATIONS

Before applying electro-osmosis to the dewatering and/or stabilization of polluted dredgings, a comprehensive laboratory study and, if possible, field program should be conducted on the specific material in order to evaluate the rate of dewatering, reduction in void ratio, increase in strength, most efficient electrical gradient, optimum time of application, moisture content at which continuity is lost, and the pollution potential of the effluent discharged. Such an investigation would also provide an opportunity to select the best type of electrode material and to appraise the advantages and disadvantages of different configurations for the drainage system.

Further research is needed to evaluate the effects of electro-osmosis on the shear strength and drainage characteristics of dredgings for different treatment times after the majority of consolidation and drainage has occurred. The intermittent application of electro-osmosis to reduce the total amount of energy expended has been reported in the literature, and this possibility should be studied to aid in assessing its economical application to the problem of dewatering dredged spoil.

CHAPTER 8

ELECTRICAL SOUNDING

Included in this chapter are the results and interpretation of electrical resistivity sounding surveys made at the Island Site and Riverside Site in the Toledo Harbor area. The purposes of this study were (a) to examine the electrical resistivity characteristics of typical dredged wastes as they are found in landfill sites, and (b) to evaluate the suitability of this technique for identifying vertical and horizontal variations in resistivity, which can usually be associated with trends in composition, consistency, and depth of fill. To aid in the latter evaluation, this survey was coordinated with simultaneous programs of borehole exploration and refraction seismic profiling, and the results of these studies are given in other parts of this report.

EQUIPMENT AND MEASURING TECHNIQUE

The resistivity meter (Soiltest Model ER-2) used in this work employs a set of four bronze electrodes, two for applying a measured current and two for measuring the gradient of the induced electrical field. Polarization effects are avoided by use of cyclically reversing direct current. The technique consists of taking electrical measurements about a single station with an electrode array of varying spacing in order that the effects of resistivity variations with depth can be examined, and a number of such individual stations along a line constitutes a profile. In each case the survey was performed along a profile which extended from

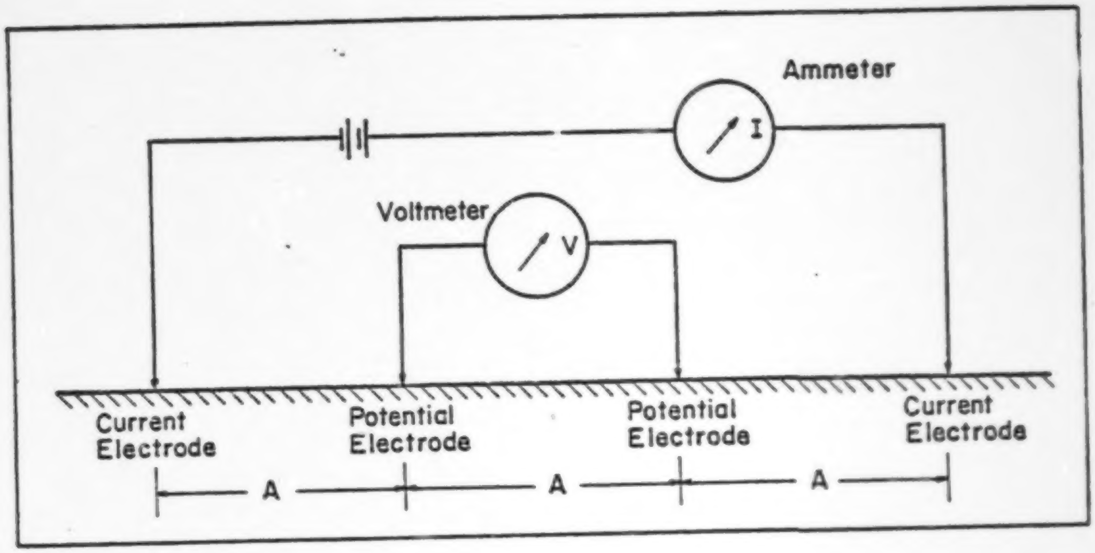
Ammeter
I
Voltmeter
V
Current Electrode
Potential Electrode
Potential Electrode
Current Electrode
A
A
A

Figure 8-1. Wenner Electrode Configuration

the inlet pipe to the outlet weir. The four electrodes were equally spaced along a line in a Wenner configuration, as shown in Figure 8-1; then a measured current was applied across the outer pair of electrodes, and the resulting potential difference between the inner pair of electrodes was measured. Since this potential difference is influenced primarily by the mass of soil between the surface and a depth approximately equal to the electrode spacing, variations of resistivity with depth can be investigated by varying the electrode spacing.

METHOD OF INTERPRETATION

Interpretation of the data is based on the concept of an "apparent resistivity", which is the resistivity of a homogeneous half-space that would theoretically produce the same relation between the applied current and the potential difference. For the Wenner electrode array, the apparent resistivity is given by

$$\rho_a = 2\pi A(V/I) \tag{8-1}$$

where ρ_a is the apparent resistivity (ohm-cm), A is the electrode spacing (cm), I is the current (amperes), and V is the potential difference between the inner electrodes (volts). Since the particular resistivity meter used in this study was calibrated to give a direct digital readout of the quantity $[2\pi\ V/I]$, the apparent resistivity, ρ_a, was obtained simply by multiplying the reading by the corresponding electrode spacing, A. Two methods were used to interpret the results reported herein; these are the Barnes Layer Resistivity Method (Barnes, 1954) and the Moore Cumulative Method (Moore, 1945).

Barnes Layer Resistivity Method

The Barnes Layer Method uses the assumptions that (a) the soil behaves as a set of horizontal layers in which the thickness of each is equal to the increment in electrode spacing, and (b) the soil layers at depths greater than the electrode spacing do not affect the apparent resistivity. It is further assumed that each layer possesses a uniform resistivity which represents some average for the layer. Accordingly, the layers are treated as a group of resistors in parallel, and we have

$$\frac{1}{R_L} = \frac{1}{R_n} - \frac{1}{R_{n-1}} \tag{8-2}$$

where R_L is the resistance of a particular layer, L, R_n is the total resistance of the entire sequence of parallel layers down to and including layer L, and R_{n-1} is the total resistance of the sequence of layers above layer L (given by the values of V/I for electrode spacings equal to the depths of the bottom and top of layer L, respectively). The layer resistivity, ρ_L, is then taken as

$$\rho_L = \frac{2\pi A_L}{1/R_L} \qquad (8\text{-}3)$$

where A_L is the hypothetical layer thickness, or increment in electrode spacing. Use of this method allows the construction of block diagrams that illustrate changes in resistivity with depth at a given station.

Moore Cumulative Method

The Moore Cumulative Method involves plotting the cumulative apparent resistivity versus the corresponding electrode spacing, A, and breaks in the slope of the resulting curve are found by drawing straight lines through sequences of plotted points. The intersection of any two consecutive line segments gives the location of a break in slope, and, provided there are no lateral resistivity variations due to large boulders, etc., a relative change in resistivity is assumed to occur at a depth approximately equal to the electrode spacing.

FIELD WORK

The first electrical sounding measurements were taken on July 6, 1971, at a station near the outlet weir of the Island Site, and on July 7, 1971, a profile of 9 stations, shown in the inset to Figure 8-2a, was laid out. Initially, a path along the profile line was cut through heavy vegetation, and the stations were located by a survey. The electrical soundings were made with electrode spacings of 2, 4, 6, 8, ..., 22 feet; the initial trial station near the weir was an exception, in that electrode spacing increments of 3 feet were used. The data obtained were quite consistent, and no significant anomalies were encountered. The observed variation in the resistivity values between individual stations along the profile for given electrode spacings was expected, because grain size, grain size distribution, mineralogy, porosity, chemistry of the pore fluid, natural water content, and many other parameters vary as a consequence of the process which governs the deposition of these dredgings as the slurry flows away from the inlet pipe towards the outlet weir. The change in conditions between the fill material and the underlying soil accounts for the increasing values of resistivity with increasing depth. Other variations in resistivity may be due to nonhomogeneities of the fill or underlying soils, as well as the inherent errors in the measuring device.

On July 8, 1971, work similar to that described above was started at Riverside Site along the profile shown in the inset to Figure 8-3a, but the resistivity meter malfunctioned after measurements at Stations 10, 12, and 13 were taken. On July 26, 27, and 28, 1971, a second field trip was undertaken, and the remaining measurements along the indicated profile were completed. As with the Island Site, a path was cut through the dense vegetation, and the stations were located by use of a tape. Electrode spacing increments of two feet were used at all stations until a maximum spacing of 22 feet was reached. The data obtained at Riverside Site were similar to those obtained at the Island Site, and no major anomalies were encountered. A rather large difference in the apparent resistivity between Stations 10 and 23 was found, but this is explained by the fact that Station 23 lies close to the inlet pipe where a substantial amount of coarse material varying from sand to gravel is present. Such a difference can be accounted for by variations in the porosity, mineralogy, and water content of the dredgings. The existence of extremely high contact resistance at this particular station also adversely affects the precision and reliability of this resistivity measurement.

ANALYSIS OF DATA

The longitudinal variation in resistivity was interpreted in terms of the average apparent resistivity given by Equation (8-1), which is based on a Wenner Electrode configuration. The variation in resistivity with respect to depth was initially analyzed by use of the Barnes Layer Resistivity Method given by Equation (8-3), but the boundaries of interest were not readily apparent. Accordingly, the Moore Cumulative Method was adopted, and it appeared to be more suitable for the interpretation of the data under consideration.

The data from both sites showed common trends, and typical plots of the observed variations are illustrated in Figures 8-2 and 8-3. There was considerable variation in resistivity in the longitudinal direction at a given depth; stations close to the inlet pipe showed high values of resistivity, whereas values at the stations near the weir were significantly lower. These observations are quite reasonable, since the soil particles in the hydraulic fill are sorted according to a physical process which is a function of the velocity, grain size, concentration of solids, and depth of fluid in the basin. In the vertical direction resistivity values were high at the surface, decreased to some intermediate depth, and then increased. Such a trend was expected because the deposits have a variable moisture content, governed near the surface by desiccation and near the bottom by gravity drainage; hence, the center part of the layer possesses the highest water content. Although the apparent layer resistivity may also be influenced by changes in the soil matrix, it is difficult to evaluate this effect quantitatively.

Island Site

A typical resistivity profile for the Island Site is shown in Figure 8-2a, where the longitudinal variation in the average apparent resistivity is plotted for electrode spacings of 10 and 12 feet. As can be readily seen, the values of resistivity for a particular spacing decrease rapidly with increasing distance from the inlet pipe for a distance of several hundred feet, after which they remain almost constant throughout the remaining length of the profile. Local variations showing opposite trends are probably due to measuring errors and are not significant. Although the interpretation of electrical sounding data is not simple, it is known that resistivity is affected by mineralogy, porosity, and water content, and these parameters can, in turn, be correlated with grain size and grain size distribution, and this is precisely the relationship being addressed in this study. Since grain size analyses of samples taken along the indicated profile confirm the fact that there is a longitudinal variation in grain size and grain size distribution, the longitudinal changes in resistivity for a particular layer can be related to these variations. In general, grain size and grain size distribution influence the porosity and natural water content of the fill material, and hence there is a double effect on the resistivity of the soil. Although the composition of the soil and its mineral components influence the electrical resistivity, there is not enough information available to advance conclusive statements with regard to these parameters.

The typical block diagram shown in Figure 8-2b (block diagrams for

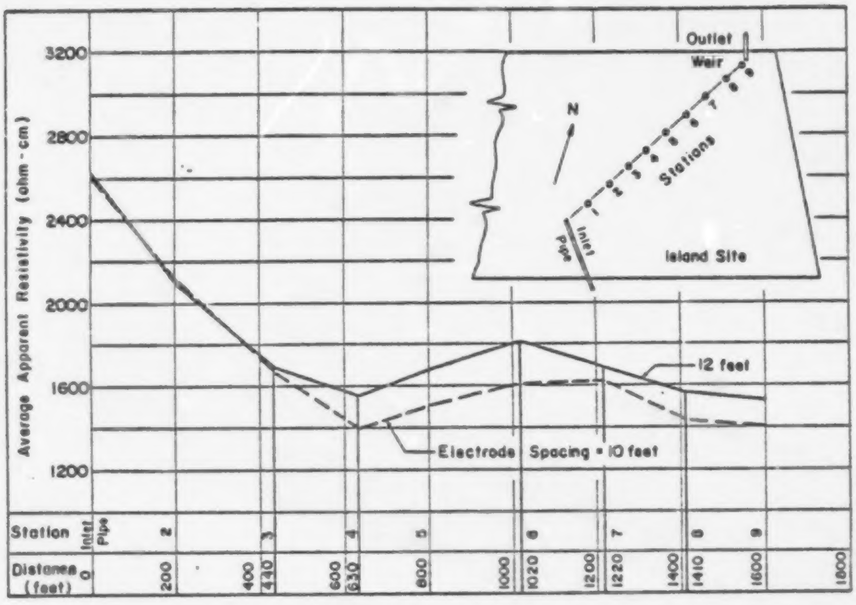

(a) Resistivity Profile

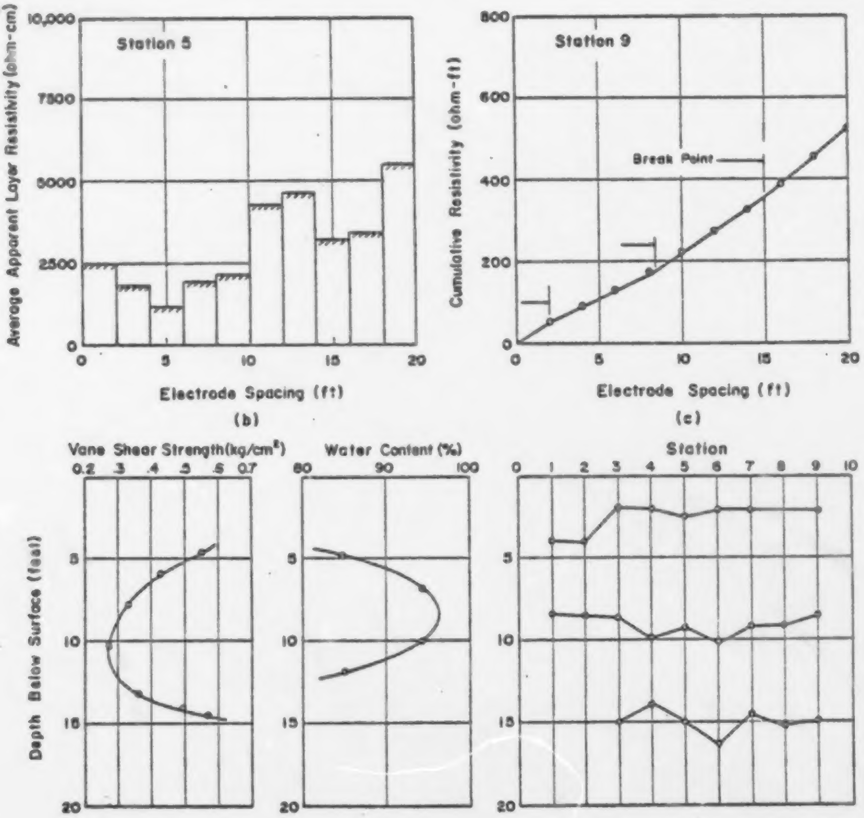

(b) (c)

(d) (e) (f)

Figure 8-2. Resistivity Profile and Supplemental Data from Island Site

all stations are given in Figure 8-4) illustrates the variation with depth in the apparent layer resistivity of the fill, as interpreted by the Barnes method. The top of the deposit has a relatively high resistivity, which decreases to a depth of about 5 feet and then increases to a depth of 10 to 14 feet. Although the block diagram itself does not allow the direct prediction of the cause of this particular relationship, the supplementary shear strength and water content data given in Figures 8-2d and 8-2e provide a clue to the reasons for the changes.

Figure 8-2c shows a typical plot of results obtained by the Moore Cumulative Method. In general, the break points or changes in slope of the curve seem to describe three regions. The characteristics of the uppermost few feet cannot be detected directly from the plot, but direct field observations indicate that there exists an upper desiccated crust which can be expected to have a high resistivity. The region associated with the second break point seems to be characterized by the high water content of the middle portion of the fill, and the lowest region from approximately 12 to 16 feet deep seems to be associated with a change in the soil type, that is, the transition from the fill material to the original ground surface. This interpretation is substantiated by the shear strength and water content data given in Figures 8-2d and 8-2e. Graphs similar to Figure 8-2c have been plotted in Figure 8-5a for all stations on the Island Site, and the break points obtained from the Moore Cumulative Method are shown in Figure 8-2f on a longitudinal profile for which the horizontal scale is not uniform. The break points indicating the three individual layers under consideration occur quite consistently along the longitudinal profile, and hence the above interpretation seems very reasonable.

Riverside Site

The resistivity profile for Riverside Site is given in Figure 8-3a for electrode spacings of 10 and 12 feet. Although a large decrease in resistivity was found between the inlet and Station 23, the resistivity values for all other stations were nearly the same over the entire profile. The increase in resistivity with increasing distance from Stations 18 to 15 is unexpected, but this may be due to a boundary effect caused by a buried dike which formed part of a special study several years ago at Riverside Site. Since the deposition process at Riverside Site is identical to that on the Island Site, longitudinal size sorting of particles must be expected, and the high apparent resistivity close to the inlet pipe is probably due to the presence of a coarse material with its associated mineralogy, porosity, and natural water content. As with the Island Site, grain size analyses of samples taken from Riverside Site support this interpretation.

The typical block diagram shown in Figure 8-3b (similar block diagrams for all stations are given in Figure 8-4) is very similar to that given in Figure 8-2b, and it indicates the same general phenomena. Specifically, a substantial increase in resistivity is encountered at a depth of approximately 10 feet, and the variation of the resistivity within the middle region is probably due to a high water content. The supplemental shear strength and water content data given in Figures 8-3d and 8-3e confirm the trend indicated by the electrical sounding data. The desiccated upper crust varies between 2 and 4 feet thick and exhibits relatively high apparent resistivity values, as shown in the block diagrams.

A typical cumulative resistivity plot is given in Figure 8-3c, and the existence of definite regions similar to those on the Island Site

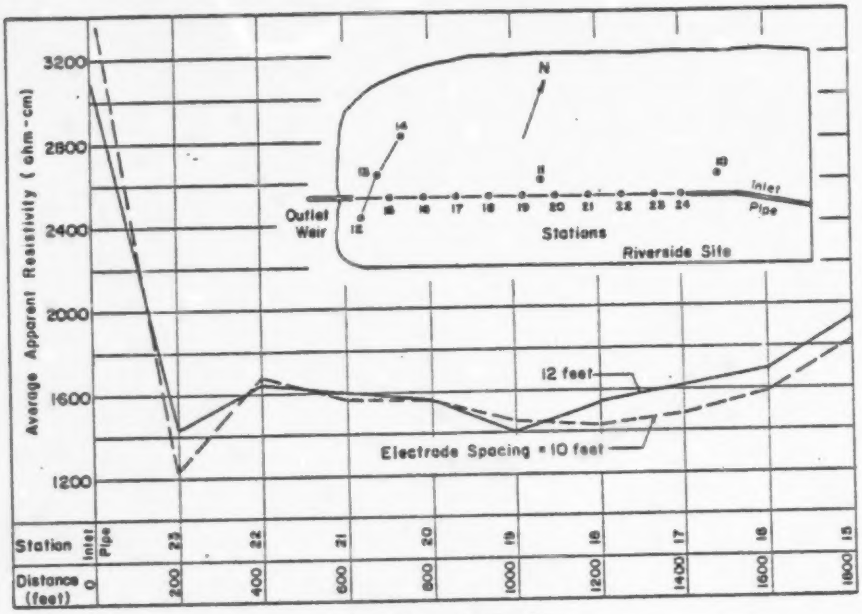

(a) Resistivity Profile

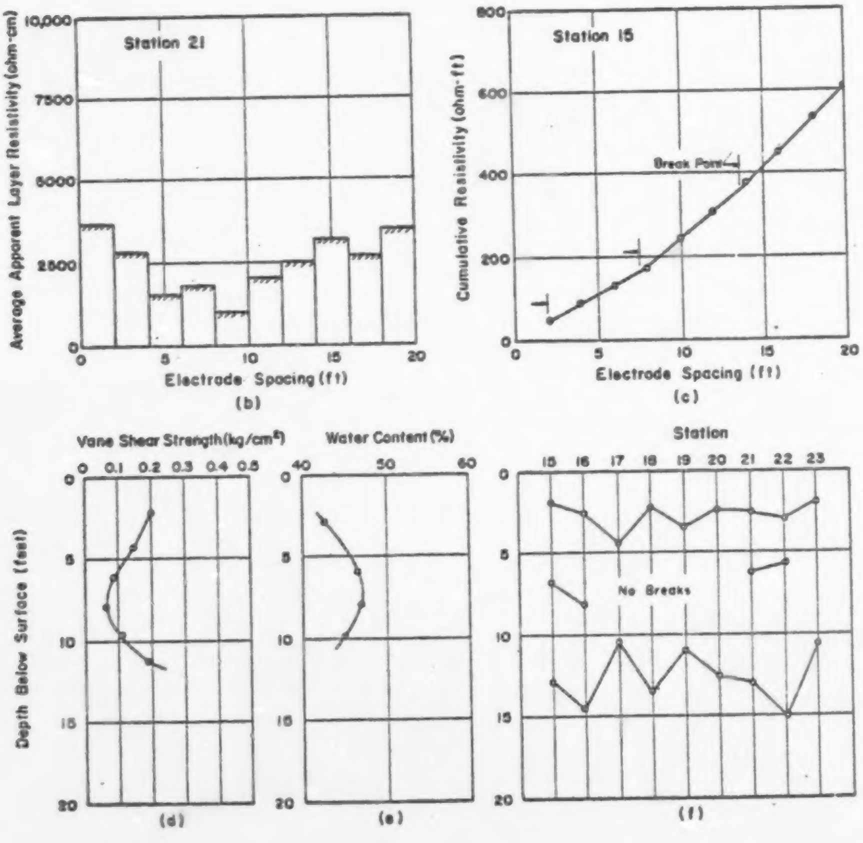

Figure 8-3. Resistivity Profile and Supplemental Data from Riverside Site

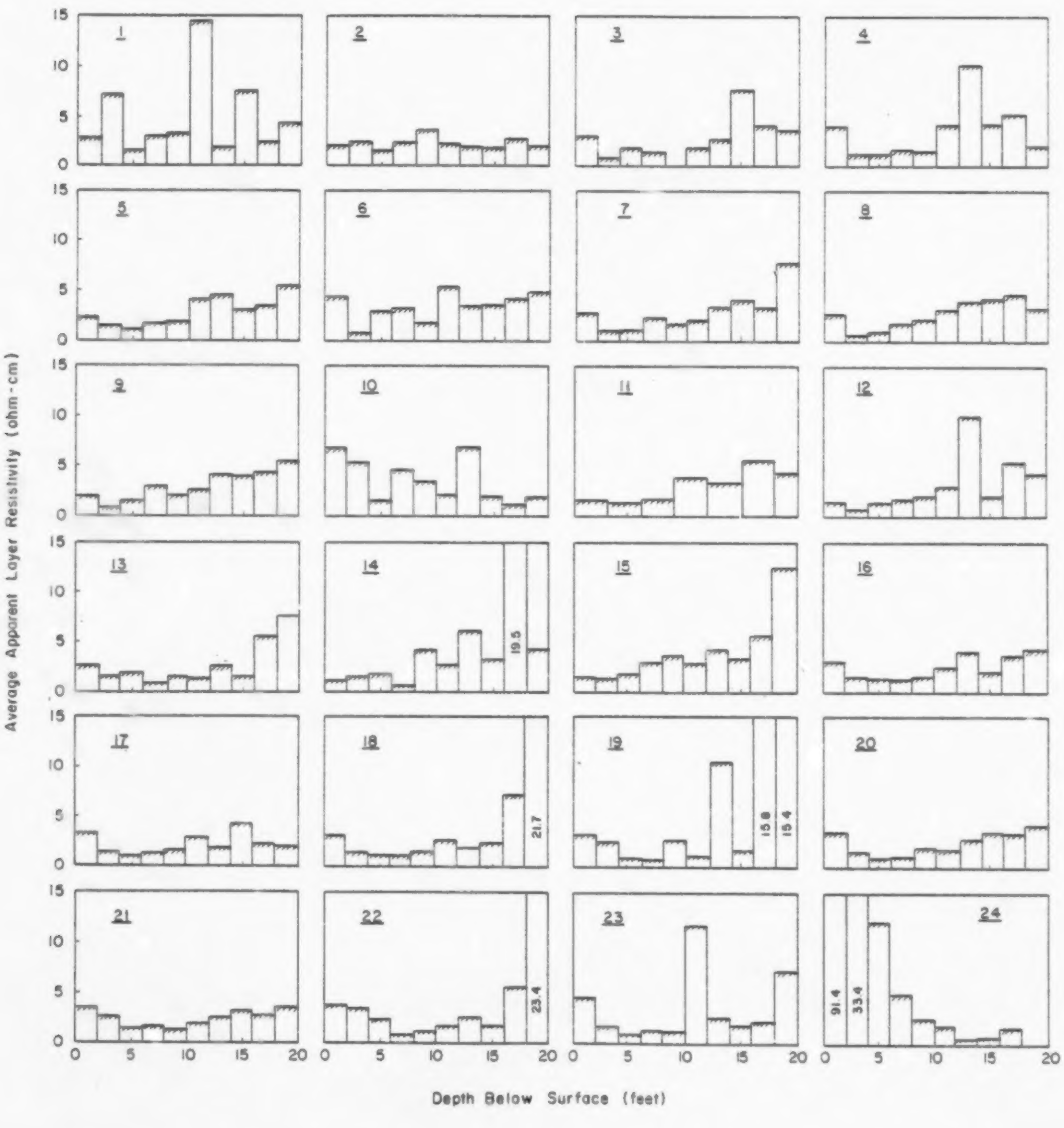

Figure 8-4. Average Apparent Layer Resistivities

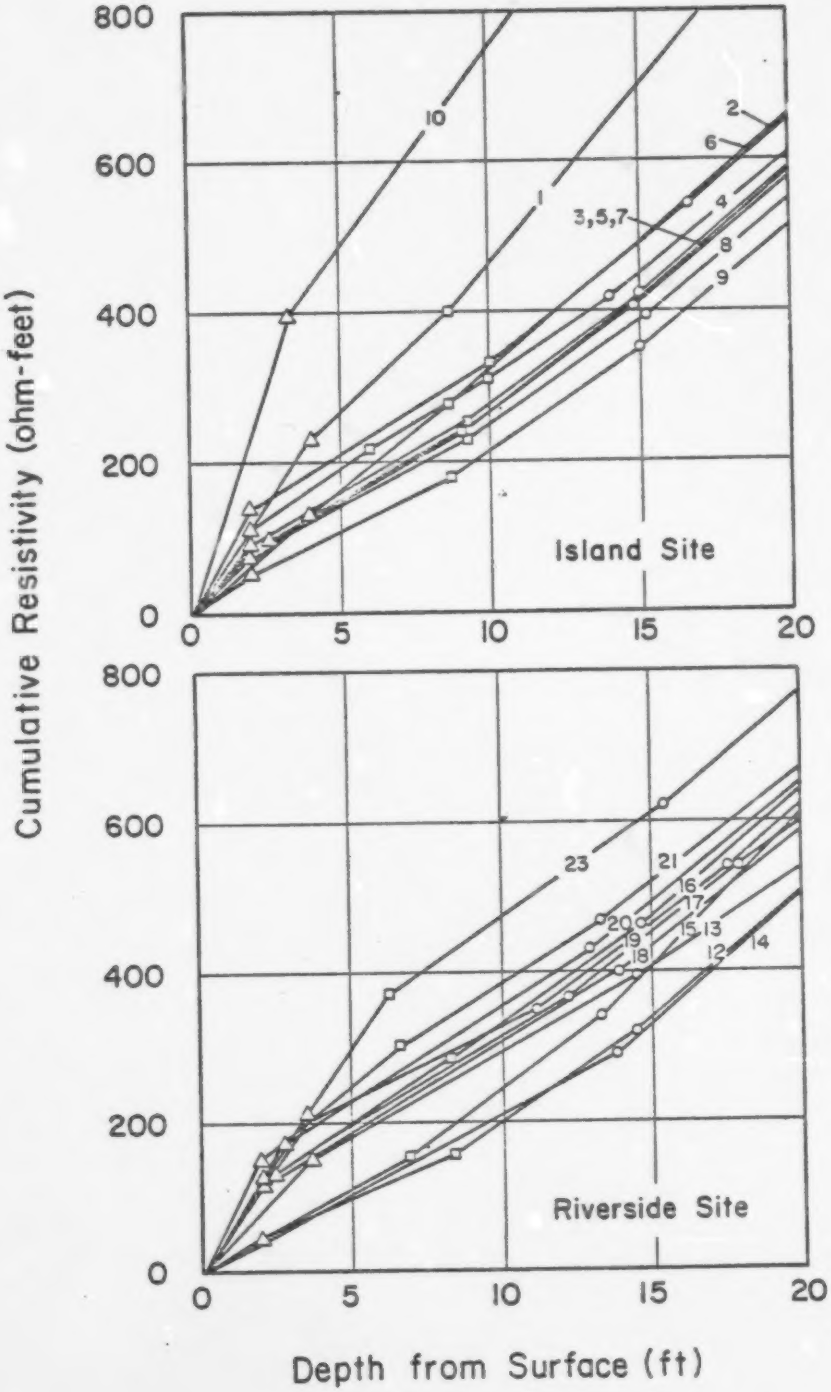

Figure 8-5. Cumulative Resistivity Curves

can be observed. The break points determined from the various supplemental graphs shown in Figure 8-5b have been plotted in Figure 8-3f, which presents the relationship between the depth of the break point and its location along the profile, where the scale along the profile is not uniform. The deepest of the three regions is on the order of 10 to 15 feet relative to the existing ground surface, and this suggests a change in the soil type, which is probably indicative of the original ground surface prior to deposition of dredgings.

CONCLUSIONS

Based on the results and interpretation of the electrical sounding survey reported herein, the following conclusions may be advanced:

1. The general trends exhibited by the Island Site and Riverside Site are similar.

2. Three phenomena apparently caused changes in the apparent resistivity values; these are (a) water content variations, (b) porosity and mineralogy changes, which are associated with grain size and grain size distribution, and (c) a change in the soil conditions. It appears that the longitudinal variations in the average apparent resistivity are due primarily to the sorting of particle sizes during the depositional process, and the variations with depth are caused mainly by water content changes.

3. The original ground surface before the deposition of dredgings was identifiable within reasonable limits by measuring the change in electrical resistivity with depth and interpreting the results in terms of the Moore Cumulative Method. By use of such a procedure the depth of dredgings at the Island Site was found to vary from 12 to 16 feet and at Riverside Site from 10 to 15 feet. The indicated variations in depth may be due to an undulating topography, inherent errors associated with the method, or a combination of both.

4. The electrical sounding technique is useful for detecting qualitative changes in soil conditions, but it must be supplemented by additional data in order to deduce reliable quantitative changes.

CHAPTER 9

SEISMIC SURVEY

The seismic refraction of layered soils is usually analyzed by assuming a constant velocity for each individual layer. Such an assumption gives reasonable results for the average velocity of each layer, but it does not provide any information about possible variations of velocity within the layer. Furthermore, if there is a high-velocity soil overlying a low-velocity soil, the presence of the latter will not be determined by use of conventional seismic refraction methods.

For the case reported herein the seismic response of a soft hydraulic fill overlain by a crust of desiccated material is studied by introducing some modifications to the standard seismic refraction field test and the associated interpretation procedure. The field tests were conducted by placing explosive charges (a) on the surface, (b) within the fill, and (c) near the surface of the original ground underlying the fill; the geophones and recording system utilized were standard equipment. Other tests using surface shots were conducted on a similar unfilled site in the vicinity to obtain additional data on the original ground conditions. As expected for a rather heterogeneous , consolidating soil, the response of the fill did not obey a constant-velocity law.

The interpretation of results is undertaken by first analyzing wave propagation in a semi-infinite mass with a one-dimensional variation of velocity, and the problem is solved graphically for the general case by introducing the appropriate boundary conditions. Then, a piece-wise linear variation of the velocity with depth is assumed, and the problem is solved analytically. A digital computer is used to determine the response of a fill with a widely varying velocity distribution, and results are plotted in the form of charts which give arrival times at different distances as a function of fill characteristics. The interpretation consists of selecting a theoretical response curve which best fits the one obtained in the field. The final step in this work is the comparison of the resulting velocity profiles with the soil strength profiles obtained by use of field vane shear tests. The analysis is completed by relating the results to the sedimentation and consolidation processes.

OBJECTIVES

The primary objective of this work is to evaluate the variations in material and consistency of a hydraulic landfill composed of maintenance dredgings, and this is accomplished in part by studying the propagation velocity of pressure waves within such a fill. We are interested in the variation of this velocity with depth, as well as its variation along a typical profile extending between the outlet and the inlet of the fill. The variation of velocity with depth will provide information about the consolidation process in the soil, and the variation of velocity along a horizontal profile will give information about the sedimentation process. Although the absolute value of the propagation velocity of pressure waves has significance for soils, the relative values and the variations from point to point are of primary interest in this particular study.

As a second objective, an attempt is made to evolve testing and interpretation procedures for evaluating these types of soils by use of seismic refraction techniques. Emphasis will be given to establishing the manner in which the field test should be conducted and the recorded data should be analyzed. Finally, the third objective is to analyze the velocity profiles and to study their correlation with other observed characteristics of the fill.

PRESENTATION OF THE DATA

Most of the data presented herein were obtained from Riverside Site in Toledo, Ohio, during the period from July 26 to 28, 1971, but some supplementary tests were conducted at the nearby Penn 7 Site. In this section a general discussion of the test procedure used in this work is presented, and recorded data are tabulated in Table 9-1. Following a brief explanation of how the response would be interpreted if a constant-velocity profile were hypothesized, the inapplicability of such a model is shown by examining the general trends of the data. Accordingly, a more general method of analysis is developed to interpret these data.

Test Procedure

In seismic refraction surveying, a burst of energy in the form of mechanical vibrations is imparted to the earth by means of an impact or an explosive charge, and the arrival times of the signal at various points on the ground surface are observed. The relations among the travel times to points at various distances from the energy source provides some information about the nature of the layered system.

Previous to the work described herein, an attempt was made to conduct seismic tests on a similar fill (Island Site) by use of an engineering seismograph with a hammer to provide the excitation energy. However, due to the poor ability of this soil to transmit the signals, it was impossible to record any response with the relatively low energy input afforded by a hand hammer. This difficulty was overcome at Riverside Site by the use of dynamite charges at different depths within the fill, rather than at the surface. A diagrammatic description of the seismic refraction method, as

Table 9-1. Summary of Data from Seismic Survey

Location	Shot Number	Location of Shot Point and Extreme Geophone (feet)	Geophone Spaci (feet)	Depth of Charge (feet)	Size of Charge S=dynamite stick B=blasting cap	Arrival Times (milliseconds, ±0.2 ms)											
						Geophone Number											
						1	2	3	4	5	6	7	8	9	10	11	12
Penn 7	1	0 - 120	10	3	½ S	8.0	14.4	20.4	26.6	30.4	34.8	38.2	41.6	42.8	43.4	45.0	48.0
	2	120 - 0	10	3	½ S	47.3	46.5	44.6	42.6	42.8	42.1	43.8	40.4	33.1	23.0	16.2	6.8
	3	0 - 360	30	3	1 S	18.6	30.7	42.1	46.8	55.9	62.0	71.6	74.1	73.9	71.7	71.8	70.6
	4	0 - 360	30	4	1 S	18.6	32.1	43.2	48.5	58.8	62.7	73.5	77.0	71.8	73.8	74.2	73.0
	5	360 - 0	30	3	1 S	71.4	68.6	71.2	69.2	71.4	68.7	71.5	61.0	50.0	47.0	39.2	25.4
	6	360 - 0	30	3	2 S	72.2	70.0	73.4	70.6	73.0	71.0	70.4	61.6	52.6	48.8	40.6	26.4
	7	0 - 360	30	4	2 S	18.2	31.9	42.8	47.8	58.8	65.5	72.8	75.3	72.5	76.9	75.0	74.3
	8	360 - 0	30	2½	2 S	78.7	77.4	76.8	76.8	80.3	75.5	76.8	68.8	57.8	55.4	46.2	31.0
Transverse Line at Riverside Site	9	300 - 180	10	0	2 B	12.1	20.9	29.3	38.6	47.6	56.4	65.2	74.0	82.7	92.5	101.3	109.5
	10	300 - 180	10	0	4 B	12.3	20.1	29.5	38.2	47.0	56.0	64.8	73.3	82.3	92.5	100.7	109.7
	11	300 - 180	10	5	2 B	33.5	44.4	46.5	49.5	50.3	54.6	59.6	66.0	66.9	70.1	77.4	80.9
	12	300 - 240	5	11	2 B	27.7	29.3	37.3	34.8	32.6	37.6	39.2	33.8	38.1	38.9	41.1	42.6
	13	300 - 180	10	11	½ S	29.9	34.7	34.7	35.6	37.0	39.5	43.4	49.4	51.9	52.9	60.5	64.9
	14	180 - 300	10	11	½ S	67.1	61.1	55.1	52.6	50.4	48.4	48.8	50.6	47.9	44.7	43.9	36.5
Longitudinal Line at Riverside Site	15	90 - 150	5	9	½ S	16.7	16.7	18.3	19.0	24.0	27.4	31.6	36.6	36.3	35.9	35.3	35.7
	16	90 - 210	10	9	½ S	17.6	19.7	28.7	36.4	36.2	36.2		40.0	45.3	44.3	43.5	47.7
	17	90 - 450	30	10	½ S	27.4	36.5	45.3	45.1	56.9	64.0	65.8	74.6				
	18	90 - 450	30	3	½ S	31.4	52.8	61.2	63.9	72.7	79.8	85.0	82.9	85.0	85.0	93.8	97.2
	19	510 - 150	30	10	½ S				71.0	71.8	70.6	65.6	65.8	55.7	48.5	46.5	28.1
	20	510 - 150	30	2½	½ S							165.8	139.2	113.1	86.3	59.9	35.1
	21	510 - 150	30	11	1 S	82.0	77.8	73.7	70.7	72.1	69.1	63.7	65.6	56.2	48.2	45.6	
	22	510 - 150	30	3	1 S	127.7	124.3	123.7	112.4	113.8	109.8	104.4	85.4	78.7	68.5	60.9	35.9
	23	940 - 1000	5	3	2 S	8.8	12.5	17.2	22.2	26.4	30.6	35.2	40.4	45.4	50.0	55.4	59.8
	24	940 - 1000	5	10	1 S	18.1	17.6	19.0	20.2	21.6	22.7	24.1	25.0	26.2	28.0	30.2	32.4
	25	940 - 580	30	10	1 S	23.9	31.3	42.3	57.1	62.4	68.1		70.5	71.3	80.5	82.3	83.7
	26	520 - 880	30	9	1 S	71.6	66.0	64.0	66.6	65.0	62.2	63.0	52.8	46.4	44.4	34.4	24.2
	27	560 - 720	5	10	1 S	18.8	17.6	17.8	17.8	19.2	22.0	25.6	27.4	28.6	28.2	27.8	31.8
	28	560 - 200	30	10	3 S	22.2	29.2	39.4	48.8	[illegible]	58.4	63.8	67.8	64.4	67.6	68.0	67.8
	29	940 - 1300	30			78.8	77.0	77.2	76.6	75.8	71.2	71.6	65.6	60.4	50.2	36.6	23.8
	30	1360 - 1000	30	10	2 S	22.0	35.2	50.0	58.5	65.6	67.8	72.6	70.8	72.6	71.2	72.2	73.0
	31	1360 - 1300	5	11	1 S	20.0	20.4	19.2	19.0	20.4	21.4	24.6	25.2	27.6	30.6	33.0	36.0
	32	1360 - 1300	5	2	½ S	6.4	10.6	14.8	19.6	24.0		33.4	37.8	42.4	46.4	51.7	55.5
	33	1340 - 1700	30	11	2 S	76.8	66.6	65.6	63.5	63.1	59.2	58.6	64.7	54.4	47.8	32.5	21.9
	34	1700 - 1640	5	11	1 S	14.2	[illegible]	21.2	22.6	22.8	21.2	22.4	24.0	26.8	27.0	29.5	32.9
	35	1700 - 2060	30	11	2 S	71.8	71.8	69.0	67.8	65.6	66.8	76.0	68.2	63.4	56.5	42.6	33.0
	36	2090 - 1730	30	4	2 S	34.8	50.4	55.2	59.4	63.8	71.1	85.2	85.7	87.5	87.5	88.0	88.4
	37	2090 - 2030	10	4	½ S	8.8	21.0	30.0	39.4	47.4	48.0	49.4	51.0	53.4	55.2	56.8	59.2
	38	2030 - 2090	10	1	1 S	61.6	61.8	59.0	56.8	56.4	53.6	45.8	36.8	28.1	23.2	14.0	6.8

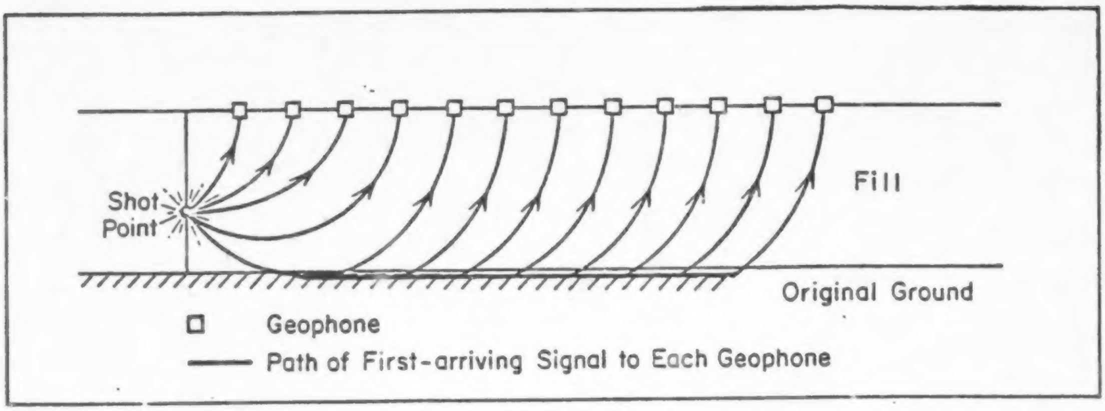

Figure 9-1. Diagrammatic Description of the Seismic Refraction Method

used in this study, is given in Figure 9-1. As a consequence of the low strength of the fill, it was possible to place the charges manually by pressing them into the fill with a plastic tube. In the vicinity of the inlet pipe, where more granular materials were deposited, a hand auger was used to place the charge. The geophone lay-out and the recording system were the same as used in the standard procedure. The equipment used was a Geo-Space GT-2B refraction seismograph, a 12-channel instrument which records the traces of 12 geophones on a polaroid paper print. Clear and well-defined signals were recorded in most cases, and a complete set of data was obtained.

Data

Eight tests were performed at the Penn 7 Site, a future dredgings disposal area in the vicinity of Riverside Site, to measure the response of the original ground, which presumably is similar to that underlying the landfill at Riverside Site. Then, a total of thirty tests were conducted on the fill at Riverside Site. A plan of the location of these tests is shown in Figure 9-2. The line of each shot is indicated in Table 9-1 by expressing in feet the distance of the shot point and geophone number 12 from the outlet weir;

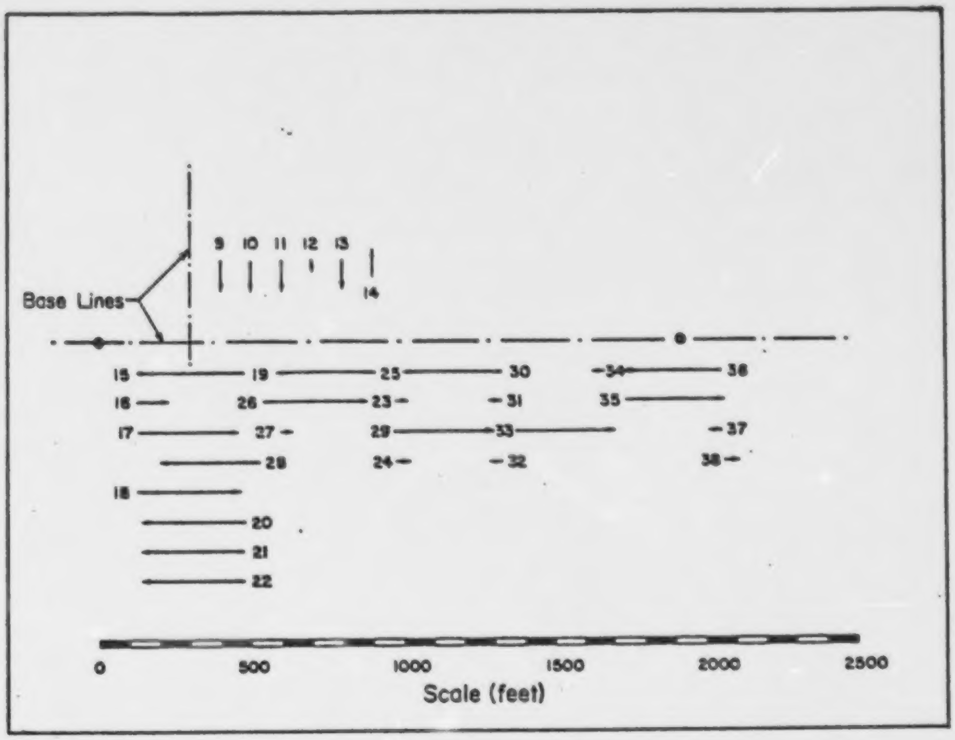
9
10
11
12
13
14
Base Lines
15
19
25
30
34
36
16
26
23
31
35
17
27
29
33
37
28
24
32
38
18
20
21
22
0
500
1000
1500
2000
2500
Scale (feet)

Figure 9-2. Lay-out of the Seismic Tests at Riverside Site

these points represent the extremes of the line, and their order indicates the direction of the shot. An arbitrary origin is chosen in the Penn 7 Site to show the relative locations of Shots 1 to 8 conducted in this area. In the same table is given the spacing of the geophones for each shot, the depth at which the explosive was placed, and the size of the charge employed. The data, which include the arrival times at each of the twelve geophones on the line, were obtained by carefully reading photographic records of geophone signals by use of a magnifying lens and a finely divided scale; probable errors are believed to be on the order of ± 0.1 ms. In addition, there is a possible error of ± 0.1 ms due to the testing procedure. Therefore, any scatter greater than ± 0.2 ms is considered to be attributable to soil conditions.

Theoretical Response for Constant Velocity Profile

In order to demonstrate the need for a more general interpretation procedure for these tests, this section presents the theoretical response based on the assumption of a constant velocity profile within the fill. The next section will compare actual data with that deduced from this simplified model, and this comparison will provide the basis for the way in which the standard procedure should be modified. The time for a compression wave in a constant-velocity fill to travel between an explosive charge at a depth S and a geophone on the surface is given by

$$t = \frac{1}{V_F} (x^2 + S^2)^{\frac{1}{2}} \tag{9-1}$$

where t is the travel time, V_F is the velocity of the fill material, x is the horizontal distance between the shot and the geophone, and S is the depth of the shot. If the fill is underlain by a layer of higher velocity, the path of the first-arriving signal at a distant geophone will be partly in the layer of higher velocity; the travel time for the signal is then given by

$$t = t_B + \frac{x}{V_B} \tag{9-2}$$

where t_B is the time intercept for the bottom waves, and V_B is the velocity of the bottom material. The meaning of the time intercept t_B is shown in Figure 9-3, which is a hypothetical plot of travel time versus distance for the conditions postulated. The value of t_B can be easily found from the expression

$$t_B = \frac{2H-S}{V_B} \cot i \tag{9-3}$$

where H is the thickness of the fill, and i equals $\sin^{-1}(V_F/V_B)$. Note that x_c in Figure 9-3 is the "critical distance", or the distance on the ground

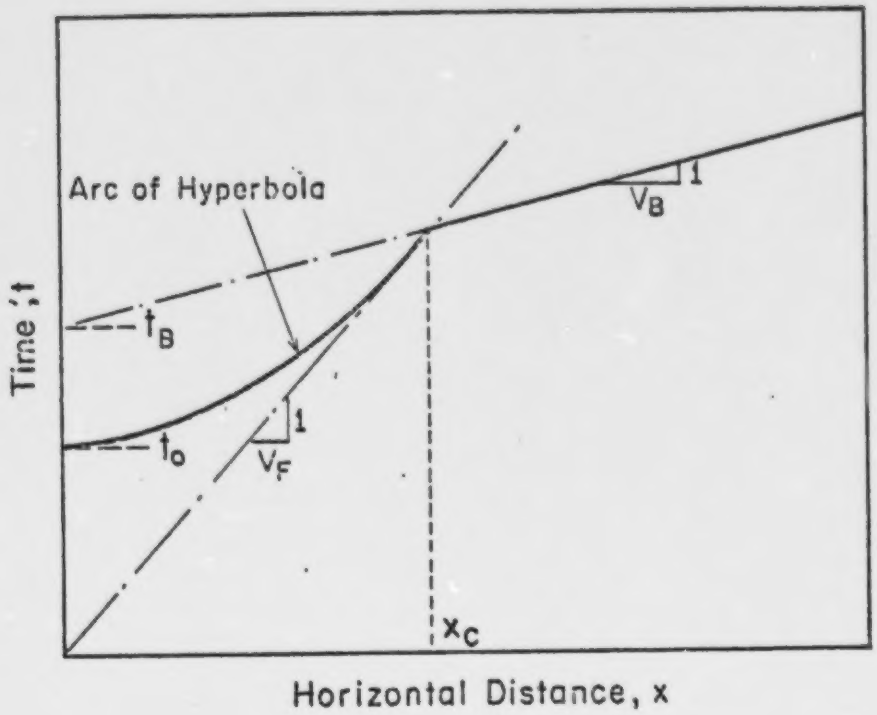

Figure 9-3. Theoretical Response for Two Layers with Constant Velocity

surface at which the direct wave reaches the point at the same time as the refracted wave. The graphical expression of these relations on the t-x plot is an arc of hyperbola (intercepting the t axis at $t_o = S/V_F$) for the fill response and a straight line corresponding to the bottom wave. If bed-rock were present at sufficiently shallow depth, a third portion of the curve, consisting of a straight line of lower slope, would be expected.

General Trends of Actual Response

There are several features of the actual response that make it different from the ideal seismic test results illustrated above, and these features will constitute the basis for the development of the interpretation procedure. Three of the most important general characteristics obtained directly from an overall analysis of the data are considered in this section.

Air Waves.-- Looking at the data corresponding to Shots 9 and 10, we see that they describe almost exactly a straight line with a slope that corresponds to a velocity of 1.14 ft/ms. In addition, the sense of the first-arriving wave as recorded on the photograph is opposite to that normally observed. These considerations lead to the conclusion that the impulse exciting the geophone is an airborne wave in these cases. The homogeneity of the air explains the fact that the data are described so well by a straight line. The slope of this line gives the propagation velocity of a pressure wave in air, and the unusual type of signal recorded on the photograph can be explained as an initial downward movement of the geophone, rather than the upward movement which would be caused by the vertical component of a ground wave; the geophones used do not register horizontal movements.

Once it is recognized that initial signals caused by air waves are a possibility, an interpretation method must be developed to distinguish between air waves and ground waves and, if possible, to account for the circumstances which control the appearance of such waves. It will be shown that airborne signals can be properly analyzed and that they can be helpful in the interpretation procedure.

Cap Delays.-- In the standard interpretation procedure the fact that all arrival times are out of phase by an unknown constant time does not seriously affect the results, because the slopes of the lines and the abscissae of the break points are unchanged, and these are the features upon which the method is based. In this case, however, absolute arrival times are needed, and hence this unknown constant time must be determined. The main causes of this initial delay time are cap delays and apparent delays due to errors of alignment in the recording system. The first cause gives a constant delay which is the same for each geophone, whereas the second produces a delay which is different for each geophone. An independent investigation directed to this point gave very small cap delay times, which were on the order of 1.4 ± 0.2 ms. The investigation consisted of a special series of seismic tests in which the geophones were closely spaced. Also, the characteristic delay time given by the manufacturer of the cap was considered. These determinations of cap delay agreed closely with those calculated by theoretical considerations from the survey data. The second cause of delay (that is, due to the recording system) was corrected in the normal manner by a series of calibration shots. The data analyzed herein have been corrected for the effects of these time delays.

Variation of Velocity with Depth.-- To illustrate the variation of velocity with depth, Shots 11 and 12 are examined. The charge in Shot 11 was placed at a depth of 5 feet, whereas in Shot 12 it was placed in the same hole at a depth of 11 feet. The respective arrival times at a distance of 10 feet in the horizontal plane were 32.1 ms for the shallow shot and 27.9 ms for the deeper shot. For a constant-velocity model the arrival time for the second case should have been about 39 ms to be consistent with the first case. This anomaly can not be handled by a constant-velocity model, but it presents no problem when dealing with a more general model. Although this point has been illustrated by only one example, it can be seen that this type of result is typical of the data in Table 9-1.

METHOD OF ANALYSIS

Since the general trends of the recorded response from this site can not be interpreted on the basis of a constant velocity model, the problem of pressure wave propagation in a medium with spatially varying characteristics is addressed. A graphical solution is found for cases in which the propagation velocity is a generalized function of depth, and an analytic solution is determined for cases in which this variation can be expressed as a piece-wise linear function. The latter variation is selected for the interpretation advanced in this study, and a digital computer is used to prepare charts which give arrival times as functions of different constants describing the velocity distribution. The interpretation procedure consists of using these charts to determine the soil characteristics which agree most closely with the recorded response.

Propagation of Pressure Waves in a Continuum

The principle of minimum time defines the ray path between two given points P_1 and P_2 in a continuum, and this can be expressed as

$$\frac{\partial}{\partial C}\left\{\int_{P_1}^{P_2}\frac{ds}{V(s)}\right\}_C = 0 \tag{9-4}$$

where C represents the ray path, s is the distance along C, and V is the propagation velocity of the medium, which is assumed to be isotropic, although, in general, it varies with s. Equation (9-4) can be solved with relative ease if the variation of velocity is assumed to be a unique function of depth, that is, there is no spatial variation in any given horizontal plane, and such a situation is treated in the following section.

Medium with Uni-directional Variation of Velocity

Letting V be a function of one variable, which is chosen as the y axis of the reference system, we may write Equation (9-4) as

$$\frac{\partial}{\partial C}\left\{\int_{P_1}^{P_2}\frac{ds}{V(y)}\right\}_C = 0 \tag{9-5}$$

which can be expressed in terms of the horizontal coordinate, x, as

$$\frac{\partial}{\partial C}\left\{\int_{P_1}^{P_2}\frac{(1+y'^2)^{\frac{1}{2}}}{V(y)}\,dx\right\}_C = 0 \tag{9-6}$$

The above equation is a particular form of the Euler-Lagrange differential equation, and its solution can be found in any book on variational calculus; specifically, this solution may be written as

$$(x-x_o) = A\int_{y_o}^{y}\frac{V(\eta)}{(1-A^2V^2(\eta))^{\frac{1}{2}}}\,d\eta \tag{9-7}$$

where x_o and y_o are the coordinates of the excitation point and A is a parameter, particular values of which are associated with particular ray paths emanating from the excitation point. Equation (9-7) can be written in differential form as

$$dx = \frac{A\,V(y)}{\left\{1-A^2V^2(y)\right\}^{\frac{1}{2}}}\,dy \tag{9-8}$$

or

$$1+\left(\frac{dy}{dx}\right)^2 = \frac{1}{A^2V^2(y)} \quad . \tag{9-9}$$

By use of the inclination angle i of the ray path, as shown in Figure 9-4, we may write

$$\frac{V}{\sin i} = \frac{1}{A} \quad , \tag{9-10}$$

which is a form of Snell's law. Equation (9-10) is a very simple form of the field equation governing the propagation of pressure waves in a continuum, and it may be interpreted graphically in the following manner. Differentiation of Equation (9-10) gives

$$\frac{dV}{V} = \frac{di}{\tan i} \quad . \tag{9-11}$$

If R is the radius of curvature of the ray path, we have the following relations:

$$R\, di = ds \tag{9-12}$$

$$dy = (\cos i)\, ds \tag{9-13}$$

$$dV = \frac{dV}{dy} (\cos i)\, ds \tag{9-14}$$

which can be used to transform Equation (9-11) to

$$R \sin i = \frac{V}{dV/dy} \quad . \tag{9-15}$$

The geometrical meaning of Equation (9-15) is that the ordinate of the center of curvature of any ray path at any point is the subtangent of the velocity versus depth curve at that point. Accordingly, points CC and ST in Figure 9-4 must lie on a horizontal line. This geometrical condition is the graphical expression of the field equation of the problem. As shown later, this interpretation will allow the construction of the ray paths from the source point to any other given point within the continuum.

The second point of interest is the definition of the time required for the impulse to reach a given point. This time is a scalar function whose gradient is tangent to the ray path, and it has a modulus equal to

$$|\text{gradient } t| = 1/V \quad . \tag{9-16}$$

The horizontal component of this gradient is

$$\frac{\partial t}{\partial x} = \frac{1}{V} \sin i \tag{9-17}$$

which, with the use of Equation (9-10), becomes

$$\frac{\partial t}{\partial x} = A \tag{9-18}$$

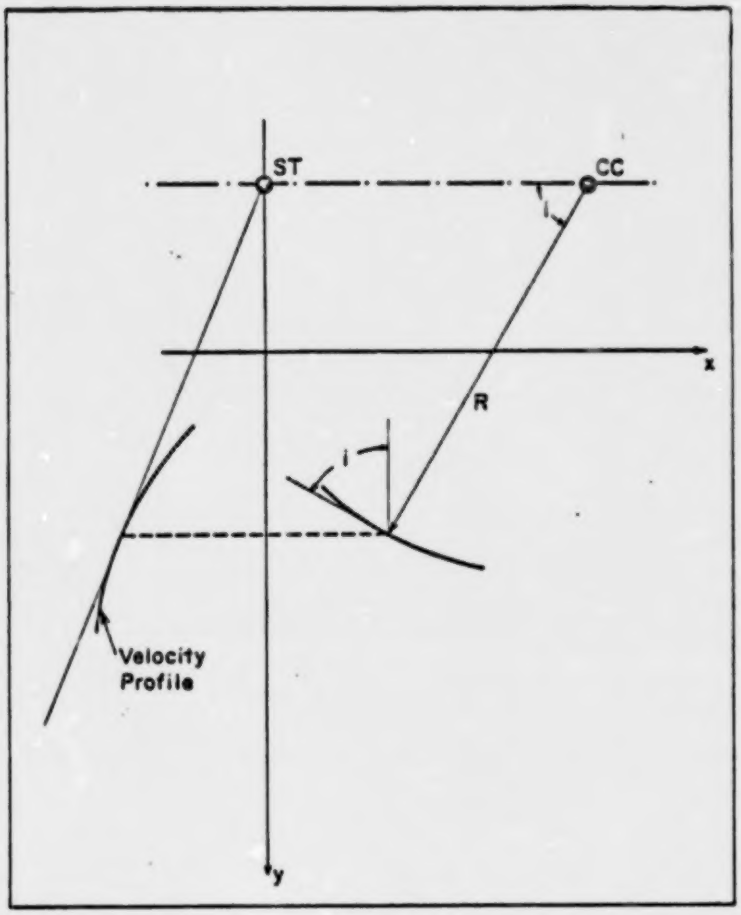

Figure 9-4. Geometrical Interpretation of Snell's Law

Equation (9-18) allows us to state that the horizontal component of the time gradient is constant along the ray paths. Since this component of the gradient is the slope of the arrival time versus distance plots, this condition will facilitate a graphical determination of the arrival time at each point once the ray path is known. Note that the value of A according to Equation (9-10) is precisely the reciprocal of the velocity at the lowest point of the ray path, where the angle i is a right angle.

Graphical Determination of Time-Distance Plot

Use of the two conclusions derived from the geometric interpretation of the differential equation for this problem allows the solution to be found in a graphical manner. Figure 9-5 shows an arbitrary velocity profile which is approximated by a series of chords. In this way the continuum is divided

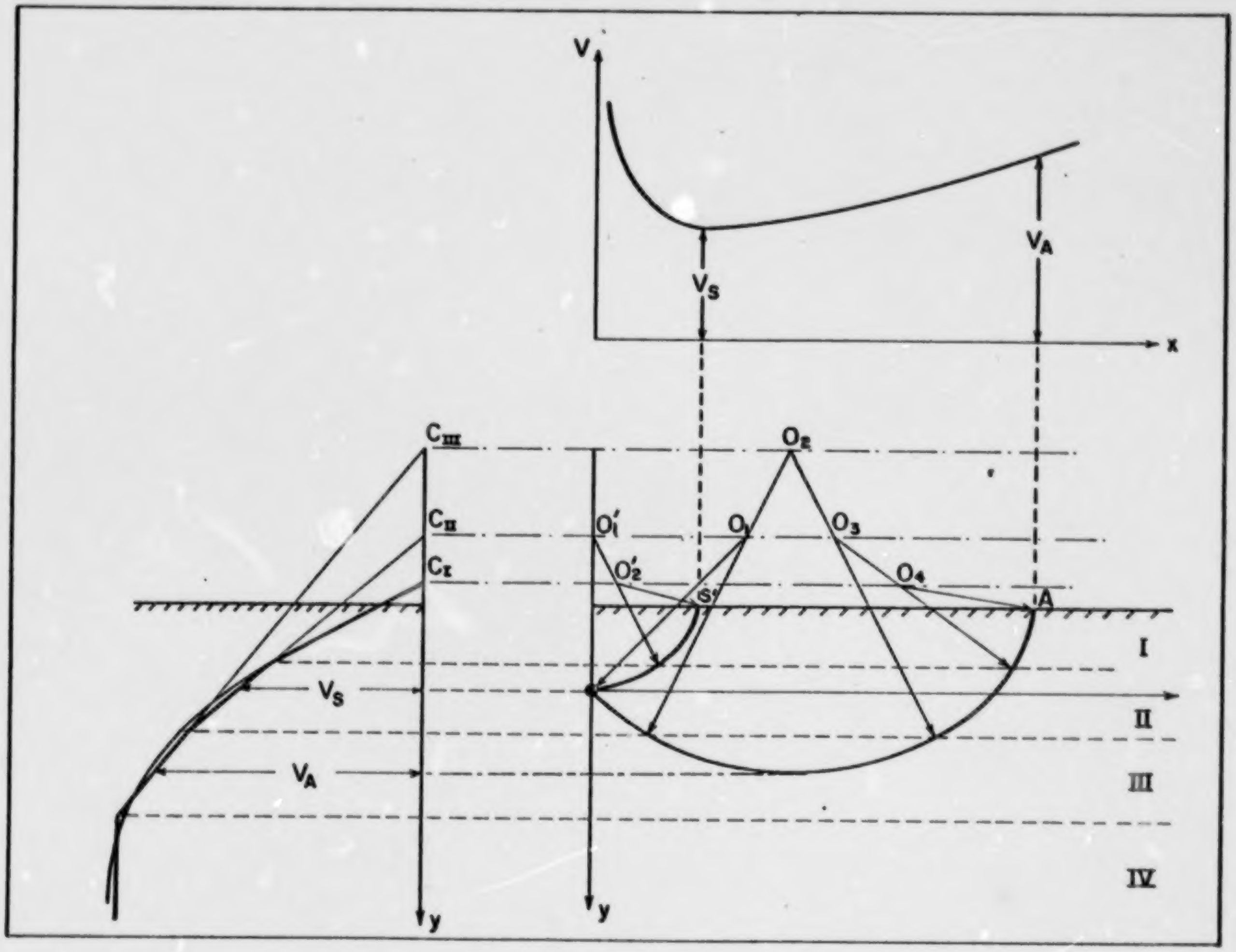
V
x
V_S
V_A
C_{III}
C_{II}
C_I
O_2
O_1'
O_1
O_3
O_2'
O_4
S'
A
I
II
III
IV
y
y

Figure 9-5. Graphical Determination of Seismic Response

into horizontal zones I, II, III,... whose corresponding subtangent intersections are C_I, C_{II}, C_{III},..., and ray paths within these zones will have their centers of curvature at the horizontal lines passing through C_I, C_{II}, C_{III},..., respectively. Taking any center, 0_1, on the locus of centers corresponding to the zone where the source is placed, the first part of the ray path is constructed. When entering a different zone, the center of curvature is moved to a new position, 0_2, at the corresponding level, and a second circular arc is drawn. These steps are repeated until we reach a point on the horizontal surface where the geophones are placed. When this has been achieved, the apparent velocity is simply the velocity corresponding to the lowest point of the ray path.

A repetition of this process will allow several points of the apparent velocity-distance plot to be defined, and the integration of this plot by any of the usual graphical means will yield directly the time-distance plot. Note that the time intercept of these plots can be determined previously as

$$t_o = \int_0^S \frac{dy}{V} \tag{9-19}$$

which corresponds to the time for the vertical,straight ray path from the source to the point above it at the level of the geophones. In Figure 9-5 two ray paths are drawn by use of centers 0_1, 0_2,... and $0'_1$, $0'_2$,..., respectively. Although some interesting properties could be derived for the response of a continuum with an arbitrary velocity profile, the complexity of this model precludes its widespread use, and the interpretation procedure employed herein will be based on a simpler model, which is reasonably representative of actual field conditions encountered.

Layer of Finite Thickness with a Linear Variation of Velocity

The field conditions for the fill area under consideration can be represented by an infinite continuum consisting of the air, the consolidating fill (deposited dredgings), and the original ground. In this study the propagation velocities of pressure waves in the air and in the original ground are obtained from airborne and original ground signals, respectively, by use of conventional techniques. The problem thus reduces to one of finding the response of a given layer between two semi-infinite media with constant velocity. In order to obtain a sufficiently simple solution for use in interpretation, a linear variation of the velocity with depth is assumed within the fill; a diagram of this model is shown in Figure 9-6.

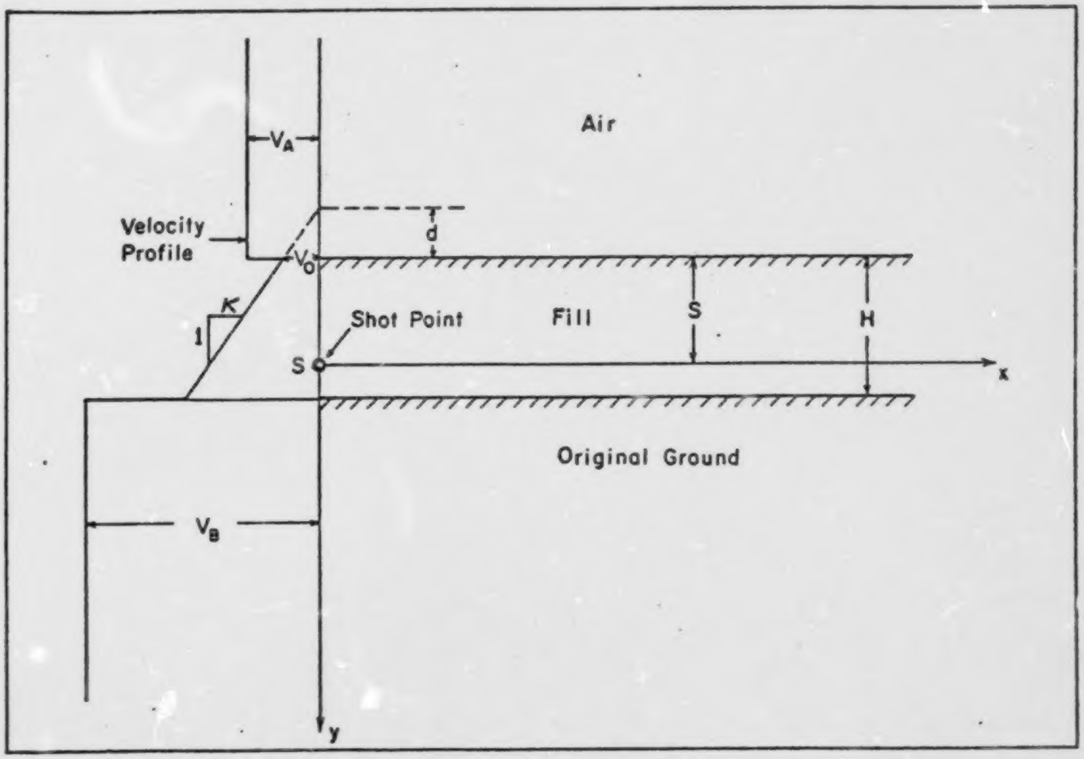

Figure 9-6. Model with Piece-wise Linear Velocity Profile

The propagation velocities in the air and the ground are termed V_A and V_B, respectively, and other variables in this model are the depth of the shot, S, the lowest velocity of the fill, V_o, the slope of the velocity profile, κ, and the thickness of the fill, H.

Even though the resulting formulae are derived for this case, they can be modified when a crust of constant velocity overlies the fill layer or when the velocity within the fill is discontinuous due to inclusions of higher or lower velocity. This model can also be modified to handle velocity variations with depth in the original ground. The manner in which these modifications affect the response can be determined by use of the same formulae. For example, the effect of a desiccated crust can be simulated by assuming the geophones to be placed under the crust, solving for this case, and adding to the resulting times the time required for a wave to pass through the crust; this type of modification should be performed for each shot, and it should constitute part of the interpretation. The solution for the model given in Figure 9-6 is found by considering individually the three parts into which the velocity profile is divided; however, the wave propagation within the fill is analyzed first.

Ray Paths.-- For the coordinate system given in Figure 9-6 the variation of velocity is given by

$$V(y) = \kappa(y + d + S) \tag{9-20}$$

where

$$d = \frac{V_o}{\kappa} \; . \tag{9-21}$$

According to the geometrical interpretation of the general problem, the ray paths in this particular case will be arcs of circles having their centers on the line $y = -(d + S)$ and passing through the origin of the coordinate system. Such a family of circles can be expressed by the parametric equation

$$x^2 + y^2 + 2(d + S)y - 2\lambda x = 0 \tag{9-22}$$

where the centers and radii of these circles are

$$\text{centers} = (\lambda, -(d + S)) \tag{9-23}$$

and

$$\text{radii} = (\lambda^2 + (d + S)^2)^{\frac{1}{2}} \tag{9-24}$$

Isochrones.-- The family of isochrones, which are orthogonal to the ray paths, is described by a set of circles centered on the y axis and described by equations of the form

$$x^2 + y^2 - 2\mu y = R^2 - \mu^2 \quad . \tag{9-25}$$

The orthogonality condition, which can be expressed as

$$R^2 + \lambda^2 + (d + S)^2 = \lambda^2 + (\mu + d + S)^2 \tag{9-26}$$

and simplified to

$$R^2 = \mu^2 + 2\mu(d + S) \quad , \tag{9-27}$$

can be substituted into Equation (9-25) to obtain

$$x^2 + y^2 - 2\mu(y + d + S) = 0 \tag{9-28}$$

which is the parametric equation of the isochrones.

Time Associated with Each Wave Front.-- Each value of μ in Equation (9-28) defines a wave front position or an isochrone which is the locus of points that receive the wave signal simultaneously at time t. This time can be obtained by integrating along any ray path between the shot point and the isochrone, and it may be written as

$$t = \int_S^A \frac{dS}{V} \quad . \tag{9-29}$$

The integral in Equation (9-29) can be evaluated by use of the polar coordinate system shown in Figure 9-7, where

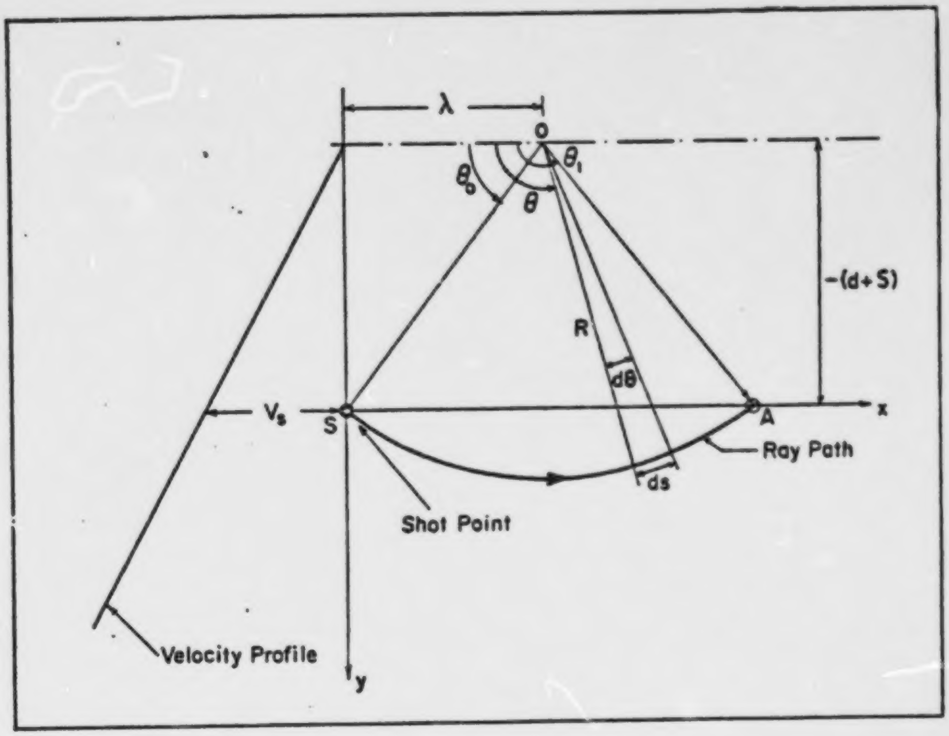
λ
O
θ_o
θ
θ_1
-(d+S)
R
dθ
V_s
S
A
x
Ray Path
ds
Shot Point
Velocity Profile
y

Figure 9-7. Path of Integration to Determine Arrival Times

$$ds = R\,d\theta \tag{9-30}$$

and

$$V = \kappa R \sin\theta \quad . \tag{9-31}$$

Substitution of Equations (9-30) and (9-31) into Equation (9-29) yields

$$t = \frac{1}{\kappa}\int_{\theta_o}^{\theta_1} \frac{d\theta}{\sin\theta} \tag{9-32}$$

which can be integrated to obtain

$$t = \frac{1}{\kappa}\,\ell n\left\{\tan\frac{\theta}{2}\right\}\Big|_{\theta_o}^{\theta_1} \quad . \tag{9-33}$$

Equation (9-33) can be written in any of the following forms:

$$t = \frac{1}{\kappa}\sinh^{-1}\left\{\cot\theta\right\}\Big|_{\theta_o}^{\theta_1} \tag{9-34}$$

$$t = \frac{1}{\kappa} \cosh^{-1}\left\{\csc \theta\right\}\Big|_{\theta_o}^{\theta_1} \tag{9-35}$$

$$t = \frac{1}{\kappa} \tanh^{-1}\left\{\cos \theta\right\}\Big|_{\theta_o}^{\theta_1} \tag{9-36}$$

If L is defined as the horizontal distance between points S and A, θ_o and θ_1 can be expressed as

$$\cot \theta_o = \frac{L}{2(S + d)} \tag{9-37}$$

$$\theta_1 = \pi - \theta_o \quad . \tag{9-38}$$

When the values are substituted into Equation (9-34), we obtain

$$t = \frac{2}{\kappa} \sinh^{-1} \frac{L}{2(S + d)} \quad . \tag{9-39}$$

By specifying that point A is at the isochrone associated with the parameter μ, we get

$$L^2 = 2\mu(d + S) \tag{9-40}$$

which allows the time associated with each isochrone to be stated explicitly as

$$t(\mu) = \frac{2}{\kappa} \sinh^{-1}\left\{\frac{\mu}{2(d + S)}\right\}^{\frac{1}{2}} \tag{9-41}$$

Time-Distance Plot.-- The arrival times at the points of the line along which the geophones are placed are obtained by first seeking the corresponding isochrones. Any point on this line has the coordinates (x,-S), and the associated isochrone will have a parameter μ such that the coordinates of the point satisfy Equation (9-28); thus, we obtain

$$x^2 + S^2 - 2\mu d = 0 \quad . \tag{9-42}$$

Substitution of the value for μ obtained from Equation (9-42) into Equation (9-41) yields directly the equation of the time-distance plot corresponding to waves transmitted through the fill:

$$t(x) = \frac{2}{\kappa} \sinh^{-1}\left\{\frac{x^2 + S^2}{4d(d + S)}\right\}^{\frac{1}{2}} \quad . \tag{9-43}$$

Equation (9-43) can be expressed in terms of velocities by use of Equations (9-20) and (9-21):

$$t(x) = \frac{2}{\kappa} \sinh^{-1}\left\{\frac{(\kappa x)^2 + (V_S - V_o)^2}{4V_S V_o}\right\}^{\frac{1}{2}} \tag{9-44}$$

where V_S is the velocity at the depth of the shot.

Some Features of the Solution.-- There are certain features of the time-distance plot that should be pointed out and discussed. The apparent velocity at the level of geophones, obtained by taking the derivative of Equation (9-44), is

$$V(x) = \frac{\kappa x}{2} \left\{1 + \left(\frac{2d + S}{x}\right)^2\right\}^{\frac{1}{2}}\left\{1 + \left(\frac{S}{x}\right)^2\right\}^{\frac{1}{2}} \quad . \tag{9-45}$$

Using Equation (9-22) to evaluate the radius of curvature of the ray path emerging at the line of the geophones at point x, we get

$$R(x) = \frac{x}{2} \left\{1 + \left(\frac{2d + S}{x}\right)^2\right\}^{\frac{1}{2}}\left\{1 + \left(\frac{S}{x}\right)^2\right\}^{\frac{1}{2}} \quad . \tag{9-46}$$

The combination of Equation (9-46) with Equation (9-45) allows the velocity to be written as

$$V(x) = \kappa R(x) \quad . \tag{9-47}$$

The apparent velocity at any point along the ground surface is proportional to the radius of curvature of the ray path at that point. According to Equation (9-47), there is a minimum for V(x). Since the center of curvature must be placed at the horizontal line $y = -(d + S)$, we have

$$R(x) \geq d + S \quad . \tag{9-48}$$

The minimum value of the radius of curvature yields the minimum value of the apparent velocity:

$$V_{min} = \kappa(d + S) = V_S \tag{9-49}$$

which gives an inflection point on the time-distance plot. The location of this inflection point can be obtained from Equation (9-22) as

$$x_{inf} = \left\{S(2d + S)\right\}^{\frac{1}{2}} \qquad (9\text{-}50)$$

and the corresponding time is

$$t_{inf} = \frac{2}{\kappa} \sinh^{-1} \frac{S}{2d} \qquad (9\text{-}51)$$

From this situation it can be deduced that the time-distance plot has an inflection point at which the apparent velocity is the same as that at the depth of the shot, and the apparent velocity from the time-distance plot is always equal to or greater than that corresponding to the depth of shot. At the origin of the x axis, the emerging ray is straight and, according to Equation (9-47), the apparent velocity is infinite, and the time-distance plot has a horizontal tangent. The corresponding time intercept can be found from Equation (9-43) as

$$t_o = \frac{2}{\kappa} \sinh^{-1}\left\{\frac{S}{z} \left(\frac{1}{d(d + S)}\right)^{\frac{1}{2}}\right\} \qquad (9\text{-}52)$$

These features, which have been discussed for the particular model selected, could be derived for the general case. In the latter situation the same conclusions apply with a different time intercept and a different location of the inflection point, but with the same values for the apparent velocity.

Bottom Waves.-- The time-distance plot corresponding to bottom waves, which are refracted at the interface between the fill and the original ground, is a straight line with a slope that is the inverse of the bottom velocity, V_B, and a time intercept which is evaluated as follows. First, the center of the ray path within the fill is found by imposing the condition of refraction. Since the apparent velocity of any ray refracted at the bottom is V_B, the radius of curvature of the ray path within the fill is

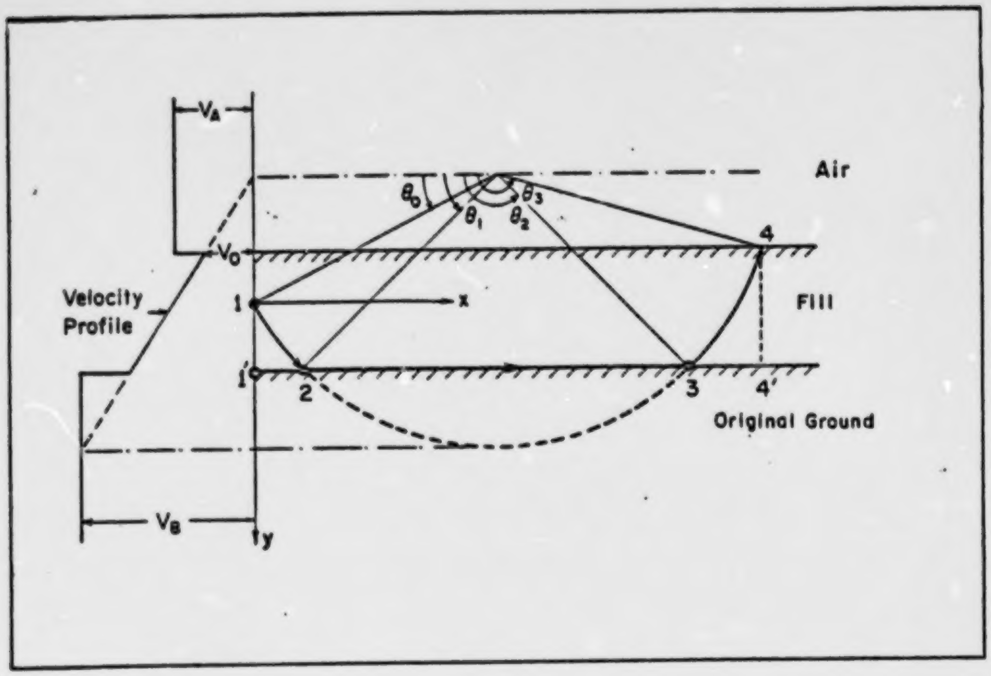

V_A
Air
θ_0
θ_1
θ_2
θ_3
4
V_0
Velocity Profile
1
x
Fill
1'
2
3
4'
Original Ground
V_B
y

Figure 9-8. Refraction at the Bottom of the Fill

$$R = \frac{V_B}{K} \quad . \tag{9-53}$$

If we complete the ray path in the fill with an imaginary arc extending into the bottom layer, as shown in Figure 9-8, the lowest point of this prolongation of the ray would be at the level where the prolongation of the fill velocity profile intercepts the bottom velocity. According to the notation given in Figure 9-7, the time intercept can be evaluated as

$$\begin{aligned} t_B &= \left[t_{12} + t_{23} + t_{34}\right] - \left[t_{1'2} + t_{23} + t_{34'}\right] \\ &= t_{12} + t_{34} - t_{1'2} - t_{34'} \end{aligned} \tag{9-54}$$

where the subscripts indicate the path along which the times are evaluated. Equation (9-35) may be used to obtain

$$t_{12} + t_{34} = \frac{1}{\kappa}\left\{\cosh^{-1}\left(\frac{1}{\sin\theta_o}\right) - \cosh^{-1}\left(\frac{1}{\sin\theta_1}\right) + \cosh^{-1}\left(\frac{1}{\sin\theta_2}\right) - \cosh^{-1}\left(\frac{1}{\sin\theta_3}\right)\right\} \qquad (9\text{-}55)$$

and

$$\sin\theta_o = \frac{V_S}{V_B} \qquad (9\text{-}56)$$

$$\sin\theta_1 = \sin\theta_2 = \frac{V_H}{V_B} \qquad (9\text{-}57)$$

$$\sin\theta_3 = \frac{V_o}{V_B} \qquad (9\text{-}58)$$

where

$$V_H = V_o + \kappa H \quad . \qquad (9\text{-}59)$$

Substitution of Equations (9-56) through (9-59) into Equation (9-55) yields

$$t_{12} + t_{34} = \frac{1}{\kappa}\left\{\cosh^{-1}\frac{V_B}{V_o} + \cosh^{-1}\frac{V_B}{V_S} - 2\cosh^{-1}\frac{V_B}{V_H}\right\} \quad . \qquad (9\text{-}60)$$

Time $t_{1'2}$ may be evaluated by

$$t_{1'2} = \frac{R(\cos\theta_o - \cos\theta_1)}{V_B} \quad , \qquad (9\text{-}61)$$

which, by use of Equations (9-56) through (9-59), becomes

$$t_{1'2} = \frac{1}{\kappa}\left\{\left[1 - \left(\frac{V_S}{V_B}\right)^2\right]^{\frac{1}{2}} - \left[1 - \left(\frac{V_H}{V_B}\right)^2\right]^{\frac{1}{2}}\right\} \quad . \qquad (9\text{-}62)$$

Similarly, we obtain

$$t_{34'} = \frac{1}{\kappa}\left\{\left[1 - \left(\frac{V_o}{V_B}\right)^2\right]^{\frac{1}{2}} - \left[1 - \left(\frac{V_H}{V_B}\right)^2\right]^{\frac{1}{2}} \quad . \qquad (9\text{-}63)$$

Use of Equations (9-60), (9-62), and (9-63) allows Equation (9-54) to be written as

$$t_B = \frac{1}{\kappa}\left\{\cosh^{-1}\frac{V_B}{V_o} + \cosh^{-1}\frac{V_B}{V_S} - 2\cosh^{-1}\frac{V_B}{V_H} + \right.$$

$$\left. + 2\left[1 - \left(\frac{V_H}{V_B}\right)^2\right]^{\frac{1}{2}} - \left[1 - \left(\frac{V_S}{V_B}\right)^2\right]^{\frac{1}{2}} - \left[1 - \left(\frac{V_o}{V_B}\right)^2\right]^{\frac{1}{2}}\right\} \qquad (9\text{-}64)$$

Air Waves.-- The minimum value of the apparent velocity from the time-distance plot for fill waves is the velocity corresponding to the depth of the shot. When this velocity is lower than the propagation velocity of pressure waves in the air, waves will be refracted at the ground surface and airborne signals will be recorded. The response of an air wave on a time-distance plot is a straight line with a slope that is the inverse of the wave propagation velocity in air and with a time intercept which is evaluated as follows. The ray path for such a wave is shown in Figure 9-9. Following a procedure similar to that explained for bottom waves, we find the time intercept of an air wave to be

$$t_A = t_{12} - t_{1'2} \qquad (9\text{-}65)$$

where t_{12} and $t_{1'2}$ can be calculated as

$$t_{12} = \frac{1}{\kappa}\left\{\cosh^{-1}\frac{V_A}{V_o} - \cosh^{-1}\frac{V_A}{V_S}\right\} \qquad (9\text{-}66)$$

and

$$t_{1'2} = \frac{1}{\kappa}\left\{\left[1 - \left(\frac{V_o}{V_A}\right)^2\right]^{\frac{1}{2}} - \left[1 - \left(\frac{V_S}{V_A}\right)^2\right]^{\frac{1}{2}}\right\} . \qquad (9\text{-}67)$$

The use of Equations (9-66) and (9-67) allows Equation (9-65) to be written as

$$t_A = \frac{1}{\kappa}\left\{\cosh^{-1}\frac{V_A}{V_o} - \cosh^{-1}\frac{V_A}{V_S} + \left[1 - \left(\frac{V_S}{V_A}\right)^2\right]^{\frac{1}{2}} - \left[1 - \left(\frac{V_o}{V_A}\right)^2\right]\right\} . \qquad (9\text{-}68)$$

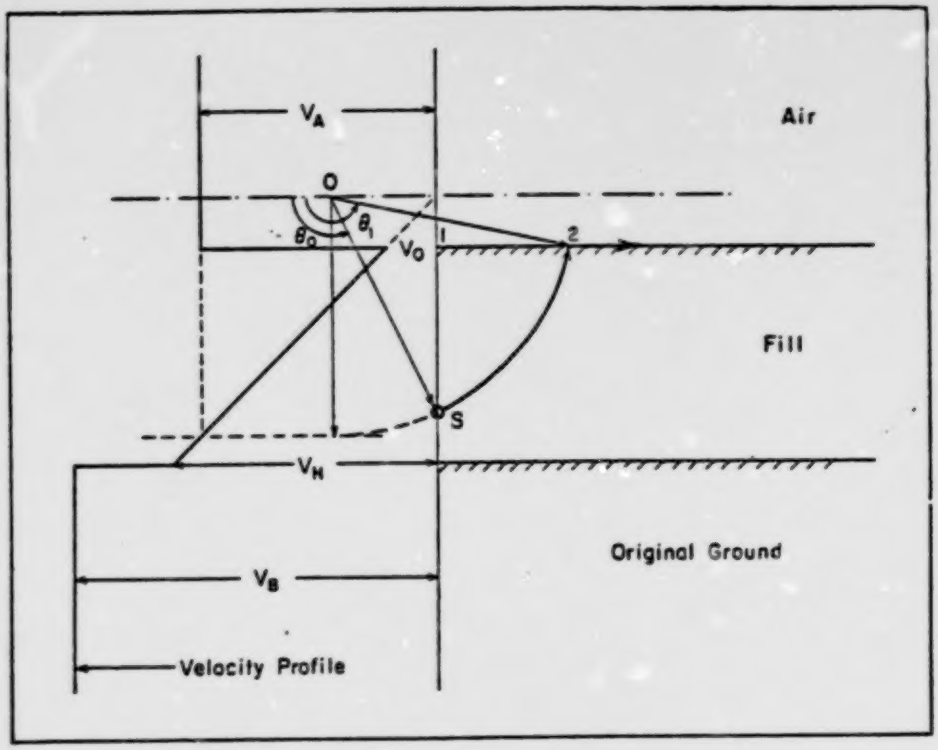

Figure 9-9. Refraction at the Surface of the Fill

The distance at which air waves appear can be evaluated by equating the times corresponding to fill and air waves, and this will yield

$$x_A = \frac{V_A}{K} \left\{ \left[1 - \left(\frac{V_o}{V_A}\right)^2\right]^{\frac{1}{2}} - \left[1 - \left(\frac{V_S}{V_A}\right)^2\right]^{\frac{1}{2}} \right\} \; . \tag{9-69}$$

Shape of the Response.-- The response of the selected model on a time-distance plot will be formed by three different components corresponding to fill, air, and bottom responses. When the velocity at the depth of the shot is higher than that in air, air waves will not appear as first arrivals; however, airborne signals are received when it is lower. For values of x lower than x_A, as given by Equation (9-69), the recorded response corresponds to a fill wave. From this point on, the first signal can be due to either a fill wave or an air wave, depending only on the velocity at the point where the explosive is placed. The third part of the time-distance plot is due to the wave propagation characteristics of the original ground. Finally,

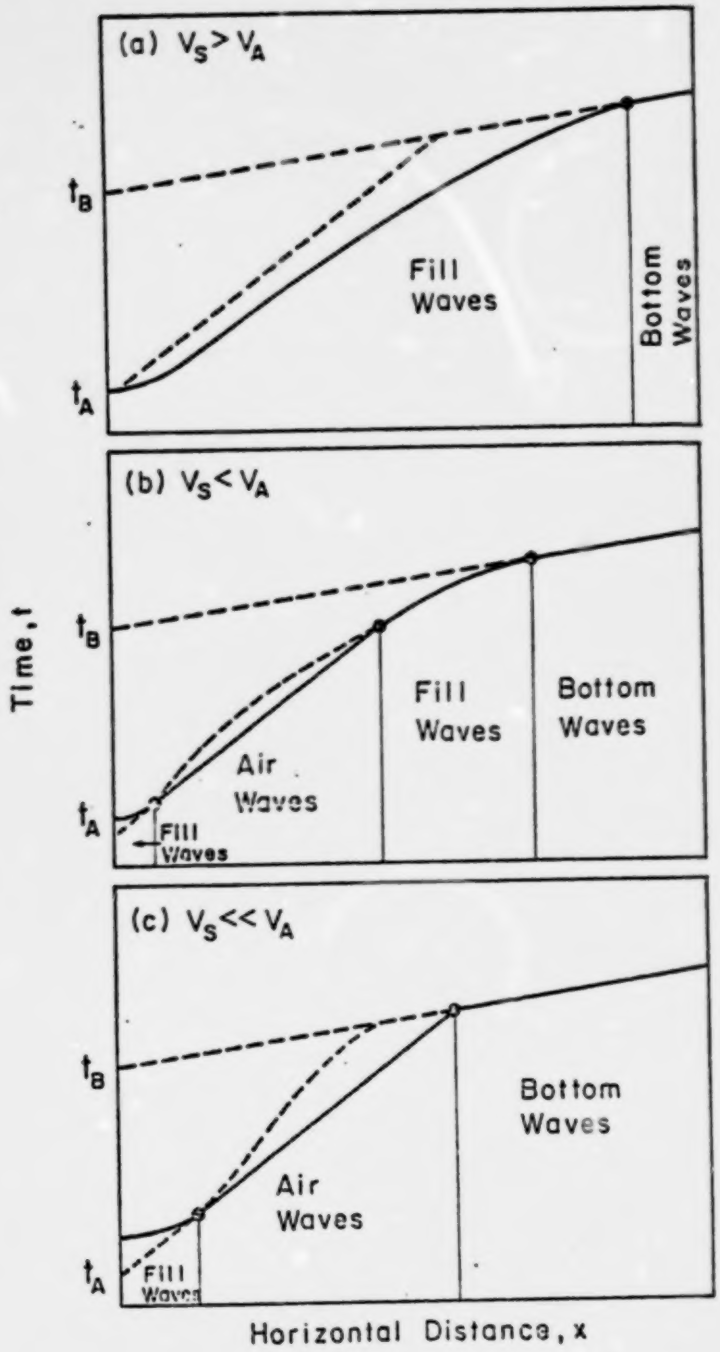

Figure 9-10. Typical Shapes of Time-Distance Plots

some signals due to a deeper layer of bed rock are received for geophones at great distances from the shot. Figure 9-10 shows three sketches of possible responses which may be obtained from this model.

Interpretation Procedure.-- The model used to simulate the response of the area tested can be described with six variables, which are the velocities of the air, ground, and fill waves at the shot point, the slope of the variation of the velocity with depth in the fill, the depth of the shot, and the thickness of the fill. The velocities of the air and ground waves are found directly by measuring the slopes of the corresponding parts (which are, theoretically, straight lines) of the time-distance plot. The thickness of the fill and the depth of the shot were measured in the field, and the two remaining quantities, which are concerned with the velocity profile within the fill, are determined by the interpretation procedure described. A digital computer was used to evaluate the foregoing formulae over a wide range of values for V_o and K, the constants which define the velocity profile, and the results are given in Figures 9-11 through 9-14.

The contours in Figures 9-11, 9-12, and 9-13 represent values of the time (in milliseconds) for the signal to reach a geophone at a horizontal distance of x feet from the shot point; each chart is for a particular value of the horizontal distance x and a particular value of the shot depth S. The contours in Figure 9-14 give the values of the time intercept, t_B (see Figure 9-3 or 9-10), for various values of S. Two charts with different scales for V_o, the minimum value of the velocity in the profile, are provided for each case considered; in one case V_o is varied between 0 and 0.16 ft/ms, whereas in the other case a variation from 0 to 1.6 ft/ms is plotted. These graphs allow the different arrival times to various geophones, as well as the type of signal (air, fill, or bottom wave), to be read. If the appropriate graph is entered with the recorded arrival time to the first geophone, we may select a curve which gives the V_o-K

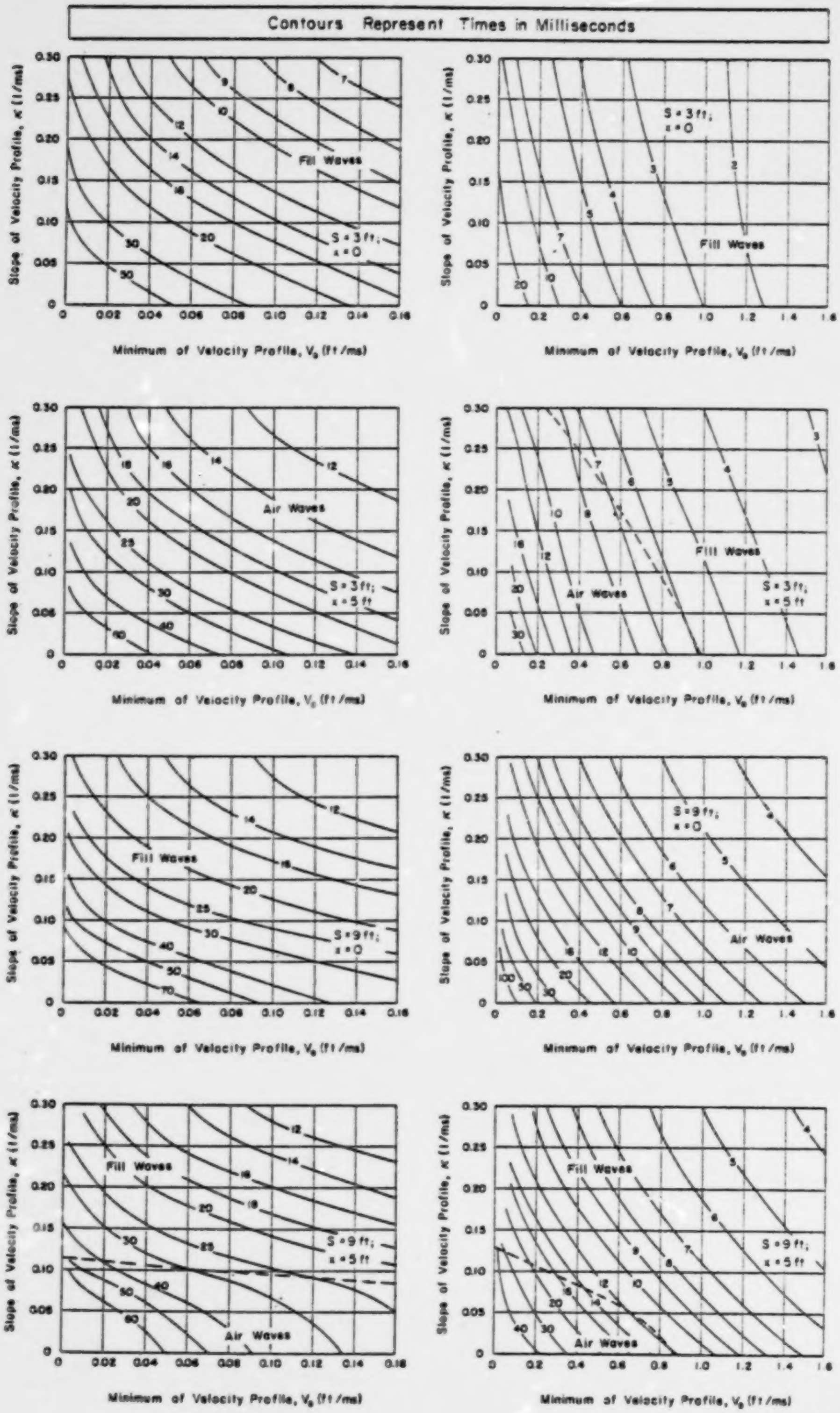

Figure 9-11. Seismic Response Curves for Horizontal Distances of 0 and 5 Feet

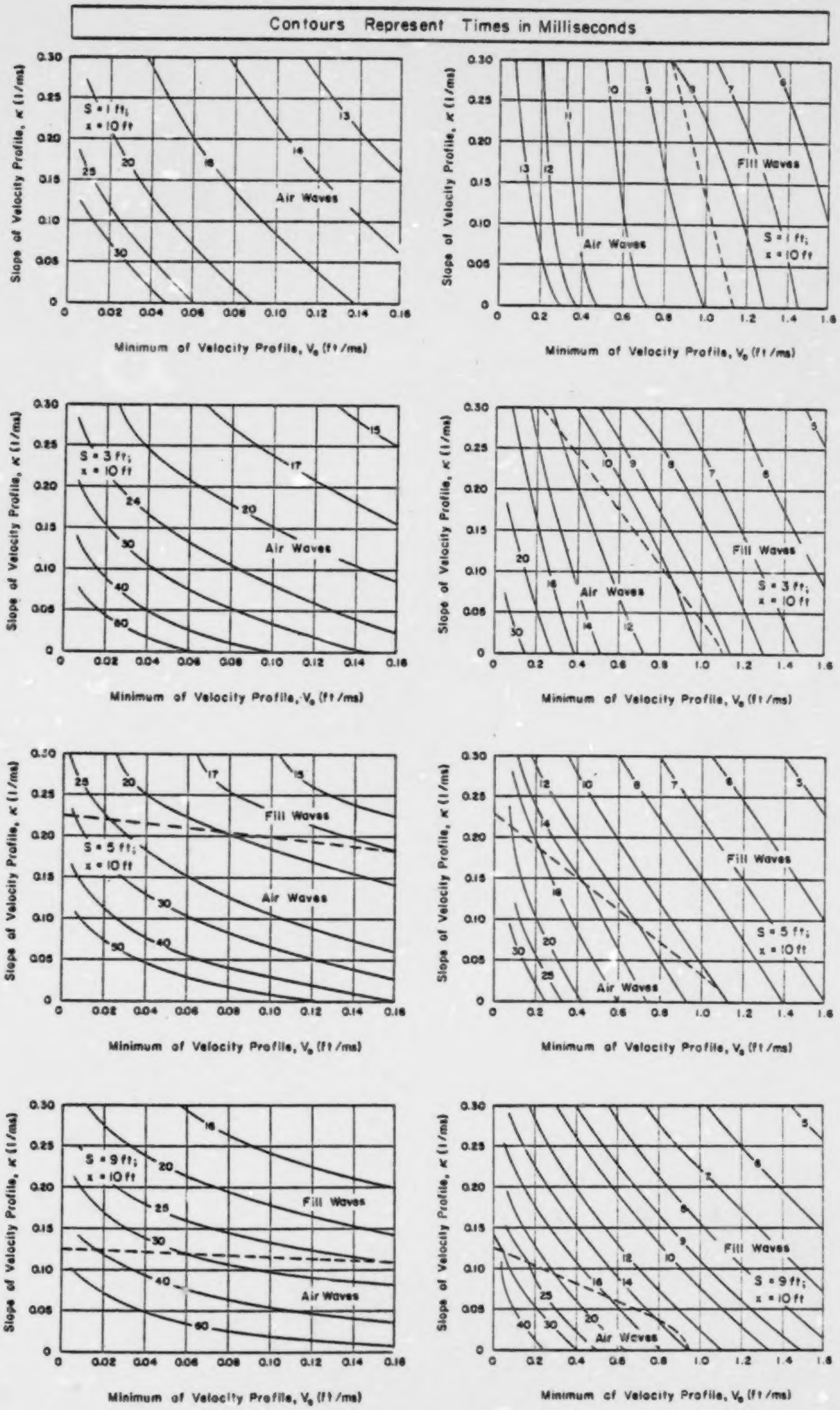

Figure 9-12. Seismic Response Curves for Horizontal Distance of 10 Feet

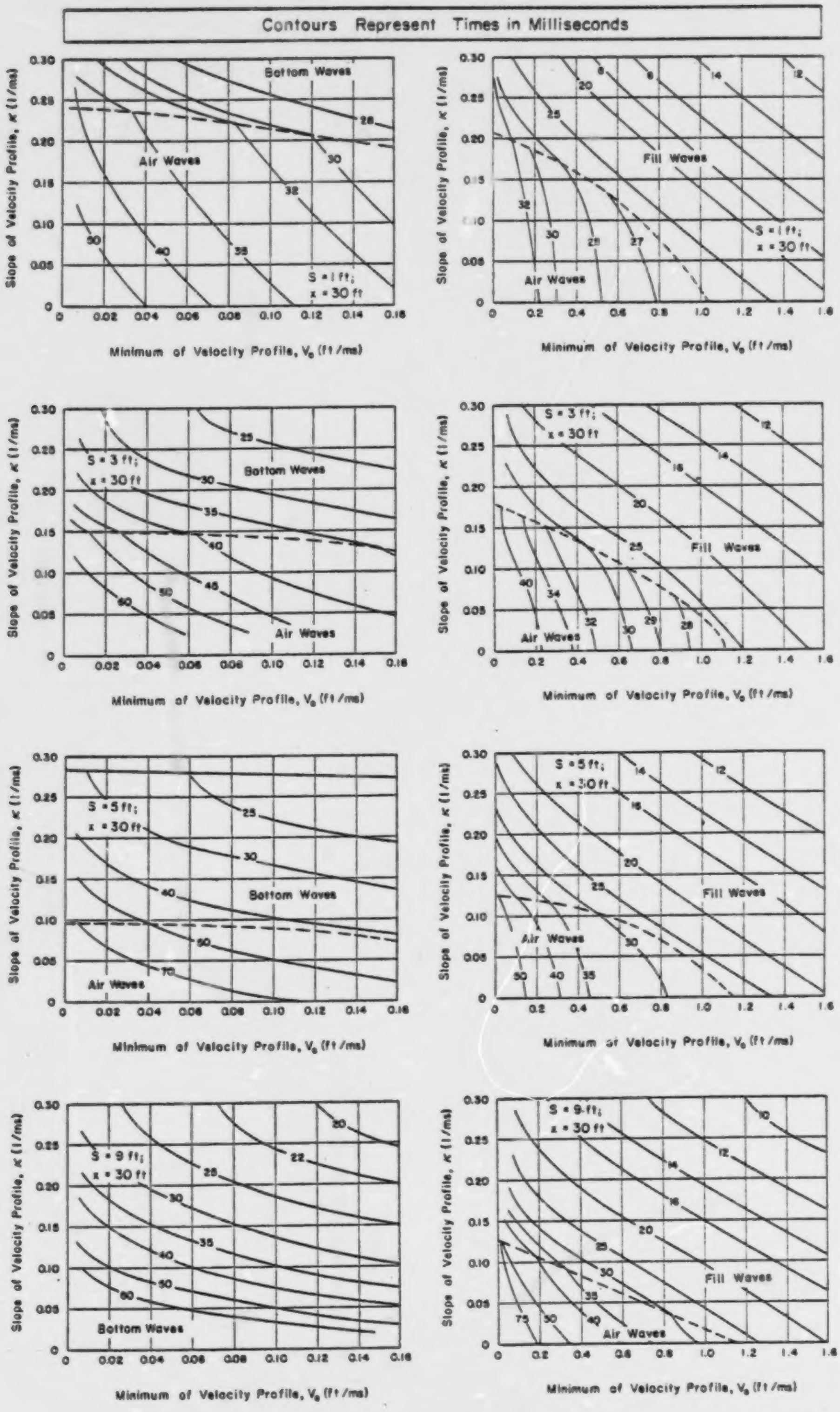

Figure 9-13. Seismic Response Curves for Horizontal Distance of 30 Feet

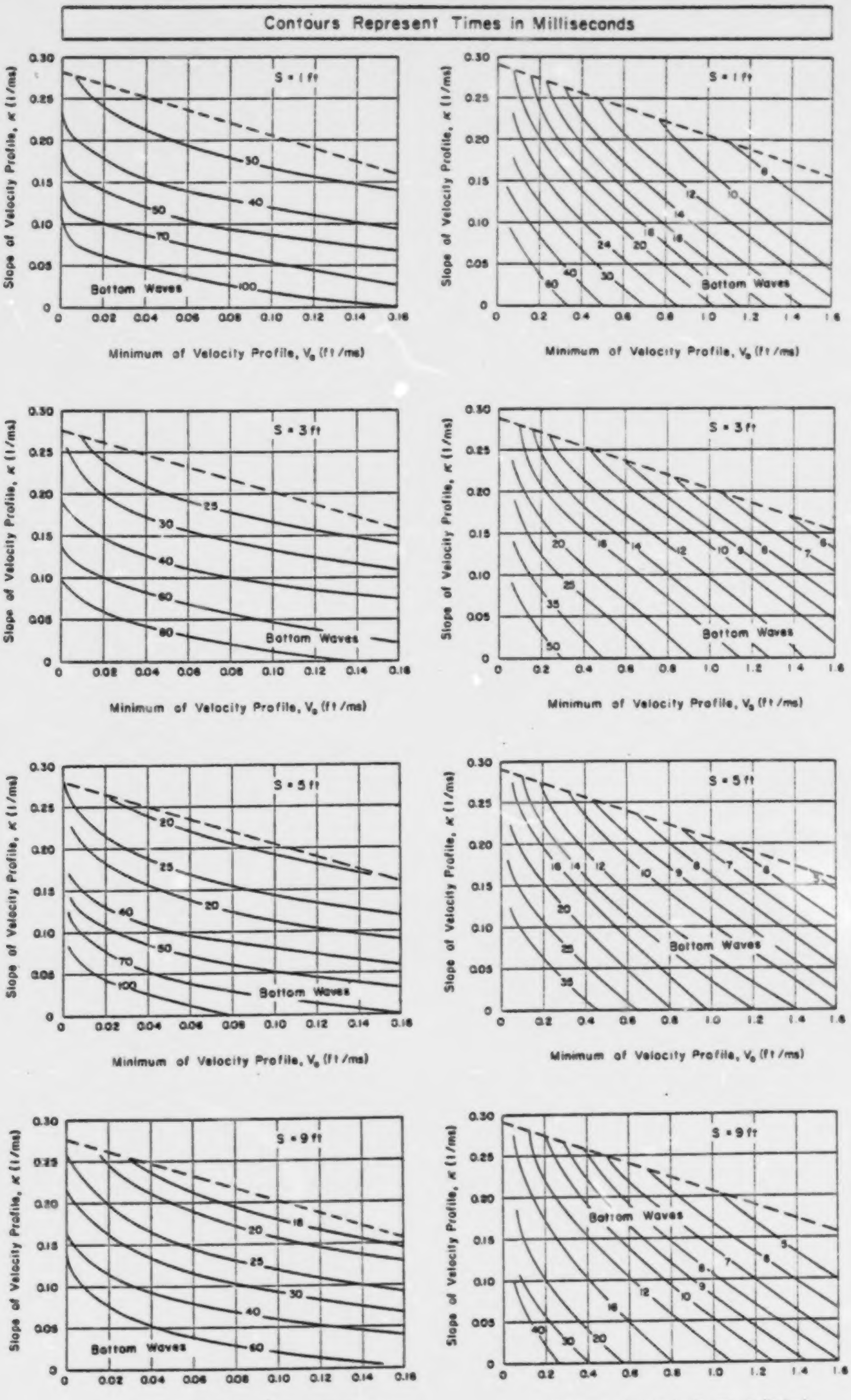

Figure 9-14. Seismic Response Curves for Bottom Waves

relation that would yield the same arrival time as the model. For the same shot, repeating the process on the appropriate chart for the arrival time to the second geophone, we obtain a different V_o-κ relation. The intersection of the two curves obtained by use of the first and second geophones will give particular values for V_o and κ. The results obtained by use of arrival times to the third, fourth, etc. geophones should agree with those obtained from the first two geophones. However, since the field conditions are more complicated than those of the model, the values of V_o and κ defined by use of the data from the first two geophones gives some scatter when applied to predict the response for other geophones. Therefore, engineering judgment is used to select values for V_o and κ such that this scatter is minimized, and the linear variation of velocity assumed in the model will approximate the erratic velocity profile of the actual fill. As is appropriate for all interpretation techniques, a theoretical model constitutes the basis for the interpretation, but an appreciation for actual field conditions must be incorporated into the procedure and the theoretical response must be modified to account for features not included in the model. Accordingly, the results obtained from such analyses must be used with an appreciation of the interpretation procedure employed.

INTERPRETATION OF RESPONSE

Data recorded in the field are interpreted on the basis that the response is modeled by a soil layer with a linear variation of velocity with depth. In cases where this model is not suitable due to the presence of a desiccated crust, the existence of a layer of softer organic soil of much lower velocity, or a soil layer with much higher velocity, the model is modified to allow a proper interpretation. The response of a continuum with a general velocity profile is always borne in mind when interpreting these cases.

Penn 7 Site

Shots 1 to 8 were conducted at the Penn 7 Site. For Shots 1 and 2, the geophones were spaced at 10 feet and the depth of the charge was 3 feet. The response can be approximated by two straight lines with the following velocities and break points:

Shot 1: $V_1 = 1.62$ ft/ms; $V_2 = 4.20$ ft/ms; $x_c = 57$ ft

Shot 2: $V_1 = 1.25$ ft/ms; $V_2 = 5.80$ ft/ms; $x_c = 43$ ft

Based on the results from those two shots, which were run in opposite directions, the conventional interpretation procedure for horizontal strata suggests the presence of two constant velocity layers. The indicated depth of the interface between these two layers is

Shot 1: $H_1 = 18.9$ ft

Shot 2: $H_1 = 13.7$ ft

Shots 3 and 4 were conducted with the same lay-out, but with a slightly different depth of charge and a geophone spacing of 30 feet. Shots 5 and 6 had a lay-out with the same spacing in the opposite direction to that of Shots 3 and 4, but essentially the same depth of charge was used. Shots 7 and 8 were on the same line and with the same spacing as Shots 3 and 5, respectively. When interpreted according to the conventional technique, this group of shots yields a ground profile similar to that described by Shots 1 and 2, but, since they were conducted with a 30-foot spacing, a third layer of higher velocity is detected. The velocities and thicknesses of these layers vary somewhat according to the shot from which they are obtained, and the general results may be described as

$$0.77 \text{ ft/ms} \le V_1 \le 1.94 \text{ ft/ms}$$

$$4 \text{ ft/ms} \le V_2 \le 5 \text{ ft/ms}$$

$$V_3 \simeq 10 \text{ ft/ms}$$

$$14 \text{ ft} \le H_1 \le 19 \text{ ft}$$

$$H_2 \simeq 100 \text{ ft}$$

Although this unsophisticated interpretation can be challenged, it does illuminate some interesting features, among which are the following:

1. Shots 4 and 8, conducted on the same line but with charge depths of 4 and 2.5 feet, respectively, yield a quite different response. The arrival time to the first geophone is 18.6 ms for Shot 4 and 31.0 ms for Shot 8.

2. When a constant velocity is assumed for the upper layer, the value of the velocity varies between 0.77 and 1.94 ft/ms, depending on the shot from which it is deduced.

3. The time intercept, if obtained by linear extrapolation, is negative for Shot 2.

The first of these features suggests that the depth of the charge has an important effect on the response of this particular soil; from the second feature, we may infer a lateral variation of the velocity at the top of the original ground; and the third feature illustrates that the time-distance plot for these shots is not composed of straight lines near the origin. Also, the variation in the indicated thickness of the surface layer suggests a dipping interface. When the response of these shots is interpreted on the basis of the foregoing analysis, these features can be explained. As previously discussed, the response of a soil with a depth-dependent velocity profile has an inflection point at which the slope gives the velocity at the depth of the shot point. The straight lines used for a conventional interpretation of these shots can be taken as the slopes at their inflection points, and, with a consideration of the different depths at which the charges were placed, the following variation of velocity can be obtained:

Shot	Depth (feet)	Velocity (ft/ms)
8	2.5	0.77
1,2,3,5,6	3	1.46
4&7	4	1.94

These values of the velocity are approximate and can not be accurately determined due to the large spacing of the shots. The velocity at the deepest point increases to 4 or 5 ft/ms; according to this interpretation, the depth of bedrock is about 82 feet. A generalized velocity profile for the original ground is advanced in Figure 9-15 on the basis of these considerations.

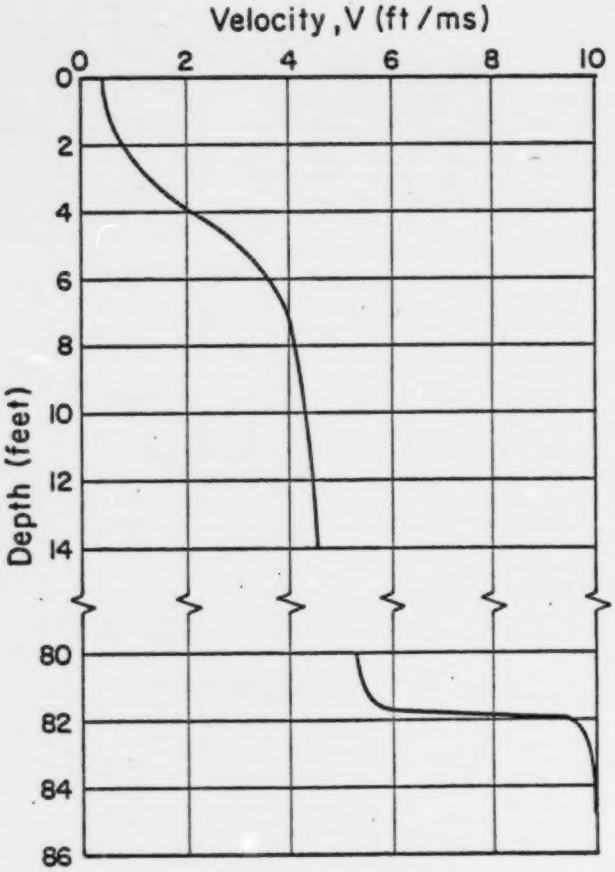

Figure 9-15. Velocity Profile at Penn 7 Site

Riverside Site

The seismic response of the fill is analyzed by interpreting each of the shots in a manner similar to that previously described. Duplicate shots on the same line and with the same spacing are analyzed together. Shots 9 through 14 on the transverse line are considered first, and then the remaining shots on the base line are examined.

Transverse Base Line.-- For Shots 9 and 10 the blasting caps were embedded a few inches, and the signals received by the twelve geophones indicated a downward initial motion due to air-borne compression waves. The arrival times are described with almost no scatter by straight lines which are characteristic of the propagation velocity of pressure waves in air at this site on this particular day, that is, $V_A = 1.14$ ft/ms. No other signal was recorded on the 120-foot line covered by the geophones. From these two shots it can be concluded that the wave propagation velocity in the soil at the top of the fill is lower than that in the air.

Shots 11 and 12 were conducted on the same line as Shots 9 and 10, but at depths of 5 and 11 feet, respectively. Upon comparison with Shots 9 and 10, they show the influences of the embedment of the charge on the seismic response. Shot 11 gives an air-borne signal which indicates that the velocity of the fill at a depth of 5 feet is lower than that of the air. Since the magnitude of the charge (2 blasting caps) was relatively small, the air-borne signals are weak, thereby allowing the slower ground signals to be detected on the same record. Shots 12 and 13 originate at a depth of 11 feet and yield bottom wave data at all geophones. The arrival time to the geophone at a horizontal distance of 10 feet from the charge is 29.9 ms for Shot 13, which is at a depth of 11 feet, and 33.5 ms for Shot 11, which is 5 feet deep. Although the geophone in the first case is at a greater distance from the source than in the second case, the arrival time is less than for the second case. This fact, however, is explained by the variation of velocity with depth. A comparison of the time-distance plots of these shots and Shot 2 from the Penn 7 area is given in Figure 9-16. Using the appropriate charts, which correspond to the spacing and depth of each shot, we obtain

$$V_o = 0.10 \text{ ft/ms}$$

and

$$\kappa = 0.11 \text{ ft/ms/ft.}$$

The desiccated crust overlying this fill is about one foot thick and may alter these results. To account for this effect the depth of the shot can be taken to be one foot less, and the time required to pass almost vertically through the crust can be added to the arrival times. If this is done, the improved values for V_o and κ are found to be

$$V_o = 0.10 \text{ ft/ms}$$

and

$$\kappa = 0.12 \text{ ft/ms/ft}$$

when the velocity of the crust, V_c, is assumed to be 1 ft/ms. The latter value is chosen on the basis of actual values obtained from other shots, as is shown subsequently. Shots 12 and 14 on the same line yield a response which is in good agreement with this velocity distribution. If values of V_o and κ are selected by use of the data from Shot 14, we obtain

$$V_o = 0.10 \text{ ft/ms}$$

and

$$\kappa = 0.09 \text{ ft/ms/ft} \quad .$$

However, this lower value of κ is associated with a thicker fill, which corresponds to the point at which the charge of Shot 14 was placed. Hence, both values of κ obtained from this set of shots can be considered equivalent in the sense that they yield similar velocities for points near the crust and

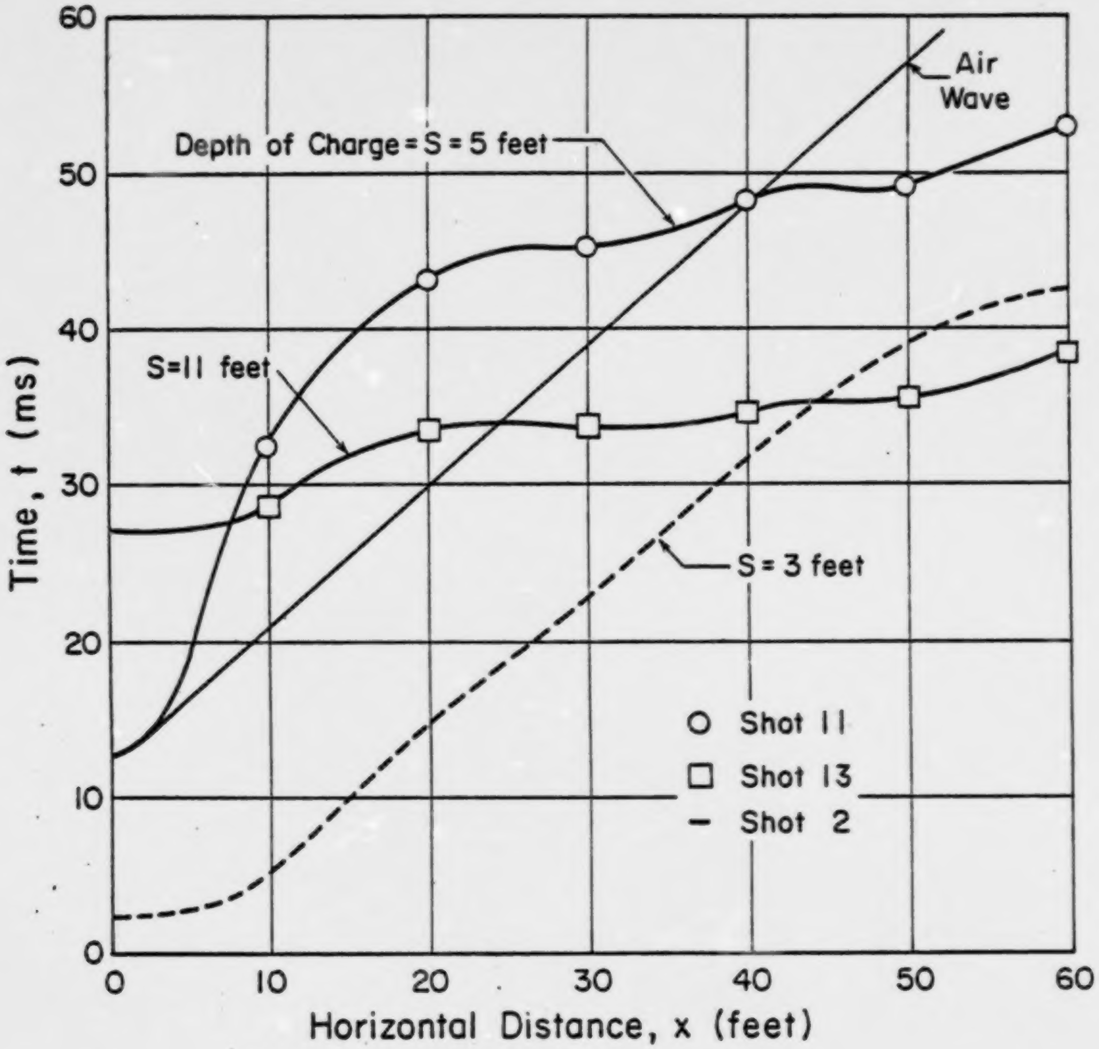

Figure 9-16. Comparison of the Seismic Response at Penn 7 and Riverside Site

near the bottom. Finally, the velocity profile shown in Figure 9-17a for the area covered by the transverse line represents the indicated interpretation of Shots 9 through 14.

First Part of Longitudinal Base Line.-- The base line, which extends from the outlet weir to the inlet pipe, is divided for purposes of this analysis into four longitudinal sections, each with a length of about 500 feet, and a localized region in the vicinity of the inlet pipe. The response of the first part (0 to 500 feet) is studied by use of Shots 15 through 18. The most interesting data obtained from these shots are:

1. The bottom velocity, V_B, deduced from the last portion of the response, is about 3.5 ft/ms.
2. The time intercept, t_A, of the air wave from Shot 18 is 3.4 ms.
3. The time intercepts, t_o, of the fill waves from Shots 15 and 16 are both approximately 17 ms.
4. The difference, Δt, in the arrival times of Shot 17 (at a depth of 10 feet) and Shot 18 (at a depth of 3 feet) is an average of 16.5 ms.
5. The time intercepts, t_B, of the bottom waves are 18 ms for Shot 17 and 34.5 ms for Shot 18.

With these data and the assumption of a 1-foot thick desiccated crust with an average velocity of 1 ft/ms, the values of V_o and κ that best describe the response are

$$V_o = 0.27 \text{ ft/ms}$$

and

$$\kappa = 0.10 \text{ ft/ms/ft.}$$

As far as the analysis of the fill characteristics at this site is concerned, it is clear that the closest geophones yield the more valuable data. In fact, for spacings of 30 feet the signal is almost always due to bottom waves, and the response is governed primarily by the conditions of the ground over which the fill is placed. However, an analysis of the shots with large geophone spacings will yield some interesting features concerning

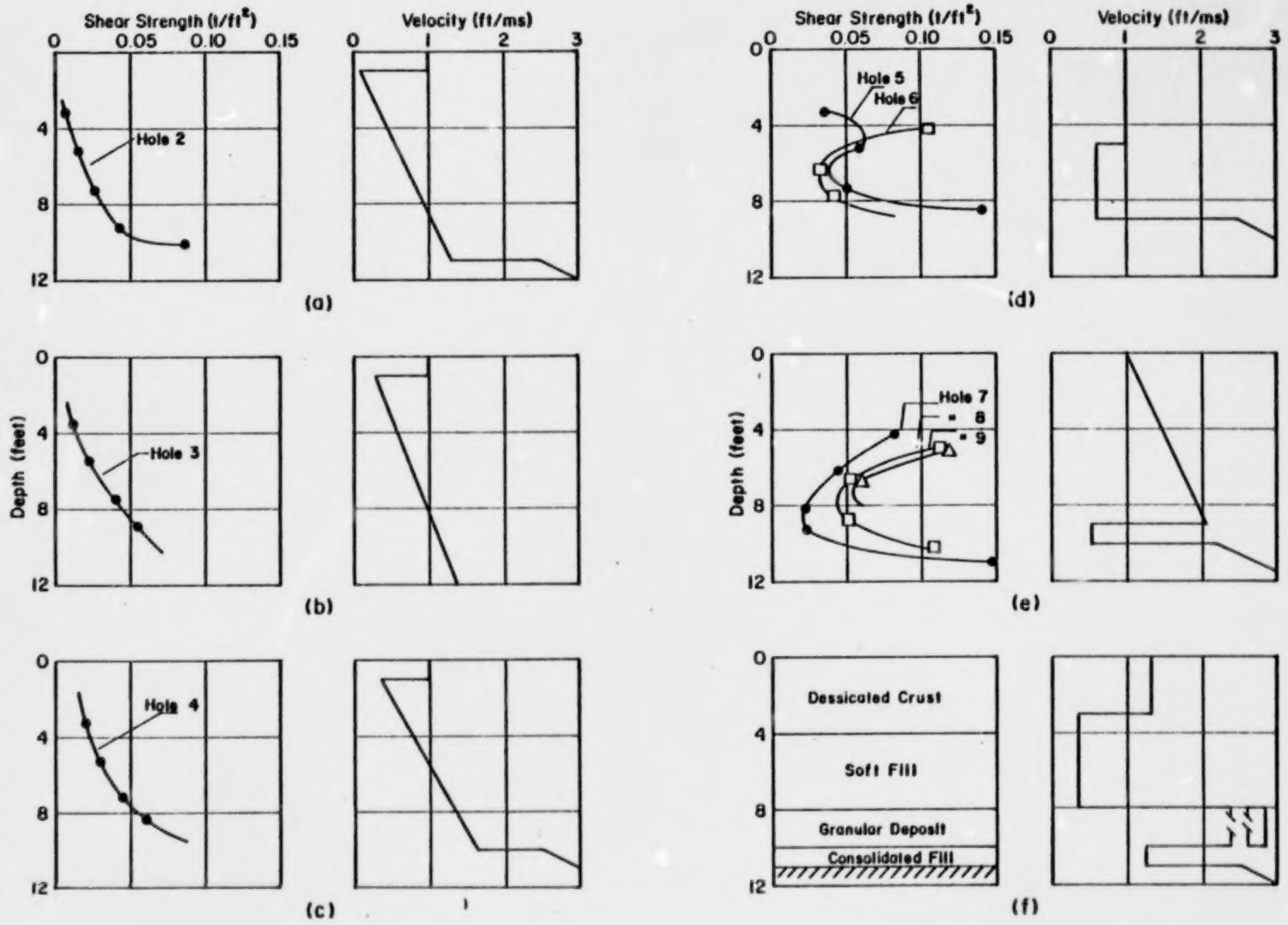

Figure 9-17. Velocity and Shear Strength Profiles at Riverside Site

the conditions of the bottom of the fill. The arrival times for geophones 4 through 6 of Shot 16 are almost equal; actually, the signal was received at geophone 6 slightly sooner than at geophone 4, which is much closer to the excitation source. This situation, which might normally be considered due to some error in the test procedure, is repeated in Shots 15 through 22, which have geophones placed at that location of the base line (that is, from 40 to 60 feet). This part of the response represents a decrease of 8 ms in the arrival times for the geophones which are located beyond it. This same feature is repeated at points between 90 and 110 feet along the base line. One possible explanation for this type of response, where the geophones farther from the source receive the wave impulse sooner than the closer ones, is given by the sketch of Figure 9-18. The existence of a dike across the base line at the 40 to 60 foot location would cause the signal to arrive at point A on the dike before it arrives at point B, which is closer to the excitation point. A metal pipe passing through the dike would cause the signal to arrive almost simultaneously at points C and D at 90 to 110 feet along the base line. This interpretation could be substantiated somewhat if a closer spacing were used to test this area; very probably the location of the pipe and its length could be determined from the response.

Shots 19 through 22 were conducted at the end of this first part of the base line, and the most important feature of these shots are:

1. The arrival times for geophones 2, 3, 4, and 5 of Shot 19, which is 10 feet deep, and Shot 22, which is 3 feet deep, differ by about 20 ms.
2. The time intercepts, t_B, for the bottom waves are 20.5 ms for the deep shots and 40.5 ms for the shallow shots.
3. The time intercepts, t_A, of the recorded air wave for Shots 20 and 22 are 7.0 ms and 7.9 ms, respectively.

At this extreme of the first portion of the base line, no shots were conducted with closely spaced geophones; hence, the values for V_o and κ are not

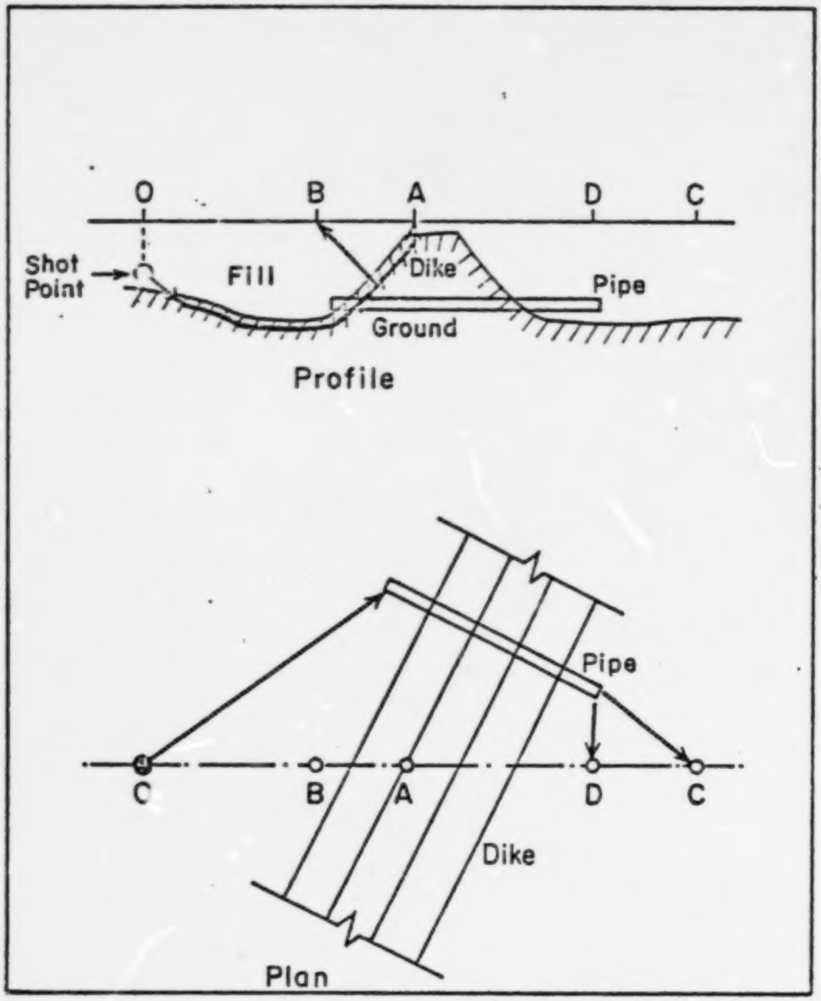
O
B
A
D
C
Shot Point
Fill
Dike
Pipe
Ground
Profile
Pipe
C
B
A
D
C
Dike
Plan

Figure 9-18. Explanation of Anomalous Response at Riverside Site

defined as well as they are for the other end. However, based on the indicated features, we may obtain values of

$$V_o = 0.15 \text{ ft/ms}$$

and

$$\kappa = 0.10 \text{ ft/ms/ft.}$$

The transmissibility of the fill is slightly poorer at this end, but this could be correlated with the existence of the previously mentioned dike, which could facilitate the accumulation of softer material at this point. The difference, however, is quite small, and the intermediate velocity profile given in Figure 9-17b is deduced as a result of this step of the interpretation.

Second Part of Longitudinal Base Line.-- At the end close to the 500 foot point of the base line, Shots 26 and 27, both of which are deep shots, were conducted . The time intercept, t_B, of the bottom waves from these shots is 12 ms. Values for V_o and κ may vary from $V_o = 0.20$ ft/ms and $\kappa = 0.225$ ft/ms/ft to $V_o = 1.09$ ft/ms and $\kappa = 0$. The intermediate values of

$$V_o = 0.36 \text{ ft/ms}$$

and

$$\kappa = 0.14 \text{ ft/ms}$$

can be used to describe the response of these shots, as well as Shot 25, which was run at the other end of this part of the base line. This interpretation is shown in Figure 9-17c.

Third Part of Longitudinal Base Line.--As we approach the inlet pipe, the desiccated crust becomes thicker, and the model based on a linear variation of velocity with depth must be modified. If we assume a crust of thickness c overlying a softer constant-velocity layer of thickness m, the time to intercept, t_B, of the bottom wave, when the shot point is at the bottom of the softer layer, can be expressed as

$$t_B = \frac{m}{V_F} \cos \alpha + \frac{c}{V_c} \cos \beta \tag{9-70}$$

where α and β are given by

$$\sin \alpha = \frac{V_F}{V_B} \tag{9-71}$$

$$\sin \beta = \frac{V_c}{V_B} \tag{9-72}$$

where V_F, V_c, and V_B are the velocities of the fill, crust, and bottom, respectively. The response of the fill waves is given by the following system of equations:

$$t = \frac{m}{V_F}\,\frac{1}{\cos i_F} + \frac{c}{V_c}\,\frac{1}{\cos i_c} \tag{9-73}$$

$$x = m \tan i_F + c \tan i_c \tag{9-74}$$

$$V_c \sin i_c = V_F \sin i_F \tag{9-75}$$

which defines t as a function of x. The time intercept of the fill wave is

$$t_o = \frac{m}{V_F} + \frac{c}{V_c} \quad . \tag{9-76}$$

If the shot is made within the crust, the time intercepts for the bottom and fill waves are

$$t_B = 2\,\frac{m}{V_o} \cos \alpha + \frac{2c-S}{V_c} \cos \beta \tag{9-77}$$

and

$$t_o = \frac{S}{V_c} \quad . \tag{9-78}$$

For the air waves we obtain

$$t_A = \frac{S}{\cos \alpha}\left(\frac{1}{V_c} - \frac{\sin \alpha}{V_A}\right) \tag{9-79}$$

or

$$t_A = S\left[\frac{V_A^2 - V_C^2}{V_A^2\ V_C^2}\right]^{\frac{1}{2}} \tag{9-80}$$

Shot 23, at a depth of 3 feet, is interpreted with this type of model. The time intercept of the air wave is 1.1 ms, and, if V_A is taken as 1.14 ft/ms, Equation (9-80) yields a velocity of 1.0 ft/ms for the top crust. For this shot a bottom wave is recorded with a time intercept, t_B, of 24 ms, which, according to Equation (9-77), allows us to write

$$2\frac{m}{V_o} \cos \alpha + (2c-3) \cos \beta = 24 \text{ ms.} \tag{9-81}$$

Shot 24, which was conducted at the same location, but at a depth of 10 feet, yielded a bottom wave with a time intercept, t_B, of 13.5 ms, which, by use of Equation (9-70), allows us to write

$$\frac{m}{V_o} \cos \alpha + \cos \beta = 13.5 \text{ ms} . \qquad (9\text{-}82)$$

From the final parts of the time-distance plots for these shots, the bottom velocity, V_B, can be obtained as 3.5 ft/ms. Using this value for the bottom wave velocity and assuming a fill thickness of 10 feet, we can determine the following for V_o:

$V_o = 0.66$ ft/ms , for $m = 7$ ft

$V_o = 0.60$ ft/ms , for $m = 5$ ft .

The resulting interpretation for this part of the base line is given in Figure 9-17d.

Fourth Part of Longitudinal Base Line.-- Along this part of the base line, which is very close to the inlet pipe, the material is more granular, and the corresponding velocities are higher. It is noted, however, that some delay exists for the bottom waves which appear quite far from the excitation point, and this fact suggests the presence of a softer soil overlain by an upper layer of higher velocity. In Shot 32, which was placed at a depth of 2 feet, an airborne wave with a time intercept, t_A, of 0.8 ms was recorded; use of the charts in Figures 9-11 through 9-14 allows us to deduce a velocity of 1.0 ft/ms for the top part of the profile. Bottom waves with time intercepts, t_B, of 6.7 ms were recorded for Shots 30 and 31, and an apparent bottom velocity, V_B, of 2.2 ft/ms can be interpreted. The time intercept, t_o, of the fill waves from Shot 31 is 17.5 ms. From these data we obtain a velocity profile wherein the velocity increases with depth from the given value of V_o at a rate given by $\kappa = 1.2$ ft/ms/ft. The softer soil, which can explain the low values for the bottom wave delays and the high values for the fill wave delays, could have a thickness of about 1 foot and a velocity, V_F, of 0.4 ft/ms or a different thickness and velocity according to this ratio. The interpretation for this part of the base line is shown in Figure 9-17e.

Region Near Inlet Pipe.-- Shots 34 to 38 were conducted in the area near the inlet pipe, and the interpretation of the response in this area is summarized in Figure 9-17f. If Shots 37 and 38 are interpreted according to conventional procedures, a two-layer system is obtained, and the results are

Shot 37:
$V_1 = 1.09$ ft/ms
$V_2 = 5.60$ ft/ms
$D = 19.3$ ft

Shot 38:
$V_1 = 1.32$ ft/ms
$V_2 = 5.60$ ft/ms
$D = 27.8$ ft

where D is the thickness of the top layer. It is known that the thickness of the fill is much less than that obtained by this interpretation, and this difference is due to the lower velocity layers within the fill; these can not be detected by shots which are conducted near the surface, and no deep shots were performed due to the difficulty of boring a hole to place the charge. Values for the velocities are, however, correct, and these suggest the presence of a high velocity layer ($V = 5.6$ ft/ms) within the fill. Based on the approximately known value of the fill thickness and the high values of the time intercepts for the bottom waves, ($t_B = 35$ ms for the shot at a depth of 4 feet, and $t_B = 39$ ms for the shot at a depth of 1 foot, we obtain $V_F = 0.30$ ft/ms for the fill below the high velocity layer. The reason for the existence of this relatively high velocity layer is probably due to the deposition of boulders, coarse gravel, and sand when the inlet pipe was above each particular point. Accordingly, the location of this high velocity layer should be deeper at some distance away from the pipe and shallower near the present position of the pipe. At the other side of the inlet pipe, where Shots 34 and 35 were conducted, this high velocity layer is not detected, and a response similar to that obtained in the middle of the fill area is recorded. However, the response of Shots 35 and 36, which span both sides of the inlet, shows clearly the abrupt difference between the two sides by a sudden change in arrival times. Note the difference in the arrival times for geophones 6 and 7 of Shot 35; the signal is received 10 ms sooner on the geophone located 30 feet farther from the excitation point.

DISCUSSION OF RESULTS

Discussed and analyzed herein are the velocity profiles obtained for the unfilled Penn 7 Site and the filled Riverside Site. The resulting velocity profiles are correlated with the data obtained by use of the field vane shear test, and a tentative explanation is advanced for the low velocities recorded within the fill area. Finally, based on the experience obtained from this work, the testing procedure is criticized, and some improvements are recommended for incorporation into future work to facilitate a better analysis of the data.

Response of the Unfilled Area at Penn 7

As shown in Figure 9-15, the velocity associated with most of the profile of this area is about 4 to 5 ft/ms, which corresponds to sandy soils. On the other hand, the presence of sandy soils is verified by the results of borings made at this site for different purposes. However, the most interesting feature of the velocity profile is the very low value of the velocity for the upper part (to a depth of 4 feet) of the fill. The velocity at the bottom of the fill was expected to be similar to that of the unfilled area, but such low values of the velocity are not found. It can be argued that the placement of a fill over the ground increases its capability to transmit pressure waves, and this reasoning can be accepted if the capability to transmit pressure waves is associated with the state of stress of the soil.

For a relatively high value of the confining stress, the velocity is governed by the compressibility and density of the soil skeleton, but for low values of the confining stress, as is the case near the surface, the mechanism for transmitting pressure waves could be different. In effect, if the contact between grains is loose, the propagation of the wave from grain to grain involves not only a compression of the grains themselves, but also relatively important motion of the grains in order to make the contact with other grains sufficiently tight to transmit the wave. This type of mechanism may involve relative slip between grains. If this is the case, the propagation velocity of pressure waves is governed by the confining stress. On the other hand, it is known that confining stress plays an important role in the compressibility of soils, and the equivalent modulus of elasticity changes greatly with stress level. This dependency of the velocity on confining stress for low stress levels was also found when testing for cap delays in a compact sandy soil with very close spacings. When the charge was embedded less than one foot, the first signal was given by an air-borne wave, and this indicates a very low velocity at the top of the soil where the confining stress is very low. A tentative relationship between the propagation velocity of pressure waves and the confining stress is proposed in Figure 9-19a on the basis of the results from the shots at the Penn 7 Site. For stress levels higher than 0.6 to 0.7 ton/ft^2 the velocity does not seem to depend on the stress level, whereas for lower values of stress the velocity decreases considerably to very small values. The existence of velocities lower than those of air waves is, however, difficult to explain. It is possible that the propagation of the air waves within the soil is attenuated so that the corresponding signal is not strong enough to be recorded by the geophones; then, the slower soil wave is recorded as a primary wave.

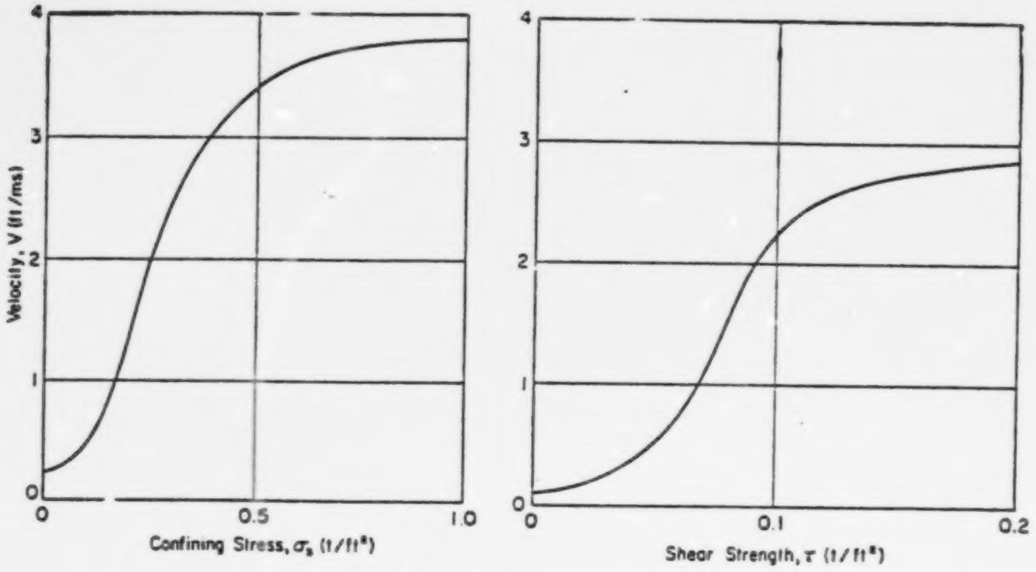

Figure 9-19. Velocity-Confining Stress-Shear Strength Relationships

Response of the Filled Area at Riverside Site

The fill area at Riverside Site has been divided into six parts -- a transverse base line near the outlet weir, four parts along a longitudinal base line between the outlet and the inlet, and one part near the inlet pipe. The velocity profiles for each of these parts yield a velocity on the order of 1 ft/ms for the upper desiccated crust and a lower velocity for the fill, which exhibits values of the velocity as low as 0.1 ft/ms. It is known that the shear strength of a consolidating soil is controlled primarily by the effective stress, which, in turn, is associated with the degree of consolidation. If the propagation velocity of pressure waves depends on the stress level for low stresses, a correlation should be expected between the propagation velocity and the shear strength of the soil; this is shown in Figure 9-19b. The velocity profiles obtained by use of this interpretation procedure are correlated with the results of field vane shear tests. In the desiccated crust, where the effective stress should be higher due to the negative pore pressures caused by evaporation, the corresponding velocities are higher than those of the consolidating fill. Comparisons of typical strength-velocity relationships are shown in Figure 9-17.

When considering the response near the inlet pipe, the low velocities are more localized, and the consolidated crust becomes thicker and more granular. Near the region of the inlet pipe, the general profile is described in Figure 9-17f. At some depth there is a layer of coarse granular material, which was probably deposited when the inlet pipe was placed at that point. Soft fill was deposited over this layer as the inlet pipe was moved to a different position. Finally, the crust at the top of the fill was probably dessicated during the interval between filling operations. Based on the general trend of these response data, the fill area can be divided into several zones, as shown in Figure 9-20, and these zones can be characterized

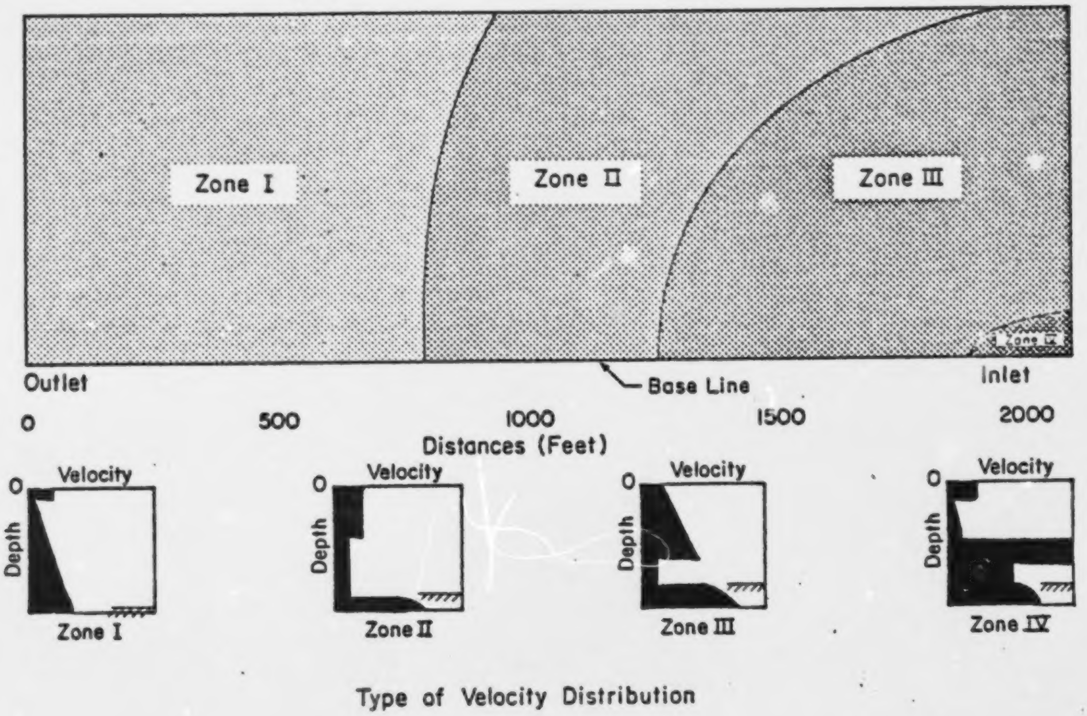
Zone I
Zone II
Zone III
Zone IV
Outlet
Base Line
Inlet
0
500
1000
1500
2000
Distances (Feet)
Velocity
Depth
0
Zone I
Velocity
Depth
0
Zone II
Velocity
Depth
0
Zone III
Velocity
Depth
0
Zone IV
Type of Velocity Distribution

Figure 9-20. Seismic Response Zones at Riverside Site

as follows. In Zone I the crust is thin (about one to two feet) and the underlying fill, which comprises about eighty per cent of the profile, is very soft. In Zone II the crust is thicker (about half of the profile) and the underlying fill is in a more advanced stage of consolidation and therefore has a higher velocity. In Zone III the consolidation is almost complete, as would be expected for more granular soils, and the weak unconsolidated material constitutes a minor part of the profile. Finally, Zone IV, which is associated with the region near the inlet pipe, consists of a high-velocity coarse granular material overlain by a softer soil. The deposition of this soft soil is probably due to the low velocities of the flow behind the inlet pipe and near the enclosing dike. This soft soil is overlain by a higher-velocity desiccated crust.

Testing Procedure

As has been shown, the conventional testing procedure with surface excitations will yield air-borne waves when the fill transmissibility is lower than that of the air. The presence of low-velocity soil is not detected by this type of seismic procedure, and it is necessary to embed the excitation points if the fill response is to be measured. On the other hand, based on the experience gained in this work, some recommendations concerning the geophone spacing, energy input, air wave control, and cap delay control are advanced in order to facilitate the obtaining of a better set of data.

Embedment.-- Since the response of any given shot will yield the velocity at the depth of the shot, a well defined velocity profile could be obtained if several shots were conducted at different depths at the same point. The number of shots that should be conducted at each point depends on the desired degree of refinement of the investigation, but at least two different depths should be tested at each point.

Spacing.-- The fill response is based solely on the data obtained from the geophones near the shot point. For ease in interpretation the same geophone spacing should be used for all shots. For example, if the thickness of soft soil to be studied is 20 feet, the following spacing is suggested:

Geophone number	1	2	3	4	5	6	7	8	9	10	11	12
Distance (feet)	0	1.5	3	6	12	20	30	40	50	60	70	80

Spacings can be varied proportionally for other values of the thickness.

Energy Input.-- For this work the explosive charge was varied from two blasting caps to two sticks of dynamite, and this variation of energy input had no apparent effect on the response. The appropriate energy input for a particular case will be the minimum required to produce a well-defined response at the most distant geophone, and this will generally have to be determined by trial.

Air Wave Control.-- When the velocity of the soil in which the shot is conducted is lower than that of the air, the first recorded signal corresponds to an air-borne wave. If one could determine by field trial a combination of energy input and amplifier gain that would permit the recording of the later arrival of the ground waves, a considerable advantage in the interpretation would be provided.

Cap Delays.-- The delay of the cap should be known or determined by a separate test. The procedure used in this work to define the cap delay consisted of firing surface shots with very closely spaced (3 feet) geophones. The time intercepts of the recorded air waves yields directly the cap delays. However, the value obtained was different than that provided by the manufacturer of the caps, probably because of batch-to-batch variability in the manufacture. For interpretation of the type described herein, the delay should be determined by tests on a random sample of a number of caps from the batch to be used.

CONCLUSIONS

Based on the results of this seismic survey, the following conclusions can be advanced:

1. Horizontal and vertical variations in the material and consistency of a hydraulic landfill composed of maintenance dredgings can be determined qualitatively from a seismic refraction survey, but a quantitative evaluation requires use of supplementary information from boreholes or vane shear tests.

2. A method of testing and interpretation has been developed to enable subsequent studies of a similar nature to be conducted and analyzed more effectively.

3. Velocity profiles for the specific cases analyzed were found to correlate very well with data obtained from independent sources.

CHAPTER 10

ENGINEERING PROPERTIES SOIL TESTS

The results of an extensive program of soils engineering tests are reported in this chapter. These data are concerned primarily with the evaluation of the dredgings as materials from which to construct a useful landfill. The engineering property tests are grouped into six categories, and they examine the classification, strength, consolidation, compaction, compressibility, and permeability characteristics of a variety of dredgings from different locations. In addition to the usual classification tests (particle size analysis, water content, unit density, specific gravity, and Atterberg limits), the findings of two mineralogical studies are presented. The section on shear strength includes the results from both field and laboratory vane shear tests and from laboratory unconfined compression and triaxial compression tests. Laboratory vane tests were conducted on the "undisturbed" tube samples taken from the field and on samples subjected to drainage, consolidation, and electro-osmotic treatment. Consolidation tests were conducted on "undisturbed" samples of suitable strength and consistency, and compaction and compressibility tests were performed on three surface materials. Six direct permeability tests were conducted, and approximate values for the permeability were determined from the consolidation and drainage test data; in addition, the electro-osmotic coefficient of permeability was computed from the electro-osmosis test data.

CLASSIFICATION TESTS

In general, the procedures for conducting soil classification tests are reasonably well standardized, and, with the exception of the particular deviations described, the methods outlined by Lambe (1951) were employed in this work. Essentially standard procedures were used to determine the Atterberg limits, water content, unit weight or density, and specific gravity. The Atterberg limits were conducted on material that was air-dried to the appropriate water content. Since the organic matter in the samples tested was completely humified, the results obtained are considered to be valid; this is in contradistinction to the use of the Atterberg limit tests on peaty soils, where the results are usually erratic and the tests are generally considered inappropriate. Due to the high percentage of fines in these dredgings, hydrometer tests were conducted in most cases to determine the grain size distribution; approximately 50 grams of material were used with 15 cubic centimeters of calgon solution (concentration of 0.3 moles per liter) added as a dispersing agent. Sieve analyses were conducted on samples containing more than 20 percent (by weight) of particles not passing a 200 mesh sieve. Typical grain size distributions for four samples are given in Figure 7-1, and the effective grain size, D_{10}, percentage of clay (less than 2 microns), and uniformity coefficient, $U = D_{60}/D_{10}$, for over 30 samples are plotted on various figures of the set from Figures 10-1 through 10-17. Also included in several of these figures are values for the specific gravity, dry density, Atterberg limits, and water content as functions of depth for various locations (bore holes) in the fill area. The interpretation and significance of these results are treated in Chapter 11.

MINERALOGICAL ANALYSES

Two series of tests, one at the University of Wisconsin-Milwaukee and the other at Northwestern University, were conducted to determine the mineralogy of these dredgings. The results of the tests performed at the University of Wisconsin-Milwaukee on nine different dredgings are reported in Table 10-1. Standard X-ray diffraction methods were used with heat and glycol treatments, and estimates of the relative amounts of each mineral present in the less-than-2-micron material are based on integrated peak intensities and mass absorption coefficients. Table 10-2 contains the results of the mineralogical analysis performed at Northwestern University on seven samples of dredgings; after being air-dried, these samples were tested for organic matter by use of hydrogen peroxide (H_2O_2) and for carbonates by use of 1N hydrochloric acid. Powder samples of the material passing the 200 mesh sieve were used for X-ray analyses. The clay-size particles (less than two microns) were separated by mixing the material in a blender with a dispersing agent and then placing the mixture in a centrifuge to remove all particles larger than 2 microns. Sedimented samples were formed by allowing the decanted suspension to evaporate slowly, and three slides were prepared for each sample. One slide was X-rayed after air-drying, one after heating overnight at 500°C, and the third after treatment with glycol. The X-ray scans were performed on a Philips Norelco goniometer, and the data were obtained on a strip chart recorder.

STRENGTH

This section presents the results of the strength testing programs, together with a description of the testing equipment and methods, and a

Table 10-1

Quantitative Mineralogical Analyses

Sample	Illite (%)	Kaolinite (%)	Mixed Layer (%)	Carbonate (%)	Percent of Total Carbonate	
					Calcite	Dolomite
C1DM	70	30	Trace	32	70	30
C2DM	60	20	20	29	65	35
C3TO	50	15	35	36	55	45
C4TO	50	15	35	36	60	40
C5TO	60	20	20	39	--	--
D1DM	65	35	Trace	25	--	--
D2DM	60	15	25	27	45	55
D3TO	50	15	35	28	60	40
D4CO	75	25	Trace	40	--	--

Table 10-2

Qualitative Mineralogical Analyses

Sample	Minerals Positively Present	Minerals Possibly Present
C3TO	Mica (Illite) Kaolinite Vermiculite Carbonates Some organic matter	Quartz
C7MW	Mica (Illite) Kaolinite Quartz Dolomite Carbonates	Vermiculite
C8MW	Mica (Illite) Dolomite Carbonates Some organic matter	Seprolite Vermiculite
C9MW	Mica (Illite) Kaolinite Dolomite Quartz Carbonates Some organic matter	Vermiculite
C22TO	Mica (Illite) Kaolinite Vermiculite Dolomite Quartz Carbonates	
D4CO	Mica (Illite) Kaolinite Montmorillonite Dolomite Carbonates Organic matter	Vermiculite
D6TO	Mica (Illite) Kaolinite Vermiculite Quartz Dolomite Some carbonates	

complementary section in Chapter 11 gives a detailed discussion of these test results with their interpretation and significance.

Testing Equipment and Procedures

The major strength testing equipment utilized in the field was the Swedish vane borer, but some supplementary tests were conducted with a Pilcon miniature field vane. In the laboratory a miniature vane was employed, and a number of conventional compression tests were performed on standard equipment. The vane was selected because it is ideally suited for testing the very soft, weak soils which were usually encountered in this testing program, whereas triaxial and unconfined compression tests were used on the stiffer materials.

Swedish Vane.--The vane consists of four rectangular blades attached to a shaft. To conduct a strength test, the vane is pressed into the soil in the direction of the shaft until the desired position is reached; then it is rotated slowly through a torque measuring device until a peak torque (failure) is reached. Most of the pioneering work on the development of this test procedure was done in Sweden and is reported in The Vane Borer by Cadling and Odenstad (1950), wherein a vane rotation rate of six degrees per minute is suggested as a compromise between expediting the conduct of the test and minimizing the rate effects on the strength behavior. This rate has since been incorporated into the standard procedure, and it was used on this project both in the field and in the laboratory. The equipment used was identical to that reported by Cadling and Odenstad (1950) and the torque measuring device was built in Norway especially for this equipment. The latter allows controlled measurements by means of a gear driven system in which a handle is rotated uniformly at a rate of 30 revolutions per minute, thereby causing the vane to rotate at 6 degrees per minute, and a precise torque spring is used to measure the applied torque.

The test procedure does not require a bore hole; the vane, which is inside a protective housing, was pressed into the soil to the desired depth, whereupon the vane was extended about 20 inches beyond its housing to its testing position. Next, the torque head was fitted to the supporting pipe and attached to the vane shaft, using the pipe as the reaction for the applied vane torque. After the peak torque was achieved and recorded, the vane shaft was rotated rapidly through 20 revolutions to remold the soil in the zone where the shear strength was determined. Then, the test was conducted again in the usual manner to measure the remolded strength. Following this operation, the vane was retracted into its protective housing, the apparatus was advanced to a new test depth, the vane was extended, and another test was performed as indicated above. This sequence was repeated until the bottom of the fill was encountered, in which case the vane could no longer be advanced manually. A calibration chart provided with the equipment gives the shear strength as a function of the number of degrees of rotation of the torque spring indicator for each size of vane used. This chart, in turn, is based on the relationships among the area of the envelope generated by rotating the vane through one revolution, the average shear strength developed on that surface, and the applied torque; the details of these relationships are given by Cadling and Odenstad (1950).

Laboratory Vane.--The theory and techniques discussed above are equally applicable to the miniature laboratory vane, except that there is no protective housing; at the completion of each test the vane is simply pressed from one test depth to the next. The miniature vane apparatus used for these tests was designed and manufactured in England by Leonard Farnell and Company, Limited. As with the Swedish field vane, the laboratory vane also incorporates calibrated springs and a geared operation to allow control over the rotation rate of the vane.

Pilcon Vane.--The Pilcon vane is a miniature field vane which may be used in the upper 3 feet of the fill. It does not have a protective housing and is pressed into position by hand. Rotation is accomplished manually without the benefit of a geared mechanism. Accordingly, a controlled rotation rate is difficult to achieve.

Compression Tests.--Unconfined compression and triaxial compression (UU) tests were conducted at a constant strain rate of approximately one percent per minute. All specimens had a length-to-diameter ratio of about two, and the unit weight and water content were determined for each specimen. Two types of samples were tested; tube samples of the stiffer materials from the field were tested to obtain so-called "undisturbed" strengths, and a series of compacted specimens were tested to determine their classical strength parameters, c and ϕ, where c is the cohesion intercept and ϕ is the angle of internal friction.

Results

The results of the vane shear strength determinations in the field and the miniature laboratory vane shear strength tests on the tube samples are given as a function of depth in Figures 10-1 through 10-18. Figures 10-1 through 10-9 show these relationships for various bore holes, whereas Figures 10-10 and 10-11 illustrate the variation of shear strength along a line between the discharge pipe and the outflow weir. Figures 10-12, 10-13, and 10-14 give analogous data obtained from the Island Site. All the data given in Figures 10-1 through 10-14 were obtained during the

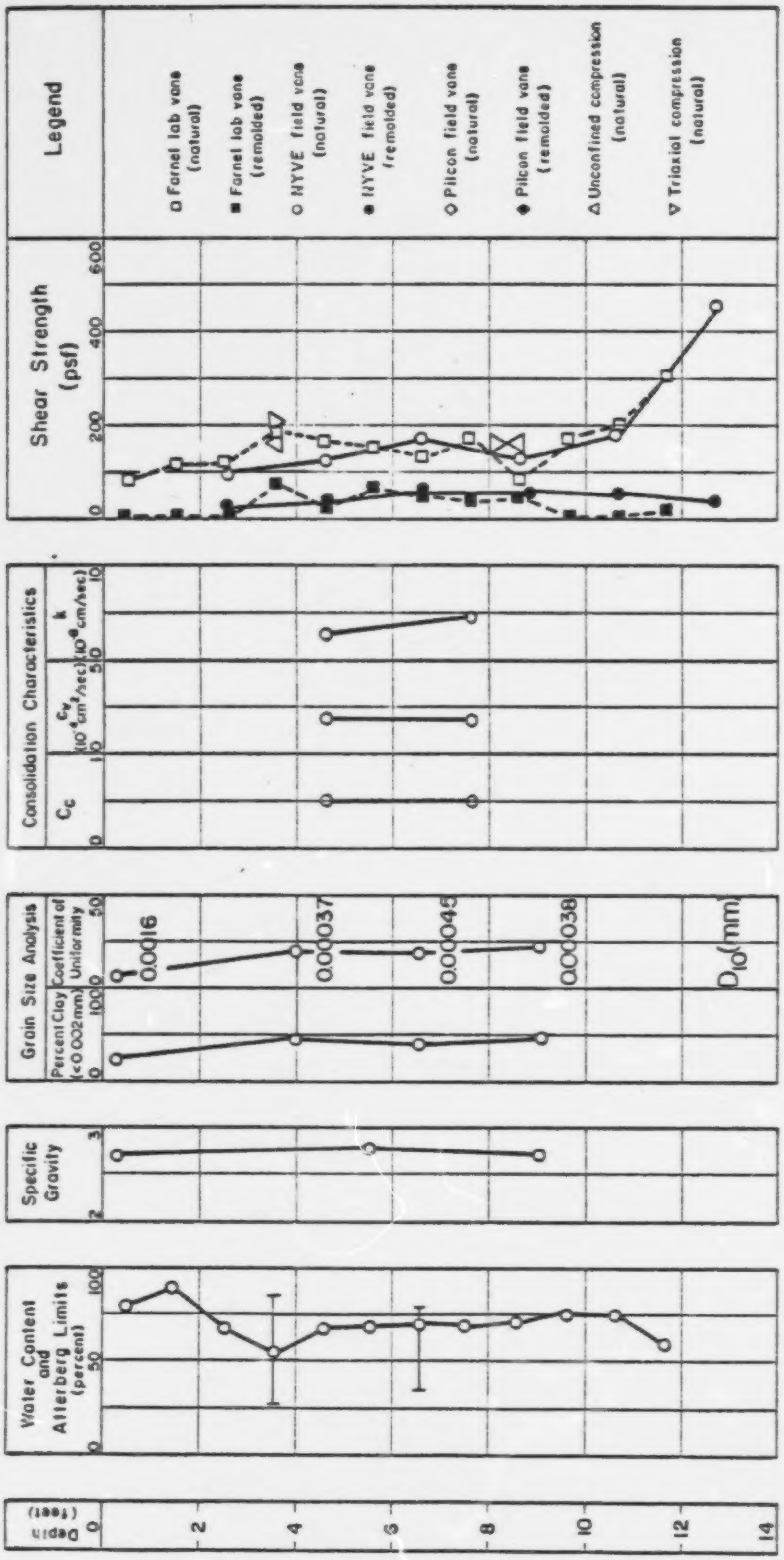

Figure 10-1. Field and Laboratory Test Data from BH-1 at Riverside Site

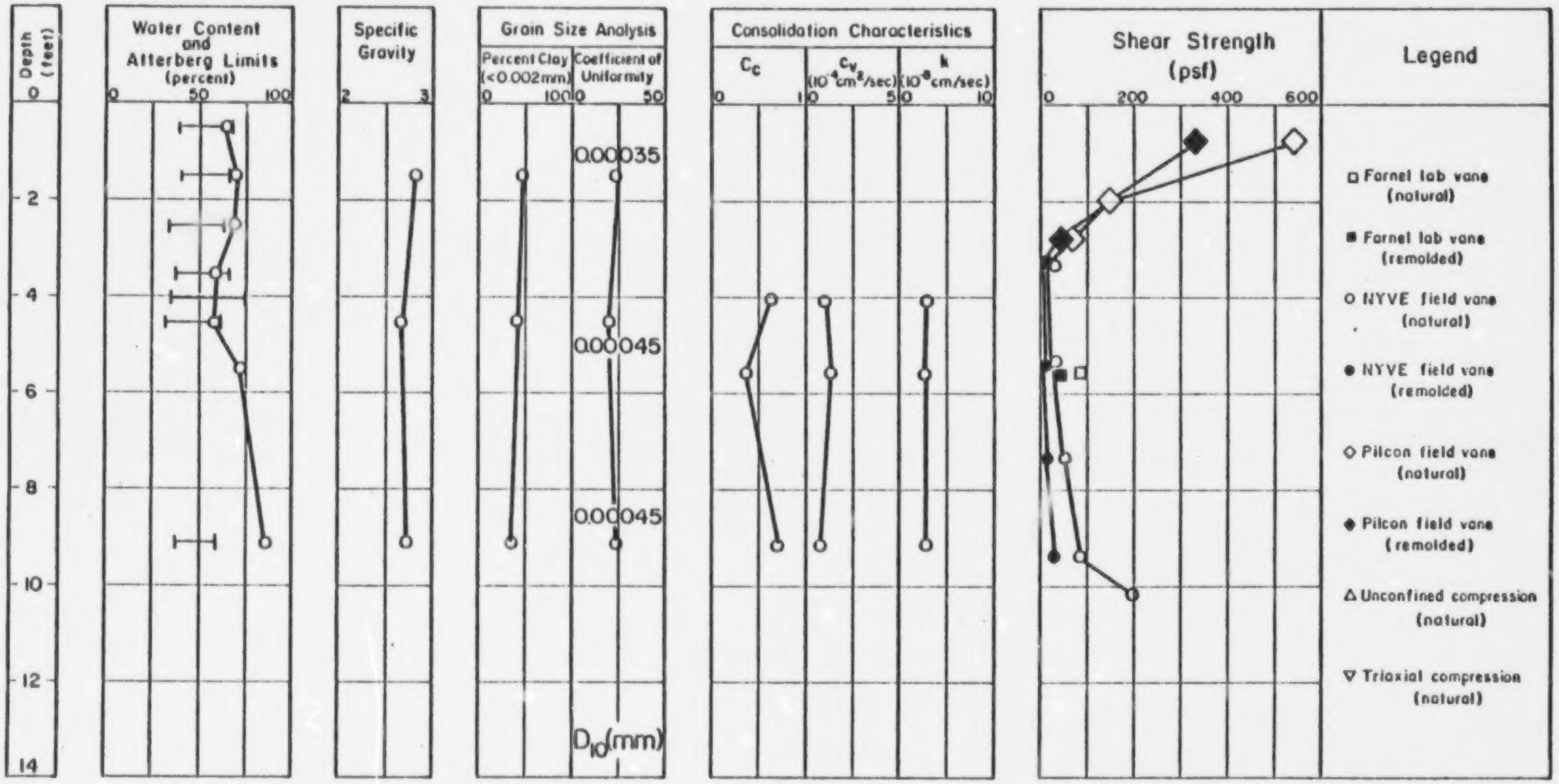

Figure 10-2. Field and Laboratory Test Data from BH-2 at Riverside Site

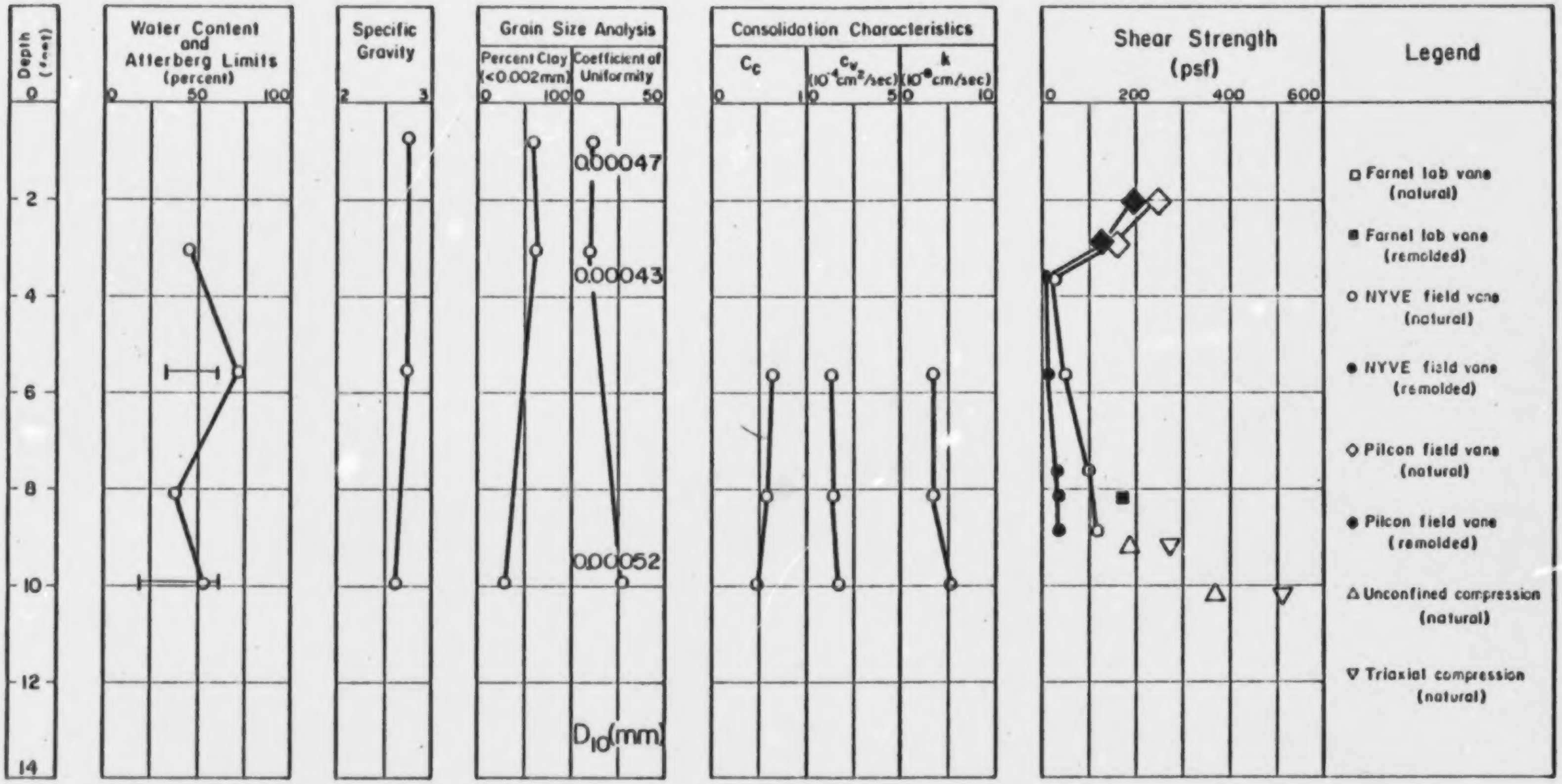

Figure 10-3. Field and Laboratory Test Data from BH-3 at Riverside Site

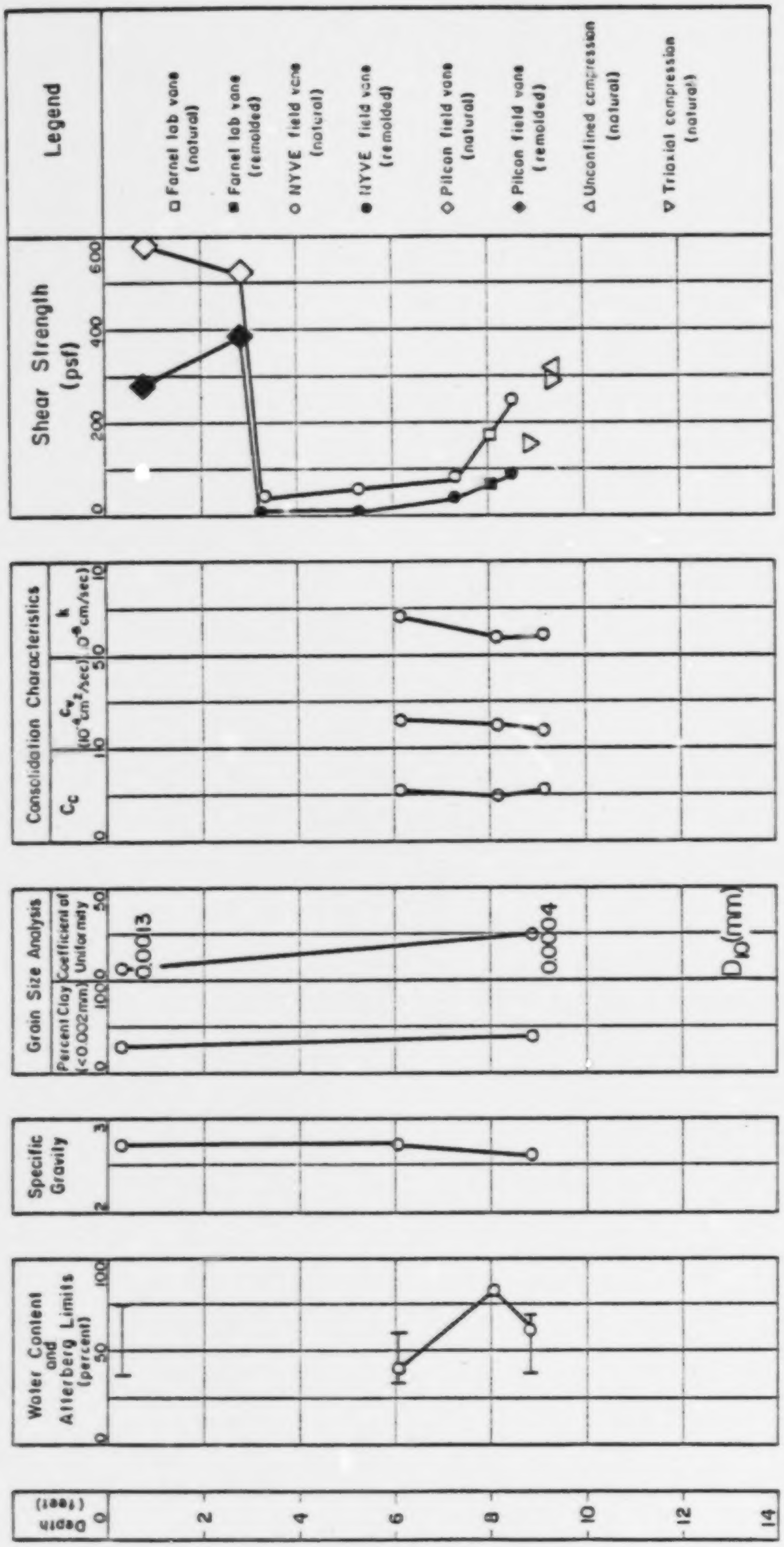

Figure 10-4. Field and Laboratory Test Data from BH-4 at Riverside Site

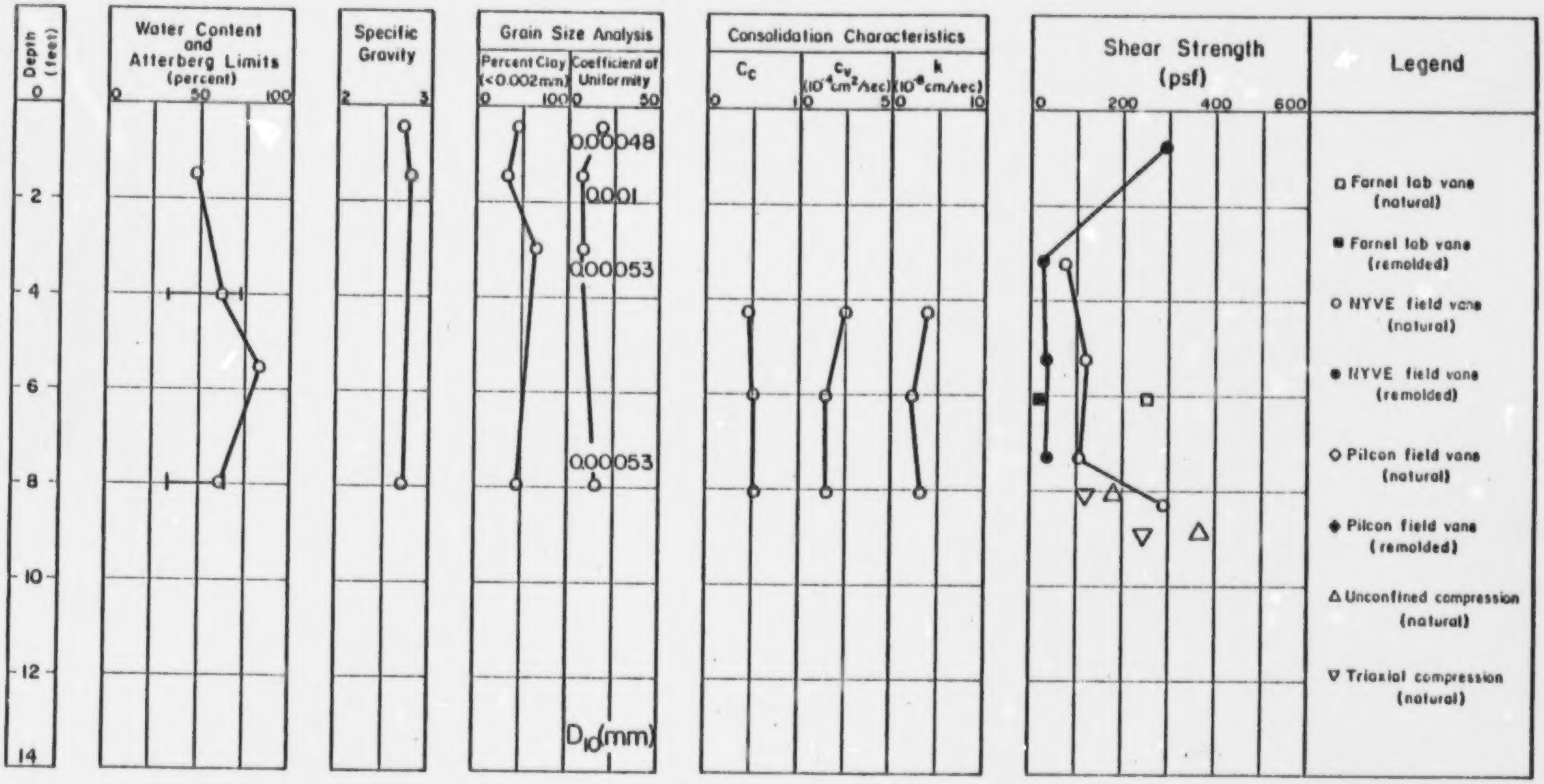

Figure 10-5. Field and Laboratory Test Data from BH-5 at Riverside Site

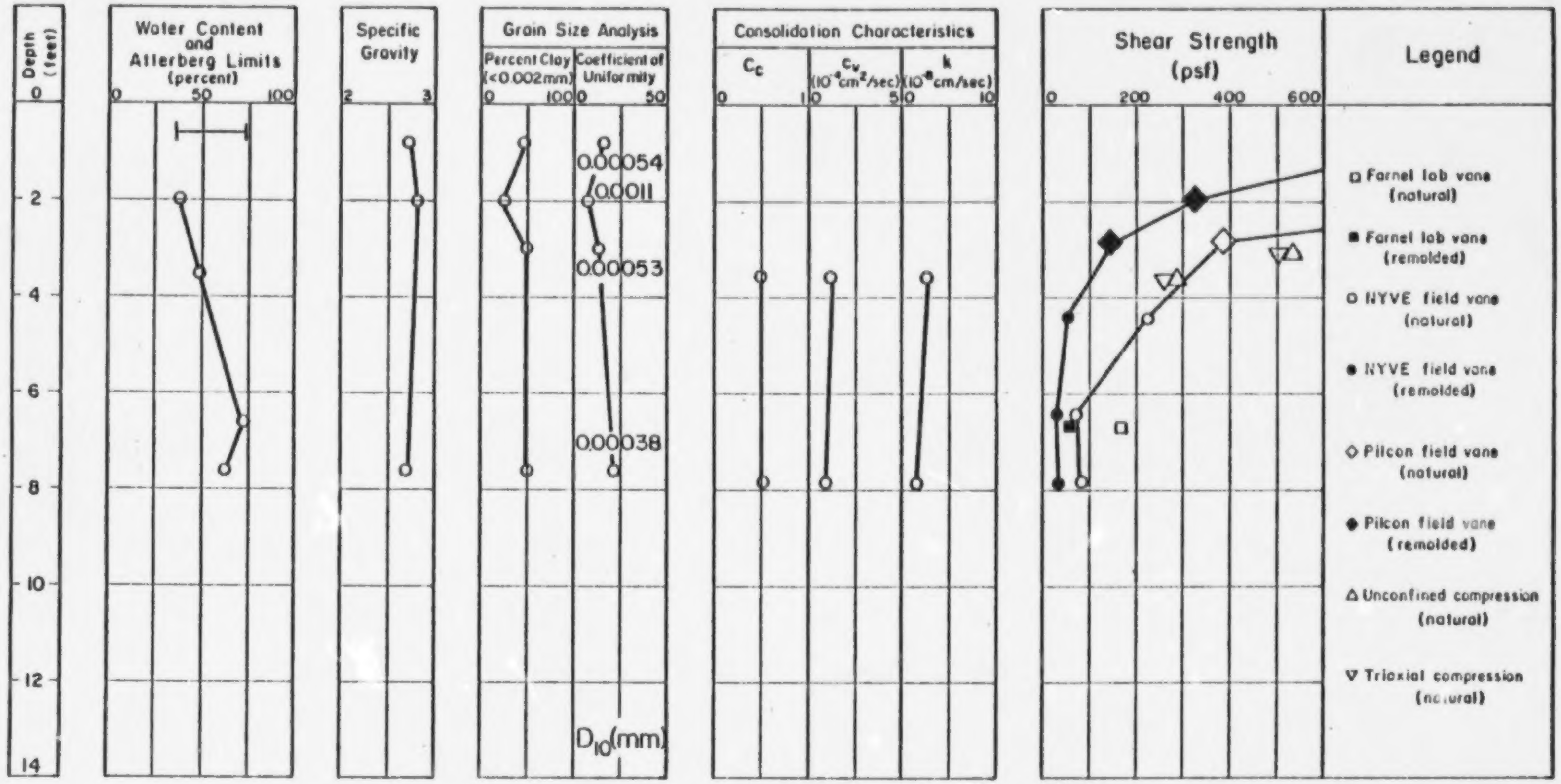

Figure 10-6. Field and Laboratory Test Data from BH-6 at Riverside Site

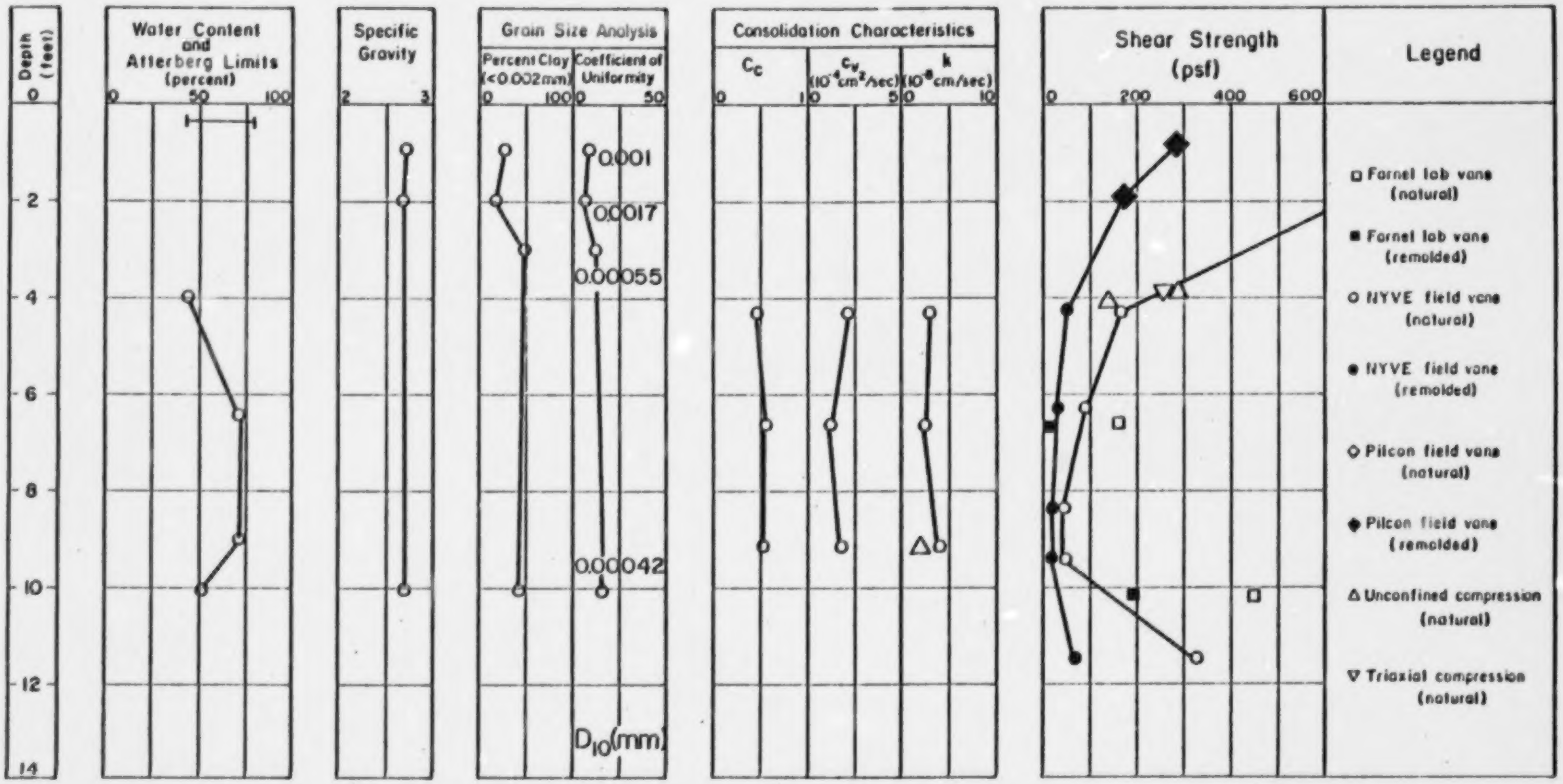

Figure 10-7. Field and Laboratory Test Data from BH-7 at Riverside Site

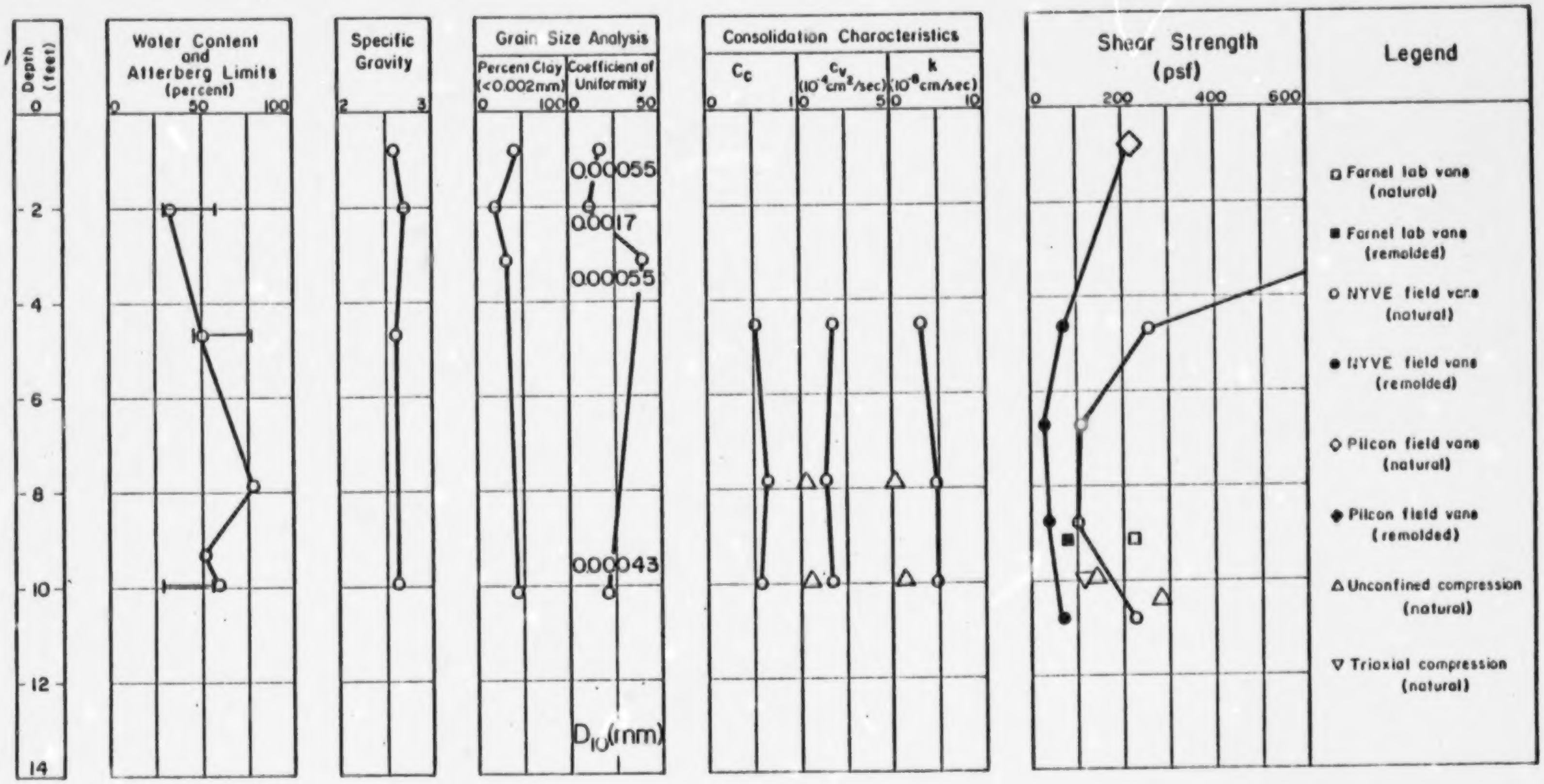

Figure 10-8. Field and Laboratory Test Data from BH-8 at Riverside Site

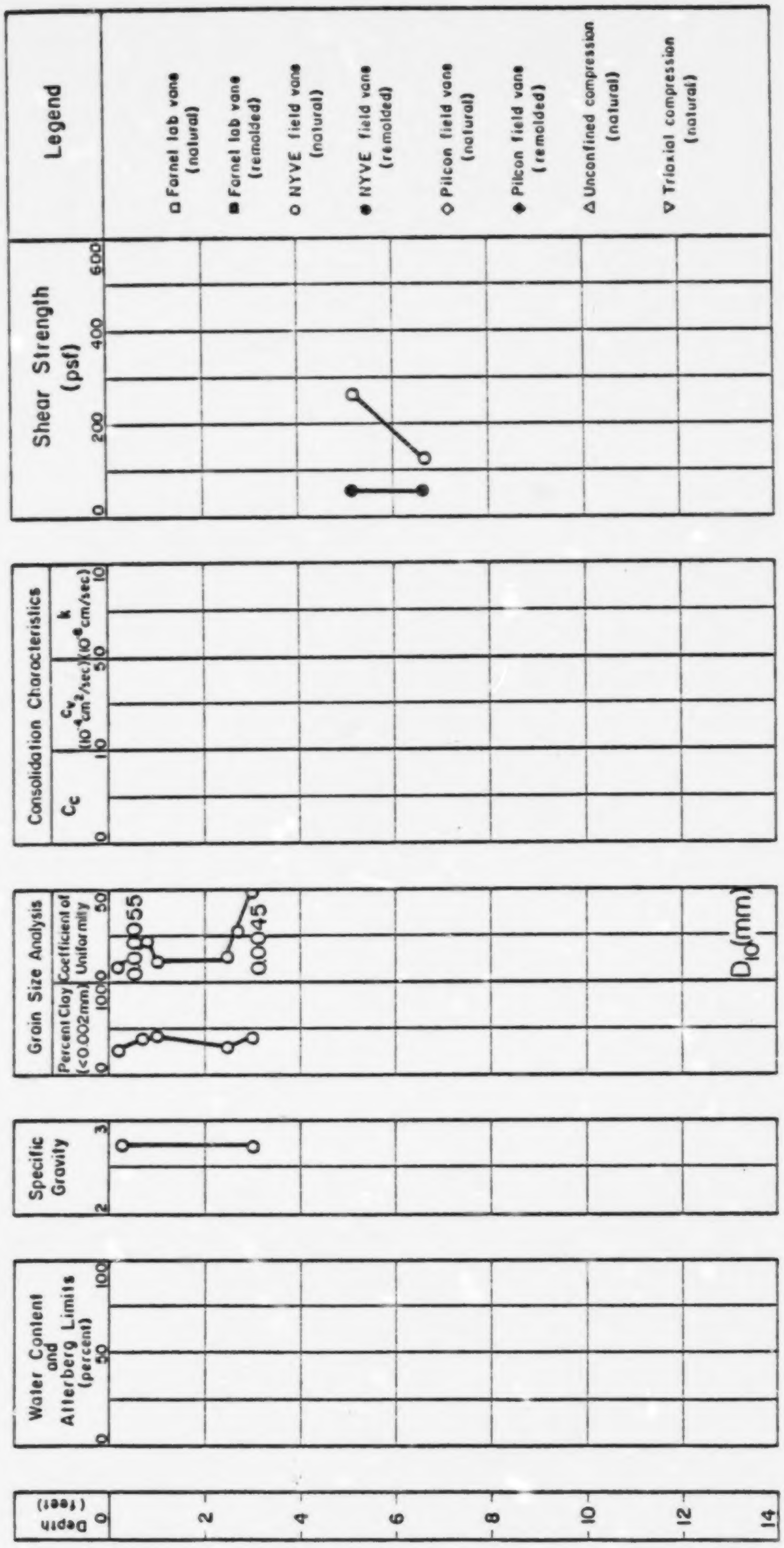

Figure 10-9. Field and Laboratory Test Data from BH-9 at Riverside Site

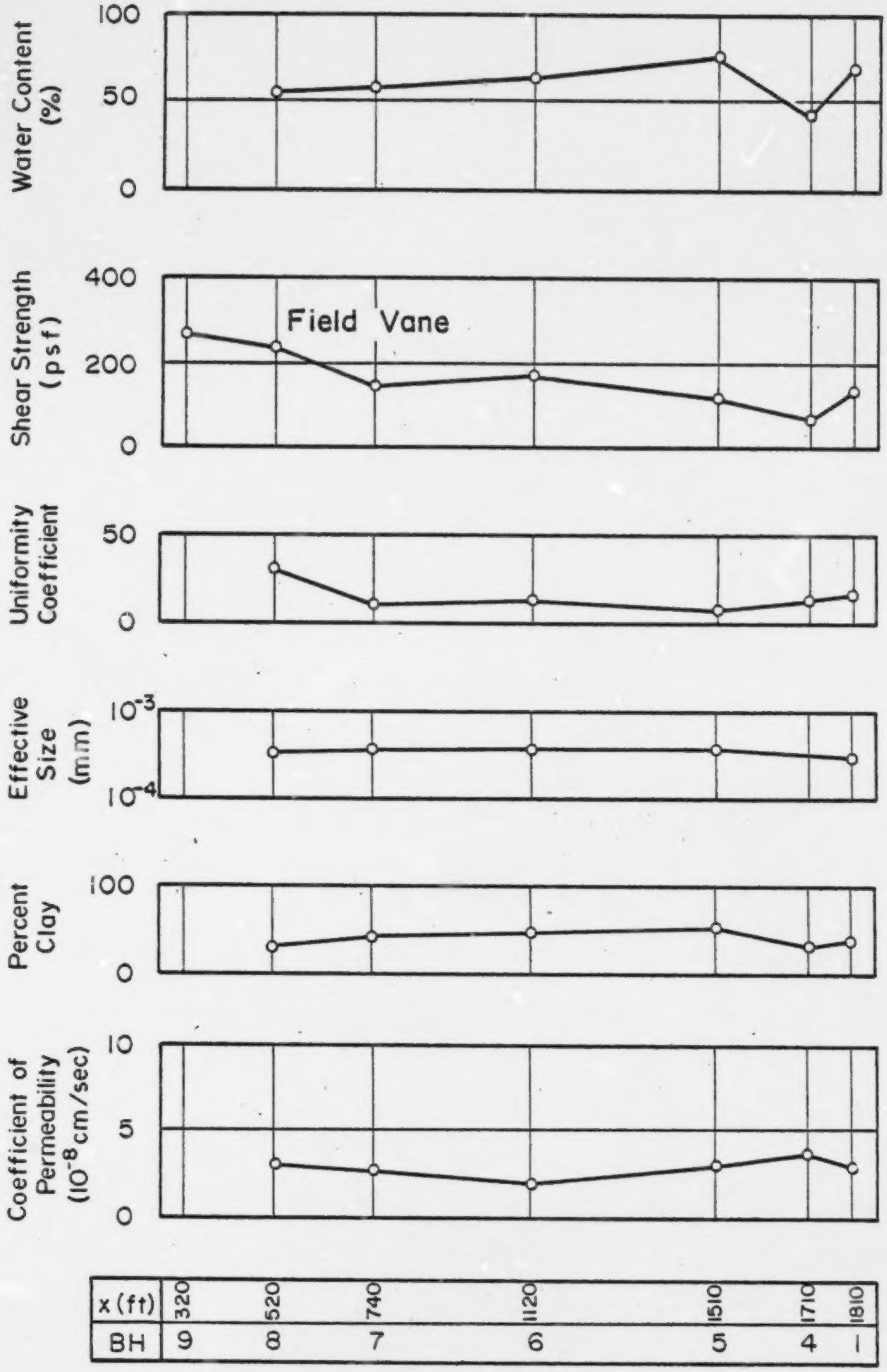

Note: x = distance from discharge pipe

Figure 10-10. Longitudinal Profile of Test Data from Riverside Site at Depth of Five Feet

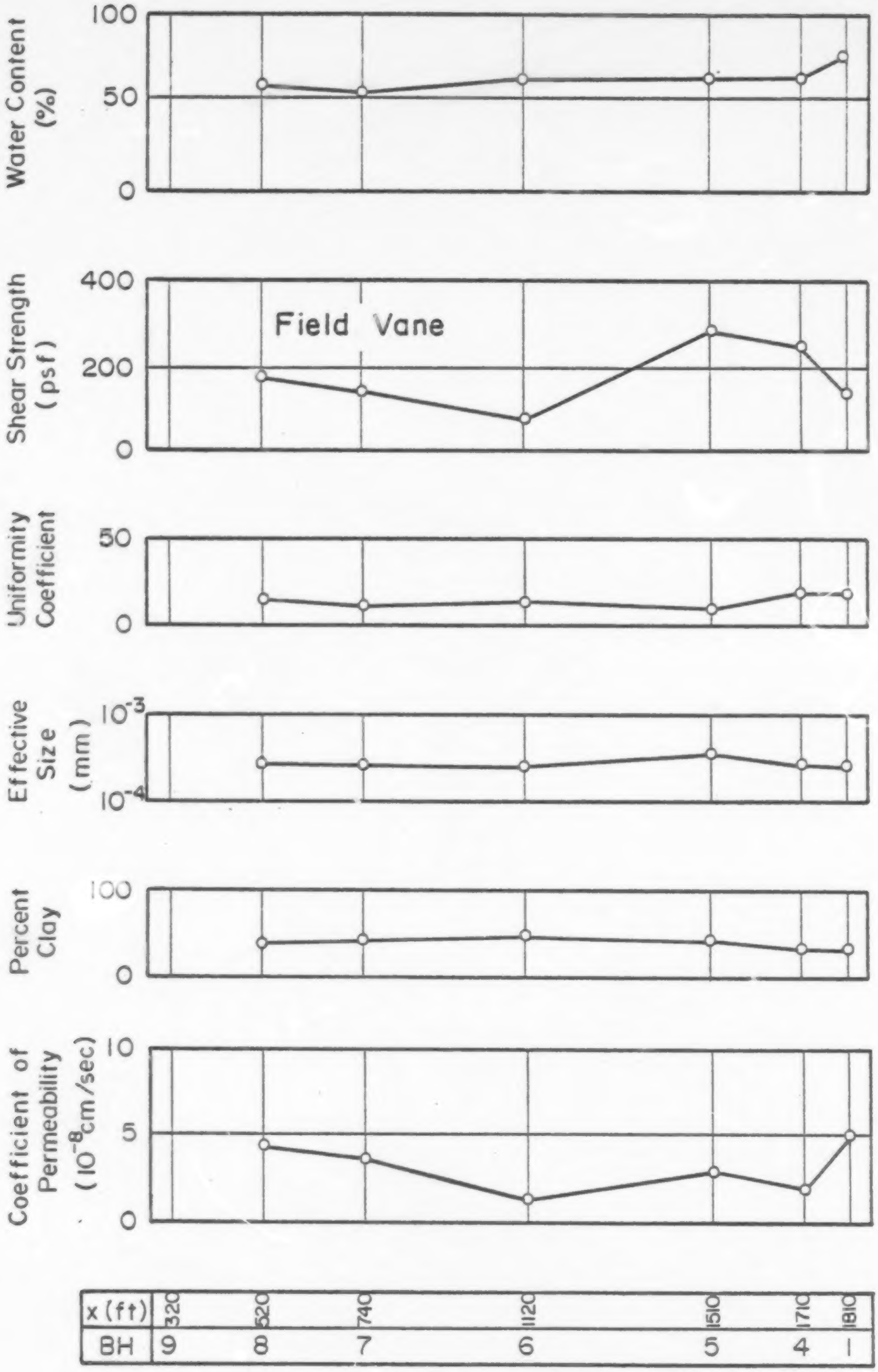

Note: x = distance from discharge pipe

Figure 10-11. Longitudinal Profile of Test Data from Riverside Site at Depth of Eight to Ten Feet

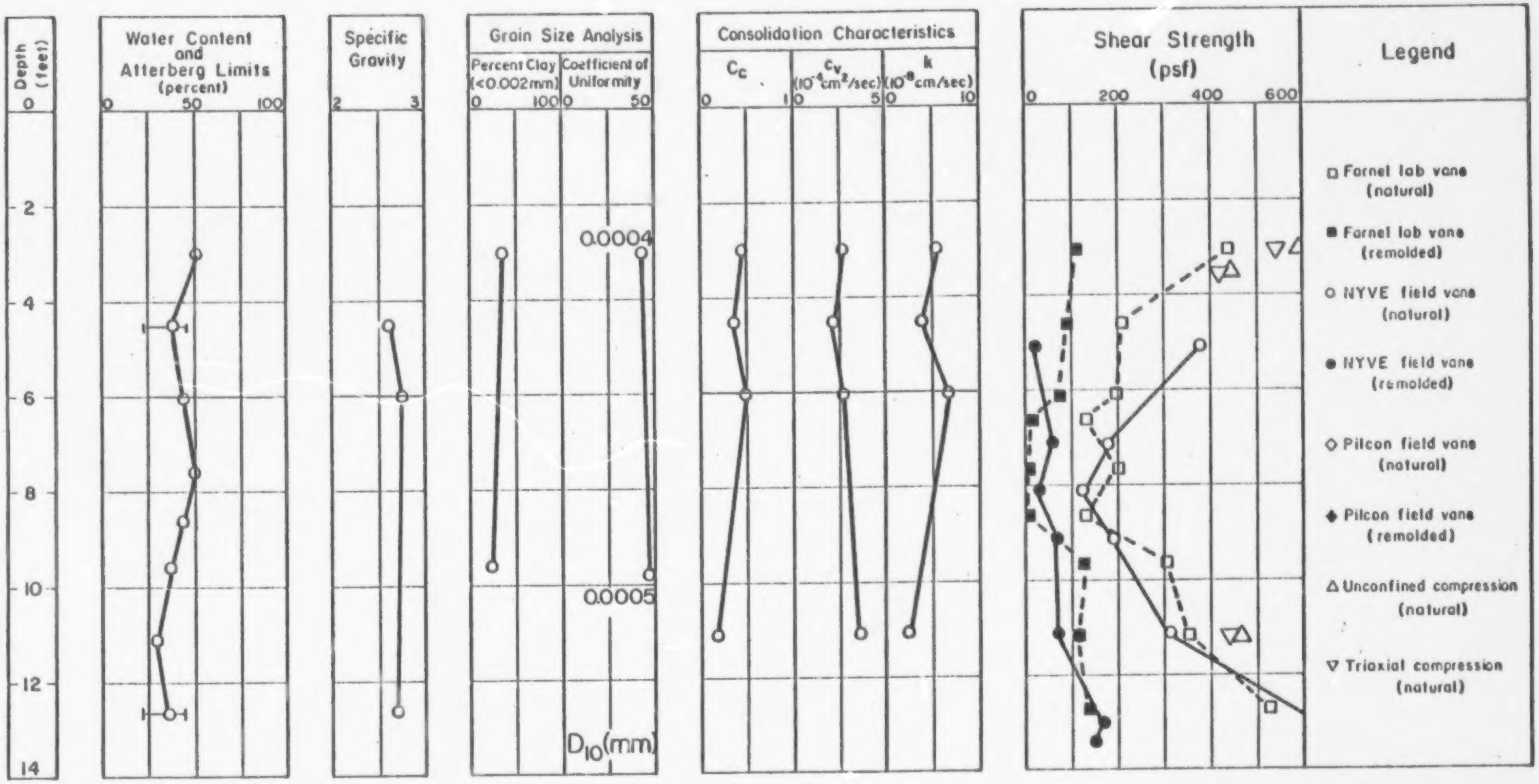

Figure 10-12. Field and Laboratory Test Data on Samples from Island Site near Overflow Weir

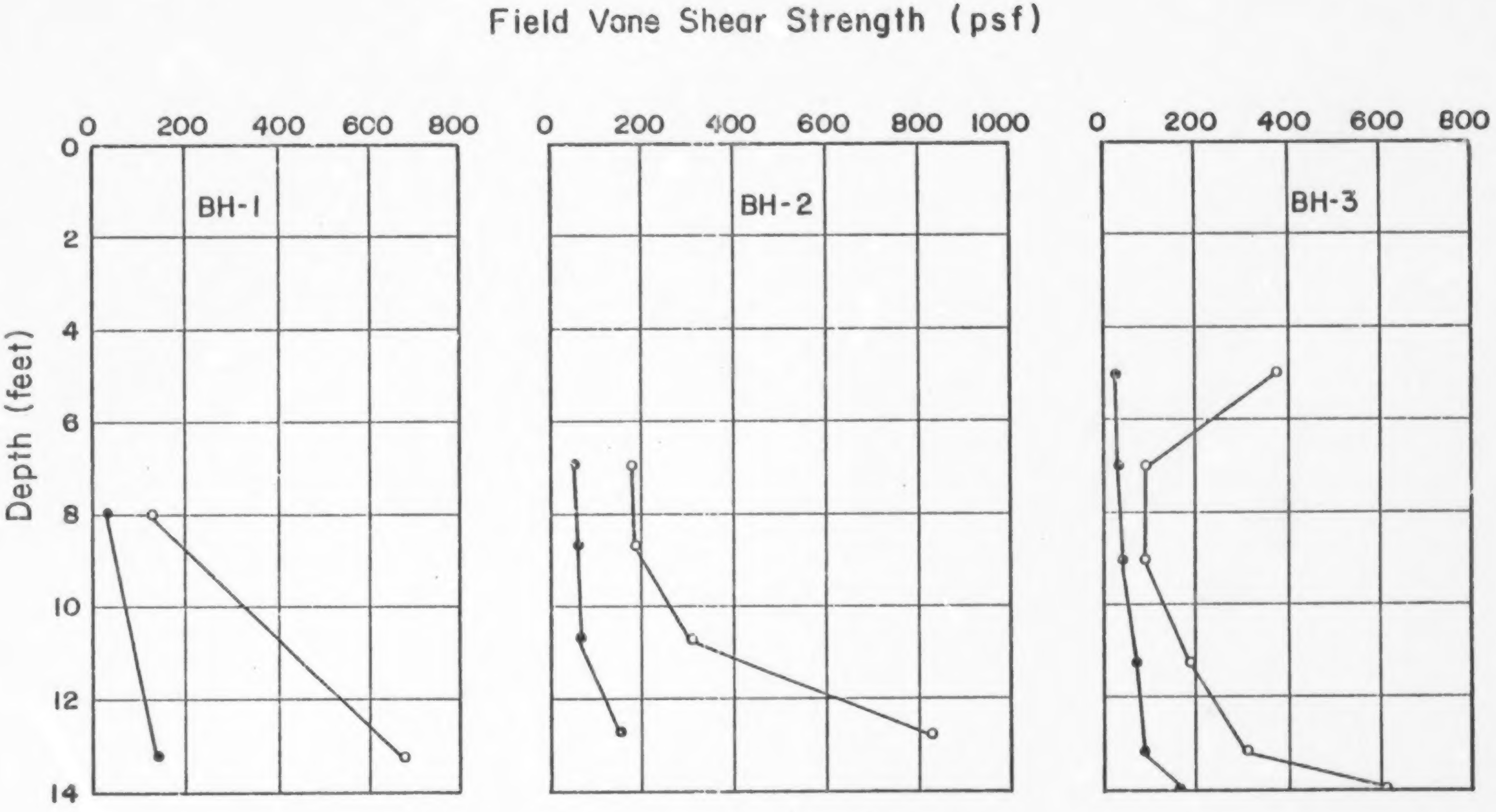

Figure 10-13. Field Shear Strength versus Depth from BH-1 through BH-3 at Island Site

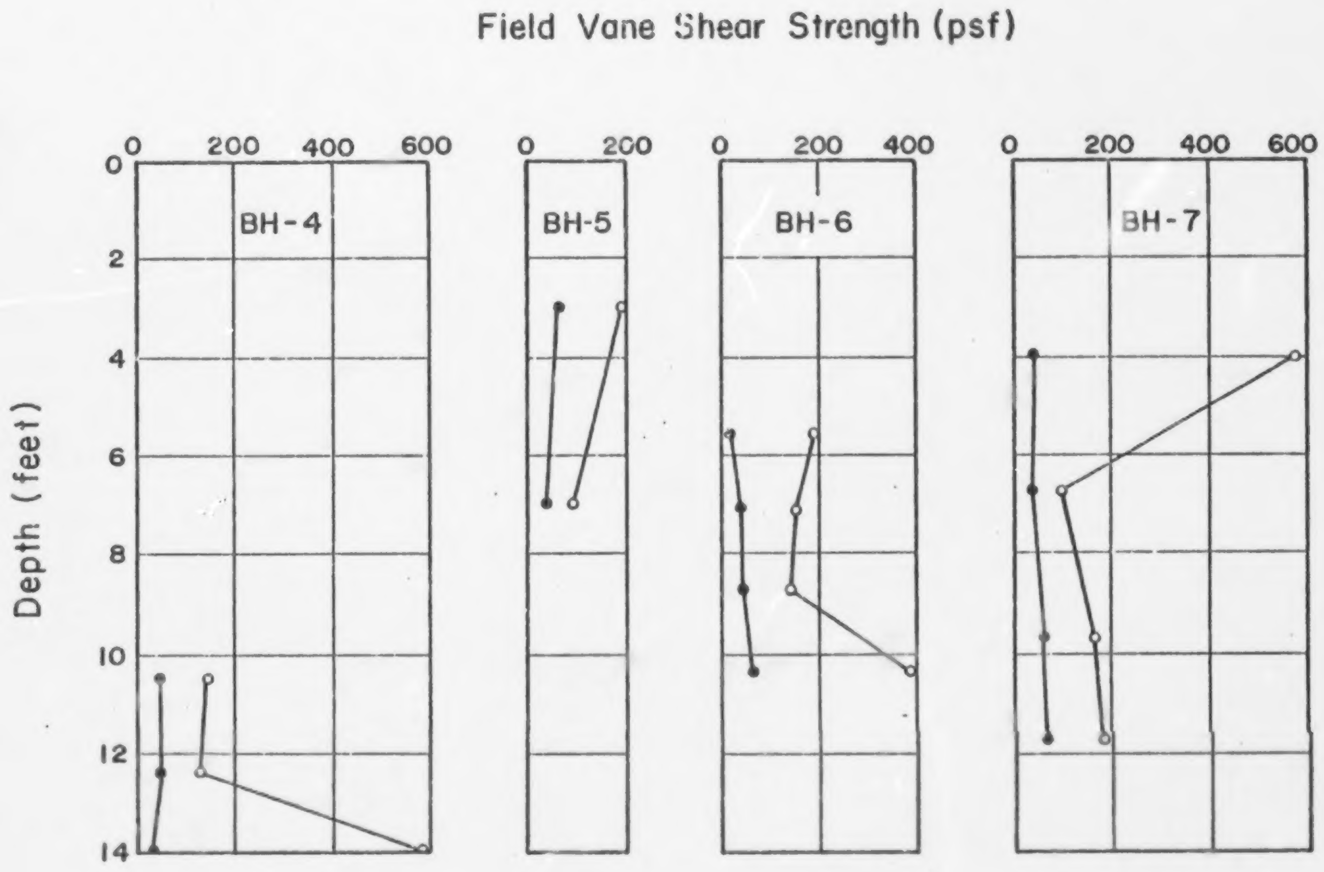

Figure 10-14. Field Shear Strength versus Depth from BH-4 through BH-7 at Island Site

summer of 1971, whereas those presented in Figures 10-15 through 10-18 were obtained from Riverside Site during the summer of 1972. Figure 10-19 gives a comparison of the undisturbed field vane strengths determined at Riverside Site in 1971 with values obtained at virtually the same locations in 1972.

Miniature laboratory vane tests were made on the sediments from the drainage tests, and the results are reported in Figures 10-20, 10-21, and 10-22. Figures 10-23, 10-24, and 10-25 give the stress-strain plots and the associated failure envelopes for the materials which were compacted at optimum water content in the Harvard miniature mold. Failure of the stiffer specimens occurred by rupture at relatively small strains, whereas the specimens of the softer materials were presumed to have failed at 20 percent strain or the maximum principal stress difference, whichever came first.

CONVENTIONAL CONSOLIDATION

A series of conventional consolidation tests was conducted on an apparatus in which the loads were applied by dead weights acting through a system of lever arms. The 3-inch diamter tube samples from the field were extruded and trimmed to fit a 2.5-inch diamter consolidometer ring; most of the rings were of 1-inch thickness, but some tests were conducted in 0.75-inch or 1.25-inch rings. After fitting the soil specimen to the ring, it was placed in the consolidometer, submerged, and loaded in the usual manner of doubling the previous load for each new loading. The stresses ranged from 0.158 kilograms per square centimeter to 10.1 kilograms per square centimeter, with each load increment usually being maintained for 24 hours. After full loading was achieved, the load was

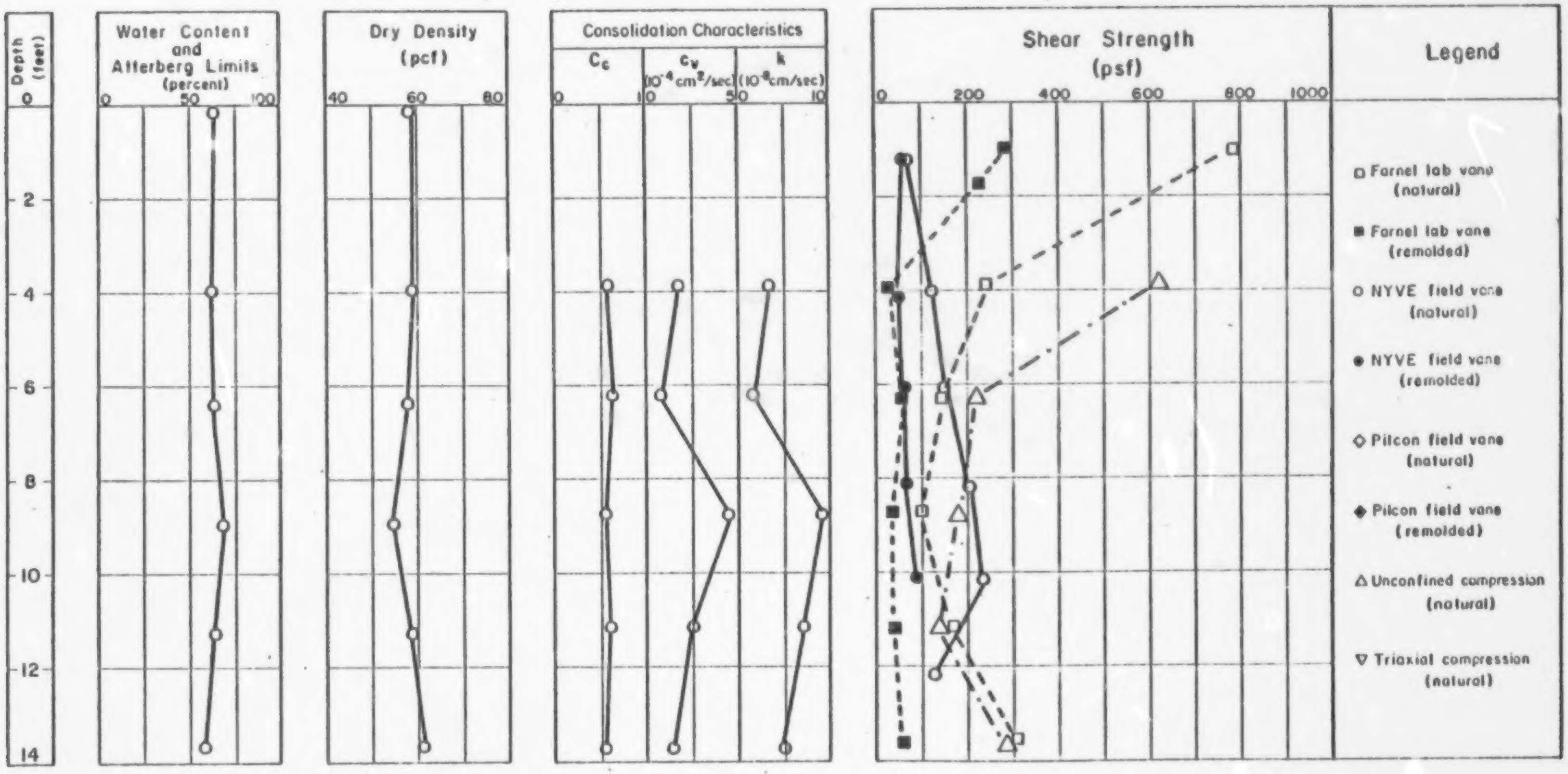

Figure 10-15. Field and Laboratory Test Data from BH-10 at Riverside Site

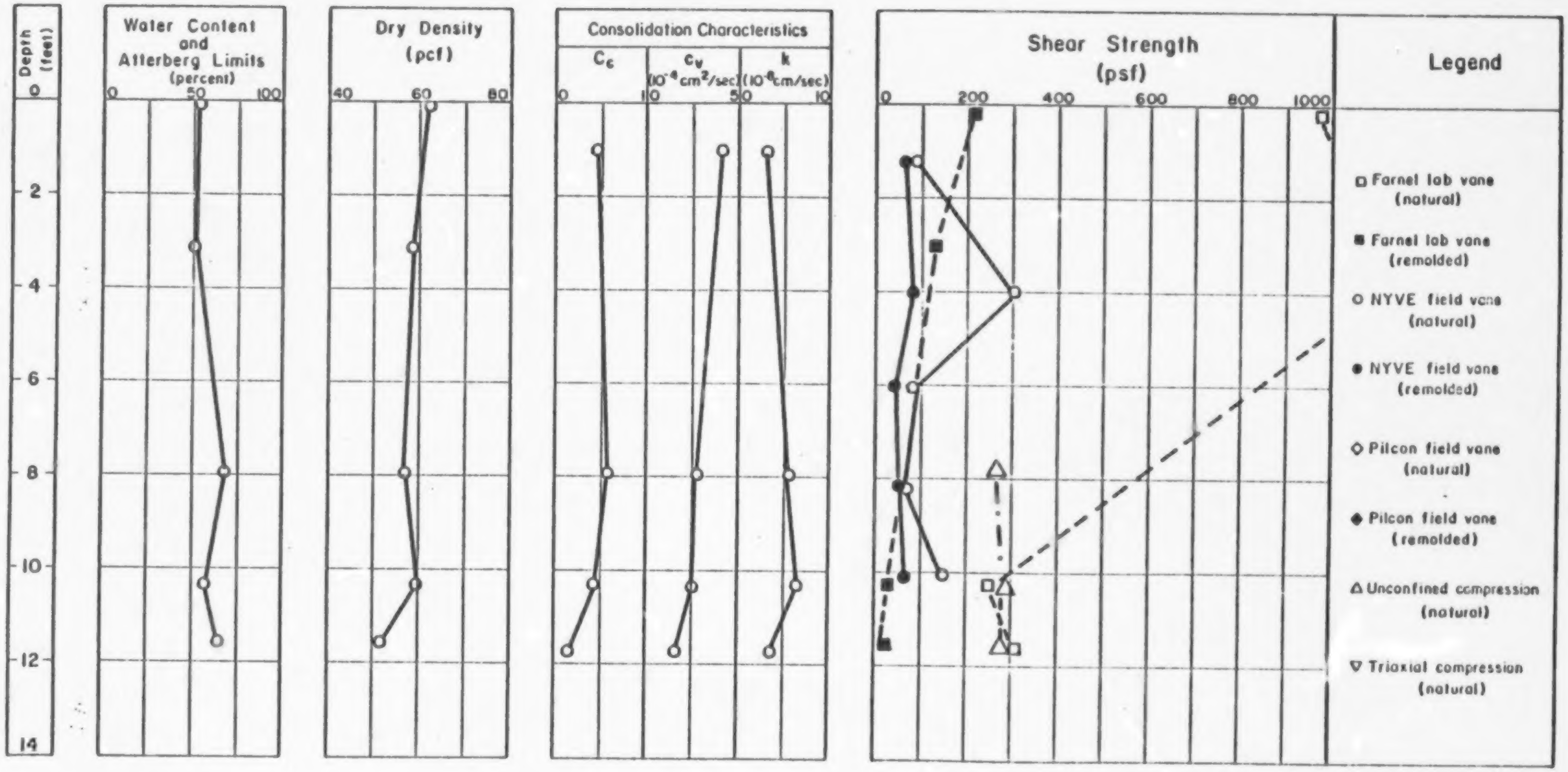

Figure 10-16. Field and Laboratory Test Data from BH-16 at Riverside Site

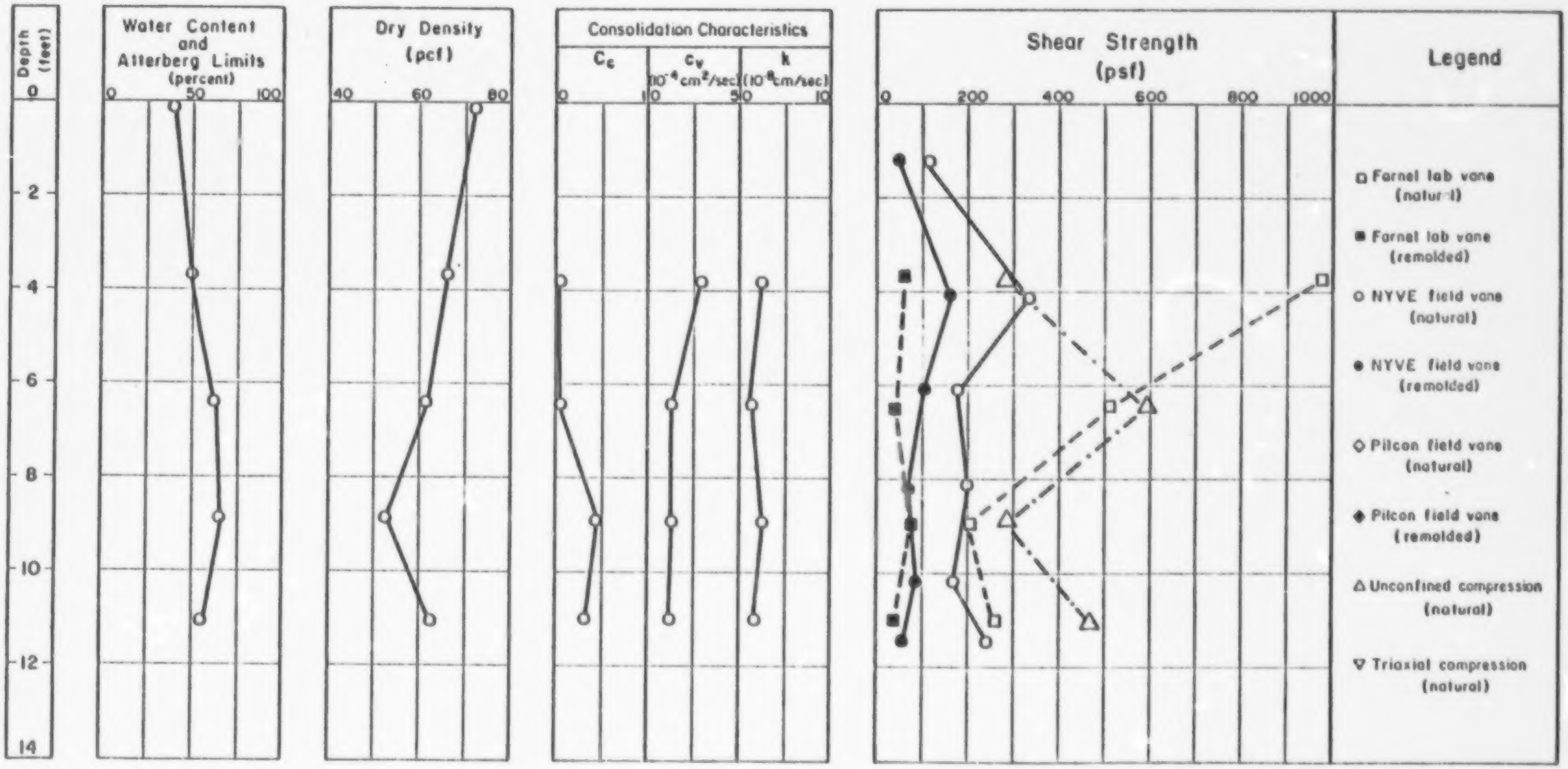

Figure 10-17. Field and Laboratory Test Data from BH-18 at Riverside Site

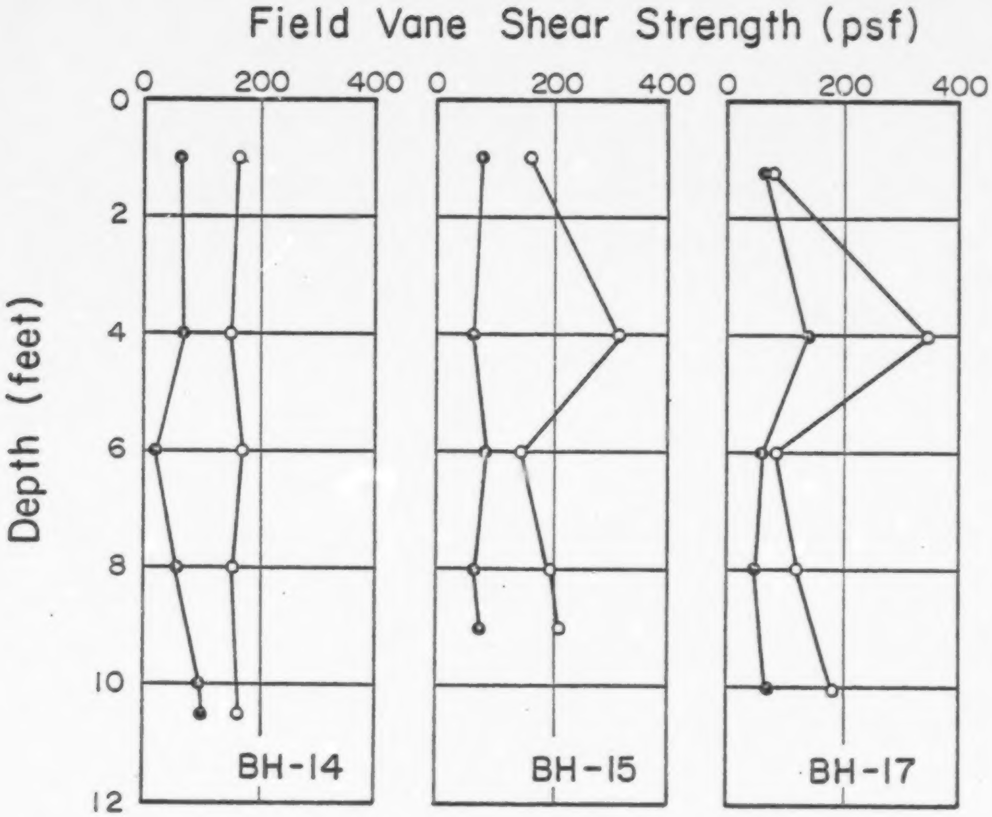

Figure 10-18. Field Shear Strength versus Depth from BH-14, BH-15, and BH-17 at Riverside Site

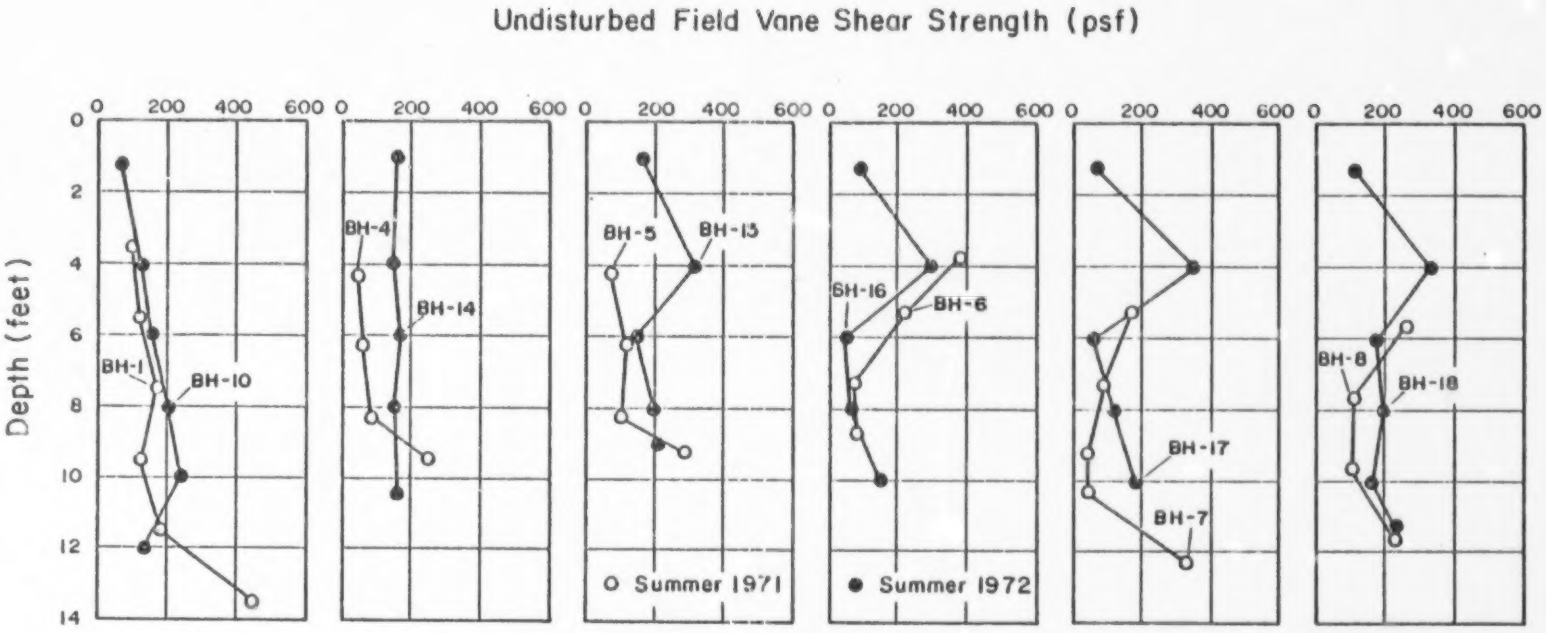

Figure 10-19. Comparative Plots of Field Shear Strength at Riverside Site in 1971 and 1972

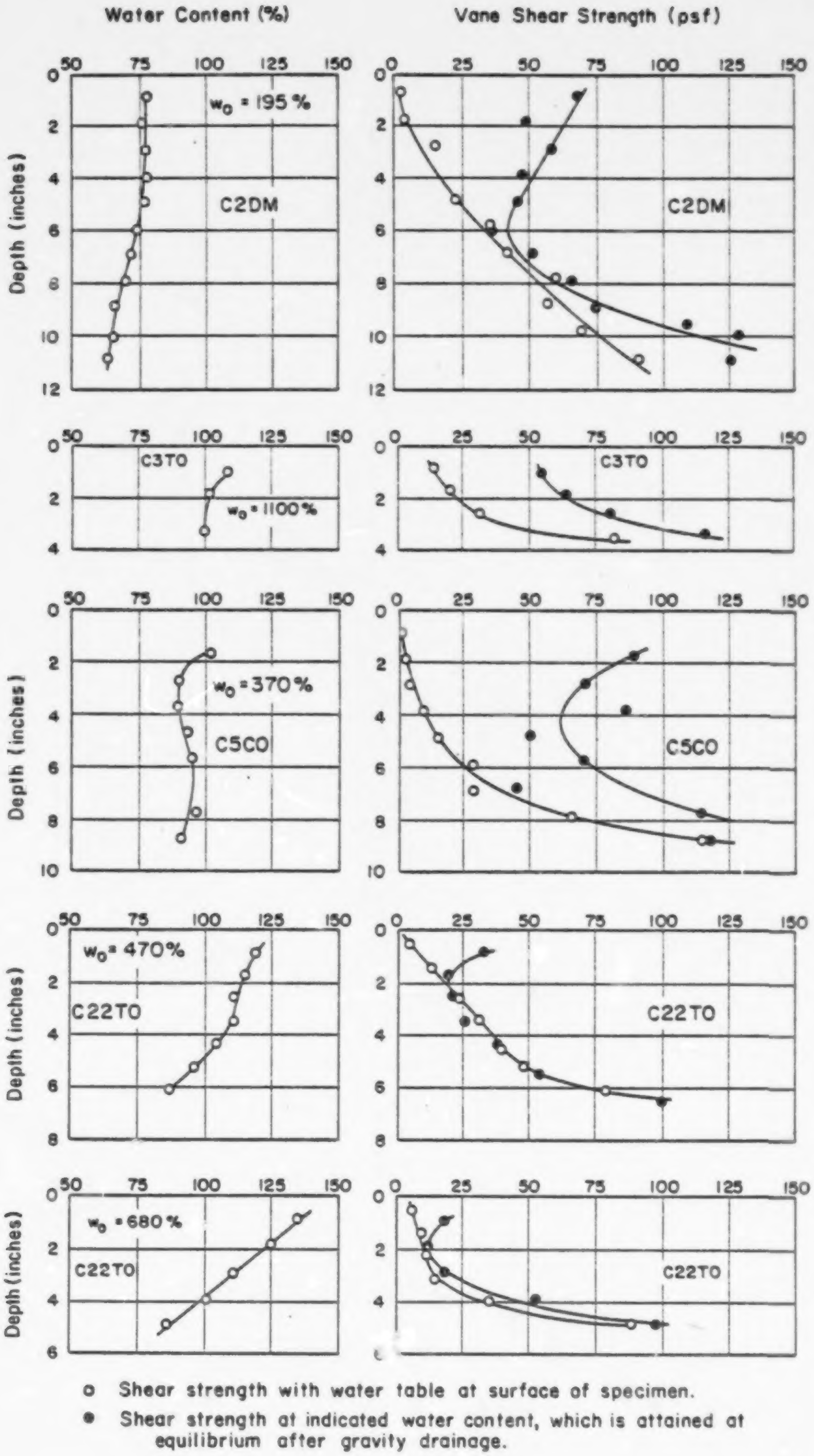

○ Shear strength with water table at surface of specimen.

● Shear strength at indicated water content, which is attained at equilibrium after gravity drainage.

Figure 10-20. Laboratory Shear Strength and Water Content versus Depth in Gravity Drained Specimens

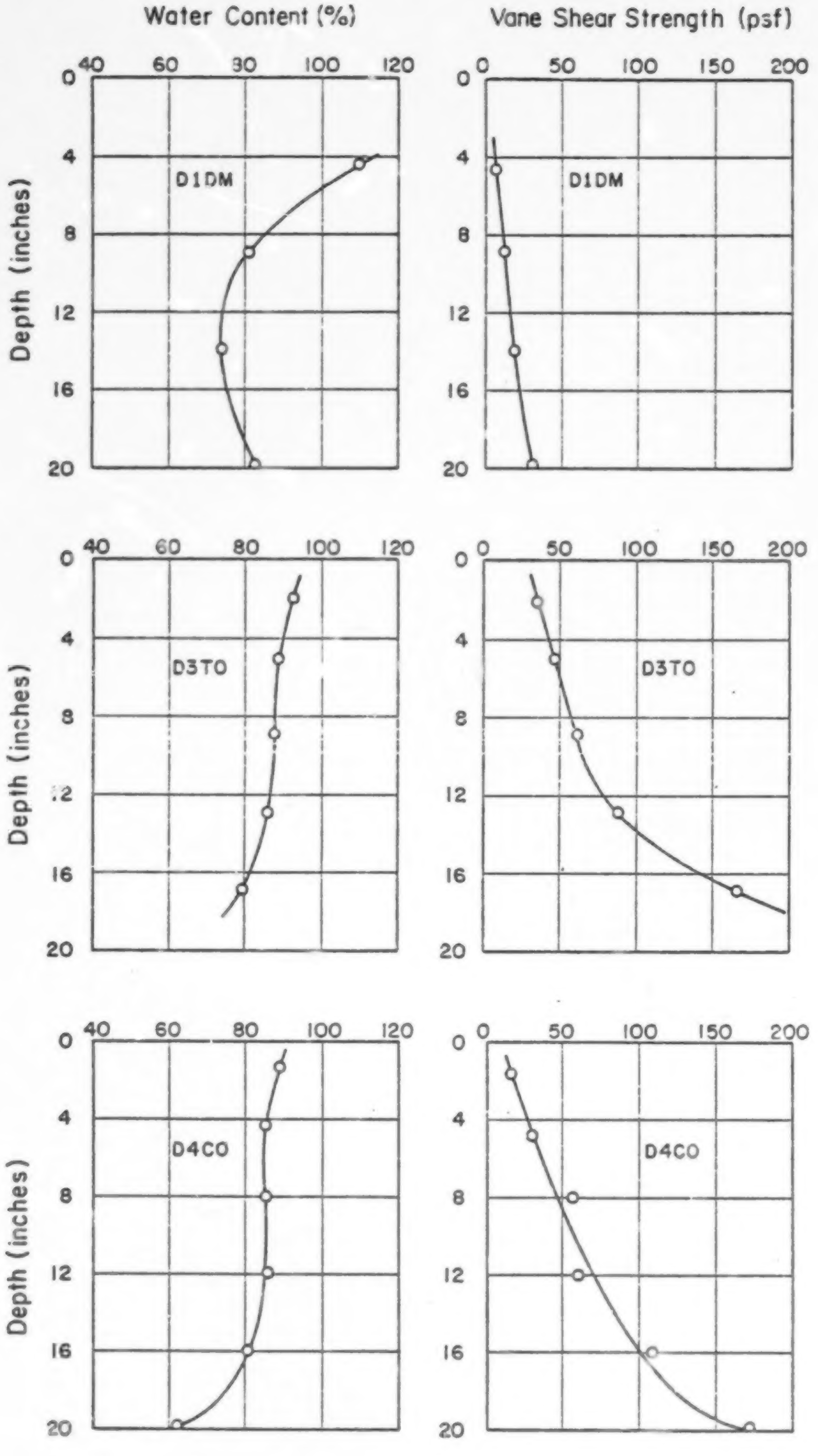

Figure 10-21. Laboratory Shear Strength and Water Content versus Depth in Gravity Drained Specimens

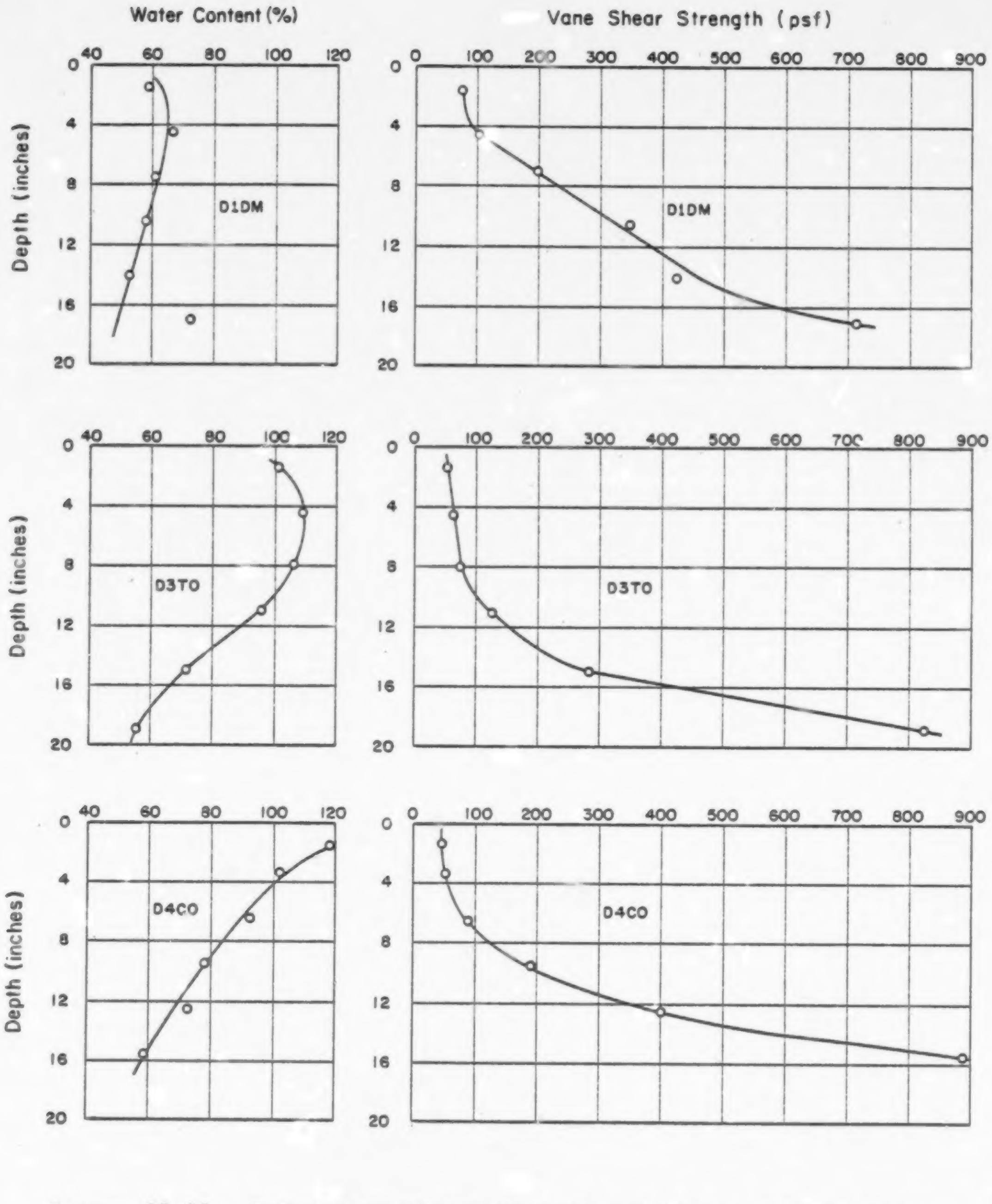

Figure 10-22. Laboratory Shear Strength and Water Content versus Depth in Vacuum Drained Specimens

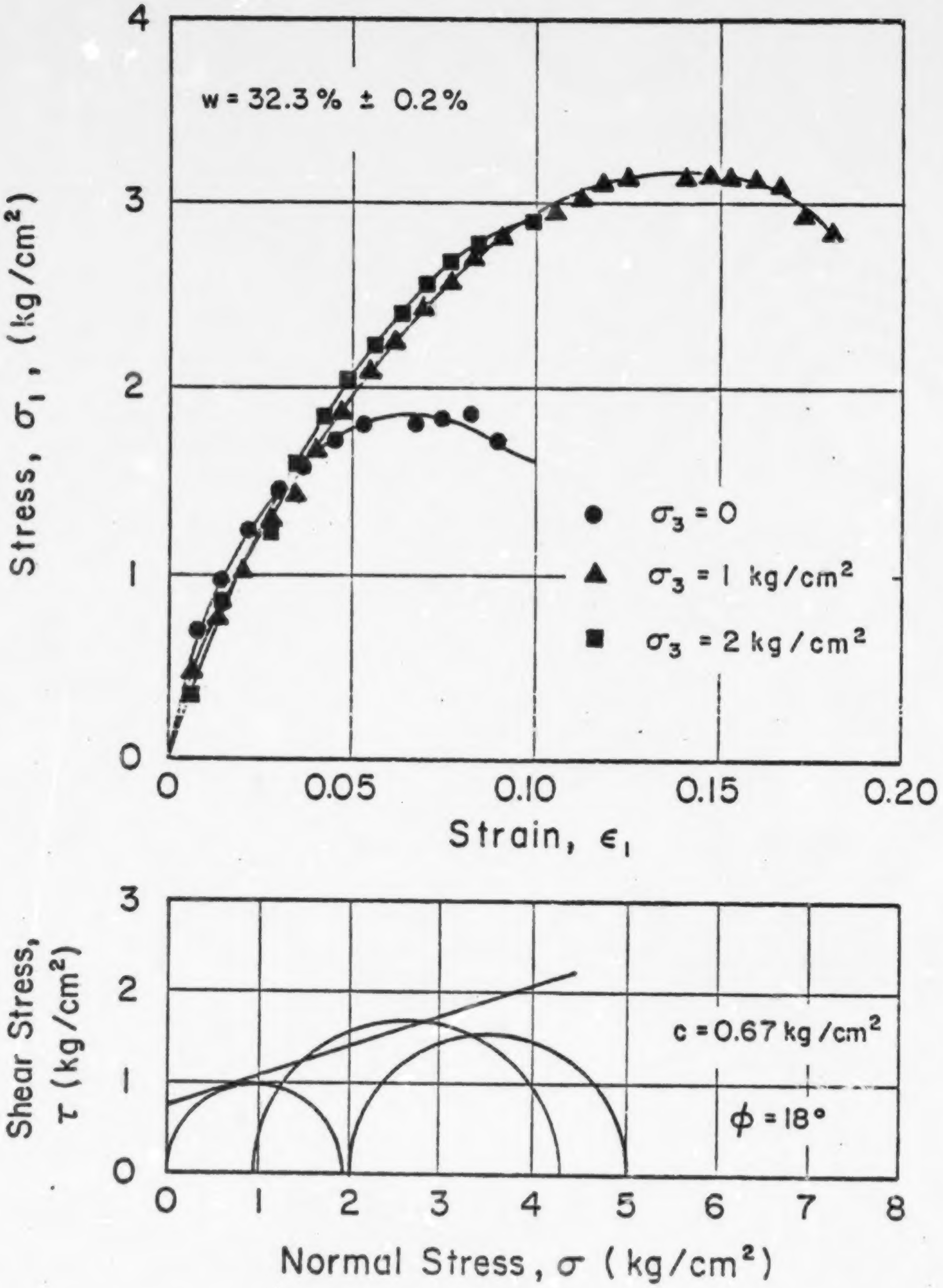

Figure 10-23. Stress-Strain-Strength Data on Compacted Dredgings from Vicinity of BH-10

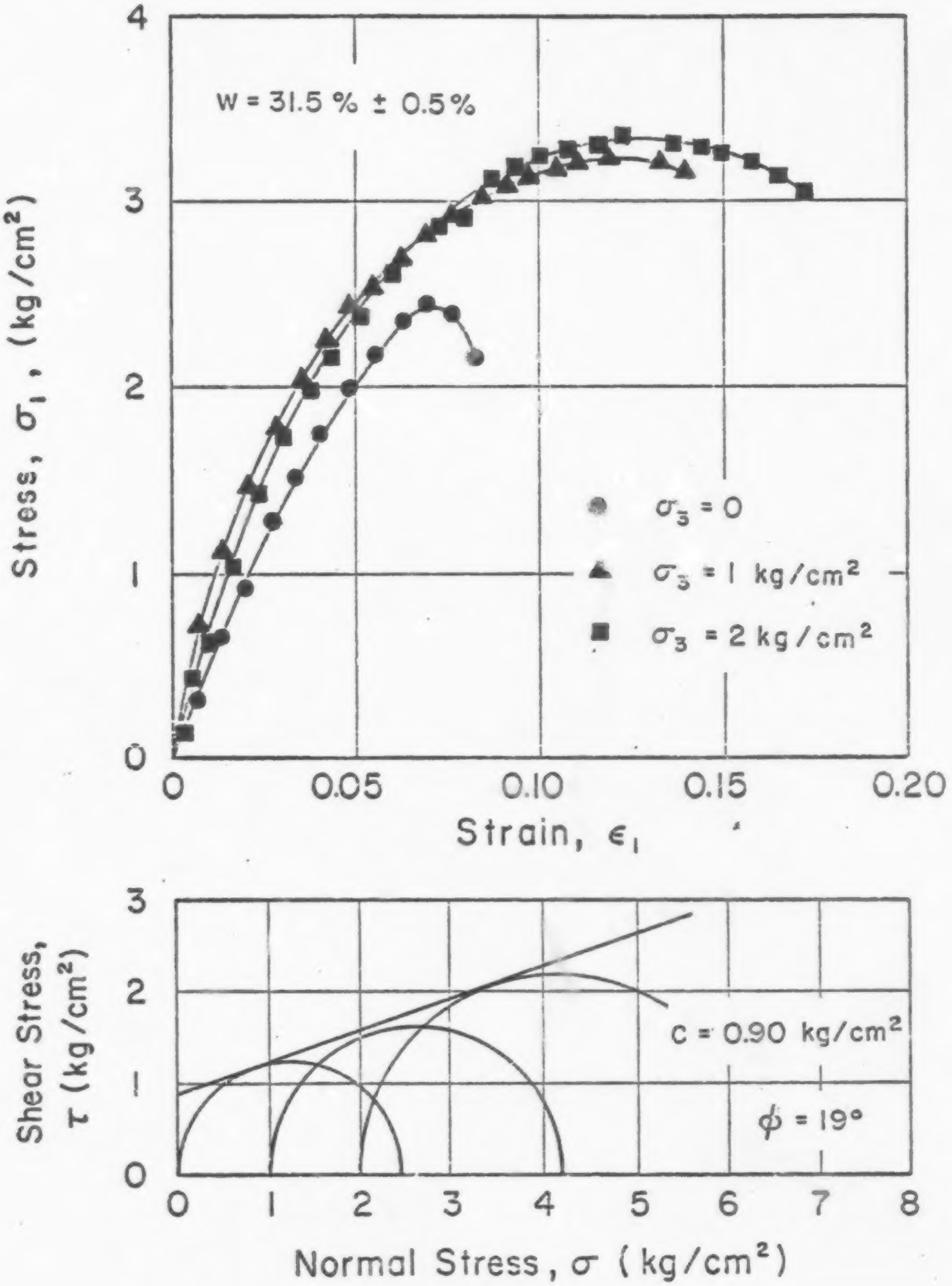

Figure 10-24. Stress-Strain-Strength Data on Compacted Dredgings from Vicinity of BH-16

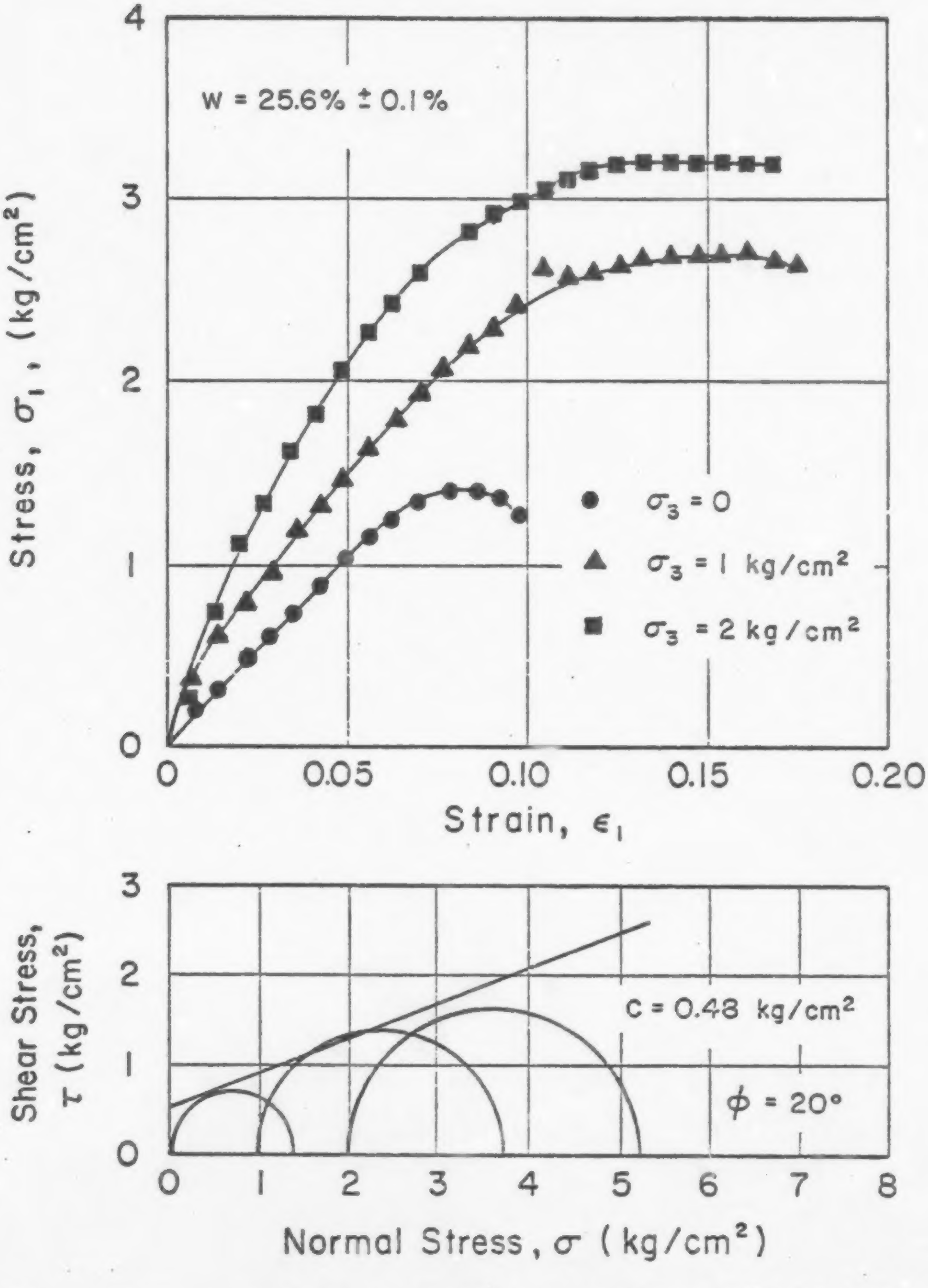

Figure 10-25. Stress-Strain-Strength Data on Compacted Dredgings from Vicinity of BH-18

removed systematically to develop the rebound curve. For each load increment, the deformations were converted to void ratios, e, and these were plotted against the logarithm of time, log t, to facilitate the determination of primary consolidation and the value of the coefficient of consolidation, c_v; from theoretical considerations (Terzaghi, 1943), c_v may be computed from the expression $c_v = 0.196\ h^2/t_{50}$, where h is one-half the specimen height for conditions of double drainage, and t_{50} is the time for one-half of primary consolidation to occur. The void ratio, e, associated with the end of primary consolidation under a given stress, p, is usually plotted versus that load to develop an e-log p curve for each specimen. The slope of this curve in the higher load ranges usually becomes nearly linear, and this slope is termed the compression index, C_c. Consolidation tests were conducted on 26 samples taken from Riverside Site and the Island Site in 1971 and on 13 samples taken from Riverside Site in 1972; the coefficients C_c and c_v are summarized in Figures 10-1 through 10-9, 10-12, 10-15, 10-16, and 10-17.

COMPACTION

When considered for engineering use, the compaction characteristics of a soil are of considerable interest. Accordingly, three samples of spoil were selected from Riverside Site and tested in the laboratory to determine their moisture-density-compaction relationships; the three samples were E115 from near BH-10, which was in the vicinity of the outflow weir, E134 from near BH-16, which was about midway between the outflow weir and the discharge pipe, and E146 from near BH-18, which was about 500 feet from the discharge pipe where the spoil enters the fill. Two series of compaction tests were conducted to study the conventional moisture-density relationships, and an additional series was performed to investigate the effect of compactive effort on the peak density of dredgings and the variation of density with depth in the compaction mold.

Standard Proctor compactive effort was used in the first series of tests, and the resulting moisture-density relationships are presented in Figure 10-26. In general, the response is characterized by the typical compaction curve, which has a peak density at the optimum moisture content and lesser densities at higher and lower water contents. Although there is not much difference in the results for the samples taken near BH-10 and BH-16, the peak density for the sample from the vicinity of BH-18 is substantially higher, exhibiting a value of about 86 pounds per cubic foot while the other two samples had peak densities around 78 pounds per cubic foot. In addition, the optimum water content for the sample from near BH-18 is about 28 percent, which is somewhat lower than the values of 33 and 38 percent for the other two samples. Since a comparison of the organic contents of these three samples reveals little variation, the major reason for these differences is presumed to be due to grain size and gradation.

The second series of tests was conducted on samples compacted with the Harvard miniature device (Wilson, 1950), and a study of the test results presented in Figure 10-27 indicates the same trends as those discussed above for a standard Proctor compactive effort. Although the optimum moisture content does not vary appreciably in these tests, the greater compactive effort of the Harvard miniature test does develop greater densities (about 100 pounds per cubic foot compared to 86 pounds per cubic foot for the material from near BH-18, and about 91 pounds per cubic foot compared to 78 pounds per cubic foot for the material from the

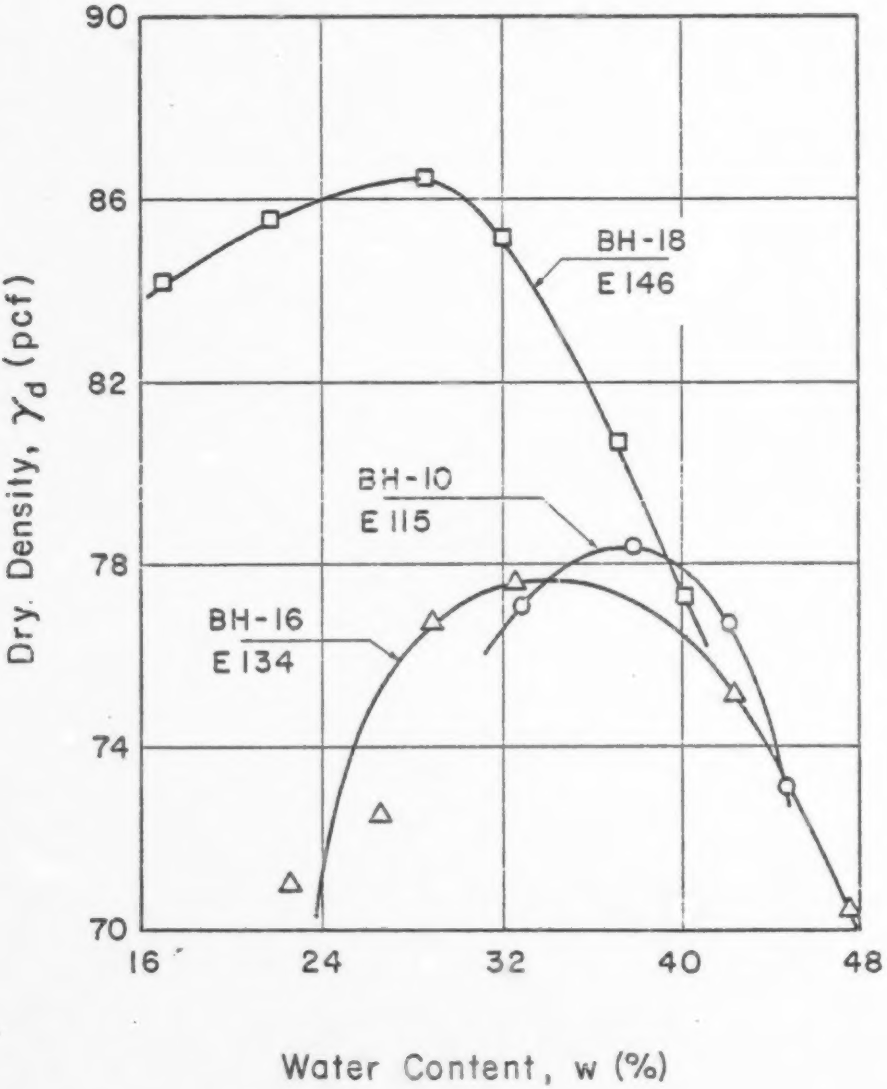

Figure 10-26. Standard Proctor Compaction Curves

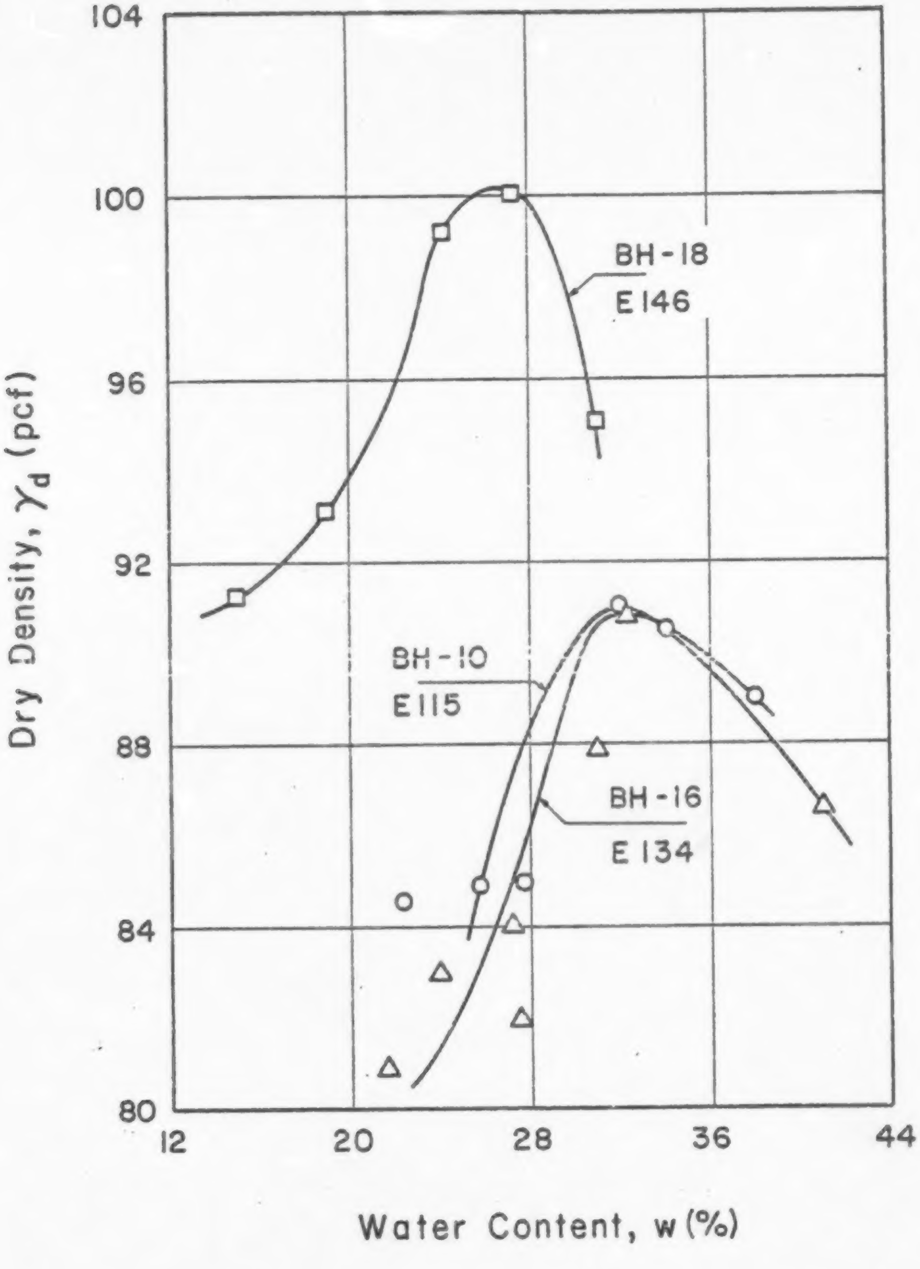

Figure 10-27. Harvard Miniature Compaction Curves

vicinity of BH-10 and BH-16. The samples prepared by the Harvard miniature technique were subjected to strength tests, and the results obtained are reported in the section on strength properties.

A third series of tests was performed to determine the peak densities obtained for different compactive efforts. These tests were conducted in a specially designed, sectioned mold 2.5-inches in diameter and 5 inches high; a diagram of the mold is shown in Figure 10-28. To obtain medium densities the standard Proctor energy per unit volume (12,400 foot-pounds per cubic foot) was used. The dense condition was achieved by compacting the material with a unit energy equivalent to that specified for the modified AASHO procedure (56,300 foot-pounds per cubic foot). Finally, the loose samples were prepared by using a unit energy equal to 20 percent of that specified for the standard Proctor procedure (that is, 2,480 foot-pounds per cubic foot). The results for this latter series of tests are given in Figure 10-29, which suggests that the peak dry density may reasonably range between about 60 and 100 pounds per cubic foot, depending on the compactive effort and the material characteristics (assuming compaction at optimum moisture content).

While preparing the test specimens in the specially sectioned mold discussed above, a minor study was undertaken to determine the variation of density with depth within the compaction mold; this was done on the material from near BH-16, and the results are presented in Figure 10-30. Although the medium density condition yielded somewhat erratic results, the loose and dense conditions indicated consistently higher densities for greater depths. This is quite reasonable, because the lower material receives additional energy as the upper layers are being compacted.

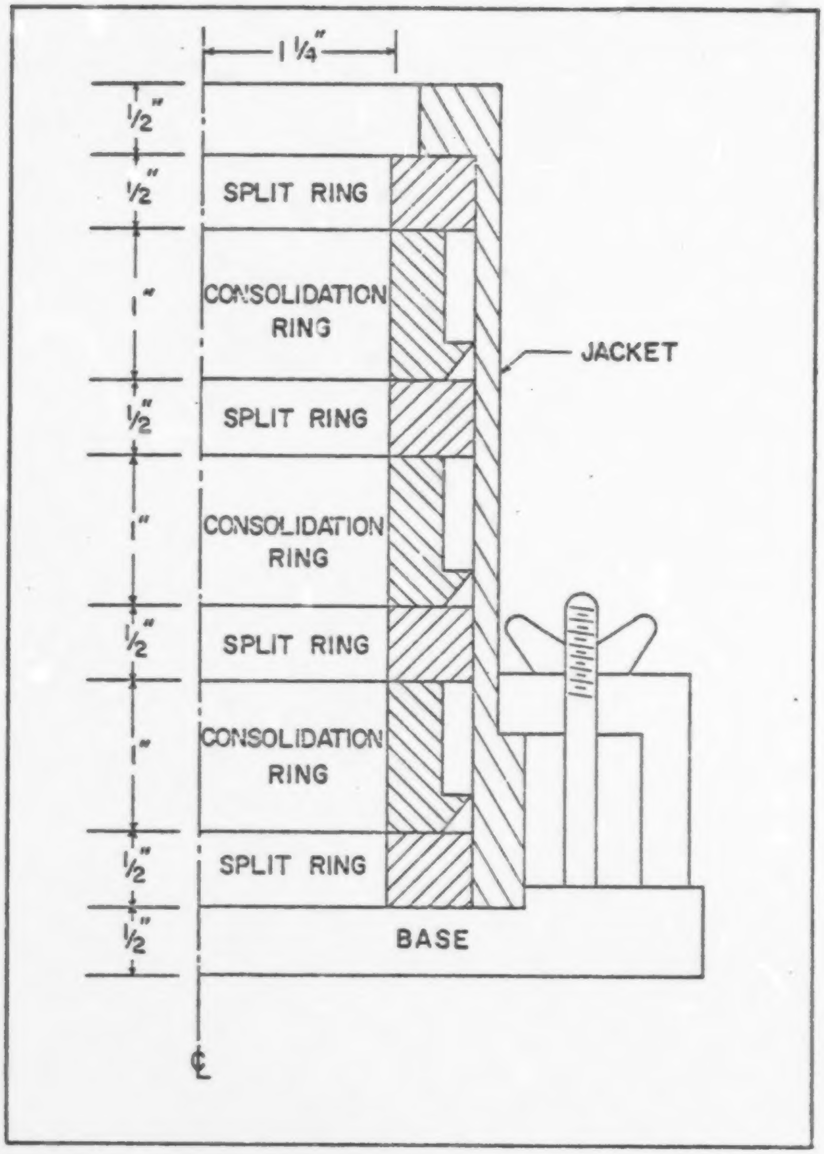
1 1/4"
1/2"
1/2"
SPLIT RING
1"
CONSOLIDATION RING
JACKET
1/2"
SPLIT RING
1"
CONSOLIDATION RING
1/2"
SPLIT RING
1"
CONSOLIDATION RING
1/2"
SPLIT RING
1/2"
BASE
℄

Figure 10-28. Cross-section of Split Ring Compaction Mold

Summary of Dry Densities (pcf)

E_c ($\frac{ft\text{-}lb}{ft^3}$)	BH-10(E115)	BH-16(E134)	BH-18 (E146)
2,480	63.6	63.2	72.2
12,400	75.5	73.5	83.3
56,300	83.4	82.1	94.4

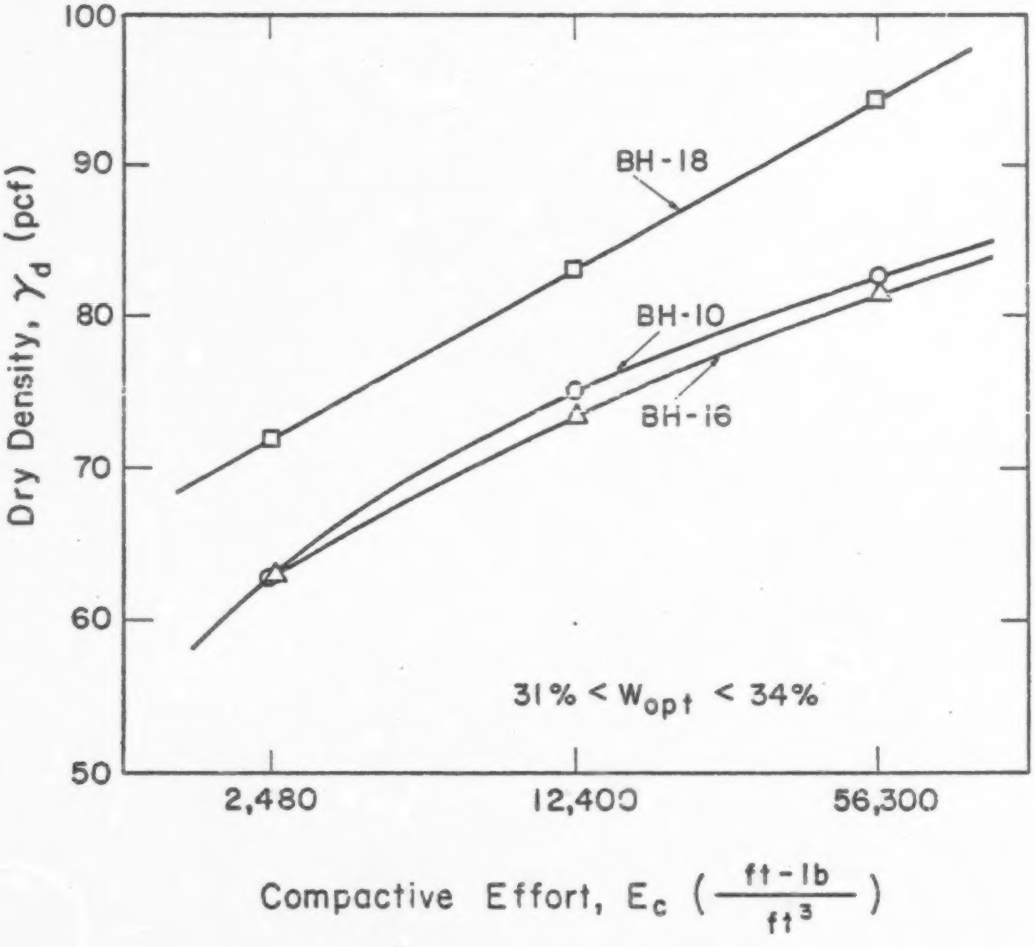

Figure 10-29. Maximum Dry Density versus Compactive Effort for Three Different Dredgings

Dry Densities of BH-16 (E134) Material (pcf)			
$E_c\left(\frac{ft\text{-}lb}{ft^3}\right)$	2,480	12,400	56,300
Top Ring	61.5	63.4	77.5
Middle Ring	63.2	73.5	82.1
Bottom Ring	64.0	70.0	86.1

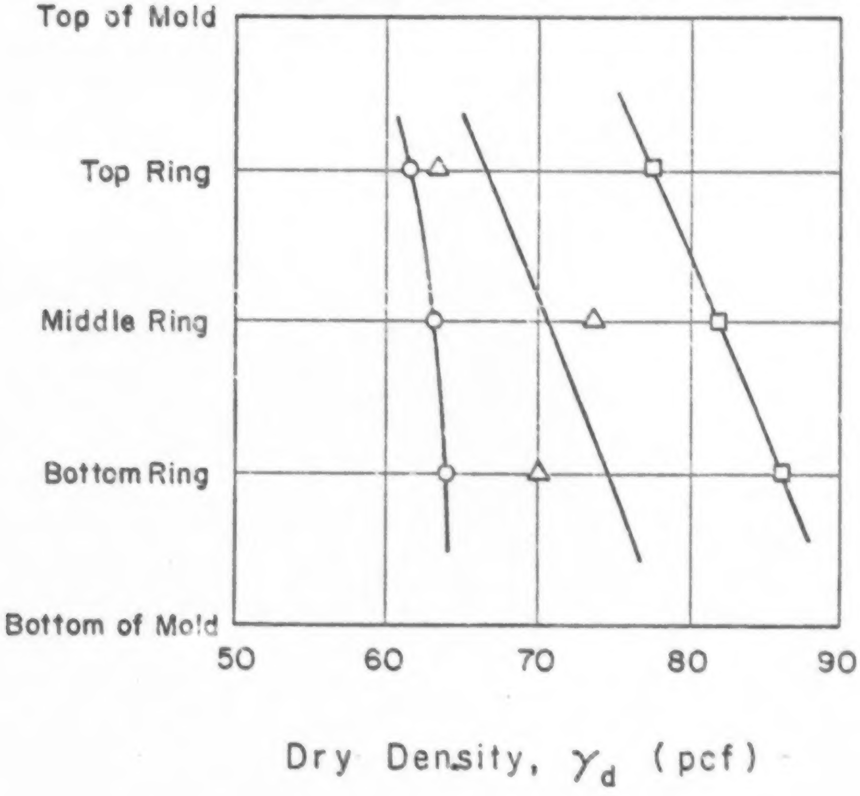

Figure 10-30. Dry Density at Different Locations within the Mold

COMPRESSIBILITY

After the dredgings were compacted into the specially designed, sectioned mold, the outer casing of the mold was removed, the ends of the material in each of the three rings were trimmed, and the trimmed specimens and their constraining rings were placed in a consolidometer to investigate their compressibility under uniaxial strain conditions. The results of these tests, together with similar data for bedding sand, Vicksburg clay, and Grundite (for comparative purposes), are given in Figure 10-31. Of these materials, sand exhibits the highest moduli for comparable relative conditions (that is, low, medium, or high density), and for a given material the denser states are associated with the higher moduli. Although the dredgings are generally more compressible than all three soils (bedding sand, Vicksburg clay, and Grundite) included for comparative purposes, this aspect should be studied more thoroughly before definitive conclusions are drawn since the materials were at different absolute densities.

PERMEABILITY

A knowledge of the permeability of the spoil is useful for evaluating its drainage and dewatering characteristics. Most of the permeability data presented herein were obtained indirectly from other testing programs, including the drainage tests, the slurry consolidation and conventional consolidation tests, and the electro-osmosis study. In addition, a few direct permeability tests were conducted in an Anteus device with the use of back-pressure to achieve a higher degree of saturation. Included herein are the data and the test procedures used to determine the permeability from the results of the various testing programs.

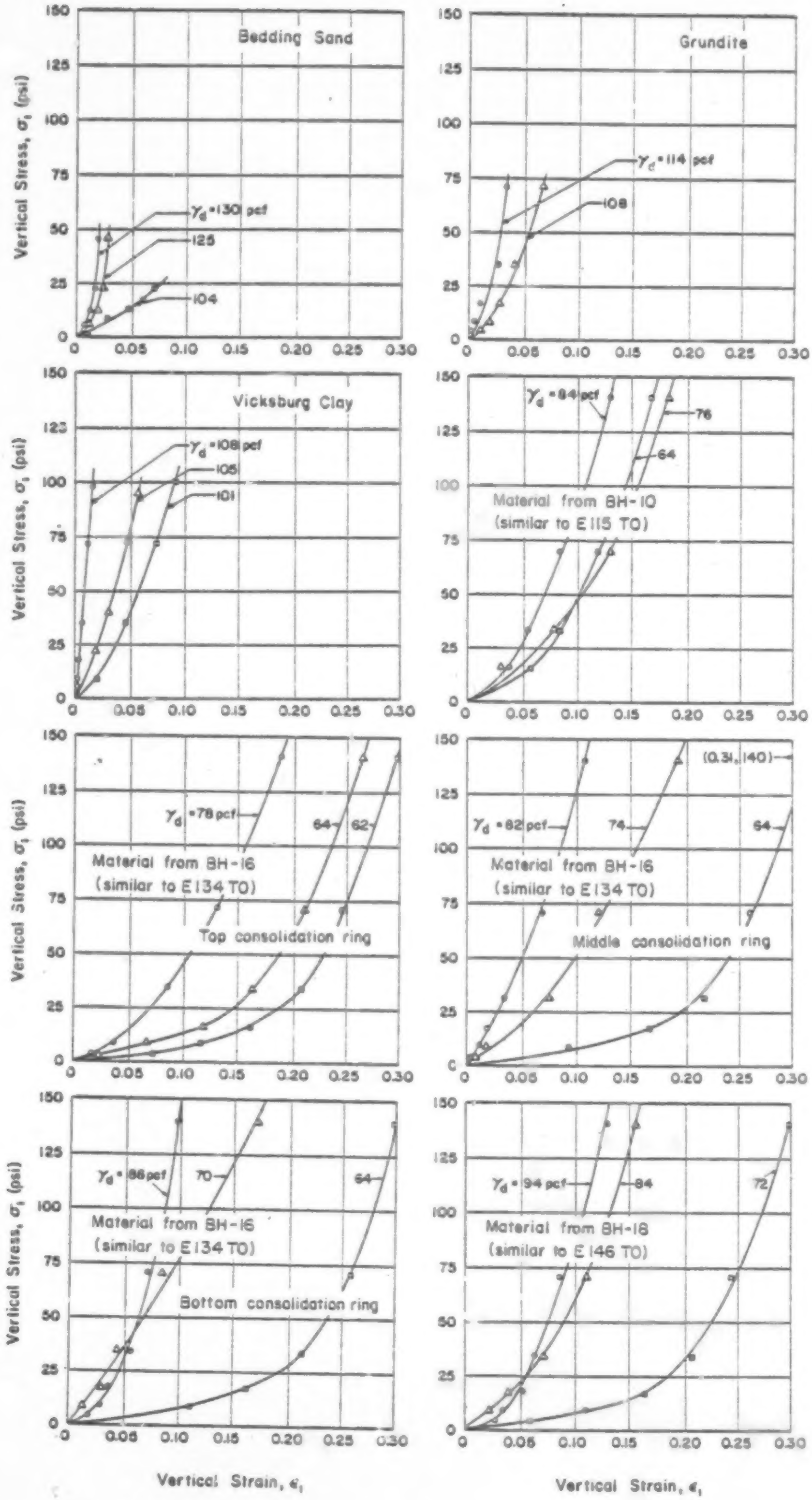

Figure 10-31. Compressibility of Various Soils and Dredgings

Electro-osmosis

The electro-osmotic coefficient of permeability, k_e, is usually defined as

$$k_e = q \Big/ \bar{v} A \tag{10-1}$$

where q is the time rate of fluid flow, A is the cross-sectional area perpendicular to the direction of flow, and $\bar{v}$ is the average voltage gradient across the sample. Very frequently, the electro-osmotic coefficient of permeability is expressed in centimeters per second per volt per centimeter, or centimeters squared per volt-second. The calculations and results shown in Tables 10-3 and 10-4 are based on the data presented in Chapter 7. The k_e values given in Table 10-3 were found by using the average quantity of flow due to the electro-osmotic action over a particular period of time (either 10, 20, or 40 hours), whereas those shown in Table 10-4 were determined by using the instantaneous value of the flow rate at a particular time (either at t = 0, or actually an instant after the flow rate attained its peak value, or at t = 6 hours). The instantaneous value of k_e at t = 6 hours is about twice that obtained when the data are averaged over the first 10 hours. The initial instantaneous value of k_e for sample D4C0 is about three times the value at t = 6 hours and about six times the value found for the average of the first ten hours.

Direct Permeability

The Anteus consolidation device was used to conduct direct permeability tests on six dredgings (Lowe, Jonas, and Obrician, 1969). The "undisturbed" samples were trimmed to fit the consolidometer ring, placed in the device, and subjected to 80 pounds per square inch back-pressure to achieve a

Table 10-3

Average Electro-osmotic Coefficient of Permeability

Sample	Time, t (hours)	Flow Rate, q (cc/sec)	Average Gradient, $\bar{v}$ (volts/cm)	Electro-osmotic Coefficient of Permeability, k_e (cm^2/volt-sec)
C22TO	20	0.00264	1.16	1.49×10^{-5}
	40	0.00246	1.23	1.31×10^{-5}
C27MM	20	0.00493	1.19	2.70×10^{-5}
	40	0.00396	1.28	2.02×10^{-5}
D1DM	10	0.00805	1.16	4.54×10^{-5}
	20	0.00611	1.21	3.30×10^{-5}
D4CO	10	0.00695	1.23	3.69×10^{-5}
	20	0.00556	1.31	2.78×10^{-5}

Table 10-4

Instantaneous Electro-osmotic Coefficient of Permeability

Sample	Time, t (hours)	Flow Rate, q (cc/sec)	Gradient at Time t (volts/cm)	Electro-osmotic Coefficient of Permeability, k_e (cm^2/volt-sec)
D1DM	6	0.0139	1.25	7.25×10^{-5}
D4CO	0	0.0333	1.00	21.8×10^{-5}
D4CO	6	0.0158	1.41	7.33×10^{-5}

higher degree of saturation. After being consolidated under a 10 psi stress for at least 12 hours, the samples were unloaded and tested to determine their permeability while still under the back-pressure. The test utilized falling head conditions, wherein the driving head fell as the head on the collecting burette rose. The initial head difference was chosen at about 1.5 feet, and the seepage length was about one inch. Accordingly, Table 10-5 gives the permeability values calculated by use of the following expression:

$$k = 0.5 \left[\ln \frac{H_1}{H_2}\right]\left[\frac{A_B}{A_S}\right] \frac{L}{\Delta t} \qquad (10\text{-}2)$$

where H_1 is the initial height of water at t_1, H_2 is the final height of water at t_2, Δt equals $(t_2 - t_1)$, A_B is the area of the burette, L is the length, and A_S is the area of the sample.

Table 10-5

Coefficient of Permeability from Direct Tests

Sample	Coefficient of Permeability (cm/sec)
E78TO	9.1×10^{-8}
E80TO	1.2×10^{-8}
E64TO	1.3×10^{-8}
E70TO	2.0×10^{-8}
E59TO	6.1×10^{-7}
E62TO	2.5×10^{-8}

Drainage Tests

The results of the drainage tests reported in Chapter 6 for samples D1DM, D3TO, and D4CO were used to compute the permeability as follows. The average flow rate, q, was determined from the total amount of water drained in the first 9 days; then, with a knowledge of the sample height and the height of water, the gradient, i, was calculated, and the permeability was computed by use of the expression

$$q = k\,i\,A \quad , \tag{10-3}$$

where A is the cross-sectional area of the test specimen. In the case of the vacuum tests, the vacuum was converted to an equivalent head, and the same procedure outlined above was used. The results of these calculations are shown in Table 10-6.

Table 10-6

Coefficient of Permeability
from Short-Term Drainage Tests

Sample	Coefficient of Permeability (cm/sec)	
	Gravity Only	With Vacuum
D1DM	3.4×10^{-6}	4.1×10^{-7}
D3TO	2.6×10^{-6}	3.5×10^{-7}
D4CO	5.1×10^{-6}	4.9×10^{-7}

Although extracting greater quantities of water in a given time, the vacuum tests employed a greater applied head and thus generated a greater flow resistance; the head for the vacuum test was about 20 times that for the gravity test, and the flow resistance was increased by a factor of about 10, as reflected in the lower values of k for the vacuum tests.

Permeability determinations were also made for samples C2DM, C3TO, C5CO, and C22TO, which were subjected to gravity drainage. Since these tests extended for longer periods of time, it was possible to approximate the permeability at points throughout the drainage process. The flow quantity, q, was averaged over some short period of time, and this value, together with the head and length of flow path associated with that time, were used with Equation (10-3) to compute the coefficient of permeability. The results of these computations are plotted in Figure 10-32, where it is seen that the permeability decreases rapidly with decreasing void ratio. The steeper curves are found for the samples with the lower initial concentrations of solids, thereby indicating a rapid drop in permeability with decreasing void ratio. The range of permeabilities extended from about 10^{-6} to 10^{-4} cm/sec, with the higher values being obtained at the beginning of the test and the lower values at the end. The thicker material (sample C2DM) had the smallest change in void ratio during the test, but it still ended with the lowest void ratio of any sample in the test series.

Conventional Consolidation

The coefficient of permeability may be computed from conventional consolidation test data by use of the following relationship:

$$k = (a_v \gamma_w c_v)/(1 + e) \quad , \tag{10-4}$$

where c_v is determined as discussed previously, γ_w is the unit weight of water, e is the void ratio, and $a_v = \Delta e/\Delta p$. In most cases, the permeability was determined when the stress on the specimen was 0.634 kilograms per square centimeter, and a_v was taken as the change in void ratio, Δe, for the load increment from 0.634 to 1.268 kilograms per square centimeter, in which case the stress increment, Δp, would be 0.634 kilograms

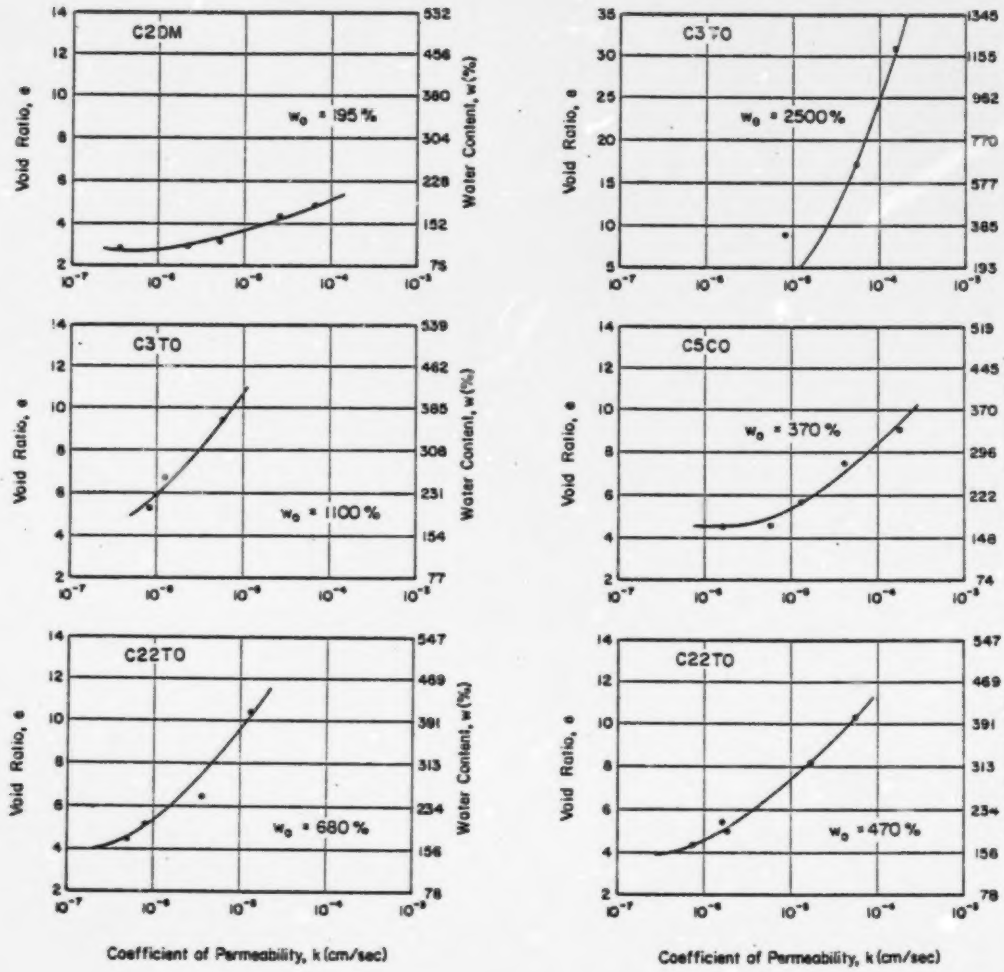

Figure 10-32. Permeability as a Function of Void Ratio or Water Content

per square centimeter. The results of these computations are given in Figures 10-1 through 10-12, and 10-15, 10-16, and 10-17, where the coefficient permeability is plotted as a function of depth for the different bore hole locations. Equation (10-4) was also used to compute the coefficient of permeability for the four materials tested in the electro-osmosis study under an applied stress of 0.6 kilograms per square centimeter and with no electrical gradient, and these results are given in Table 10-7.

Table 10-7

Coefficient of Permeability from
Single-Load Consolidation Tests

Sample	Coefficient of Permeability (cm/sec)
C22TO	3.2×10^{-7}
C27MM	5.5×10^{-7}
D1DM	2.9×10^{-7}
D4CO	9.0×10^{-7}

CHAPTER 11

INTERPRETATION AND SYNTHESIS

The purpose of this chapter is to provide an interpretation and synthesis of the detailed information presented in the preceding chapters, and an attempt is made to evolve an overall view of the entire research effort with some projected ideas of processes and programs worthy of further consideration. Following a brief review of some specific background information in order to place the test data in perspective, the results of this experimental program are discussed in conjunction with other related material to develop the concepts which are advanced. Consideration is first given to the basic engineering characteristics of the dredgings, such as particle size, gradation, mineralogy, organic content, water content, chemical constituents, density, specific gravity of solids, and Atterberg limits, and this is followed by an evaluation of the engineering properties of shear strength, compressibility, consolidation, compaction, and permeability. Finally, the overall usefulness of dredgings to construct landfills is assessed from a technical point of view, and some specific suggestions are advanced to improve the quality of both new and existing spoil disposal areas.

FRAMEWORK OF TEST PROGRAM

Although the general background for this entire study is presented in Chapter 2, some specific information is included in this section to aid in interpreting the results of the test programs conducted. Following a survey of the more active dredging sites in the Great Lakes region, it was decided to conduct the major investigative effort at

Toledo, Ohio. The polluted nature of the dredgings in this area has been recognized for some time, and diked disposal areas have been used for many years. The particular disposal areas studied most intensively in this work were Riverside Site and the Island Site (see Figure 3-13).

The Island Site was constructed in 1961 and 1962 by the placement of a 7 foot dike by hydraulic dredge. In 1966 the dike was raised to 15 feet, and in 1970 to 20 feet. The enclosed area of approximately 150 acres is nearly rectangular in plan with dimensions of about 3800 feet by 1800 feet. Riverside Site consists of approximately 34 acres and is also nearly rectangular in plan with dimensions of about 2200 feet by 700 feet. During 1968, 1969, 1970, and 1972 Riverside Site received approximately 1.19, 0.36, 0.32, and 0.27 millions of cubic yards of dredgings, respectively.

The first major sampling trip associated with this study was taken in December of 1970 to Detroit, Toledo, and Cleveland; samples included bottom sediments from the harbors, materials from the discharge pipes, and water from within and near the disposal areas. The other three major field testing and sampling efforts were conducted in Toledo in June and July of 1971 and in June of 1972; the trip in June of 1971 was concerned primarily with the Island Site, whereas the latter two were centered at Riverside Site. In June of 1971 the sampling and field testing effort at the Island Site included the successful use of the large field vane and the Osterberg piston sampler, and the usefulness and success of the 5-inch piston sampler was demonstrated at Riverside Site; this latter success led to the subsequent construction of the 3-inch piston sampler, which was even more successful. Most of the ensuing field work, including that in June of 1972, involved the use of the large field vane and the 3-inch piston sampler.

CLASSIFICATION

Analyzed in this section are some basic test results which enable maintenance dredgings to be classified in accordance with normal procedures used in soil mechanics; these data include the density, water content, particle size, gradation, specific gravity, void ratio, mineralogy, organic content, and plasticity of a representative variety of dredgings. Although some of these tests are relatively simple, others require considerable care and special equipment. Not only do these results allow classification of the dredgings, but they also provide an indication of their probable engineering behavior. For example, a knowledge of the in situ density, together with some idea of the minimum and maximum densities, can help considerably in predicting strength and compressibility characteristics. For fine-grained materials, such as maintenance dredgings, it is also important to study the plasticity relationships, which are revealed by the Atterberg limits and related indexes. In addition, the water content and pore fluid pressure can exert a significant influence on the strength reponse.

Particle Size and Gradation

As may be readily appreciated, the particle size and gradation of a given dredgings sample depend to a large extent on the history of the sample. As one typical example of such a history, the dredging cycle begins with the bottom sediments in a very loose, saturated condition; then, these sediments may be removed by the use of a hopper dredge, loaded onto a vessel, transported to the disposal site, and pumped into the area through a discharge pipe together with large quantities of water. Although this process tends to mix the solids in the water, the larger particles are rolled along the bottom of the pipe while the finer particles are carried in suspension. At the end of the discharge pipe the mixture is ejected into a large basin where a free field flow-sedimentation regime begins to function. The large heavy particles, including rocks, gravel, and lumps of clay, settle immediately in the vicinity of the discharge pipe; sand-size particles are carried further from the end of the pipe and settle rapidly as the velocity of the water decreases; finally, the silts and clays and other fines are transported still further toward the overflow weir, some even being carried over the weir if sufficient retention time is not allowed for the very fine particles to settle.

In addition, particle sizes and their distributions will depend on the nature of the materials being dredged. Although quite coarse materials may be dredged on occasion, the bulk of polluted maintenance dredgings are fine-grained materials (typically in the very fine sand, silt, and clay size ranges); this is because the harbors are usually located along streams and rivers that reach the lakes where the gradients and associated flow velocities are very small. Based on the typical gradation curves shown in Figure 7-1, and the data given in Figures 10-1 through 10-9, the dredgings studied were found to be relatively well graded, fine-grained soils. Such soils are usually characterized by slow drainage, low permeability, high compressibility, and low density.

Mineralogy and Chemistry

Experimental data have indicated that each harbor has its own unique materials and that large variations in mineralogy and chemical composition may occur within a given harbor; the latter characteristics are governed in large part by the urban and industrial wastes that are discharged into the harbor and the erosion potential of the surrounding watershed. For example, along the Calumet River and associated facilities in the Chicago area, a high percentage of the bottom materials consist of "flu-dust", which is a fine-grained material composed largely of iron oxides emitted by the adjacent steel industry. Most harbor sediments contain various petroleum products and other hydrocarbons that interact in various ways with the mineral particles to influence both the engineering properties of the material and the test procedures used to determine these properties. Since the chemical composition of a given dredgings sample is highly dependent on the localized environment from which it was taken, no general conclusions regarding the chemical nature of maintenance dredgings can be advanced. However, based on the mineralogical analyses given in Tables 10-1 and 10-2, as well as those reported by the Corps of Engineers (1969) and Hartzell (1968), most dredgings apparently contain substantial portions of the common clay minerals, such as illite and kaolinite. For example, the fine-grained materials from Marcus Hook Shoal (Hartzell, 1968) contain large amounts of illite, kaolinite, and chlorite, as well as the non-clay minerals quartz and feldspar; in addition, a large fraction of the organic material consists of fine particles of coal. The same types of clay minerals were found in the Toledo and Milwaukee sediments.

Water Content and Density

The water content and density of dredgings are very important material parameters because (a) they are directly related to such engineering properties as strength and compressibility, and (b) they determine the amount of dredgings which can be placed into a given disposal area. Although the water content of a specimen is quite easy to determine by use of standard procedures (Lambe, 1951), the determination of the in situ density is usually more difficult for dredged spoil. When sampling tubes are pressed into these materials there is a tendency for them to compress and decrease in volume due to the side-wall friction between the tube and the spoil. In this sampling program, however, the recovery obtained by use of the piston sampler was generally excellent for the softer materials, and the measured densities should be quite accurate. Some problems were encountered in trying to measure the density of the desiccated materials within the top few feet of the surface; good recovery was not obtained, and attempts to find in situ densities by use of the sand cone procedure were generally unsuccessful due to the presence of shrinkage cracks and root networks.

Since the dredgings in most recently filled disposal sites are essentially saturated except for small amounts of entrapped air or generated gas, their dry density, γ_{dry}, may be approximated from a knowledge of the specific gravity, G, of the solid particles in the dredging sample, the water content, w, of the sample, and the density of water, γ_{water}, by use of the following relationship:

$$\gamma_{dry} = \frac{G\gamma_{water}}{1 + Gw} \qquad (11\text{-}1)$$

In general, the specific gravity of the solid particles in a dredging sample varies within rather small limits and may often be approximated with reasonable accuracy; G usually lies between 2.64 and 2.72 for most soil minerals, and the values reported in Chapter 10 generally fall between 2.6 and 2.8 with an average value of about 2.7. Hence, subject to the assumption that G = 2.7, Equation (11-1) can be written as

$$\gamma_{dry} \text{ (in pcf)} = \frac{168.5}{1 + 2.7\,w} \qquad (11\text{-}2)$$

and used to conveniently approximate the in situ dry density from a knowledge of only the water content of the sample. In this regard it is interesting to note (a) the rather large variations in specific gravity (see Table 11-1) reported by the Corps of Engineers (1969) and (b) the fact that most of the values are substantially lower than those determined in this study. However, since minor variations in the testing technique can either invalidate the test or cause the result to differ significantly

Table 11-1

Engineering Properties of Typical Dredgings
(after Corps of Engineers, Philadelphia District, 1969)

SUMMARY OF DETAILED LABORATORY TESTS

Boring	Sample	Depth	Classification	Atterberg Limits			Mechanical Analysis			d	W_o	S_o	Shear Test			Consolidation Test		
				LL	PL	PI	Gr	Sand	Fines	(pcf)	(%)	(%)	Type	φ	C(tsf)	e_o	G_s	C_c
I. EDGEMOOR DISPOSAL AREA:																		
EDB-1	UD-2	13-15	Org CLAY - CL	121	42	79	0	3	97	44	109.6	98				2.854	2.56	1.13
2	UD-2	16-18	Org CLAY - OH	119	49	70	0	0	100	48	86.5	92	Q	0	0.28			
										45	88.8	90	R	12.6	0.15			
													$\bar{R}$	31.0	0			
2	UD-3	22-24	Org CLAY - OH	106	46	58	0	0	100	46	93.6	99						
3	UD-2	12-14	Org CLAY - OH	120	43	77	0	0	100	42	101.0	92						
4	UD-1	8-10	Org CLAY - OH	109	43	66	0	0	100	43	103.9	98						
5	UD-1	2- 4	Org CLAY - OH	134	51	83	0	0	100	33	147.4	99						
										38	110.8	89	Q	0	0.15			
										40	100.5	89	R	14.7	0.05			
													$\bar{R}$	30.8	0			
5	UD-3	16-18	Org CLAY - OH	122	45	77	0	0	100	43	108.5	99				2.643	2.49	0.90
5	UD-4	22-24	Org CLAY - OH	121	49	72	0	0	100	45	93.2	93	Q	0	0.25			
										43	99.7	94	R	13.8	0.20			
													$\bar{R}$	35.9	0			
5	UD-6	34-36	Org CLAY - OH	126	46	80	0	0	100	44	101.4	100				2.482	2.46	1.02
6	UD-1	4- 6	Org CLAY - OH	110	41	69	0	0	100	43	98.6	95	Q	0	0.12			
										44	93.8	93	R	14.5	0.05			
													$\bar{R}$	33.8	0			
6	UD-3	21-23	Org CLAY - OH	87	38	49	0	0	100	57	62.2	91	Q	2.5	0.25			
										52	73.9	91	R	14.5	0.13			
													$\bar{R}$	29.8.	0			
6	UD-4	29-31	Org SILT - OH	164	76	96	0	0	100	34	132.7	96				3.161	2.26	1.43
7	UD-2	17-19	Org CLAY - OH	130	45	85	0	0	100	40	111.5	96				2.918	2.50	1.00
7	UD-4	27-29	Org CLAY - OH	56	36	20	0	0	100	57	63.6	96				1.566	2.36	0.51
8	UD-2	10-12	Org CLAY - OH	107	45	62	0	0	100	46	88.1	90				2.489	2.35	0.87
8	UD-3	16-18	Org SILT - OH	51	32	19	0	3	97	72	44.2	89	Q	0	0.25			
										70	46.7	92	R	13.2	0.25			
													$\bar{R}$	37.2	0			
9	UD-2	12-14	Org SILT - OH	89	49	40	0	4	96	48	84.0	91	Q	0	0.30			
										51	77.0	93	R	15.4	0.15			
													$\bar{R}$	38.7	0			
										59	65.9	100				1.681	2.34	0.48
9	UD-3	18-20	Org CLAY - OH	96	38	58	0	0	100	58	65.8	97				1.737	2.35	0.50
II. OLDMANS NO. 1 DISPOSAL AREA:																		
OAB-1	UD-1	6- 8	Org CLAY - OH	136	49	85	0	0	100	41	108.6	98				2.771	2.49	1.28
										41	108.2	95	Q	0	0.15			
										41	98.5	91	R	12.6	0.10			
													$\bar{R}$	29.7	0			
2	UD-1	12-14	Org CLAY - OH	92	43	49	0	0	100	48	93.0	100				2.218	2.47	0.95
2	UD-2	18-20	Org CLAY - OH	193	90	103	0	0	100	31	154.8	98				3.532	2.23	1.80
3	UD-1	8-10	Org CLAY - OH	149	52	97	0	0	100	40	114.7	98				2.877	2.46	0.90
4	UD-1	4- 6	Org CLAY - OH	127	51	76	0	6	94	41	103.3	91	Q	0	0.15			
										45	88.9	90	R	16.2	0.10			
													$\bar{R}$	31.4	0			
5	UD-1	13-15	Org CLAY - OH	63	30	33	0	0	100	71	44.2	88	Q	0	0.33			
										71	42.2	87	R	15.9	0.10			
													$\bar{R}$	32.3	0			
6	UD-2	12-14	Org CLAY - OH	115	42	73	0	2	98	37	127.2	99				3.254	2.54	1.16
III. DARBY CREEK DISPOSAL AREA:																		
DCB-9	UD-1	14-16	Org SILT - OH	83	37	46	0	2	98	62	53.5	88	Q	1.7	0.45			
9	UD-3	22-24	Sandy CLAY - CL	26	20	6	0	45	55	102	23.8	100				0.626	2.65	0.12
										100	26.3	97	Q	0	0.60			
10	UD-1	10-11.5	Org CLAY - OH	114	45	69	0	5	95	45	92.5	91	Q	0	0.39			
10	UD-2	16-18	Org SILT - OH	184	91	93	0	0	100	36	139.3	99				3.230	2.29	1.36
11	UD-1	4- 6	Org CLAY - OH	135	54	81	0	4	96	42	91.8	85	Q	1.6	0.42			
										41	95.0	85	R	14.8	0.20			
													$\bar{R}$	35.8	0			
11	UD-2	12-14	Org CLAY - OH	98	38	60	0	0	100	50	83.3	97				2.202	2.36	0.61
12	UD-2	8-10	Org CLAY - OH	120	43	77	0	0	100	42	103.2	92	R	14.3	0.07			
													$\bar{R}$	38.5	0			
13	UD-1	7- 8	Org CLAY - OH	79	34	45	0	0	100	65	55.5	100				1.400	2.51	0.39
13	UD-2	12-14	Org CLAY - OH	79	31	47	0	0	100	52	77.5	99	R	10.8	0.35			
													$\bar{R}$	34.0	0			
IV. PIGEON POINT DISPOSAL AREA:																		
PPB-57	UD-1	12-14	Org CLAY - OH	103	37	66	0	12	88	51	80.6	96	Q	0	0.35			
57	UD-3	30-32	Org CLAY - OH	101	38	63	0	0	100	53	75.1	93	Q	3.7	0.18			
57	UD-4	38-40	Org CLAY - OH	91	34	57	0	0	100	62	60.3	100				1.522	2.52	0.52
										56	65.2	100	Q	0	0.28			
58	UD-1	12-14	Org CLAY - OH	93	38	55	0	5	95	56	72.8	100				1.860	2.55	0.75
59	UD-1	6- 8	Org CLAY - OH	63	28	35	0	15	85	45	56.0	97	R	13.7	0.15			
													$\bar{R}$	38.3	0			
60	UD-1	6- 8	Org SILT - OH	99	46	53	0	0	100	50	79.0	94				2.195	2.57	0.96
60	UD-2	18-20	Org Sandy	52	27	25	0	16	84	75	41.3	90	Q	0	0.35			
			CLAY - OH							79	38.2	92	R	13.6	0.23			
													$\bar{R}$	35.0	0			
60	UD-3	26-28	Org CLAY - OH	118	46	72	0	0	100	46	96.0	99				2.439	2.52	0.98
61	UD-1	4- 3	Org SILT - OH	91	49	42	0	0	100	54	56.6	79	Q	3.3	1.15			
61	UD-2	8-10	Org CLAY - OH	100	39	61	0	10	90	55	62.3	88	Q	5.8	0.55			
61	UD-3	12-14	Org SILT - OL	40	32	8	0	7	93	73	44.0	96	R	15.1	0.25			
													$\bar{R}$	35.4	0			
61	UD-4	21-22	Org CLAY - OH	70	29	41	0	0	100	61	63.6	99				1.631	2.55	0.50
61	UD-6	34-36	Org CLAY - OH	101	39	62	0	0	100	55	72.4	99				1.858	2.34	0.77
62	UD-3	19-20	Org CLAY - OH	116	42	74	0	0	100	50	85.7	99				2.185	2.53	0.77
62	UD-4	26-28	Org CLAY - OH	136	43	93	0	0	100	42	105.4	97	Q	0	0.18			
62	UD-5	34-36	Org CLAY - OH	85	36	49	0	0	100	67	53.8	100				1.378	2.57	0.43

NOTE: For the shear tests the values shown for d, W_o and S_o are the average of the set of specimens used.

Reproduced from
best available copy.

from the correct value, it may be possible that the actual range in values for the specific gravity does not vary as greatly as reported. The in situ dry densities determined in this test program generally range from about 50 to 60 pcf, whereas the dry densities of compacted dredgings may be as high as 80 to 100 pcf (with a more likely range being from 80 to 90 pcf). Average dry densities and water contents reported by the Corps of Engineers (1969) for four disposal sites varied from 49 to 58 pcf and from 70 to 93 percent, and these values correspond quite closely to those determined for this project.

Plasticity and Organic Content

The liquid limit (LL), plastic limit (PL), and plasticity index (PI) are important aids in the classification of fine-grained soils, and they serve as indicators of probable soil behavior. Hence, an extensive series of standard limit tests (Lambe, 1951) was performed on a variety of dredgings. Based on the organic contents reported in Chapter 5, these dredgings may be classified as organic soils, and it is therefore appropriate to present some related background information to aid in evaluating the significance of the test results.

When A. Casagrande (1948) developed the Unified Soil Classification System and the associated plasticity chart, he indicated that organic soils plot below the A-line. This was corroborated by L. Casagrande (1966), Skempton and Petley (1970), and others. However, Seed, Woodward, and Lundgren (1965) found that organic soils may plot slightly above the A-line in the liquid limit range from 50 to 100 percent. Recent tests by Schmidt (1965) on a soil with three different organic contents indicate that, although the organic matter contributes greatly to the water holding capacity of the soil, it produces a proportionately small increase in plasticity. In addition, L. Casagrande (1966) found that soils with fibrous organic matter plot below the A-line on the plasticity chart. It is possible that such divergent behavior is due to the fact that the limit tests are not suitable for soils with a low degree of humification (that is, with fibrous texture). Skempton and Petley (1970) state that the plastic limit can not be measured satisfactorily and the liquid limit test becomes questionable for peats with a low degree of humification.

Odell, Thornburn, and McKenzie (1960) tested twenty-three Illinois soils and found the following correlations:

$$LL = 11.14 + 4.937C_1 + 0.669C_2 + 0.112M \qquad (11\text{-}3a)$$

$$PL = 14.78 + 3.76C_1 + 0.101C_2 + 0.036M \qquad (11\text{-}3b)$$

where C_1, C_2, and M are the percentages of organic carbon, clay size particles (less than 2 microns), and montmorillonite, respectively. These equations indicate that both the liquid limit and the plastic limit may be considered as linear functions of the organic carbon content. However, Schmidt (1965), working with Paulding soils from Ohio, found that the liquid limit does not vary linearly with organic carbon content; nevertheless, Equation (11-3a) predicted the liquid limit of the Paulding soils within an accuracy of ± 15 percent. On the other hand, he found that the plastic limit is nearly a linear function of organic carbon content; for one set of test results Equation (11-3b) underpredicted the plastic limit by about 20 percent, but the agreement was remarkable for another set of test results. Schmidt also found that the plasticity index is independent of the organic carbon.

Skempton and Petley(1970), working with organic soils from England, found that the liquid limit could be correlated with the loss on ignition by the relationship:

$$LL = 50 + 5N \qquad (11\text{-}4)$$

where N is the loss on ignition at 550° C for 3 hours; this indicates that the liquid limit is a linear function of the loss on ignition. It is worth noting the similarity between the Skempton and Petley equation and the modified Odell, Thornburn, and McKenzie equation, as obtained by Schmidt:

$$LL = (46.59 \text{ to } 55.29) + 4.937C_1 \tag{11-5}$$

The only essential difference is that Equation (11-4) is in terms of the loss on ignition and Equation (11-5) is in terms of organic carbon content. According to Skempton and Petley (1970), organic carbon is roughly equal to 0.58 times the loss on ignition at 550° C for 3 hours.

In a special study conducted at Northwestern University, two clay soils, kaolinite and grundite (consisting of a high percentage of illite), were mixed individually with prescribed amounts of peat to form artificial organic soils, and the influence of the peat on the liquid and plastic limits and the plasticity index is shown in Table 11-2. The Atterberg limits of peat are given only for comparative purposes, since the usual test procedures for inorganic soils may not be appropriate for highly fibrous soils, and the results may not have the same significance for soils with high organic contents. For these tests the soil was first dried at 105° C; then, the organic content was taken as the ratio of the loss on ignition at 500° C for 4 hours to the weight after drying. These data are plotted on Figures 11-1 and 11-2. From Figure 11-1 we see that the liquid limit and the plastic limit increase linearly with organic content; in particular, the indicated relationship for the liquid limit as a function of organic content, $\overline{OC}$, is given by

$$LL = 50 + 9.0\,\overline{OC} \quad , \tag{11-6}$$

which is very similar to Equations 11-4 and 11-5. The rates of change for the liquid limit and the plastic limit are such that the organic

Table 11-2

Effect of Organic Content on Atterberg Limits of Two Soils

Material	Organic Content %	Liquid Limit %	Plastic Limit %	Plasticity Index %
Grundite	0.0	47	27	20
Grundite	2.9	72	32	40
Grundite	6.2	101	38	63
Grundite	9.4	133	44	89
Kaolinite	0.0	49	30	19
Kaolinite	8.5	125	50	75
Kaolinite	14.8	176	63	113
Peat	45.0	250	140	110

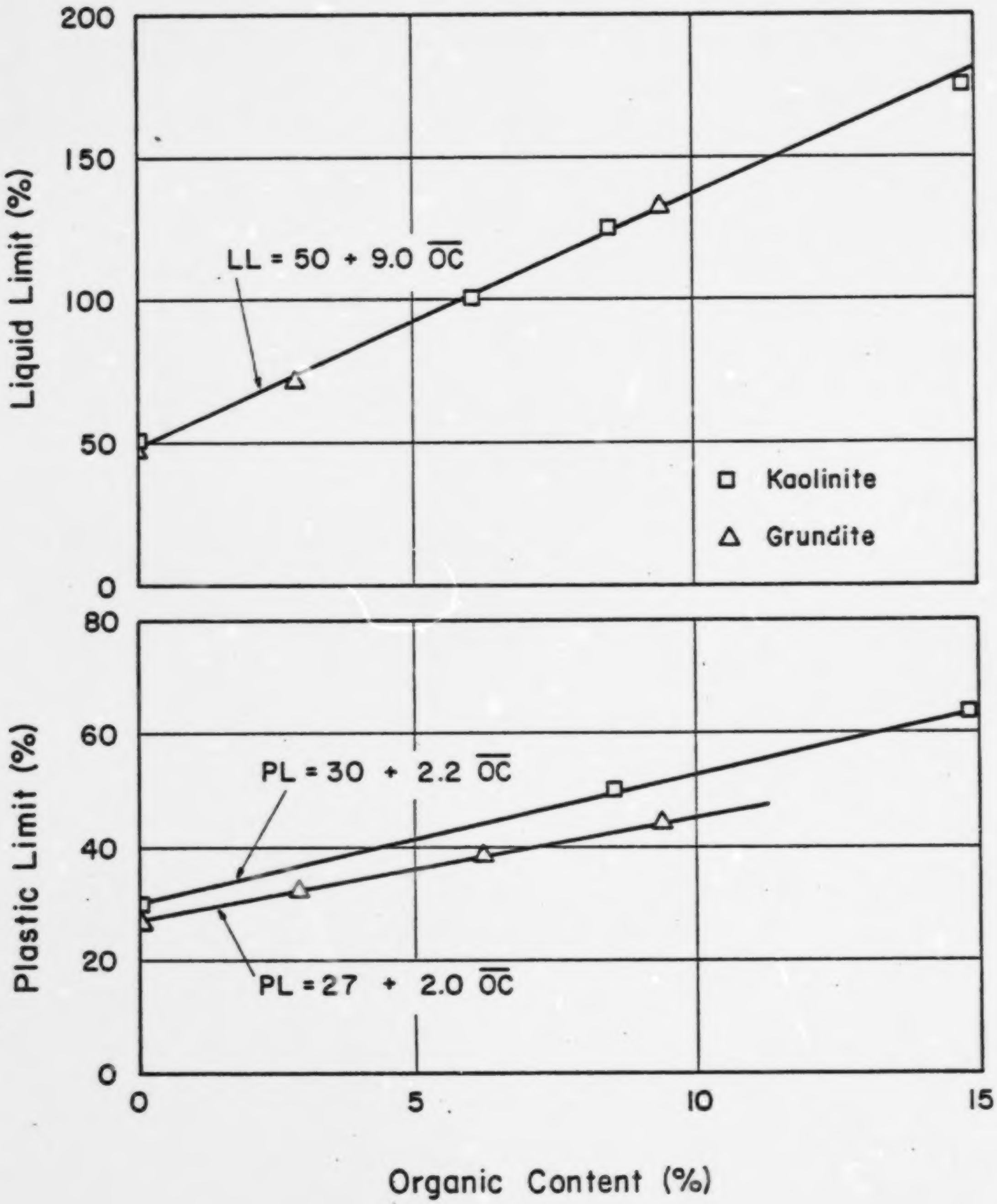

Figure 11-1. Influence of Organic Content on Atterberg Limits

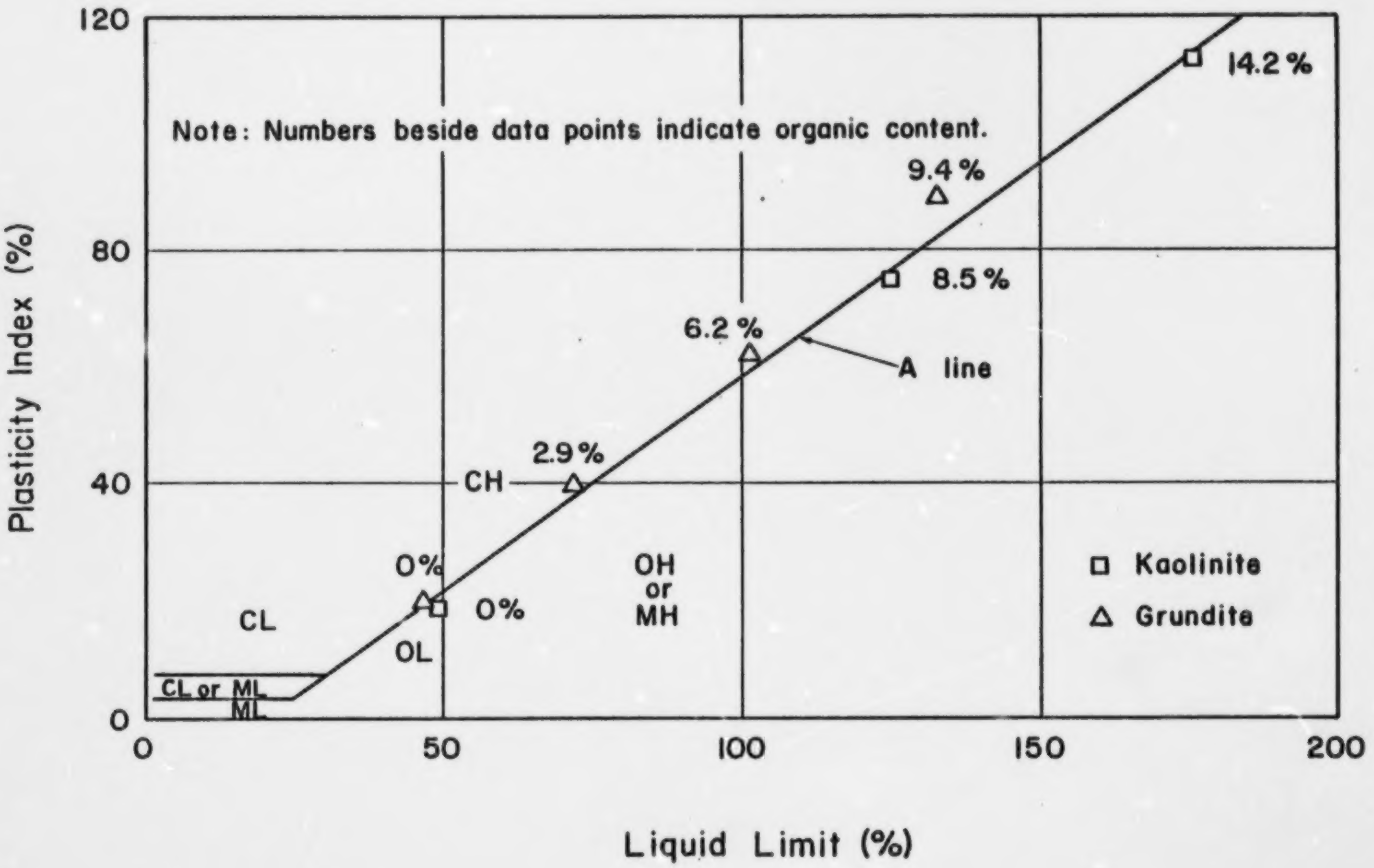

Figure 11-2. Plasticity Index versus Liquid Limit for Soils with Different Organic Contents

soil mixtures tested plot essentially along the A-line on the plasticity chart, as shown in Figure 11-2. The two different clay minerals (kaolinite and illite) exert only a minor influence of the limits of these materials, and the response is governed primarily by the organic matter.

The patterns exhibited by the preceding results are not manifested in the plasticity relationships for the dredgings. Limit test data are plotted in Figure 11-3 as a function of the organic carbon content and the ignition loss. Although the limit values generally increase with increasing values of organic carbon content or ignition loss, the indicated relationships are not well defined; this is probably due in large part to the effects of other variables, such as gradation, percentage of fines, clay mineralogy, and type of organic material. Furthermore, since the degree of decomposition of the organic matter in the dredgings is very high, the existing organic compounds have reached a chemically stable condition and do not impart to the soil the same type of behavior as organic matter with a low degree of humification. Due to the complexity of the forms of organic matter in dredgings and the complicated interaction of the various influential parameters, it will be necessary to conduct more research along the lines reported in Table 11-2 in order to isolate and study the effect of each factor and then combinations of variables. As reported in Table 11-1 by the Corps of Engineers (1969), most of the dredgings tested would probably be classified according to the Unified Classification System as OH; alternatively, a few may be classified as OL, CH, or MH.

STRENGTH

The strength of dredgings is of major interest to the soils engineer because it is directly related to the bearing capacity and stability of

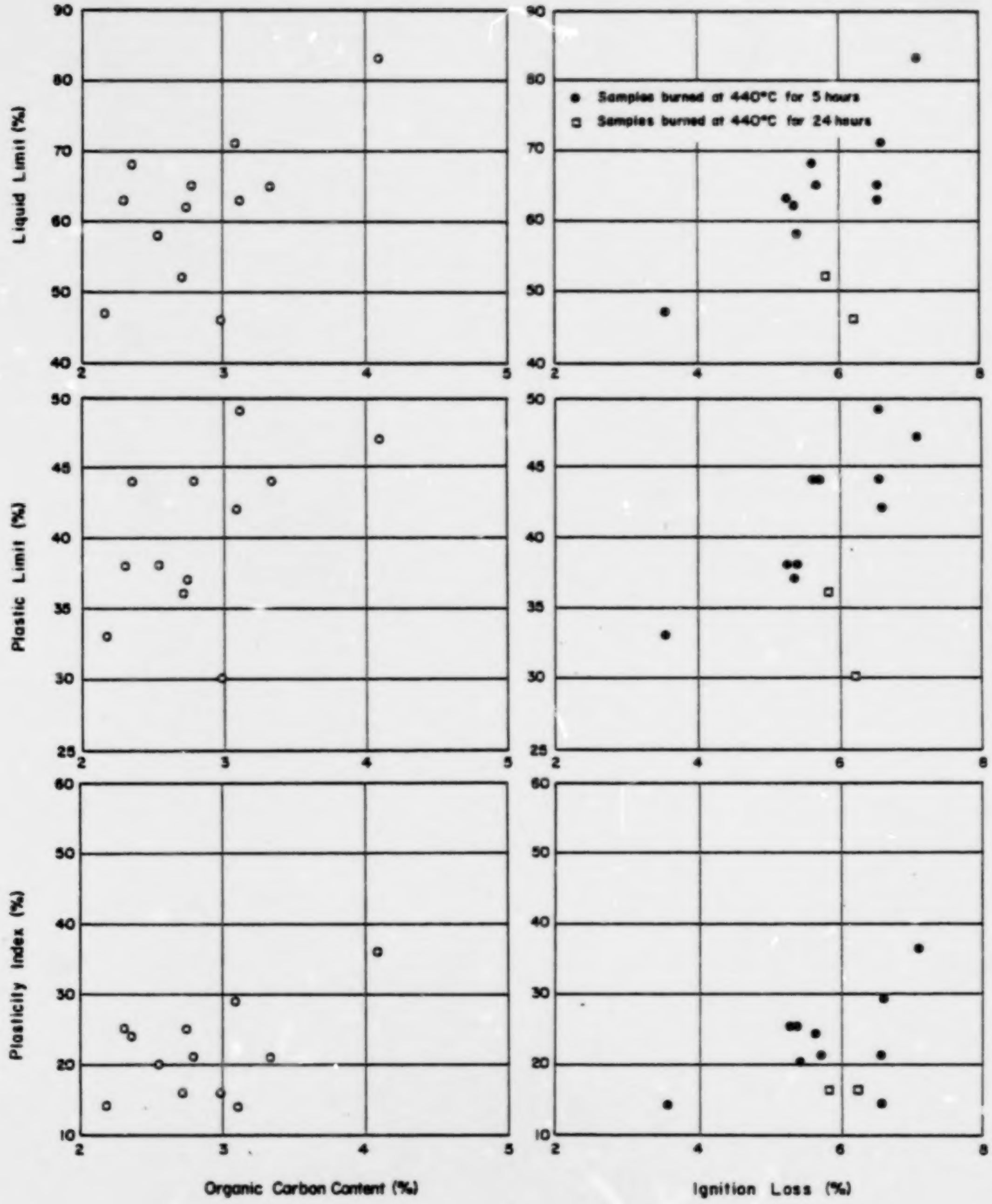

Figure 11-3. Atterberg Limits versus Organic Content for Various Dredged Materials

a landfill, and thus to its potential usefulness. There are several field and laboratory tests which may be used to determine the strength of a soil; these include vane shear, triaxial compression, and unconfined compression tests. The unconfined compression test is a special case of the triaxial compression test wherein the confining stress is equal to zero. Vane shear tests and unconfined compression tests are usually conducted under undrained conditions, but triaxial tests are commonly classified as consolidated-drained (CD or S), consolidated-undrained (CU or R), or unconsolidated-undrained (UU or Q) tests; however, all triaxial compression tests in this experimental program were of the unconsolidated-undrained (UU or Q) type. Although the strength values determined from any of these tests should ideally be identical, provided comparable drainage conditions are used during the test, substantial variations are often found in practice, and this was indeed the case in this test program. These variations may be due to a number of factors, but some of the major causes are sample disturbance, analysis or interpretation of the test, and heterogeneity and anisotropy of the soil deposit. In addition, the shear strength of a soil is influenced by a multitude of other factors, such as particle size, particle shape, gradation, density, water content, load history, mineralogy, organic content, and chemistry. The role of certain of these factors will be discussed briefly to aid in evaluating and interpreting the test results presented in Chapter 10. However, the complex interaction of the many variables that affect the shear strength of dredgings allow only certain general behavioral patterns to be established from the studies conducted, and a much more extensive test program is required to formulate detailed relationships.

In general, the shear strength of a soil increases with increasing values of density; this tendency is manifested to some degree by the test results reported herein, and a study of the variations in shear strength and density will indicate that large variations in shear strength are caused by small variations in density. It can also be seen that the shear strength generally decreases with increasing values of water content, but it is impossible to draw any specific relationships due to the complex interaction of all the influential factors. For example, the surface soils at the fill sites generally exhibited greater strengths than the materials at greater depths; this is probably due to the effects of water content and load history, since the surface soils are usually desiccated and preconsolidated to some extent. In addition, they were probably acted upon by capillary pore water tensions during the test, thereby giving apparent strengths which are higher than would be obtained if the specimens were either completely dry or submerged; therefore, a part of the indicated shear strength is due to the nature of the soil and a part is due to the conditions which exist during the test. Furthermore, Arman (1969) reported an increase in strength with an increase in the amount of fibrous organic matter in a soil; such matter was felt to act a tensile reinforcement in the soil. However, Orozco (1972) found that the unconfined compression strength generally decreased with increasing values of organic content, as shown in Figure 11-4, and the water content for maximum strength was found to be somewhat less than the water content for maximum density by compaction.

During the field trip in June of 1972 additional samples were taken and field vane tests were conducted at Riverside Site in the vicinity of bore holes 1, 4, 5, 6, 7, 8, and 9; the new bore holes are numbered 11, 14, 15, 16, 17, 18, and 19, respectively, and they are located within a few feet of the previous ones (with corresponding last digits) in order to ascertain whether any strength changes had occurred within a period of

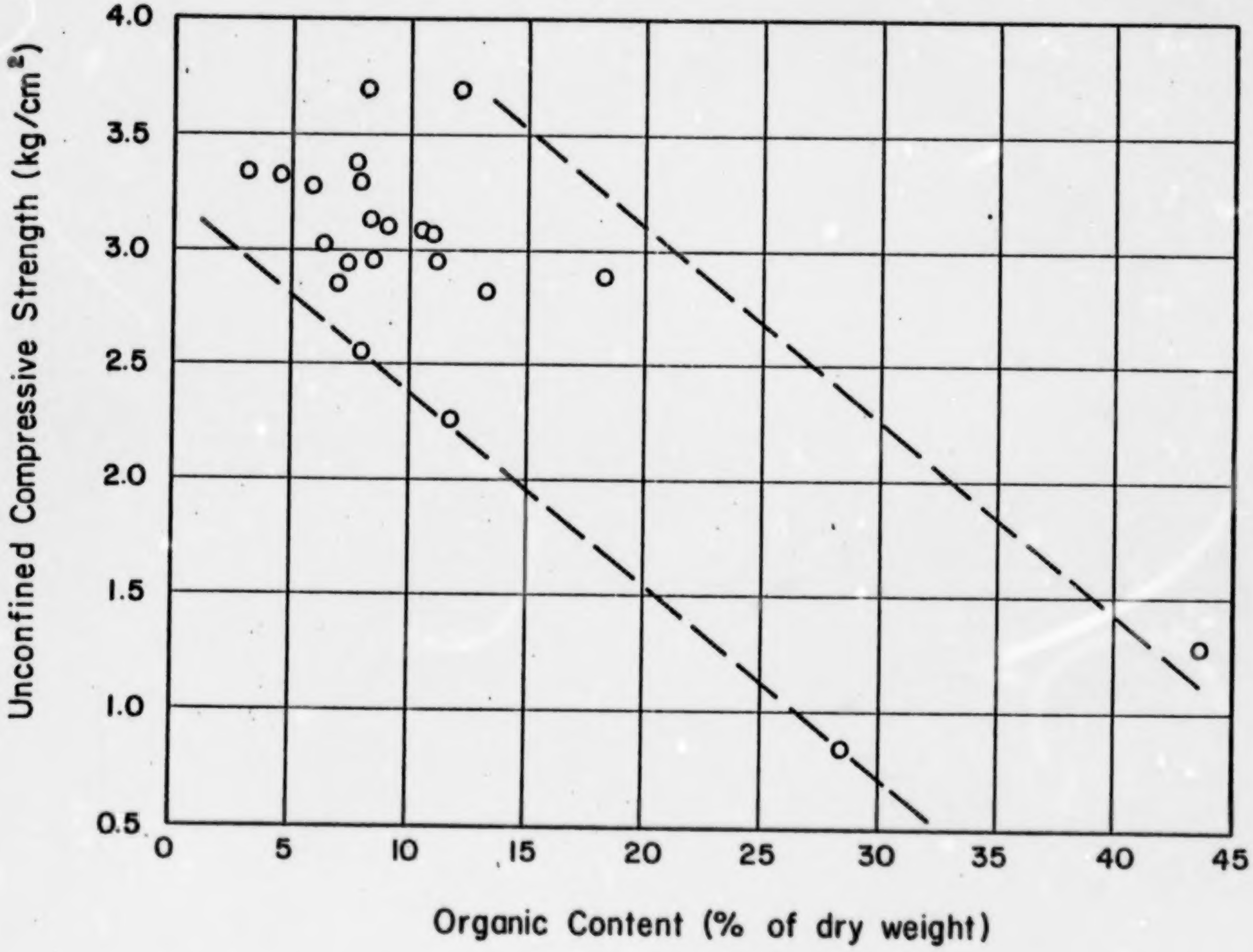

Figure 11-4. Unconfined Compressive Strength versus Organic Content (after Orozco, 1972)

one year. These strength comparisons are shown in Figure 10-19. Since this particular aspect of the research program was not anticipated in 1971, precise surface elevations at the bore hole locations were not taken at that time. Subsequent to the field work in June and July of 1971, Riverside Site received a new lift of dredgings, and the surface elevations at each respective bore hole are higher in 1972 than in 1971. Based on information concerning the volumes placed and general survey data, it is assumed that the new (1972) surface is one foot above the previous (1971) surface in relative elevation. Accordingly, the reference datum used in Figure 10-19 is that of the ground surface in 1972, and the 1971 strengths are plotted at a depth of one foot lower than that shown in Figures 10-1 through 10-9, where the values are referenced to the 1971 elevations.

A study of the data presented in Figure 10-19 reveals several interesting trends. In general, the strengths determined in 1972 are somewhat greater than those measured in 1971, but the evidence is not entirely consistent. Comparing the data from BH-1 and BH-11, we see that the strengths in 1972 are consistently higher than those in 1971, but only by a small amount; it is significant to note that these bore holes are near the outflow weir, where the soil conditions are relatively uniform and the material has a very fine-grained texture. The most dramatic strength increase was observed at BH-4 and BH-14, where the strengths in BH-14 are approximately double those in BH-4. Comparisons of strength values measured at BH-5 and BH-15, BH-7 and BH-17, and BH-8 and BH-18 give additional evidence of strength increases over most of the depths compared, but these data are not as consistent as that discussed above. The location of BH-6 and BH-16 is the only one that shows consistently smaller strength values for 1972 than for 1971.

Another feature of interest in Figure 10-19 is the larger strength shown at the 4-foot depth in BH-15, BH-16, BH-17, and BH-18; this strength increase is very likely due to the consolidation by desiccation of a previous surface. Although this phenomenon could possibly be explained by the presence of a layer of material with different properties, no other evidence was found to support this possibility. There are many other factors that may cause local variations of strength to occur; these include the presence of roots from current or previous plant growth, stems and debris embedded in the fill, and old shrinkage cracks which form localized planes of weakness.

The results of laboratory vane tests conducted on undisturbed tube samples, samples from the drainage tests, and samples from the slurry consolidometers reveal the influence of water content and density on shear strength. Most of the drainage tests show a decreasing water content with depth and a corresponding increase in shear strength. For the series of gravity drained samples presented in Figure 10-20, the initial vane tests were conducted with the samples in the tube and with a small amount of free water at the surface; following these tests, the surface water was allowed to evaporate, and the vane tests were repeated. The data from the latter tests indicate a much larger strength, especially in the top zone. This phenomenon is attributed to the development of pore water tensions due to capillary action, and this increases the effective stress and thus the shear strength; of course, the water content of the samples also decreased somewhat. The effect of decreased water content or increased density (since water content is an indirect measure of density for a saturated soil, and these samples are nearly saturated) on the shear strength is also seen by comparing the shear strengths for the same dredgings subjected to gravity drainage (Figure 10-21) and vacuum drainage (Figure 10-22). In general, the shear strengths of the vacuum drained samples are several times those of the gravity drained samples.

The results from the field vane tests follow the same general patterns indicated by the laboratory tests; in the zones beneath the desiccated top layer, where the dredgings are still at a high water content and a low density, the shear strength is low. Near the bottom the strength is greater due to the consolidation which has occurred under the overburden, and near the top the strength is greater due to the consolidating effect caused by desiccation. Any abnormally high values of shear strength at the bottom of the fill are probably due to the fact that the vane tests were conducted in the virgin material below the fill. Based on measured values of the sensitivity (defined as the ratio of the undisturbed strength to the remolded strength) of these dredgings, it appears that substantial bonding forces are developed in periods as short as one year in the field and several weeks in the laboratory. This seems to suggest the important role of the organic compounds and chemical constituents in the dredgings.

In one additional shear strength test sequence, undrained triaxial compression tests were performed on partially saturated specimens of dredgings compacted at optimum moisture content. This was done to determine the probable shear strength of dredgings in a reasonably well compacted fill. The specimens tested were obtained from the vicinity of BH-11, BH-16, and BH-18 at Riverside Site, and, as seen in Figures 10-23, 10-24, and 10-25, the friction angle in each case is found to be about 18 to 20 degrees, and the cohesion is about 1300 psf, 1800 psf, and 1000 psf, respectively. Hence, dredgings compacted at optimum water content are seen to exhibit many times the strength of dredgings placed hydraulically in a disposal area.

The results of one major study of the shear strength of dredgings has been reported by the Philadelphia District of the Corps of Engineers

(1969); rather extensive tests were made on samples from four different sites along the Delaware River between Philadelphia, Pennsylvania, and Wilmington, Delaware. In one series of undrained vane shear tests in the field and unconsolidated-undrained (Q) triaxial compression tests in the laboratory, the shear strengths ranged from about 100 psf to 1000 psf with an average of about 500 psf. This compares with shear strengths in this test program ranging from virtually zero to about 400 to 600 psf with most values being about 100 to 200 psf. In addition, the Corps of Engineers (1969) report gives data (see Table 11-1) from consolidated-undrained triaxial compression tests without and with pore pressure measurements; the latter are termed R and $\bar{R}$ tests, respectively. The results from R tests are usually interpreted in terms of total stresses, whereas those from $\bar{R}$ tests are normally expressed in terms of effective stresses (total stresses minus pore pressure). The friction angle determined from the R tests was found to be about 14 ± 2 degrees for all specimens, and for the $\bar{R}$ tests it was found to be approximately 34 ± 3 degrees. The ranges of values for the so-called cohesion are found to be approximately 300 to 900 psf for the Q tests, 100 to 500 psf for the R tests, and zero for the $\bar{R}$ tests.

In summary, this study of the shear strength of dredgings indicates that they are indeed soft, weak materials when found in a loose, saturated condition, as is often the case in the fills placed hydraulically in the low lying areas near the harbors. However, when they are dewatered and/or consolidated, their density and strength increase to the extent that they may be considered potentially useful materials for construction of a landfill; the same is true if the dredgings are dewatered and compacted. The strength characteristics of dredgings are similar to those found for fine-grained organic soils. Although the major influence of water content and density tends to mask out the minor effects due to the chemical constituents, dredgings do exhibit a relatively rapid development of significant bonding forces, which are probably due to the organic matter present and the other chemical constituents.

COMPRESSIBILITY AND CONSOLIDATION

According to normal usage, compressibility refers to the total volume change that occurs in a soil under a given load, whereas consolidation refers to the time rate at which this volume change takes place; in other words, compressibility is a measure of the load-deformation behavior, and consolidation describes the deformation-time response. As discussed in Chapter 10, the in situ compressibility of hydraulically-placed dredgings was determined by means of conventional consolidation tests on "undisturbed" samples, and the compressibility of compacted dredgings was determined by use of a specially designed test. The results of both test programs are reviewed and compared in this section; first, the conventional consolidation test data will be evaluated, and then the special compressibility data will be interpreted.

Classical consolidation theory is based on a number of idealizing assumptions, some of which may not be adequately satisfied in the case of dredgings; two of the more important of these assumptions are the existence of small strains and complete saturation. Since dredgings are usually deposited in a very loose condition, they may and do undergo very large volume changes -- changes which greatly exceed the limitations of small strain theory. In addition, dredgings have been shown to be gas-generating materials, and they may therefore be partially saturated during much of their history; much pioneering research needs to be done on the consolidation response of partially saturated soils, and even greater complexities are introduced if gases are generated internally. Nevertheless, with these limitations in mind, we may utilize the tool of classical consolidation theory to develop a first order approximation of the probable behavior of polluted maintenance dredgings. As explained in Chapter 10, the coefficient of consolidation, c_v, may be determined from an e-log t plot in accordance with standard procedures, and this coefficient may be used to predict the time rate of consolidation in a field situation. For the tests conducted in this experimental program, c_v values were found to range from about 1×10^{-4} to 4×10^{-4} cm^2/sec with a mean somewhere between 1.5×10^{-4} and 2.0×10^{-4} cm^2/sec. These values compare with an average of 1.0×10^{-4} cm^2/sec and a range of 0.6×10^{-4} cm^2/sec to 1.6×10^{-4} cm^2/sec (two values at 5×10^{-4} cm^2/sec have been excluded from a total of eighteen tests) reported by the Corps of Engineers (1969) for dredgings from four disposal sites. Use of a coefficient of consolidation equal to 1.0×10^{-4} cm^2/sec suggests that 50 percent of the total settlement due to a load applied on the surface of a 20-foot layer of dredgings would occur in about 6 years if the layer were drained at both the top and the bottom; similarly, 90 percent of the total settlement would require about 25 years. Some typical consolidation-time curves computed by the Corps of Engineers (1969) in connection with the aforementioned study of four dredging disposal sites are given in Figure 11-5.

The prediction of total settlement due to a given load is usually deduced from an e-log p curve, several examples of which are illustrated in Figure 11-6 for both undisturbed and completely remolded samples. Much laboratory research on the compression characteristics of fine-grained soils has shown that a thoroughly remolded sample will exhibit a nearly linear relationship on an e-log p plot, as illustrated by curve (a) in Figure 11-6. Although some curvature may exist at very low and very high loads, most problems of practical engineering interest involve loads which lie within the linear range. If this soil were

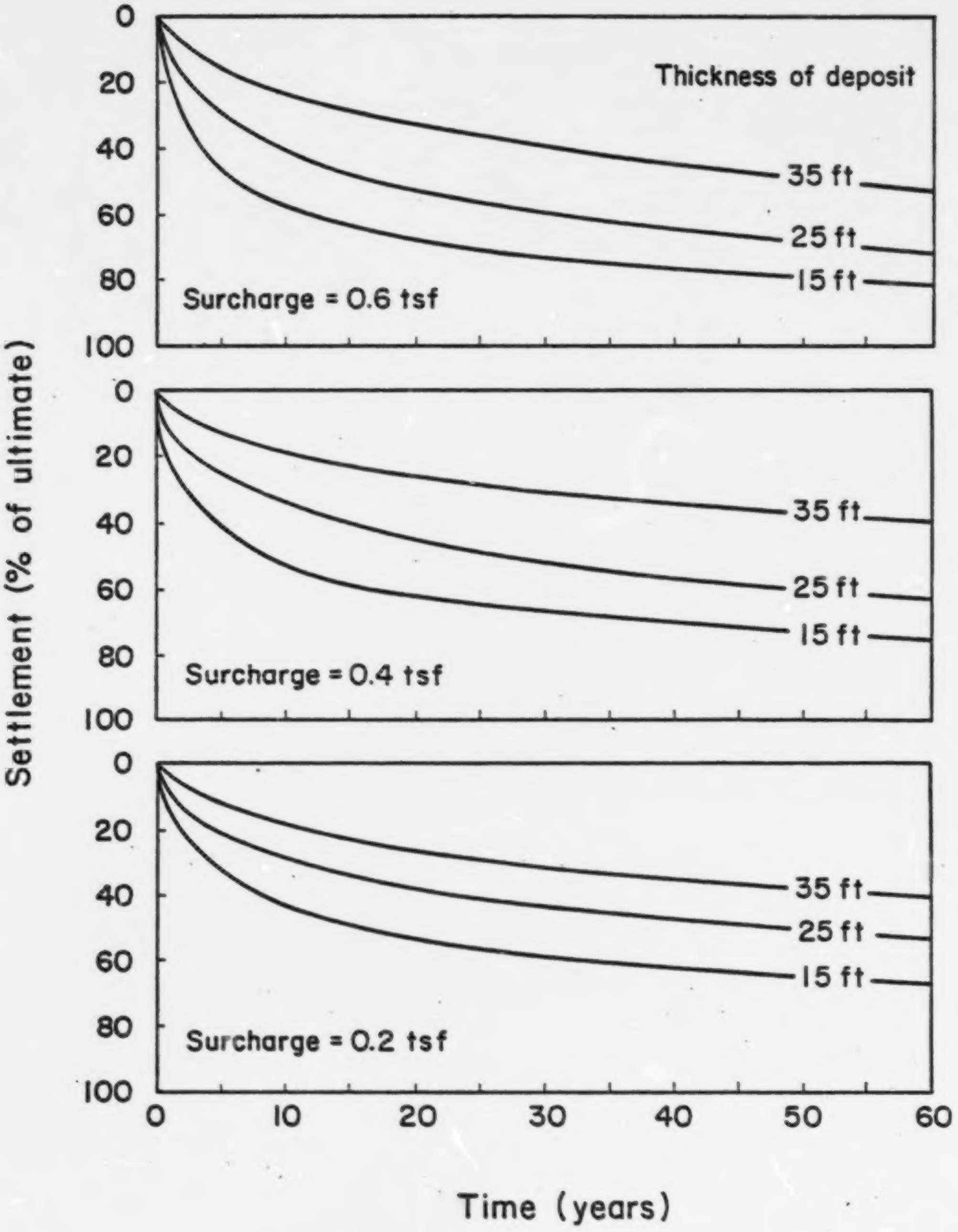

Figure 11-5. Theoretical Settlement versus Time Curves

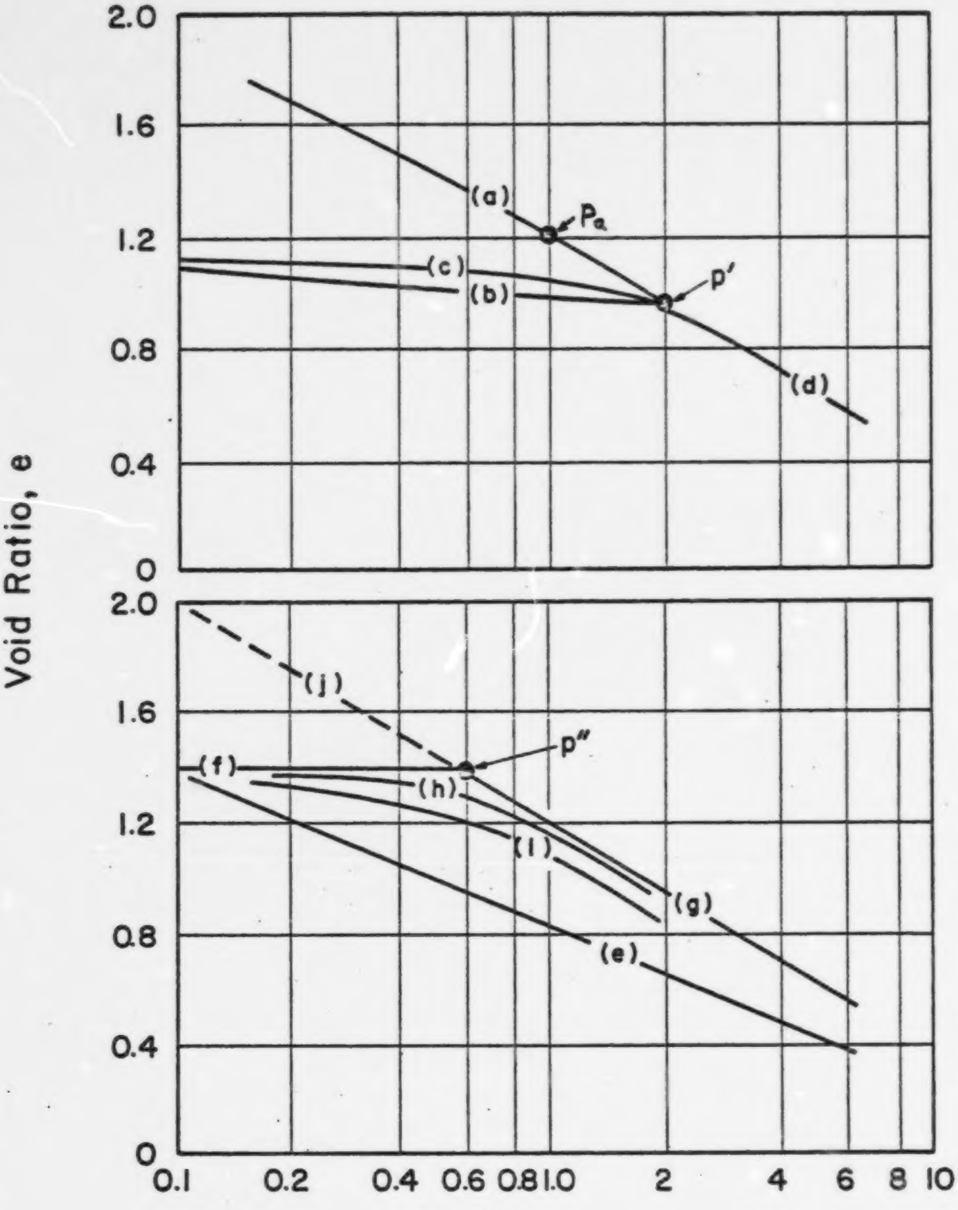

Figure 11-6. Typical Void Ratio versus Consolidation Pressure Curves

loaded to p' and then unloaded, it would rebound along curve (b) to some void ratio less than the original value; at this point the soil is said to be preconsolidated under the load p'. If the same soil were reloaded without disturbance, it would follow curve (c) with an initially flat curve taking on its maximum curvature near the previous maximum load, p', after which the response would again approach the straight line indicated by curve (d) for loads greater than p'. The portions of the e-log p curve representing load intensities greater than any that have been previously applied to the soil are called "virgin" curves; the virgin compression curve is usually linear on an e-log p plot, and its slope is defined as the compression index, C_c. With a knowledge of C_c, the settlement, S, of a layer of thickness H and initial void ratio e_o due to an applied stress, p, is given by

$$S = H \frac{C_c}{1 + e_o} \log \frac{p' + p}{p'} \qquad (11\text{-}7)$$

Alternatively, if the soil were unloaded at some point p_a along curve (a) and thoroughly remolded at its "unloaded" void ratio and water content, it would follow curve (e) upon reloading; the e-log p curve would probably be linear or nearly so, but it would have a flatter slope or smaller C_c than curve (a).

Most soils of engineering interest are found at some depth and have been subjected to some load history. If they are to be studied in the laboratory, they must be sampled, transported, trimmed, fitted into the test apparatus, and loaded. These operations involve releasing the stresses which act on the specimen in the field, and a certain amount of sample disturbance is inevitable. Ideally, if the soil could be sampled without disturbance and not allowed to rebound, its laboratory loading curve would be represented by curves (f) and (g), where curve (f) would be followed until the field consolidation stress of p" is reached and curve (g) would be followed for higher loads; curve (j) is simply a linear extension of curve (g) and represents field consolidation prior to sampling. A sample obtained without disturbance, but with rebound, would follow a loading path described by curves (c) and (d), where the effects of rebound alone are observed. However, absolutely undisturbed samples are impossible to obtain, and the effects of disturbance are observed as a partial remolding effect, as illustrated by curve (h); a specimen with greater disturbance would follow curve (i), and curve (e) illustrates the limiting case for "complete disturbance" or remolding. As demonstrated by Leonards (1962), the e-log p relationships are not only a function of the soil characteristics and history, but they are also dependent on the loading procedure followed during the test. The conventional testing procedure requires the instantaneous application of load such that the load intensity is doubled each time; other loading sequences, such as the gradual application of load, will generally result in different e-log p relationships.

All consolidation tests in this experimental program were conducted according to standard procedures, and C_c values were found to be on the order of 0.5 ± 0.1. These compare with values ranging from approximately 0.4 to 1.4 reported by the Corps of Engineers (1969). Using a C_c value of 0.5, an initial void ratio, e_o, of 2, and a preconsolidation pressure, p', of 1000 psf, we find from Equation (11-7) that a 20-foot thick layer of dredgings will settle approximately 1 foot under an added load of 1000 psf. Data reported by the Corps of Engineers (1969) indicate that about one-half of the samples tested were preconsolidated, apparently due to desiccation during the time intervals between the different deposits of dredgings, and the other half of the samples were fully consolidated under the present overburden stress. This is of interest because a fully consolidated or overconsolidated soil will not undergo additional settlement unless additional load is applied and the amount of settlement under a given load is a function of the preconsolidation stress.

In a completely separate series of tests, the compressibility of compacted dredgings was investigated; this characteristic is important in order to evaluate the benefits which can be realized by constructing a landfill of compacted materials. A special testing procedure described in Chapter 10 was used, and the results are presented in Figure 10-31. It can be readily seen that the dredgings are much more compressible than ordinary sand or clay and the loose dredgings are considerably more compressible than the dense ones. According to these data, a 20-foot layer of dredgings compacted to a medium density would settle about 6 inches under an applied load to 1000 psf.

COMPACTION

Very little compaction data has been reported on materials of a physical and chemical nature similar to that of maintenance dredgings; this is probably due in large part to the fact that they exhibit rather undesirable engineering properties and therefore have not prompted much interest to date. However, the results of a limited compaction test sequence have been reported in Chapter 10, and the significance of these results will be discussed in this section in the context of related information and the overall problem of using dredgings for landfill.

Garbe and Jeno (1968) report densities of about 84 pounds per cubic foot for the San Francisco Bay mud which was dredged and used for landfill. The material was initially dewatered by evaporation, as reported in greater detail in a subsequent section of this chapter, and then compacted at an optimum water content of 29 percent. In view of the organic content of most dredgings, it is appropriate to examine the compaction characteristics of soils with various degrees of organic content. Data reported by Holtz and Krizek (1970) indicate that a range in density from about 94 to 98 pcf is obtained by use of Standard Proctor compaction on soils with organic contents of one and a half to two percent. Orozco (1972) made an extensive study of the effect of organic content on the compaction and strength characteristics of several soils and soil mixtures, and the general range of densities was found to lie between 80 and 105 pounds per cubic foot with the higher densities being associated with the smaller values of organic content,as illustrated in Figure 11-7. In addition, oven drying was observed to change the physical-chemical nature of the soil, and Figure 11-8 shows that oven-dried samples can be compacted to significantly greater densities at lower optimum water contents than the air-dried samples.

Based on the data presented in Chapter 10 for the compaction characteristics of dredgings and the information described above for similar studies on organic soils, it appears that compacted dry densities between 80 and 90 pcf can be readily attained for most maintenance dredgings, and this will enable them to develop sufficient strength for use in many engineering applications, provided the associated settlements can be tolerated and economic considerations are favorable. In addition, the placement of dredgings in a disposal area at a density of about 90 pcf would increase the capacity of that area by approximately 80 percent, since the usual in situ densities are in the neighborhood of 50 pcf.

PERMEABILITY

It is necessary to have information on the permeability of a soil in order to develop drainage schemes for dewatering programs. Since permeability is greatly influenced by grain size, gradation, and density or void ratio, it will generally vary considerably in the different zones of a dredgings landfill. In addition, due to the existence of sand and

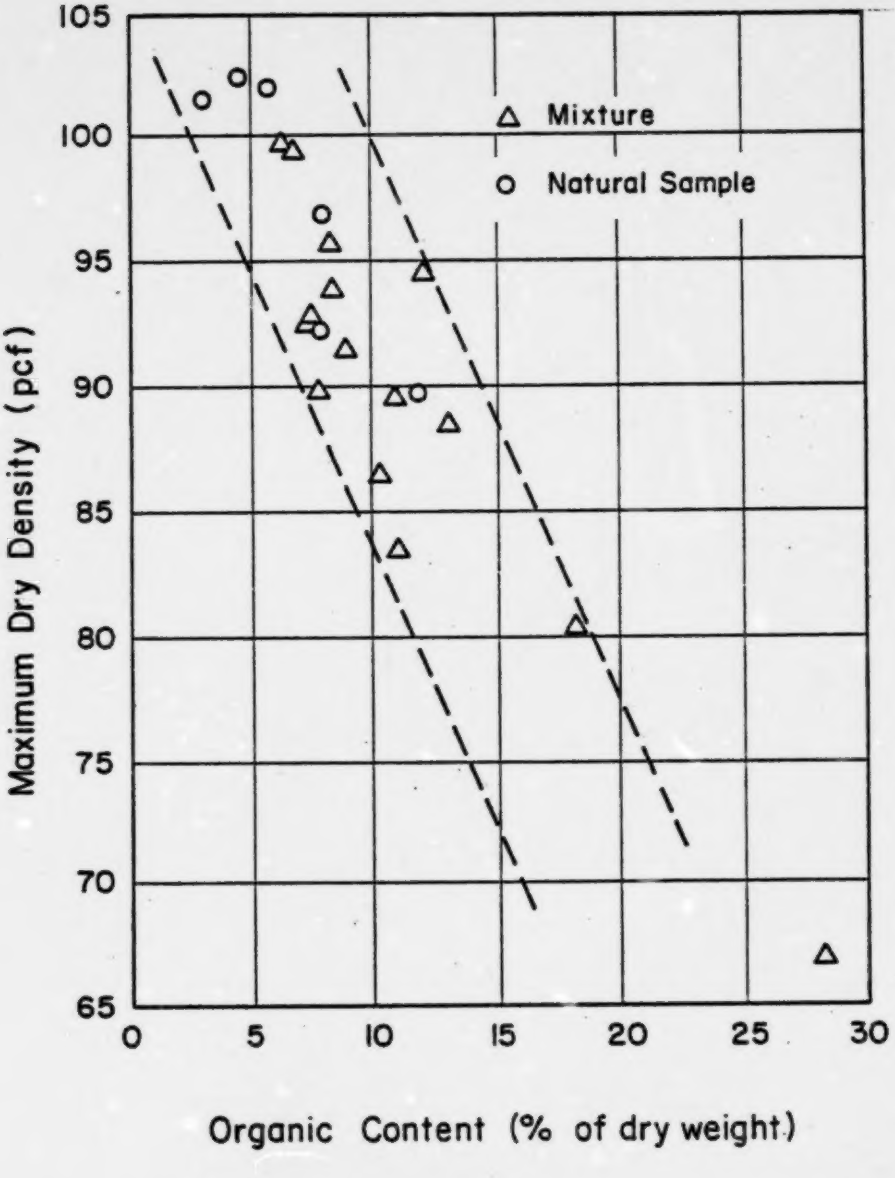

Figure 11-7. Maximum Dry Density versus Organic Content (after Orozco, 1972)

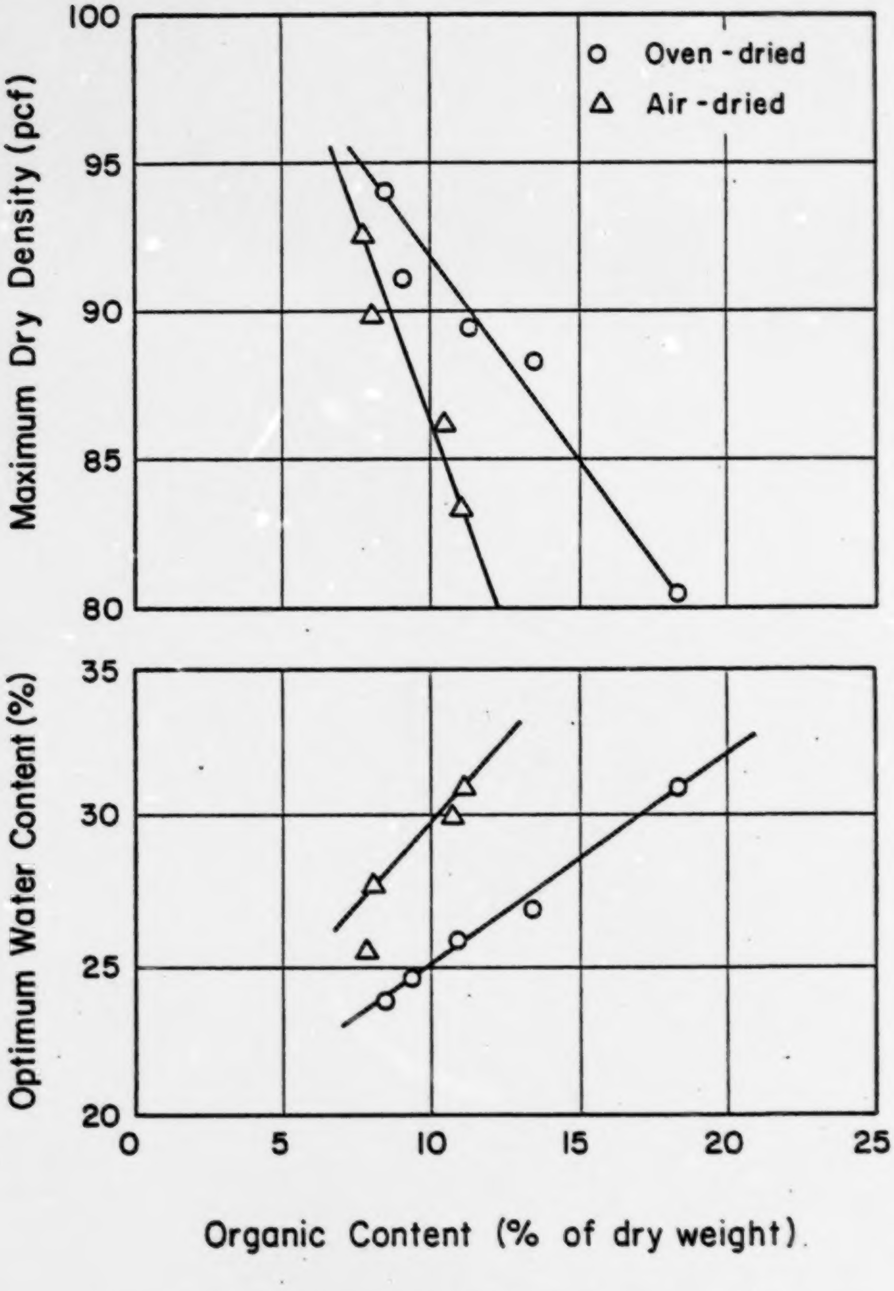

Figure 11-8. Comparisons Between Oven-dried and Air-dried Samples (after Orozco, 1972)

silt lenses and peaty material from the annual growth of vegetation, the average permeability is probably greater in the horizontal direction than in the vertical. Thus, the fill as a whole would be expected to be heterogeneous and anisotropic with respect to permeability. For this reason the data from any and all laboratory permeability tests must be viewed with caution, because it represents only discrete points in a problem which is governed more realistically by a global response. Therefore, the permeability data reported in Chapter 10 are presented as order-of-magnitude values to aid in planning more precise laboratory and/or field permeability testing programs and to facilitate preliminary calculations for drainage schemes.

Little is known regarding the effect of organic content on the permeability of a soil. Some evidence (Arman, 1970) indicates that, if organic matter of a fibrous nature is added to a clay or silt, the coefficient of permeability, k, increases rapidly until the organic content reaches about 40 percent, after which there is not much additional change. However, exactly the opposite happens for sands, with the coefficient of permeability stabilizing again at about 40 percent organic content. In the plot of k versus organic content, the curves for sand, silt, and clay converge at around 40 percent organic content to a constant value -- the sand from above and the clay and silt from below -- that seems to be the coefficient of permeability of the organic matter alone. Although the above behavior was reported for the case of fibrous organic matter, there was no data concerning the effect of finely divided organic matter on the permeability (that is, organic matter with a particle size similar to silt or clay). However, organic matter in dredgings may have a more complex influence on permeability, depending upon the degree of humification and the chemical composition of the organic matter. While fibrous peaty material may provide an open, porous, permeable soil, a fine-grained organic matter may adsorb water and swell, thereby blocking the pore passages and impeding the flow of water through the soil. In a similar fashion, fats, grease, and oil may tend to obstruct the pore passages in a fine-grained soil.

Research indicates that the degree of saturation exerts a large influence on the permeability of a given soil. Since many of these polluted dredgings are actively decomposing various organic compounds and generating gases in the process, the entrapped gases tend to block pore passages and thereby constitute a complex and influential factor in the permeability of these materials. Although these relationships have not been studied in this project, they are recognized as important considerations for further research.

The electro-osmotic permeability involves a special situation in which the water is moved through the pore passages under the influence of an electrical gradient. Although certain similarities exist between electro-osmotic fluid flow and hydraulic pressure fluid flow, the physics of the situation suggests that there are substantial differences. For example, in fluid flow due to a hydraulic gradient various soluble ions may translocate with the pore fluid and leave the soil as it is drained, or they may be leached from the soil as fresh water becomes available from precipitation; however, in fluid flow due to an electrical gradient the electrical current causes the cations to migrate toward the cathode, and they carry the water with them. In the latter process the soil is depleted of its cations much more rapidly than in the former process, and the major effect is noticed quickly in a soil subjected to electro-osmotic treatment.

As indicated previously, the permeability tests conducted as part of this research effort were exploratory in nature, and their purpose was to identify ranges of values for several different circumstances. Although permeability tests were not conducted on the coarse-grained materials that are usually deposited near the discharge pipe, experience indicates that these materials have a relatively high permeability. Since the bulk of maintenance dredgings are fine-grained, the major interest in this program was directed toward a study of these materials. Three different testing techniques were used to determine the coefficient of permeability for these materials; in addition to direct permeability tests, measures of the coefficient of permeability were deduced from the data obtained from the drainage tests and the consolidation tests. Although classical consolidation theory indicates a relationship between the permeability of a soil and its consolidation characteristics, this is usually regarded as an indirect measure, since it is dependent on other influential variables and certain assumed theoretical relationships. For example, a consolidating soil exhibits a continuously decreasing permeability, and the computed value therefore depends on the time at which the calculation is made. The details of the testing procedures employed and the associated interpretation of the data are given in Chapter 10. With these ideas in mind, it is not surprising to note the range of permeability values reported in Chapter 10. The significance of these data lies only in the order of magnitude for the values that may be associated with specific materials; in particular, the E materials exhibit a coefficient of permeability on the order of 10^{-8} cm/sec, whereas the C and D materials have a coefficient of permeability on the order of 10^{-7} cm/sec. Based on test data from two C materials and two D materials, the electro-osmotic coefficient of permeability was found to be on the order of 10^{-5} cm^2/volt-sec.

DEWATERING OF DREDGINGS

Although dewatering is one of the most effective procedures for improving the engineering properties of polluted maintenance dredgings, there has been relatively little study of this subject. However, some experience has been gained from the work of Dames and Moore (McNely, 1966) with San Francisco Bay mud, a special study by Greeley and Hansen (1969), and a report by the Philadelphia District of the Corps of Engineers (1969) Although an extended definition of dewatering might include field loading with its associated consolidation, this section will consider only dewatering by evaporation, gravity drainage with or without a vacuum, and electro-osmosis.

Evaporation

All experience to date suggests that evaporation holds the greatest promise for the economical dewatering of dredgings; this is based on observations made at the Island Site, Riverside Site, Penn 8,and Grassy Island and special studies conducted by Dames and Moore (McNely, 1966) and Greeley and Hansen (1969). Although an investigation of evaporative losses of water from dredgings was not a specific part of this laboratory or field research program, the following field observations bear directly on this subject. In December of 1970 Riverside Site at Toledo had just been completely filled, and the entire area was a sea of very soft slurry; all free water had drained from the surface, and the consistency of the material was such that it could be easily poured. Six months later this area was covered with a dense growth of vegetation from 8 to 10 feet high with lower stems up to an inch in diameter, and it could easily be traversed on foot, although most areas were too soft to support normal vehicles. Despite the fact that these general observations can not proportion the water lost by evaporation and that lost by drainage to the underlying soils, the major effect near the surface was undoubtedly due to evaporation, since the lower materials were still at relatively high water contents. In addition, McNely (1966) reports an experience concerned with the evaporative drying of San Francisco Bay mud at Mariner's Island, where the material was placed hydraulically to depths of about 3 feet and initial dry densities of about 22 pounds per cubic foot; within seven months the thickness decreased to about half of the original thickness and the dry density doubled.

Garbe and Jeno (1968) report the results of a field test in which mechanical equipment was used to agitate the dredgings, thereby accelerating the drying process. This reclamation project involved the use of a hydraulic dredge to fill former tidal marshes with the bottom material (organic silty clay; LL $\cong$ 100 percent and PI $\cong$ 50 percent) from Belmont Slough, and the results achieved in a little more than a month are shown in Figure 11-9 for materials placed at several different depths and subjected to various degrees of mixing. A comparison of the final water contents of the non-conditioned materials indicates that the thin lift (12 inches) dried from over 200 percent water content to about 110 percent, whereas the thick lift (48 inches) dried to about 170 percent; hence, the benefits to be derived by the use of thin lifts is readily apparent. The conditioning of the materials in the 16- and 21-inch lifts consisted primarily of manipulating them with a dozer to accelerate evaporation; some experimentation with a special screw rig was also very successful. This densification procedure was a success in that it yielded a usable fill for about $1.00 per cubic yard, whereas it would have cost about $1.50 per cubic yard to import and place select fill material. The thinner lift (16 inches) was easier to handle and compact than the thicker lift (21 inches), and it yielded a lower water content (about 40 percent compared to about 60 percent).

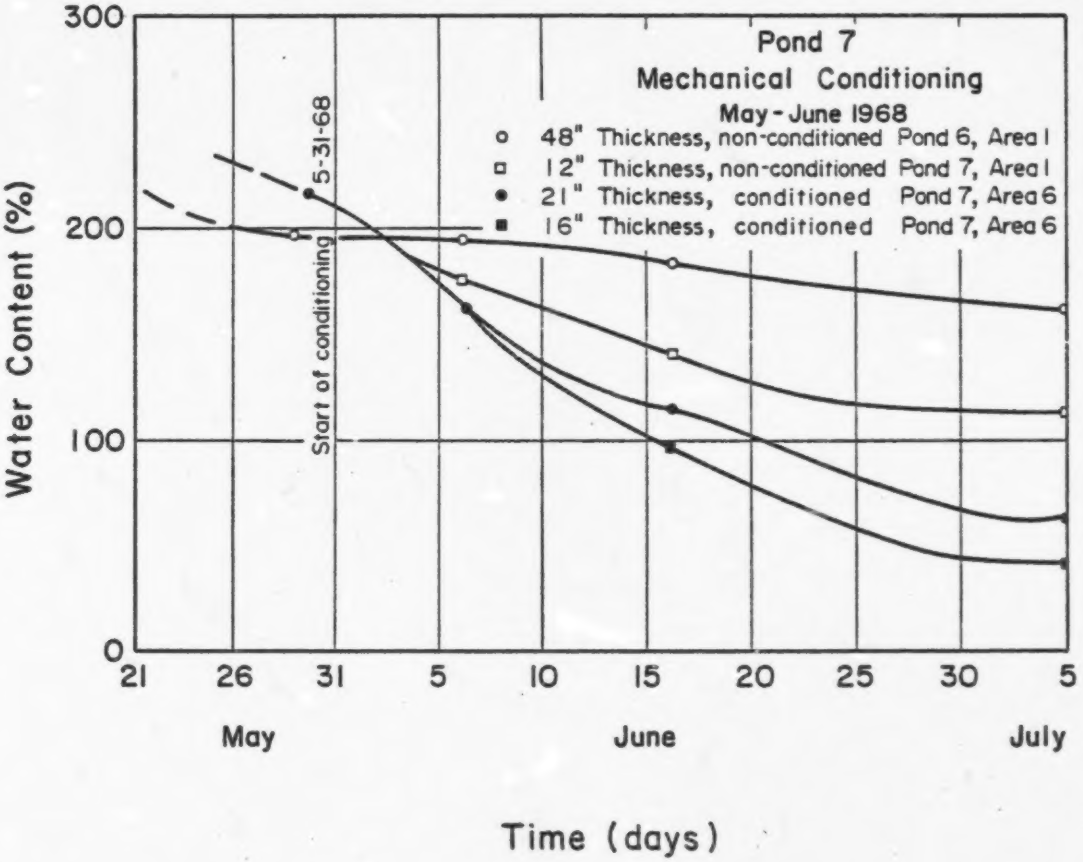

Figure 11-9. Field Study of Evaporation Losses (after Garbe and Jeno, 1968)

Greeley and Hansen (1969) report the results from a series of laboratory evaporation tests on dredgings taken from the Calumet River in Chicago, Illinois. This program consisted of drying dredgings which were placed in depths of 2, 4, 8, and 12 inches, with and without mixing, at a fairly uniform temperature ($74^{o}F$) and relative humity (58 percent). Mixing, when used, was done three times per day for the 4- and 8-inch samples and at one-hour intervals for the 2-inch samples; there was no mixing of the 12-inch sample. The test data plotted in Figure 11-10a indicate that nearly linear relationships were obtained for the percentage water content loss versus time. The thinner lifts dried more rapidly than the thicker ones, and the mixed layers dried more rapidly than the unmixed ones for each particular thickness. Figure 11-10b shows the specific relationships between the drying rate and the thickness of the sample for both the mixed and unmixed samples, and Figure 11-10c illustrates drying rate of the mixed layers as a percentage of the drying rate for the unmixed layers; it can be seen in the latter plot that greater relative effects are achieved by mixing the thicker layers.

As a consequence of the above study, Greeley and Hansen proposed the construction of drying beds, as shown in Figure 11-11, and the predicted results are given in Table 11-3. Based on their economic analysis, the average annual production of 200,000 cubic yards of dredgings from the Chicago area could be dried at a cost of about $1.28 per cubic yard if placed hydraulically, or about $0.85 per cubic yard if placed by truck from a clamshell dredge. Costs for the dredging operations or for the movement of the dredgings into and out of the drying areas are not included in the above estimates. It was recommended that field studies would have to be conducted to give more appropriate information from which to deduce improved cost estimates.

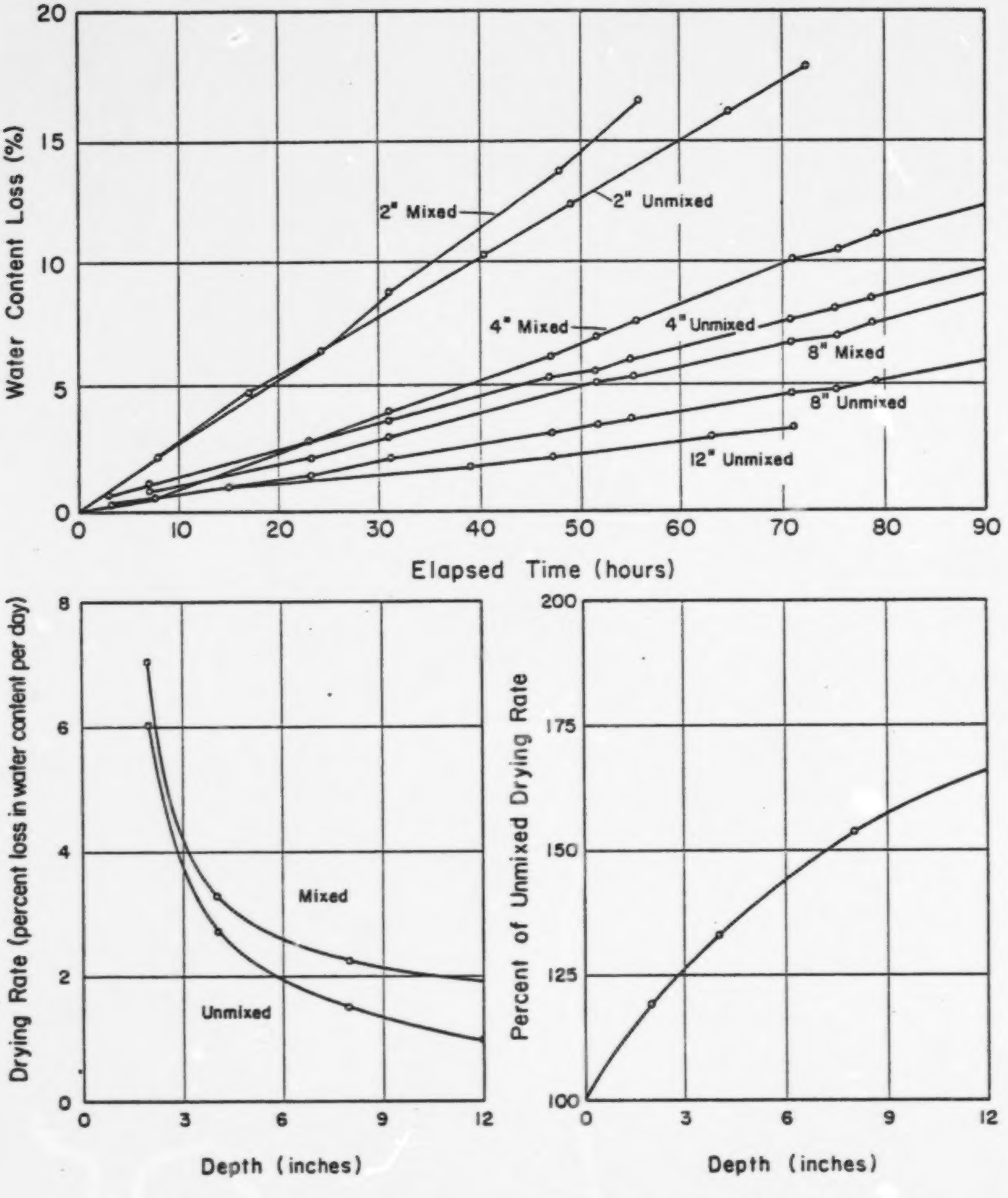

Figure 11-10. Laboratory Study of Evaporation Losses (after Greeley and Hansen, 1969)

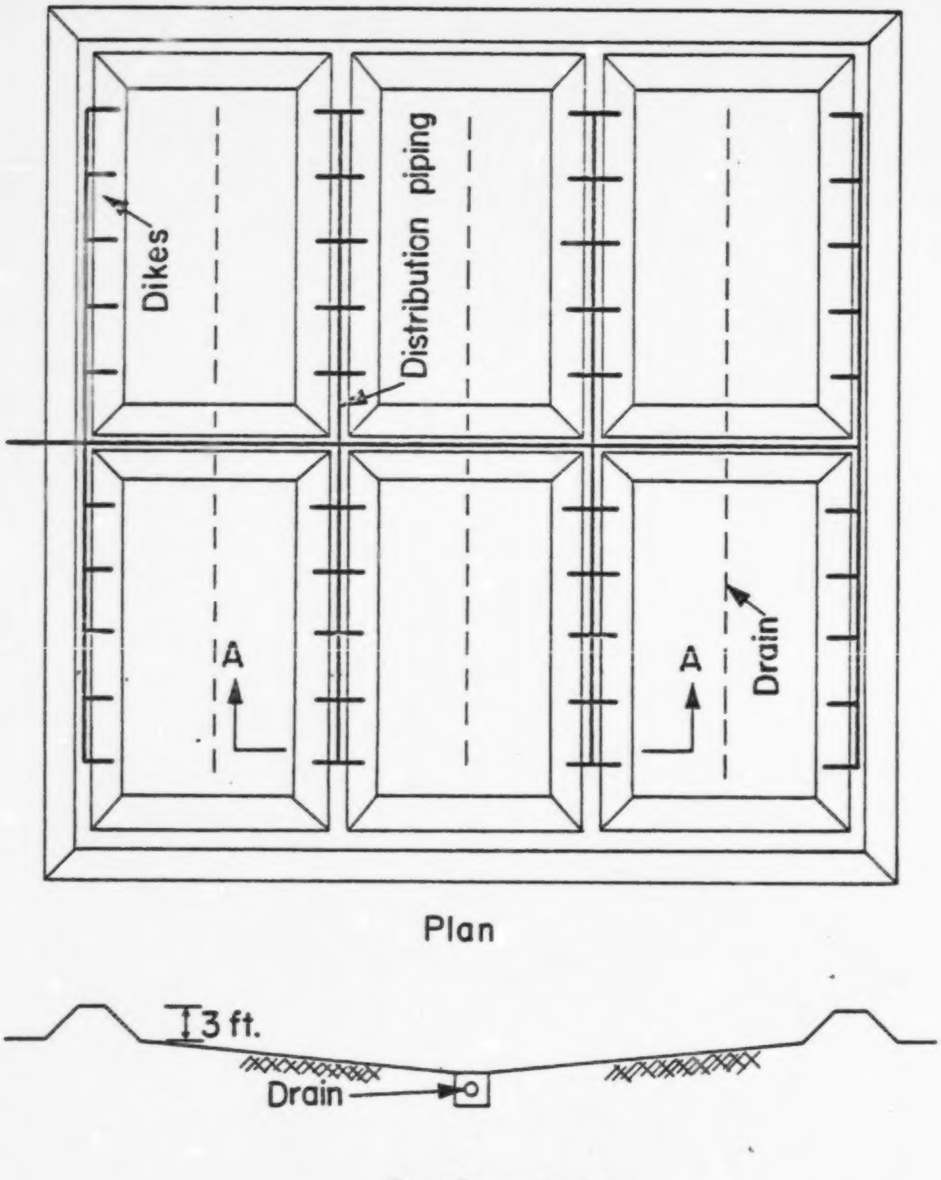
Dikes
Distribution piping
A
A
Drain

Plan

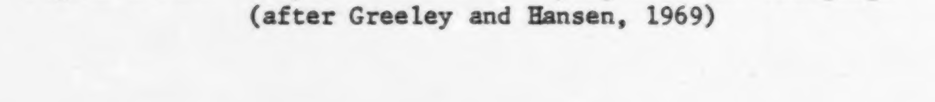

Section A-A

Figure 11-11. Proposed Scheme of Drying Beds for Dredgings (after Greeley and Hansen, 1969)

Table 11-3

Predicted Field Performance of Drying Beds
(after Greeley and Hansen, 1969)

Depth of fill (inches)	2.0	4.0	8.0	12.0
Drying rate (% per day)	6.0	3.0	1.5	1.0
Filling rate (days per acre)	0.3	0.6	1.3	1.9
Drying time (days)	8.3	16.7	33.3	50.0
Removal rate (days)	0.4	0.7	1.1	1.5
Drying cycle (days)	9.0	18.0	35.7	53.4
Volume (cubic yards per acre)	268	536	1072	1608
Volume (cubic yards per acre per day)	29.8	29.8	29.9	30.1
Area for 2000 cubic yards per day (acres)	67.0	67.0	67.0	67.0
Area required (acres)	141	114	85	63
Application rate (cubic yards per day)	4200	3400	2550	1900

Gravity and Vacuum

Field information concerning the gravity drainage of spoil areas is generally lacking and often partially confused with evaporative losses, which usually occur simultaneously. One quite good study of dewatering by gravity drainage has been reported by the Philadelphia District of the Corps of Engineers (1969); however, the primary concern of this study was to provide more capacity for spoil disposal in a given area rather than to increase the strength and density of the dredgings. Nevertheless, valuable information on increases in density can be obtained from the results reported. For example, a system of parallel drainage ditches spaced 200 to 300 feet apart was estimated to accelerate considerably the dewatering and densification of spoil areas. A spoil deposit with a depth of 15 feet was predicted to undergo a surface settlement on the order of 2 inches per foot of ditch depth; this would correspond to an increase in dry density of about 1 percent per foot of ditch depth. The corresponding figures for a spoil depth of 30 feet were projected to be about 3 to 4 inches settlement and about 1 percent increase in density per foot of ditch depth. A system of 5-foot ditches was calculated to cost about $200 per acre, and 15-foot ditches were anticipated to cost about $1700 per acre. It is stated further that drying periods from 2 to 5 years (with exceptions to 10 years) are required for a dredgings spoil area to reach a condition where agricultural equipment can be supported. The use of sand drains and surcharging to cause densification was projected to cost between $19,000 and $35,000 per acre for a 30-foot fill deposit; however, calculations suggest that rates of consolidation would be increased by about 20 to 100 times the rate due to a surcharge only.

Although spoil areas have the reputation of draining slowly and remaining soft for many years(or indefinitely in some cases), this situation really reflects the lack of drainage. If adequate opportunity for drainage is provided, the data from the laboratory tests described in Chapter 6, although quite variable, suggest that a 10 to 20 percent decrease in volume would occur relatively quickly.

Very little attention has been given to the possibility of using vacuum as a method of preloading a spoil area to accelerate the dewatering process. The use of vacuum can provide a load equivalent to 10 or 15 feet of soil surcharge. Although Nichols (1972) reports that vacuum drainage has been used as a method of consolidation, he states that it has certain drawbacks in practical application; however, further details of his experience are not given. The laboratory data reported in Chapter 6 indicate that (a) rapid drainage is achieved with the aid of a vacuum and (b) the major benefit is achieved soon after application (that is, the flow rate is greatest at the beginning and decreases with time). The most beneficial and economical treatment of dredgings by vacuum would depend on the thickness of the deposit, the intensity of the vacuum, and the initial water content and drainage characteristics of the particular dredgings. Additional consideration will be given to the use of vacuum in the following section in conjunction with dewatering by electro-osmosis.

Electro-osmotic Dewatering

The data reported in Chapter 7 are used in this section to calculate the anticipated quantity of flow per watt-hour of energy per cubic yard of dredgings. In addition, some consideration is given to a scheme that would simultaneously apply vacuum and electro-osmotic forces to dewater dredgings rapidly. The calculations involve the use of flow quantities from only the bottom half of the sample (where the pressure gradient and electrical gradient are additive), with the flow quantity caused by the pressure gradient being subtracted from the total flow quantity caused by both the pressure gradient and the electrical gradient to give the flow quantity due to the electrical gradient only. Average values of data over the first 10- and 20-hour periods were used for samples D1DM and D4CO and over the first 20- and 40-hour periods for samples C22TO and C27MM; appropriate flow quantities were determined from the experimental curves at the specified times, and the energy consumed during the associated time interval was taken as the area under the current-time curve multiplied by the applied voltage. The effectiveness of the electro-osmotic treatment is expressed in Table 11-4 as the quantity of water per watt-hour of energy per unit volume of slurry. A study of these calculations indicates that the quantity of water removed from each of the four materials varies from about 3 to 6 gallons per watt-hour per cubic yard for treatment times of 10, 20, or 40 hours; also, the effectiveness is nearly the same for each material for both time periods selected. However, the energy consumption would increase sharply for time periods longer than those selected, since, as seen in Table 11-5, approximately 75 to 95 percent of the total flow occurs in the selected time periods, and additional treatment would produce little additional drainage. Before applying this information to a field problem, it is necessary to evaluate (a) the efficiency associated with a given field problem (although the data presented in Chapter 7 indicate that significant power losses occur in the treatment process, the above calculations use the total power, including the losses) and (b) the scaling factors associated with extrapolating this information to a field problem, since the energy consumption values utilized in the above calculations are based on the laboratory data.

Table 11-4

Flow Efficiency for Electro-osmotic Dewatering of Dredgings

Sample	Time (hours)	Flow Efficiency	
		$\frac{\text{milliliters}}{\text{watt-hour x liter}}$	$\frac{\text{gallons}}{\text{watt-hour x cu. yd.}}$
C22TO	20	17.9	3.62
	40	17.9	3.62
C27MM	20	24.6	4.97
	40	23.1	4.66
D1DM	10	30.4	6.14
	20	27.4	5.54
D4CO	10	13.0	2.62
	20	12.9	2.60

Table 11-5

Comparison of Dewatering Rates With and Without an Electrical Gradient

Sample	Time	Electrical Gradient			
		None		1 volt/cm	
		Total Flow (liters)	Flow from Bottom (liters)	Total Flow (liters)	Flow from Bottom (liters)
C22TO	6 days	0.91	0.48	1.15	0.96
	20 hours	0.50 (55%)	0.24 (50%)	0.60 (52%)	0.43 (45%)
	40 hours	0.71 (78%)	0.35 (73%)	0.89 (77%)	0.71 (73%)
C27MM	6 days	0.89	0.45	1.17	1.07
	20 hours	0.56 (63%)	0.28 (63%)	0.73 (63%)	0.64 (60%)
	40 hours	0.76 (85%)	0.38 (85%)	1.05 (90%)	0.95 (89%)
D1DM	6 days	0.59	0.31	0.94	0.80
	10 hours	0.49 (83%)	0.25 (81%)	0.67 (71%)	0.54 (67%)
	20 hours	0.57 (97%)	0.30 (97%)	0.88 (94%)	0.74 (93%)
D4CO	6 days	0.94	0.48	1.10	0.94
	10 hours	0.59 (63%)	0.29 (60%)	0.69 (63%)	0.54 (57%)
	20 hours	0.83 (88%)	0.42 (88%)	0.98 (89%)	0.82 (87%)

Suggested Dewatering Scheme

Discussed in this section is a rapid dewatering scheme that combines the effects of gravity, vacuum, and electro-osmosis. This scheme might be used in a large diked area, or it might be considered as a part of a sequence of treatments in an overall dewatering program. For sake of discussion the latter will be assumed, and a schematic diagram of the equipment and process is given in Figure 11-12. In harbors with relatively large annual volumes of polluted dredgings, a general scheme involving several stages might be employed. Initially, the spoil might be placed in diked areas in a fashion similar to that presently being used, but the areas should have a higher elevation and bottom drainage to facilitate rapid sedimentation and the removal of excess water from the surface; then, at a suitable time and spoil condition, the material could be moved into a bin, such as that illustrated in Figure 11-12, for processing, after which it could be moved into large open areas and placed in thin lifts to take advantage of evaporation. The final stage would be to move the spoil into storage areas for subsequent use as a low-grade fill material, in agriculture applications, or for other purposes.

Vey (1949) states that electro-osmotic treatment is most effective if at least a small consolidating stress is applied simultaneously; in keeping with this finding, as well as exploiting the advantage to be gained from vacuum drainage (as discussed in Chapter 6), the latter may be incorporated into the suggested drainage scheme. An approximation of the combined effect due to the simultaneous use of a vacuum and electro-osmosis may be obtained from a study of the drainage reported in Chapter 7 for the case where a stress of $0.6 \frac{\text{kg}}{\text{cm}^2}$ (about one-half of atmospheric pressure) was applied with the electro-osmotic treatment; the flow quantity due to the combined effect was about double that obtained for

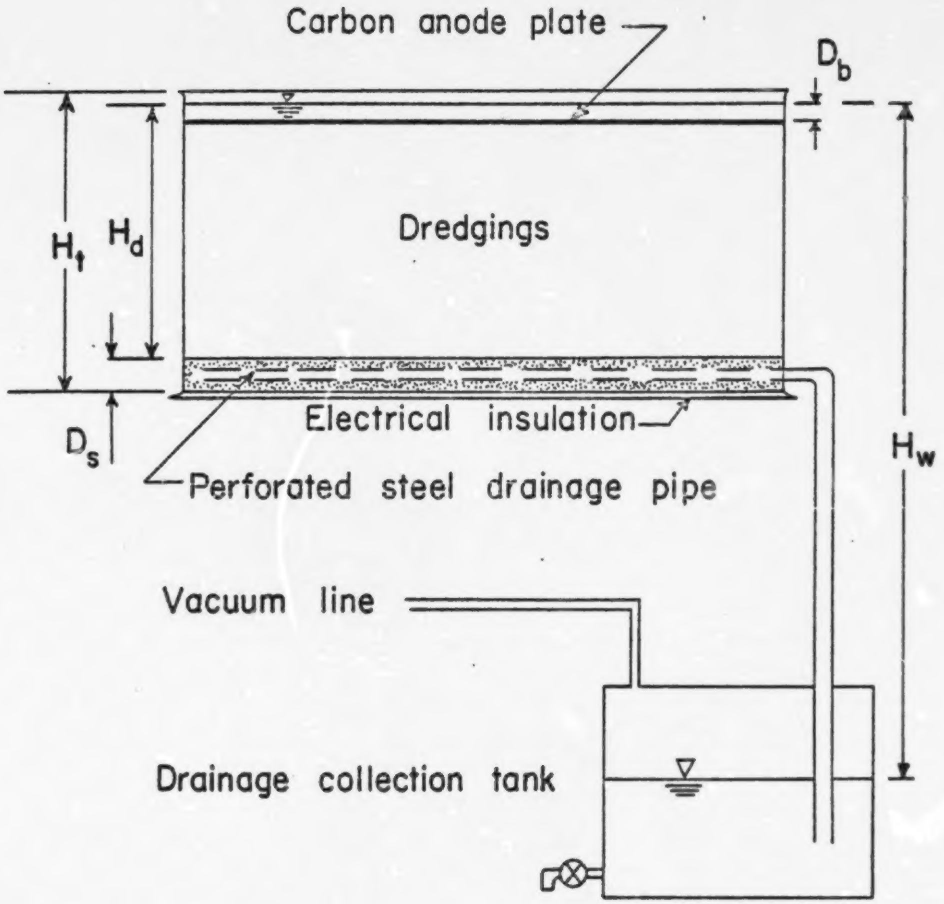
Carbon anode plate
D_b
H_t
H_d
Dredgings
D_s
Electrical insulation
Perforated steel drainage pipe
H_w
Vacuum line
Drainage collection tank

Figure 11-12. Suggested Dewatering Bin for Dredgings

electro-osmosis alone. Undoubtedly, the scheme described above would be expensive to apply in its entirety, and it could probably be justified economically only in rather unusual circumstances. However, it is possible that some part of it could be utilized to advantage in areas where disposal sites are very difficult to locate. Before meaningful economical estimates of such a dewatering scheme could be made, it would be necessary to conduct additional research under conditions which are more nearly equivalent to those of an actual installation; also, the influence of layer thickness should be studied to ascertain the role of dimensional effects. Nevertheless, based on field observations, laboratory tests and the experience of others, it seems that dredgings can be dewatered economically. Although the most promising methods of dewatering appear to involve taking advantage of evaporation losses, the rapid drainage achieved in the laboratory by use of vacuum suggests the possibility that it may be used in some phase of the dewatering process.

USEFULNESS OF DREDGINGS FOR LANDFILL

Pursuant to the major thrust of this study, this section will synthesize the preceding results in an attempt to evaluate the usefulness of dredgings for landfill, including how the dredgings may be treated and used to advantage for new fills and how existing fills may be conditioned and used. In either case the major problem lies in dewatering the spoil and increasing its density, because, once this is achieved, the spoil exhibits engineering properties characteristic of an organic silt and it is acceptable for use in many engineering applications. However, it must be emphasized that the suggestions delineated herein are developed primarily from the technical point of view; it is fully recognized that the ultimate engineering solution in any particular situation would necessarily involve an economic analysis and an environmental impact study, In general, such comprehensive analyses are extremely complicated, and their outcome depends very much on which aspects of the problem are included and the costs or benefits associated with each. For example, a landfill of compacted dredgings would not only manifest more desirable engineering properties than one consisting of hydraulically placed dredgings, but the increased density of the materials in the former case would enable approximately 80 percent more spoil to be deposited in a given disposal area; hence, this increased capacity certainly has some economic value. Of greatest difficulty to evaluate are the benefits to the environment, because these are usually very subjective.

New Fills

The two major categories of new fill that will be considered here are those fills where the dredgings are deposited initially in their final location and those in which the dredgings are moved and compacted in place at another location. In both cases appropriate planning and well-documented records will serve to enhance the usefulness of the resulting landfill. If possible, a master plan for the proposed land usage should be developed before the filling operation begins, because, by having a well defined usage for the site, the fill operation itself can be modified to achieve certain desirable effects. For example, most dredgings include significant quantitites of coarse-grained materials that produce mounds near the discharge pipe and require that the pipe be moved from time to time. By planning site usage in advance, the deposition pattern of the granular material may be adjusted to best meet the objectives of the proposed plan; this may involve placing the granular materials at the locations of future buildings to provide better quality foundation materials and thereby realize certain savings in building costs. Alternatively, the zones near the weir may be planned for use as open green areas.

Appropriate planning would also allow a more meaningful economic comparison of several alternatives for site usage, and, once a particular site usage was selected, a careful economic study of alternatives in site preparation could be undertaken. For example, the use of a given site for a wildlife refuge may require a minimum of special attention during the filling operation, whereas the use of a site as an industrial area may find it economically feasible to provide drainage systems or other dewatering schemes. Included in these economic studies would be the benefits realized by having the site in productive use soon after the filling operation is completed, compared to the relatively long periods which are usually required at present before the site is useful. Such a time consideration may even justify placing a compacted fill.

One of the major problems facing the soils engineer when called upon to give foundation recommendations for a given structure is the determination and evaluation of the nature and extent of the subsurface soils. Although a certain number of borings are indispensible to this decision, it would be most desirable to have available a record of the types of materials placed, to what depths, at what times, etc. Since the fills under consideration are placed by man, the accumulation of this information is only a matter of appropriate documentation. In particular, a small investment of effort during the filling operation may save considerable expense in soil exploration later; in addition, a soil exploration program may never fully recover the information that might be easily obtained during the fill process. Among the most important items to record are the locations of the discharge pipe and the outflow weir during the various periods of filling, since the coarser materials accumulate in the vicinity of the discharge pipe and the fines accumulate near the outflow weir. The records should also include the volumes and sources of the dredged materials, the elevation changes resulting from various seasonal depositions, and a general description and classification of the fill materials.

There are many different methods of fill placement that enhance the usefulness of landfills composed of dredgings by maximizing the opportunities for dewatering. Specifically, these include (a) placing the fill at a sufficient elevation to allow gravity drainage, (b) providing a drainage system at the base of the fill to hasten the drainage, (c) placing the fill in thin lifts to utilize evaporation more effectively, (d) utilizing vegetation to expedite the water losses by transpiration, and (e) incorporating drainage systems within the fill (as opposed to the placement of costly sand drains after fill placement). The fill should be placed in such a manner as to achieve the maximum final density consistent with economic considerations. Other stabilization procedures currently under study involve the use of chemical additives to accelerate sedimentation and to increase the strength.

A fill of greater uniformity and higher quality may be achieved by compacting the dewatered spoil. Moderate densities may be achieved by use of normal compaction procedures, and under certain special circumstances higher strength fills could be obtained by blending coarser dredgings with the fine-grained spoil to produce a well graded material.

Existing Fills

As a first step in evaluating the strength and bearing capacity of an existing fill area, it is desirable to have a knowledge of the composition of the fill. After a careful study of available records, suitable reconnaissance and a detailed subsurface exploration must be undertaken. Electrical resistivity and/or seismic refraction methods might be used to gain preliminary information of a qualitative nature on the location and extent of various zones within the fill, but these techniques would normally have to be supplemented by more quantitative investigations at discrete points. The field vane shear apparatus can be used to obtain reliable strength data on the softer soils, and manually-operated piston samplers can be used to obtain reasonably good undisturbed samples for subsequent laboratory tests. Once a fill is in place, the options for dewatering are somewhat limited; although the use of sanddrains or electroosmosis would probably be prohibitively expensive, except in very special circumstances, a system of ditches seems to offer a very economical means for dewatering existing spoil areas. However, if soft fills are placed to significant depths, the process of consolidation normally requires very long periods of time, and some measure is usually required to accelerate this process and make the land available for use in a shorter period of time. Preloading is one of the proven techniques for accomplishing this objective, and it has been used with considerable success in a large variety of similar situations. There are several variations of preloading, depending upon the desired use of the fill and the nature of the subsurface conditions. One technique, often used in soils which exhibit large amounts of secondary consolidation, involves the placement of a surcharge load considerably in excess of that load which the fill will ultimately carry. The advantages of preloading are an acceleration of settlement and an increase in strength; its disadvantages are the need for preload materials and the possibility that the soft dredgings will squeeze out from under the load. In general, however, provided a certain amount of strength gain has occurred, most landfills of dredged spoil are typical of those for which preloading has been used very successfully.

Potential Uses of Resulting Landfills

Spoil fills may be used in a variety of ways. At present, many of them are serving as wild life refuges. If this is the desired usage in a particular case, it might be advisable to seed the area with plants or to incorporate other features commensurate with the form of wild life to be encouraged. With moderate effort, most spoil fills can be made into park and recreational areas; however, despite the small loads associated with such usage, considerable benefit could be realized by the use of some dewatering and densification procedure. The medium loads caused by housing developments and light industrial buildings require relatively firm foundation materials, and this would usually dictate the use of some dewatering scheme together with either compaction or preloading; insofar as possible, buildings placed on such fills should be designed to accommodate considerable differential settlement. Loads due to heavy industrial buildings are normally transferred to the deeper subsurface materials by the use of piles or caissons, but the associated parking lots and access roads could be easily accommodated on a well designed fill of dredged spoil. However, the design of utilities and connecting light-weight additions must be designed to accept the differential settlements likely to occur between the relatively fixed main building which rests on a deep foundation and the structures within or on top of the fill material.

CHAPTER 12

CONCLUSIONS AND RECOMMENDATIONS

Based on this rather extensive, but nevertheless preliminary, investigation of the engineering properties of polluted maintenance dredgings, it appears that such spoil may be used to construct landfills of sufficient quality to serve urban and regional planning projects in a number of possible ways, such as recreational parks, wild life refuges, and areas for light industrial construction; in addition, its use as ordinary fill material and for agricultural applications is suggested. However, various other aspects of the general problem of dredgings disposal and the particular problem of placing dredgings within diked enclosures require considerably more study before definitive conclusions and well-substantiated recommendations can be deduced. Accordingly, the conclusions and recommendations advanced herein must be regarded as reasonable indications of the ultimate results anticipated at this time, and not necessarily as the final engineering judgments.

The engineering properties of most dredgings indicates that their behavior is not too different from that of a fine-grained, organic soil, the properties of which have been evaluated to some degree by previous testing and experience. The general notion that maintenance dredgings are soft and weak is only partially due to their inherent nature; the primary reason for this condition seems to be attributable to the environmental circumstances under which these dredgings are placed, namely, in low lying swampy areas with poor drainage. Although the chemical composition of polluted maintenance dredgings is often quite unique compared to that of most soils, the influence of other major factors, such as water content and density, tends to control the engineering behavior, and the unique chemical nature of the dredgings is usually subjugated to a somewhat minor role. Despite the low bearing capacity of many existing landfills, experience has proven that they can be successfully sampled and tested in situ by the use of light-weight, manually-operated equipment.

Perhaps the most important factor in determining the usefulness of dredging spoil is its water content and the associated value of dry density. Hence, dewatering is one of the most significant factors in conditioning the dredgings for subsequent use. Several techniques of dewatering, including gravity and vacuum drainage, electro-osmosis, and consolidation under an applied load, were investigated and found to be technically feasible, but their economic aspects were not studied. In addition, experience suggests that evaporation is probably one of the most useful means for dewatering thin lifts of dredgings, and further attention should be directed toward a quantitative evaluation of this procedure. It seems that considerable cost benefits could be realized by the development of economical dewatering techniques in harbors such as Toledo, Detroit, and Chicago, where relatively large volumes of spoil are dredged regularly and where suitable disposal areas are limited.

The chemistry of the fluids and solids reveals that these dredgings are rich in plant nutrients, and this is further evidenced by a rapid growth of dense vegetation at all fill sites studied. Hence, the possible use of polluted dredgings to increase food production is suggested. At a time of great national concern for the conservation of resources and the improvement of environmental conditions, it seems appropriate to direct additional study toward the possibility of recycling the growth-producing nutrients which are washed by rains into the streams and harbors and deposited in the shipping channels. Additional experience indicates that landfills of spoil may be readily used for wild life refuges or recreational parks. Also, dewatered dredgings may be compacted in a suitable manner to form a landfill of moderate density which may be suitable for parking lots or residential construction.

Certain modifications to currently used procedures for the disposal of maintenance dredgings in diked areas seem to offer the promise of considerable improvement in the characteristics of the resulting landfill. For example, substantial benefit may be realized by planning the ultimate usage of the disposal area before the fill is placed; this will enable adjustments to be made in the position of the discharge pipe, thereby allowing some control over the location and distribution of particle sizes. In addition, the height of the dikes and consequently the depth of the fill may be increased, thereby gaining the advantages that the lower layers will consolidate faster and provide additional storage space, especially if some dewatering scheme is employed, and there will be associated gains in strength and density. It may also be worthwhile to place a drainage blanket at the bottom of the fill, provided the blanket is adequately drained. Another possible improvement would be to program the disposal operation so that relatively thin lifts are placed and allowed to desiccate by gravity drainage and evaporation with or without mechanical compaction before additional spoil is deposited; this procedure would yield a moderately dense landfill throughout its entire depth.

Since no one system will be equally suitable at all sites, several alternative disposal schemes should be considered at each dredging site; these alternatives include disposal in the open waters, diked containment, transporting the materials large distances, processing them for use as compacted fill, and combining them with other solid wastes. However, the overall economics of various spoil disposal schemes needs greater attention, and no general conclusions can be advanced at this time. With regard to the use of diked containment areas in particular, the costs of leaving valuable land lie idle in the heart of expensive harbor and industrial areas must be balanced by the costs associated with accelerating the availability of these sites for some useful purpose. From a somewhat broader point of view,which is prompted by the growing concern with depletion of our resources, the economics of spoil disposal may be vastly expanded to encompass a considerably larger realm. While it may be uneconomical to dewater spoil and utilize it profitably as compacted fill or for agricultural applications, it may be possible to promote its use in these ways by reducing the price and underwriting the remaining costs as disposal expenses. The cost of this alternative would have to be compared with that for other means by which the task could be accomplished consistent with adequate protection of the environment.

The millions of dollars spent annually on dredging the waterways and the existing potential for environmental damage emphasize the need for continued research on the development of economical and efficient methods to satisfy both the disposal problem and the requirements for protection of the environment. Toward this end concerted efforts should be made to address systematically the task of defining the problem and obtaining a solution. Since the entire scope of this problem is beyond the assigned mission of any one governmental agency, a coordinated approach among several agencies is needed to develop appropriate treatment and disposal practices and to supervise the enforcement thereof.

REFERENCES

Allison, L. E. (1935), "Organic Soil Carbon by Reduction of Chromic Acid," Soil Science, Volume 40, pp. 311-320.

Allison, L. E. (1960), "Wet Combustion Apparatus and Procedure for Organic and Inorganic Carbon in Soil," Proceedings of the Soil Science Society of America, Volume 24, pp. 36-40.

American Society for Testing and Materials (1952), Special Technical Publication 142, Symposium on Exchange Phenomena in Soils, pp. 1-71.

Arman, A. (1969), A Definition of Organic Soils (An Engineering Identification), Engineering Research Bulletin Number 101, Louisiana State University, Division of Engineering Research for the Louisiana Department of Highways, Louisiana.

Arman, A. (1970), "Engineering Classification of Organic Soils," Highway Research Record 310, pp. 75-89.

Ball, D. F. (1964), "Loss-on-ignition As an Estimate of Organic Matter and Organic Carbon in Non-Calcareous Soils," Journal of Soil Science, Volume 15, Number 1, pp. 84-92.

Barnes, H. E. (1954), "Electrical Subsurface Exploration Simplified," Roads and Streets, April, pp. 81-84.

Black, C. A., Evans, D. D., White, J. L., Ensminger, L. E., Clark, F. E., and Dinauer, R. C. (1965), Methods of Soil Analysis, Number 9 in the Agronomy Series, American Society of Agronomy, Madison, Wisconsin (see article entitled "X-Ray Diffraction Techniques for Mineral Identification and Mineralogical Composition" by L. D. Whittig, pp. 671-698).

Brown, H. G., and Keffer, W. J. (1971), "Pollution Potential of Sediments," Preprint 1544, Environmental Engineering Meeting of the American Society of Civil Engineers, October, St. Louis, Missouri.

Cadling, L., and Odenstad, S. (1950), The Vane Borer: An Apparatus for Determining the Shear Strength of Clay Soils Directly in the Ground, Proceedings of the Royal Swedish Geotechnical Institute, Number 2, Sweden.

Casagrande, A. (1948), "Classification and Identification of Soils," Transactions of the American Society of Civil Engineers, Volume 113, pp. 901-930.

Casagrande, L. (1966), "Construction of Embankments Across Peaty Soils," Journal of the Boston Society of Civil Engineers, Volume 53, Number 3, pp. 272-313.

Corps of Engineers, Buffalo District (1969), Dredging and Water Quality Problems in the Great Lakes, Twelve-volume Technical Report, New York.

Corps of Engineers, Philadelphia District (1969), Long Range Spoil Disposal Study, Six-volume Technical Report, Pennsylvania.

Dominquez, R. F., and Basco, D. R. (1971), "Muddy Aspects of Water Quality Affecting Dredging," World Dredging and Marine Construction, December, pp. 22-24.

Earth Manual (1963), U. S. Bureau of Reclamation, First Edition, p. 222.

Federal Water Pollution Control Administration (1967), Michigan Harbors and Navigation Channels Bottom Sediment Analysis, Great Lakes Region, Detroit, Michigan, pp. 1-36.

Furman, N. H. (1939), Standard Methods of Chemical Analysis, Fifth Edition, Volume 1, Editor: W. W. Scott, D. Van Nostrand Company, New York.

Garbe, C. W., and Jeno, J. J. (1968), Reclamation of Hydraulic Dredge Spoil, Dames and Moore Technical Topics, San Francisco, California, pp. 1-5.

Grass, L. B. and LeMert, R. A. (1971), "Determination of Organic and Inorganic Carbon on a Single Aliquot Sample," Proceedings of the Soil Science Society of America, Volume 35, pp. 152-154.

Gray, D., and Mitchell, J. K. (1967), "Fundamental Aspects of Electroosmosis," Journal of the Soil Mechanics and Foundations Division, American Society of Civil Engineers, Volume 93, Number SM6, pp. 209-236.

Greeley and Hansen, Engineers (1969), Report on the Feasibility of Drying Dredged Material for the Ace Scavenger Company, June, Chicago, Illinois, pp. 1-14.

Hartzell, E. P. (1968), Disposal of Shoal Material From the Dredging Operation in the Delaware River, Corps of Engineers, Philadelphia District, pp. 240-260.

Heller, H. L. and Thelen, E. (1971), Building Material from Dredge Spoil, Corps of Engineers, Philadelphia District, June, pp. 1-10.

Holtz, R. D. and Krizek, R. J. (1970), "Properties of Slightly Organic Topsoils," Journal of the Construction Division, American Society of Civil Engineers, Volume 96, Number CO1, pp. 29-43.

Hutton, W. S., Hann, R. W., and Smith, R. H. (1970), A Quantitative and Qualitative Survey of Benthal Deposits Contained in the Houston Ship Channel, Technical Report Number 8, Civil Engineering Department, Environmental Engineering Division, Texas A & M University, College Station, Texas.

International Joint Commission [Canada and the United States](1970), Pollution of Lake Erie, Lake Ontario, and the International Section of the St. Lawrence River, pp. 1-174.

International Joint Commission [Canada and the United States] (1972), Agreement Between Canada and the United States of America on Great Lakes Water Quality, March 17, revised April 5, pp. 1-72.

International Lake Erie Water Pollution Board and the International Lake Ontario - St. Lawrence River Water Pollution Board (1969), Volume 1: Summary, pp. 1-151; Volume 2: Lake Erie, pp. 1-316; Volume 3: Lake Ontario and the International Section of the St. Lawrence River, pp. 1-329.

Kononova, M. M. (1961), Soil Organic Matter, Pergamon Press, London, pp. 45-46.

Kramer, J. R., and Rodgers, G. K. (1968), "Natural Processes and Water Quality Control," Paper Number Q-2, Proceedings of the Great Lakes Water Resources Conference, June, Toronto, Canada, pp. 419-432.

Krynine, D. P., and Judd, W. R. (1957), Principles of Engineering Geology and Geotechnics, McGraw-Hill Book Company, New York, pp. 126-127.

Lambe, T. W. (1951), Soil Testing for Engineers, John Wiley and Sons, Inc., New York.

Lambe, T. W. (1969), "Reclaimed Land in Kawasaki City, Japan," Journal of the Soil Mechanics and Foundations Division, American Society of Civil Engineers, Volume 95, Number SM5, pp. 1181-1198.

Leonards, G. A. (1962), Foundation Engineering, Engineering Properties of Soils, McGraw-Hill Book Company, New York.

Lowe, J., E. Jonas, and V. Obrician (1969), "Controlled Gradient Consolidation Test," American Society of Civil Engineers, Journal of the Soil Mechanics and Foundations Division, Volume 95, Number SM1, pp. 77-97.

McNely, D. J. (1966), Hydraulic Fill Area 2, Mariner's Island, Dames and Moore Office Memorandum, San Francisco, California, pp. 1-24.

Moore, R. W. (1945), "An Empirical Method of Interpretation of Earth Resistivity Measurements," Transactions of the American Institute of Mining and Metallurgical Engineers, Volume 164, pp. 197-215.

Nedved, T. K. (1969), Development of Techniques and Criteria for Determination of Sources of Shoal Deposits; Phase I: Development of Outfall Sampler (pp. 1-194); Phase II: Suspended Solids Sampling, Shoal Sampling and Tracer Studies (pp. 1-109); Phase III: Measurement of Inplace Densities of Shoal Materials (pp. 1-30); Report Number IITRI-C6157-16, United States Department of the Army, Chicago District, Corps of Engineers, Chicago, Illinois.

Nichols, C. (1972), Personal Correspondence, Dames and Moore, San Francisco, California

Odell, R. T., Thornburn, T. H., and McKenzie, L. J. (1960), "Relationships of Attenberg Limits to Some Other Properties of Illinois Soils," Proceedings of the Soil Science Society of America, Volume 24, pp. 237-300.

O'Neal G.,and Sceva, J. (1971), "The Effects of Dredging on Water Quality," World Dredging and Marine Construction, Dec., pp. 25-31.

Orozco, L. F. (1972), A Study of Compaction and Strength Characteristics of Slightly Organic Soils as a Function of Organic Content, Master of Science Thesis, Department of Civil Engineering, Northwestern Universith, Evanston, Illinois.

Penman, A. D. M., and Watson, G. H. (1967), "Foundations for Storage Tanks on Reclaimed Land at Teesmouth," Proceedings of the Institute of Civil Engineers, Volume 37, pp. 19-42.

Rutledge, P. C. (1970), "Utilization of Marginal Lands for Urban Development," Journal of the Soil Mechanics and Foundations Division, American Society of Civil Engineers, Volume 96, Number SM1, pp. 1-22.

Schmidt, N. O. (1965), A Study of the Isolation of Organic Matter as A Variable Affecting Properties of a Soil, Doctoral Dissertation, Department of Civil Engineering, University of Illinois, Urbana, Illinois.

Schollenberger, C. J. (1927), "A Rapid Approximate Method for Determining Soil Organic Matter," Soil Science, Volume 24, pp. 65-68.

Schollenberger, C. J. (1945), "Determination of Soil Organic Matter," Soil Science, Volume 59, pp. 53-56.

Seed, H. B., Woodward, R. J., and Lungren, R. (1964), "Fundamental Aspects of the Atterberg Limits," Journal of the Soil Mechanics and Foundations Division, American Society of Civil Engineers, Volume 90, Number SM6, pp. 75-108.

Shaw, K. (1959), "Determination of Organic Carbon In Soil and Plant Material," Journal of Soil Science, Volume 10, pp. 316-326.

Sheeran, D. E., and Krizek, R. J. (1971), "Preparation of Homogeneous Soil Samples by Slurry Consolidation," Journal of Materials, Volume 6, Number 2, pp. 356-373.

Skempton, A. W., and Petley, D. J. (1970), "Ignition Loss and Other Properties of Peats and Clays from Avonmouth, King's Lynn and Cranberry Moss," Geotechnique, Volume 20, pp. 343-356.

Soil Primer (1956), Portland Cement Association, p. 27.

Soil Testing Services (1968), Slag-Dredgings Fill Project, Inland Steel Company, East Chicago, Indiana, Consulting Report, Northbrook, Illinois, 34 pp.

Standard Methods for the Examination of Water and Wastewater (1971), Thirteenth Edition, American Public Health Association, New York.

Taylor, D. W. (1948), Fundamentals of Soil Mechanics, John Wiley and Sons, New York, p. 53.

Terzaghi, K. (1943), Theoretical Soil Mechanics, John Wiley and Sons, New York, pp. 266-271.

Tinsley, J. (1950), "Determination of Organic Carbon in Soils by Dichromate Mixtures," Transactions of the Fourth International Congress on Soil Science, Volume 1, pp. 161-164.

United States Department of the Interior (1967), Michigan Harbors and Navigation Channels: Bottom Sediment Analysis, Federal Water Pollution Control Administration, Great Lakes Region, Detroit Office, U. S. Naval Air Station, Grosse Ile, Michigan.

United States Department of the Interior (1969), Chemistry Laboratory Manual: Bottom Sediments, Compiled by the Great Lakes Region Committee of Analytical Methods, Federal Water Pollution Control Administration, Lake Michigan Basin Office, Chicago, Illinois.

Vey, E. (1949), The Mechanics of Soil Consolidation by Electro-osmosis," Proceedings of the Highway Research Board, Volume 29, pp. 578-589.

Walkley, A., and Black, I. A. (1934), "An Examination of the Degtjareff Method for Determining Soil Organic Matter and a Proposed Modification of Chromic Acid Titration Methods," Soil Science, Volume 37, pp. 29-38.

Water Quality Criteria (1968), Report of the U. S. National Technical Advisory Committee to the Secretary of the Interior, published by Federal Water Pollution Control Agency, Washington, D. C., pp. 1-234.

Water Quality Criteria Data Book (1970), Organic Chemical Pollution of Freshwater, Environmental Protection Agency, Volume I, Water Pollution Control Series, 18010 DPV 12/70, Washington, D. C.

Water Quality Criteria Data Book (1971), Inorganic Chemical Pollution of Fresh Water, Environmental Protection Agency, Volume II, Water Pollution Control Series, 18010 DPV 07/71, Washington, D. C.

West, P. W., and Lyles, G. L. (1960), "A New Method for the Determination of Nitrates," Analytica Chimica Acta, Volume 23, No. 3, pp. 227-232.

Whitman, R. V. (1970), "Hydraulic Fills to Support Structural Loads," Journal of the Soil Mechanics and Foundations Division, American Society of Civil Engineers, Volume 96, Number SM1, pp. 23-47.

Wilson, S. D. (1950), Small Soil Compaction Apparatus Duplicates Field Results Closely, Engineering News Record, November 2, 1950.